S.E.B.

THE MORPHOLOGY AND ELECTROPHYSIOLOGY OF LEECH NEURONES *IN VITRO* : A STUDY USING MICROFABRICATED DEVICES.

RICHARD JAMES ALFRED WILSON B.Sc.(Hons).
Department of Cell Biology.

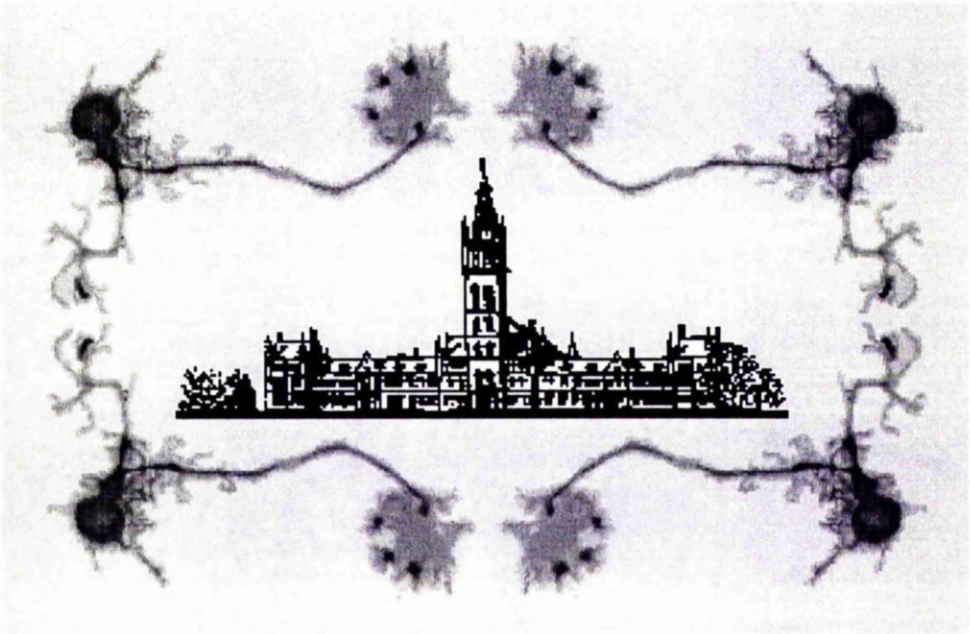

A thesis submitted to the Faculty of Science of the University of Glasgow for the degree of Doctor of Philosophy.

February, 1992.

ProQuest LLC.
789 East Eisenhower Parkway
P.O. Box 1346
Ann Arbor, MI 48106 – 1346

ACKNOWLEDGEMENTS

The generosity shown by the staff and students which make up the Department of Cell Biology has made the last three years memorable. I would like to acknowledge their friendship and thank them for their kindness.

Special thanks to Dr Susanna Blackshaw and Dr Julian Dow for their supervision and enthusiasm both during experimental work and during the writing of this thesis. I am particularly grateful to Julian for guidance both on and off the ski slopes and to Susanna for introducing me to the joys of the leech.

Special thanks also to Profs. Adam Curtis and Chris Wilkinson† for making available the necessary facilities required to complete this thesis and for providing invaluable inspiration. Regular, productive and enjoyable brain storming sessions were also held with Drs. L. Breckenridge, P. Clark, P. Connolly† & R. Lind†.

Excellent technical assistance was gratefully received from Scott Arkison (who 'lovingly' cared for the leeches), Bill Monaghan† (who skilfully operated the plasma etch and plasma CVD machines) and Mary Robertson† (who patiently bonded the planar electrode tracks to printed circuit boards). Thanks also to Andrew Hart, Carlo Mucci, Lois Hobbs† and Joan Carson†.

I would like to thank my teachers for their endeavours, especially Mr Baxter to whom I will always be indebted.

Finally, I would like to thank my parents, sisters and friends for their encouragement and understanding. Without their support, finishing would have remained a concept.

This work was supported by a Wellcome Prize Studentship.

---

†Department of Electrical Engineering

To my Parents

TABLE OF CONTENTS

List of Figures & Tables

CHAPTER ONE

CHAPTER TWO

CHAPTER THREE

CHAPTER FOUR

CHAPTER FIVE

List of abbreviations

5-HT .....Serotonin (or 5-Hydroxytryptamine)

α .....Included angle between two planes
Δ.....Optical path difference
θ.....Angle of refraction in medium
.....Conduction velocity ($m.s^{-1}$)
λ.....Wavelength (nm)
.....Length constant (cm)
τ_{foot}.....Time constant at foot of action potential (ms)
τ_m.....Membrane time constant (ms)

A .....Area (e.g. m^2)
AC.....Alternating current
BHK.....Baby hamster kidney
C .....Capacitance (e.g.μF)
CCD.....Charged coupled device
C_m.....Specific membrane capacitance ($\mu F.cm^{-2}$)
CNS.....Central nervous system
Con A .....Concanavalin A
CVD.....Chemical vapour deposition
d.....diameter (e.g. μm)
DC .....Direct current
DCC.....Dicyclohexylcarbodiimide
DMF.....Dimethylformamide
DMSO.....Dimethyl sulfoxide
DRG.....Dorsal root ganglia
ECM .....Extracellular matrix
EDTA.....Divalent selective chelator
EGF.....Epithelial growth factor
EGTA.....Ca^{2+} selective chelator
E_K .....K^+ equilibrium potential (mV)
epsp.....Excitatory postsynaptic potential
f.....Frequency (Hz)
FCS.....Foetal calf serum
Fura-2.....Fluorescent probe (Ca^{2+} indicator)
g.....Separation between two interfaces (e.g. μm)

HECT..... Hepes eagle calf serum trypose phosphate
Indo-1 ..... Fluorescent probe (Ca^{2+} indicator)
ipsp ..... Inhibitory postsynaptic potential
IRM..... Interference reflection microscopy
MOSFET..... Metal oxide semiconductor field effect transistor
N ..... Order of interference
n..... Refractive index
NA..... Numerical aperture
NGF..... nerve growth factor
PBS..... Phosphate buffered saline
W..... Half-width of differential (ms)
R ..... Resistive component of impedance
R^2..... Spearman's correlation coefficient
R_i..... Longitudinal axoplasmic resistance (Ω.cm)
R_m..... Specific membrane resistance ($\Omega.cm^2$)
R_N ..... Input resistance ($M\Omega$)
S.D..... Standard deviation
S.E.M. ..... Standard error of the mean
..... Scanning electron microscope
Sulfo-NHS... N-hydroxysulfosuccinimide
t..... Time (ms)
UV..... Ultraviolet
V ..... Membrane potential (mV)
$V_{Th(other)}$.... Membrane threshold other than at stump (mV)
$V_{Th(stump)}$... Membrane threshold at stump of processes (mV)
X_C..... Capacitive component of impedance (or reactance)
Z..... Impedance ($M\Omega$)

SUMMARY

1. This thesis considers the possibility of investigating neuronal information processing by making mulitisite recordings either from individual isolated neurones or from small neuronal networks of controlled design.
2. Isolated leech neurones were used (a) to study the effects of isolation on electrophysiological properties (Chapter 2); (b) to provide the first demonstration of the use of planar extracellular electrode arrays to measure electrophysiological properties of individual isolated neurones (Chapter 3); and (c) to investigate the use of topographical features for controlling the outgrowth of neurones in culture (Chapters 4 & 5).

3. The study into the effects of isolation confirmed and extended previous reports which showed that (a) the action potentials recorded from the cell body of isolated Retzius neurones are generally similar to action potentials recorded *in vivo* and (b) isolation causes an increase in input resistance.
4. The results of an experiment designed to show a correlation between input resistance and the length of processes, suggest that the removal of processes during extraction is not the main cause of the high input resistance of isolated cells. One possibility is that the input resistance is a direct result of a change in membrane properties.
5. This conclusion is supported by the demonstration in isolated neurones of a slow inward transient (known as anomolous rectification) that occurs shortly after the onset of large hyperpolarising current injections. This transient was not observed in dissected ganglia and has not been previously reported in leech neurones.

6. The electrophysiology of isolated neurones was also explored using extracellular electrode arrays. Specifically the electrode arrays were used to show that: (a) the conduction velocity of action potentials in P cells is faster than that of action potentials in Retzius cells (which correlates with the difference in rise time); (b) the action potentials of isolated neurones propagate from the tip of the extracted process towards the cell body (indicating that the concentration of Na^+ channels is greater at the tip of

the extracted process than in other regions); and (c) the action potential in the extracted process may have a faster rise time than that in the cell body, suggesting a difference in the average concentration of Na^+ channels.

7. The use of extracellular electrode arrays in the above experiments demonstrates: (a) the first multisite extracellular recordings of isolated neurones; (b) the first extracellular recordings made of the electrical activity that results from extracellular stimulation of the same cell; and (c) the feasibility of using these devices to investigate information processing in single cells.

8. In order to control the morphology of single neurones, and the connectivity of groups of neurones, the influence of the substratum in determining the morphology of cultured neurones was investigated. The principal result demonstrates for the first time that topography can influence the outgrowth morphology of large identified invertebrate neurones. The dimensions of the topographical features were similar to those required to align the neurites of much smaller vertebrate neurones.

9. The results also show that: (a) on planar Con A-coated substrata the outgrowth of Retzius neurones tends to be dominated by large lamellae, whereas on leech extracellular matrix (ECM) -coated substrata cells produced an elaborate network of neurites (confirming previous reports), (b) interference reflection microscopy (IRM) revealled that the neurites made a series of very close but intermittent contacts with the substratum, whereas the lamella was characterised by a large region of uniform close contact, and (c) whereas neurites were strongly influenced by topographical features the lamellar-type outgrowth was only partially aligned.

10. Based on these results a new hypothesis (the Topographical Modulating Hypothesis) is presented. The hypothesis proposes that the influence of topographical discontinuities in determining the morphology of neurones, or the orientation of migrating cells, is modulated by the molecular nature of the substrate.

CHAPTER ONE:

Introduction to multisite recordings and the leech

SUMMARY: **There are several different methods of recording the electrical activity of excitable cells (see Figure 1). Each has a different set of advantages and disadvantages (considered in Section 1.1) and as a consequence each is best suited to address a separate problem. This introductory chapter considers the advantages and disadvantages of the different methods and examines how multisite recording techniques might best be applied to unravel problems in neuronal information processing (Section 1.2). The leech nervous system is also introduced (Section 1.3) and the *in vivo* properties of the two neuronal cell types used *in vitro* in this thesis are summarised (Sections 1.4 & 1.5). Finally, the literature on leech cell culture is briefly reviewed (Section 1.6), setting the scene for the experiments in the following chapters.**

1.1 Techniques for recording neuronal activity

1.1.1 Single site recording techniques

Since their advent in the 1940's (Hodgkin & Huxley, 1945; Graham & Gerard, 1946) glass microelectrodes have revolutionised neurobiology providing an invaluable method of measuring the voltage across cell membranes. However, they do have several disadvantages which limits their application. For example, a susceptibility to vibration tends to limit the lifetime of impalements. Another disadvantage is the possibility that long term activity is modified irreversibly by the small ionic fluxes that may occur during the process of impaling a membrane. A further disadvantage is the optical problem of precisely locating the very fine tip of the electrode above the

preparation. If incorrectly positioned, the tip of the electrode may act as a knife, cutting the membrane of the process or cell body rather than cleanly impaling it. Despite these disadvantages a few highly skilled workers have used intracellular electrodes to record from axons and dendrites (e.g Cattaert *et al.*, 1992; Hild & Tasaki, 1962).

Intracellular electrodes are most frequently used to measure the voltage across a membrane, but can also be used to record current fluxes. In this mode, variable current is injected into the cell to maintain a steady voltage across the cell membrane (a technique known as the voltage clamp). The current injected exactly compensates for the current through the membrane. Thus, recording the amount of injected current gives a measure of the net current fluxes through the membrane.

As an alternative to using very sharp electrodes to impale cells, the tips can be pulled off and fire polished so as to producing a smooth blunt orifice with a diameter of a few microns. When lowered onto the surface of a cell, a seal of about 50 MΩ is formed between the membrane and the glass, creating a patch. By applying gentle suction the seal resistance can be increased to a gigaohm (forming the 'cell attached' configuration; see Figure 1.1) which effectively eliminates current leak. Thus, the tiny currents associated with the opening of channels in the area of the patch can be "captured" by the recording apparatus. This can be contrasted with the resolution of the intracellular microelectrode (when used under voltage clamp) which records the “global” current through a relatively large area of membrane. In addition, when the area of membrane is comparatively small the voltage across the patch can be clamped more accurately allowing the current which passes through single channels to be measured directly.

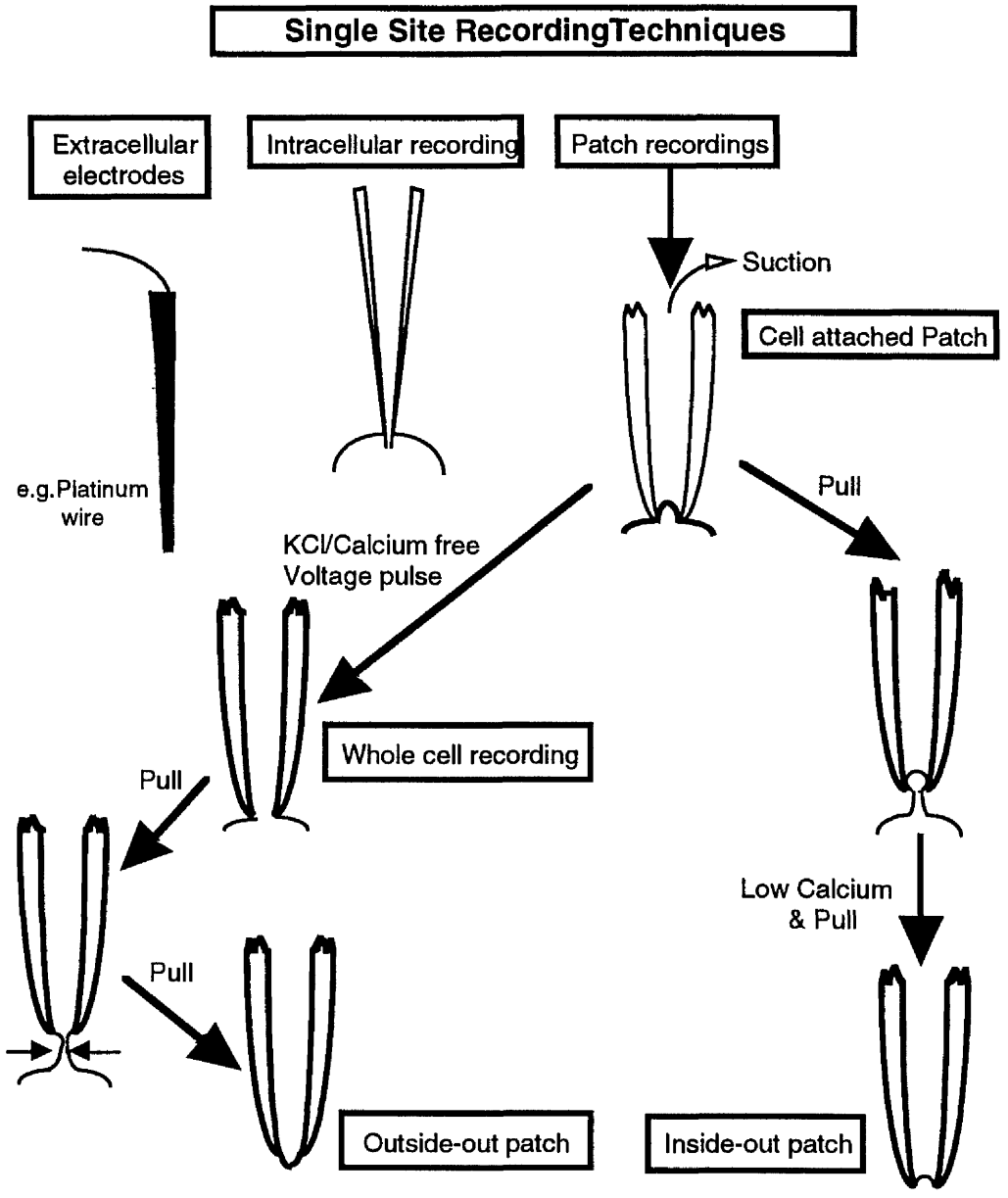

Figure 1.1: Methods of single site recording. Adapted from Hamill et al. (1981).

The patch of membrane can be manipulated in a variety of ways to create different configurations. To isolate the patch from the rest of the cell for example, the patch electrode is pulled away from the cell in a solution with a low concentration of Ca^{2+}. This leaves the membrane of the patch with the cytoplasmic surface exposed to the medium in the bath whilst the extracellular surface is exposed to the solution in the pipette (known as an

inside-out patch). An outside-out patch requires an intermediate step: the whole cell patch configuration. In KCl/Ca^{2+} free conditions, a suction or voltage pulse is sufficient to break down the membrane in the patch. In this whole cell recording mode the cytoplasm is in contact with the saline solution in the patch pipette. The salt solution of intracellular electrodes also makes direct contact with the cytoplasm, and in this respect the two approaches are similar. Like intracellular electrodes the whole cell patch is used to measure the voltage across, and the current through, a large area of membrane (equal to that of the whole cell in certain cases). However, as the tip diameter of the patch pipette is far greater than that of the intracellular electrode, the tip resistance is minimal and therefore so is the tip potential. This alleviates the need for a Wheatstone bridge circuit to compensate for tip potential, allowing membrane voltage to be measured more accurately during current injection. Unfortunately, it also means that the cytoplasm interchanges more readily with the saline which almost certainly alters its physiological balance. To transform the whole cell patch to an outside-out patch, the electrode is pulled free of the cell. As the electrode is moved away, a collar of membrane stretches from the cell to the rim of the electrode, gradually becoming narrower and narrower as the distance increases. Eventually the membrane on either side of the collar fuses and breaks away from the rest of the cell membrane, leaving the extracellular surface of the membrane patch facing outwards. The beauty of the inside-out and outside-out patches is that either side of the membrane can be selectively exposed to pharmacological agents or solutions with different ionic compositions whilst monitoring the effects on the currents from individual or small numbers of channels.

Since the cell membrane is relatively flexible, it is likely to distort somewhat to accommodate the smooth rim of the patch electrode. Thus,

unlike an intracellular electrode, precise vertical positioning is not critical and so it is possible to patch onto processes and even growth cones. This has been achieved on a variety of cell types, including cultured leech neurones (Garcia *et al*, 1989).

Unfortunately, patch electrodes have several disadvantages. The contact required with the cell is rarely reversible, especially after a gigohm seal has formed, leading to short term "one-off" recordings. A related problem is the "hit or miss" nature of forming a good seal. Misses can result in permanent damage to the cell, making it very difficult to use this technique for recording simultaneously from more than one site on any one neurone. This problem is confounded by a further disadvantage that is shared with intracellular electrodes. The bulky micromanipulators, that are required both to position electrodes in the desired location and to minimise vibration, sterically limit the number of electrodes that can be used on a single preparation.

1.1.2 Multisite recording techniques

Several additions to the electrophysiologist's arsenal promise to circumvent the difficulties of making multisite recordings. These can be divided into two classes: extracellular electrode arrays (used extensively in this project, and considered in detail in Chapter 3), and optical techniques. They differ fundamentally in that electrode arrays represent a miniaturisation of the recording site, whereas the optical techniques increase spatial resolution by way of image enlargement.

The optical techniques can be divided into two classes. The first consists of methods that utilise dyes which undergo changes in fluorescence (Grinvald & Farber, 1981), absorption (Parsons *et al.*, 1989) or distribution

(Brauner *et al.*, 1984) as a consequence of changes in either membrane potential or the intracellular concentration of an ion (Tsien, 1988). The second relies on innate properties such as birifringence and light scattering, that modulate light passing through a cell in a manner that is dependent on membrane potential.

A number of excellent reviews describe the use of dyes to monitor the activity of excitable membranes (e.g. Grinvald, 1985; Cohen, 1989; Ross, 1989; Salzberg, 1989). Here, the literature is summarised in terms of work that highlights the advantages and disadvantages of this approach.

Dyes sensitive to the concentration of specific ions

Several ions participate in the fluxes that drive the activity of excitable membranes. Dyes which undergo changes in fluorescence or absorption according to the concentration of one of these ions can therefore be used as a measure of ion-specific membrane channel activity. The detection of fast ionic fluxes that involve a relatively small number of ions are however, likely to be damped by the binding characteristics of the dye. The calcium-sensitive dyes for example, have a binding site similar to that of EGTA (a calcium chelator) making them highly specific, but also good at buffering fast transients (Tsien, 1988). The extent of this disadvantage will depend on the ionic species involved and the speed at which its channels open. The large signals of the calcium sensitive dyes and the slow time course of calcium transients offset these problems, allowing unsurpassed spatial resolution.

Figure 1.2 (overleaf): Multisite recording techniques. Both optical techniques and planar extracellular electrode arrays can be used to record neuronal excitability from multiple sites non invasively. Although optical recordings have been made using innate properties (optical apparatus for which is not shown), more usually a dye is employed which undergoes changes in absorption or fluorescence according to membrane potential, or the distribution of an ion. Each of the optical setups described can be used in either the inverted or transmitted mode.

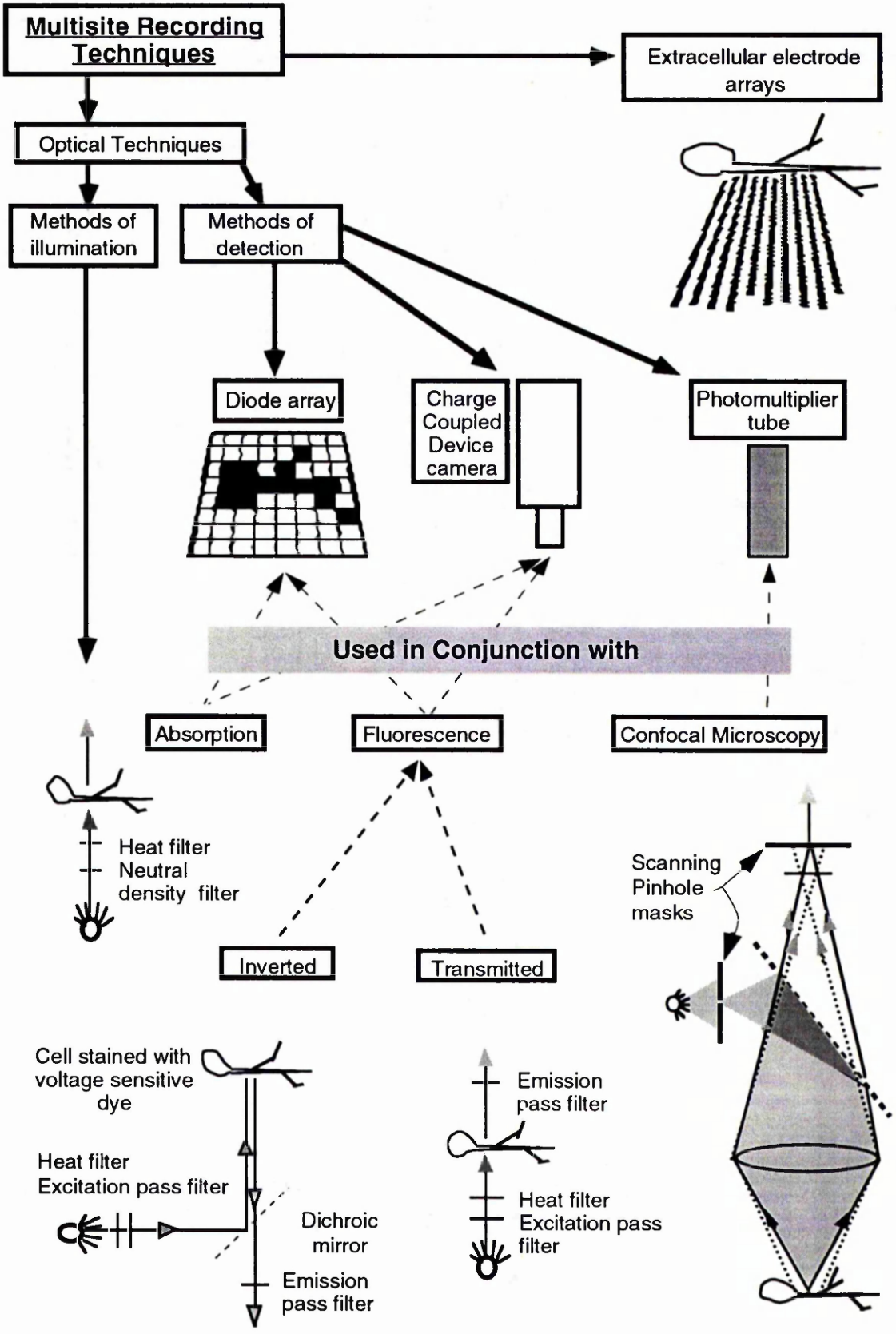
Multisite Recording Techniques
Extracellular electrode arrays
Optical Techniques
Methods of illumination
Methods of detection
Diode array
Charge Coupled Device camera
Photomultiplier tube
Used in Conjunction with
Absorption
Fluorescence
Confocal Microscopy
Heat filter
Neutral density filter
Inverted
Transmitted
Scanning Pinhole masks
Cell stained with voltage sensitive dye
Heat filter
Excitation pass filter
Dichroic mirror
Emission pass filter
Emission pass filter
Heat filter
Excitation pass filter

Thus, fura-2 has been used to measure the concentration of Ca^{2+} within different cellular compartments of smooth muscle cells and also to demonstrate the transient accumulation of calcium in hippocampal CA1 pyramidal dendrites (Williams *et al.*, 1985; Regehr & Tank, 1990). In both examples, the emitted light intensities at two excitation wavelengths were used to determine the absolute $[Ca^{2+}]$[1]. To make these "dual excitation" measurements a shutter mechanism is required to switch excitation wavelengths, reducing the sampling frequency (e.g. Kassotis *et al.*, 1987; Thayer *et al.*, 1988). A different dye (Indo-1) overcomes the need for a shutter, having a "dual emission" spectrum that has the same type of $[Ca^{2+}]$ sensitivity as the excitation spectrum of fura-2 (Grynkiewicz *et al.*,1985).

Dyes which respond directly to membrane potential can also be used to determine the contribution made by individual ionic species, if they are used in combination with specific channel blockers or modified bathing solutions. This type of approach has been applied to hippocampal slices to show that the slow, calcium dependent component of pyramidal neurone activity originates from an area that contains the apical dendrites (Grinvald *et al.*, 1982). Similarly, calcium action potentials have been found to spread from the growth cones of cultured mouse neuroblastoma (N1E-115) cells towards the soma (Grinvald & Farber, 1981).

---

[1]When excited at one wavelength, the emitted light intensity is dependent on both the concentration of dye and the amount of Ca^{2+} bound to the dye. The intensity of emitted light that results from exciting at a second wavelength is virtually independent of Ca^{2+} binding. The ratio of these two intensity values compensates for variable cell thickness or dye uptake allowing the absolute $[Ca^{2+}]$ to be determined.

Dyes directly sensitive to membrane potential

Monitoring a single ionic species may provide important information about neuronal information processing (Regehr & Tank, 1990). However, the spread and modulation of electrotonic potentials may occur in regions of a neurone where a particular species of channel is not located. Thus information about the flux of a single ionic species maybe inadequate.

Over 1,800 dyes have been synthesized that are directly sensitive to membrane potential (Grinvald, 1985). There are two types of potentiometric dyes. One type diffuses through membranes and undergoes Nernstian redistribution when a potential is applied (Brauner *et al.*, 1984). The other type is associated with the membrane itself and fluoresces according to molecular orientation or rearrangement. This latter type is likely to respond within 2 μs of an applied field, giving a temporal resolution that far exceeds that of the redistributing dyes (Salzberg, 1989).

Unfortunately, most of the fast dyes are toxic (Grinvald *et al.*, 1981b) or become so on exposure to the illuminating light ("phototoxicity"), probably through the production of oxygen radicals. This can be reduced by using deoxygenated medium and by using changes in absorption (rather than fluorescence) to measure membrane potential (Parsons *et al.*, 1989). Absorption measurements require lower excitation intensities as the photodetector receives a larger proportion of light which masks the "dark noise" inherent in the detection device. Reducing the excitation intensity minimises photobleaching, eliminating the need for correction procedures (Grinvald *et al.*, 1987), and increases the longevity of recordings. However, detecting small changes in light intensities against a bright background is more difficult than detecting the same change against a dark background.

Thus, measuring the activity in individual, small-diameter processes (where the area of membrane available for dye binding is small) may best be achieved by monitoring changes in fluorescence rather than absorption (Grinvald *et al.*, 1981b). With time, fluorescent probes may be developed that are non toxic, are less susceptible to photobleaching, and give larger signals.

Probably one of the most exciting applications of membrane bound potentiometric dyes is to inject one or a few cells iontophoretically, within a ganglion or brain slice. Using this method, it may be possible to monitor the activity of a single cell's neurites in the web of processes that constitutes the neuropil. In addition, dye binding to the membrane of non-neuronal cell types is eliminated, avoiding possible signal distortion arising through the slow excitability of glia which can be triggered by neuronal activity (Konnerth *et al.*, 1985). This kind of approach was used by Regehr & Tank (1990) using fura-2 to make Ca^{2+} recordings from dendrites in hippocampal slices. For iontophoretically-injected potentiometric dyes, the task is made considerably more difficult by the relatively small signal produced by these probes. This arises owing to the small area of plasmalemma available for dye binding and the high background caused by non-specific binding to cytoplasmic proteins and intracellular membranes that are not part of the plasmalemma. Potentially, the signal-to-noise may be degraded by a factor of ten (Grinvald *et al.*, 1987) compared to recordings of cells made *in vitro*.

A study which used neurones of the leech (introduced in Sections 1.3 to 1.6) has shown that these problems can be overcome (Grinvald *et al.*, 1987). An identifiable motor neurone (either an AE cell or an L cell) in one ganglion was injected with dye and monitored with a single photodiode. A second diode was used to record the background light. Following the intracellular stimulation of one of the mechanosensory neurones (a P cell) in

the adjacent ganglion, excitatory post synaptic potentials (epsp's) were detected in the neuropil. A number of factors contributed to this incredible resolution: high intensity light was used to maximise the fluorescent signal; the second diode was used to subtract "background" noise from each sweep; a sweep made just before stimulation was background-corrected, and then subtracted from the sweep made during stimulation (also background-corrected) reducing systematic distortion due to bleaching; 14 distortion-corrected sweeps were averaged to increase the signal-to-noise ratio; and finally a comparatively large area of the neuropil was monitored that included long lengths of processes.

Synaptic potentials have been recorded without averaging from cells grown *in vitro* using absorption measurements (Parsons *et al.*, 1989). Clearly, the main advantage of using isolated cells is that background noise can be minimised. Unfortunately, the authors were not able to detect any activity in the most distal processes, where the area monitored by each photodiode contained the least amount of membrane. This may have been a result of low dye binding in this region, rather than the electrical properties of the cells. As Grinvald (1985) quite rightly points out, the only comparisons that should be made are those between recordings made from the *same* site under different conditions. It would appear that further advances in both dyes and detection methods are required before activity can be monitored in short lengths of individual, small-diameter processes.

The use of innate optical properties

The use of innate optical properties such as birefringence and light scattering avoids the toxicity problem associated with the potentiometric dyes: recordings have been made for 10 hours without any adverse

physiological side effects (Stepnoski *et al.*, 1990). Recordings have been made from isolated nerves (Hill & Keynes, 1949; Cohen *et al.*, 1968), semi isolated neuronal tissue (Salzberg *et al.*, 1985) and single cultured *Aplysia* neurones (Stepnoski *et al.*, 1990). The literature on this promising method is relatively small, despite the excellent signal-to-noise ratios. In the study involving cultured neurones the signal-to-noise ratio was comparable to that achieved using potentiometric dyes (compare Parsons *et al.*, 1989, with Stepnoski *et al.*, 1990). One explanation for why this technique has not been used more extensively may be that success is highly preparation-dependent. Salzberg *et al.* (1985) report that changes in light scattering are associated with the secretion from the nerve terminals of the neurohypophysis in mammals, but *not* in amphibia. The potentiometric dyes seem to work far better on cultured *Aplysia* neurones than on neurones cultured from other animals, such as the leech. This may be due to the highly invaginated membrane of *Aplysia* neurones (Parsons *et al.*, 1989), which in turn could explain the excellent signal-to-noise ratios obtained using light scattering by Stepnoski *et al.* (1990).

The mechanisms responsible for the change in optical properties with membrane potential have not yet been fully characterised. A fast component superimposed on a slower transient, that occurs only after prolonged periods of activity, suggests that two separate mechanisms may be involved. The fast component may be a consequence of changes in the alignment of membrane associated molecules, or fluctuations in the width of the lipid bilayer. Volume changes (Hill, 1950) capable of altering the refractive index of the cytoplasm could explain the slower component (Cohen *et al.*, 1968). Resolving the mechanism responsible might lead to a wider use of this technique and larger signals. For example, Cohen *et al.* (1968) achieved a

ten fold improvement in their recordings of light-scattering activity in a crab nerve by viewing the preparation between two polarising filters. The first filter lets through light polarised in a single plane, the second filter blocks this light unless the plane of polarisation has been modified by the (birefringence of the) preparation. The degree of modification was found to be dependent on the membrane potential and was reduced during stimulation. Staining a preparation with a potentiometric probe increases birefringence and can leading to a further ten fold improvement in the signal-to-noise ratio (Ross *et al.*, 1977). Synthesising new dyes designed for this task may bring further improvements.

So far the merits of the optical techniques have been considered at the level of the preparation. However, their usefulness is limited by the methods of illumination and detection.

Illumination and detection devices

A number of light sources have been used for optical recordings. In order of increasing intensity, expense, and instability, the most commonly used have been tungsten-halogen lamps (e.g. Parsons *et al.*, 1989), mercury arc lamps (e.g. Grinvald *et al.*, 1987) and He/Ne lasers (e.g. Grinvald *et al*, 1981b). Lasers provide narrow-band illumination of a very small area of the preparation, reducing noise. However, this is offset by both the inherent instability (which requires additional electronics to stabilise) and the limitations of single site recordings. One adaptation to this method which seems promising, is to use a confocal system in which the laser beam is used to scan the preparation. Confocal microscopes can be used to optically "section" a fluorescently-stained preparation, removing the effects of light scattering and giving excellent spatial resolution. The draw back however is

that the present rate of scanning is too slow, leading to a low sampling frequency.

Photodiode arrays offer an alternative to the photomultiplier tube, retaining excellent temporal resolution whilst improving the spatial resolution. However, they too have difficulties. Precise mapping of the image onto the diodes cannot be guaranteed (Cohen *et al.*,1989). In addition under the present systems each diode receives light from a relatively large area (e.g. 45 μm^2 for a 40x objective; Grinvald, 1981). This is in part due to the objective of the microscope (see below) but also relates to the size of the individual diodes, each of which has a diameter in excess of a millimetre.

Improved spatial resolution can be achieved by using a Charge Coupled Device (CCD) camera. Such a camera can have a large number of light detecting elements (over 222 000) giving a resolution of 0.5 μm, using a 40x objective. Each element converts photons into electrons which it then stores. A bank of analogue-to-digital converters "reads" the number of stored photons in each element within a row, producing digital signals. The rows are read sequentially. CCD cameras have good dynamic ranges, are geometrically accurate and have excellent spatial resolution, but are limited by the time it takes to sequentially "read" each row. Thus, a camera with an array of 578 X 385 elements currently operates with a maximum sampling frequency of 100 Hz (Paul Gogan, personal communication). Again, new technology is required to overcome this difficulty.

The spatial resolution is also limited by the choice of objective. A high power objective is desirable because it not only produces a highly magnified image, but is also associated with a high numerical aperture which is essential to maximise the number of "captured" photons. However, this limits two other parameters. The first is the depth of field. To detect optical signals

from cells in intact ganglia, the depth of field should be maximised to allow for the 3-dimensional structure of the neurones (Krauthamer & Ross, 1984; Ross & Krauthamer, 1984). The second parameter is the field of view. This is limited for high powered lenses, restricting simultaneous optical recordings to a small area. Increasing the field of view reduces the spatial resolution and requires an objective with a lower numerical aperture. A 25x 0.8 NA objective is the lowest used so far to monitor the activity of single cells, yet the total field monitored by the photodetectors in this case was less than 500 μm (Parsons *et al*, 1989). This field of view appears inadequate when one considers that even small ganglia, like those of the leech, approach a millimetre in diameter. In addition, isolated neurones can be extracted with (see Chapter 2), or can grow, processes that extend over a millimetre. Thus, in many preparations only a proportion of a cells activity may be monitored at any one time.

Extracellular electrode arrays

As an alternative to optical methods, multisite recordings can also be made using extracellular electrode arrays (for a detailed consideration see Chapter 3). Electrode arrays have a practical advantage over the optical techniques: they avoid the extensive screening that is required to select the most appropriate dye for a preparation (Ross & Reichardt, 1979). They provide a technique that is truly non-invasive, allowing long term recordings. They can be used equally well to stimulate neurones[2] and are non toxic. To date, electrode arrays have three drawbacks. The first and most serious is the extracellular nature of recordings, which are influenced by *changes* in

---

[2]A photosensitive probe (designated RH-500) that can be used for stimulation, has also been developed (Faber and Grinvald, 1983).

membrane potential rather than the membrane potential *per se.* A second disadvantage, is the dependence of signal size on the distance (and configuration of the space) between the cell and the electrode. Together, these two factors tend to reduce the data available in most recordings to temporal information only. The final disadvantage is the relatively poor spatial resolution of current devices.

A co-worker at the University of Glasgow has confirmed previous claims that when a neurone forms a high resistance seal over an extracellular electrode the recordings take a form which approximates that of an intracellular electrodes (L.Breckenridge; personal communication). In addition, the problem of signal size being related to the neurone/electrode configuration may be reduced by culturing cells on electrodes in the bottom of deep grooves (R.Lind, also a co-worker at the University of Glasgow; personal communication). The problem of poor spatial resolution is addressed in Chapter 3 of this Thesis. This difficulty too can be overcome: the first demonstration of the use of extracellular electrode arrays to stimulate and make multisite recordings from the same cell is reported

1.2 The appeal of cell culture to electrophysiology

Several recent developments have highlighted the difficulties of investigating neuronal information processing in intact or semi intact preparations. This Section considers the merits of an increasingly attractive alternative: the cell culture approach.

In the seminal review of Getting (1989) understanding neuronal function by way of a reductionist approach was considered in terms of network, synaptic and cellular building blocks. He concluded that:

"*...to provide insight into principles of network operation...we need synthesis, not*

further reductionism."

and posed the following questions:

"*Do particular combinations of building blocks underlies certain tasks? Are all combinations of building blocks possible or only restricted subsets? What are the processing capabilities of the various building blocks and what do they contribute to network operation? Are there rules governing the assembly of the building blocks into networks?*" Getting (1989)

Culturing isolated neurones and "synthesising" small networks *in vitro*, appears a promising way of addressing these issues. Specifically, the cell culture approach reduces the complexities, uncertainty and inaccessibility which confronts work *in vivo*.

At the network level, it is has become clear that even the simplest behaviours are mediated by a surprisingly large number of highly interconnected neurones, in most cases without any obvious hierarchical command structure (e.g. Burrows, 1987; Lockery & Kristan, 1990; but see Larimer, 1988). In the network that controls the local bending reflex in the leech, for example, sensory information is distributed between a large number of neurones which share the responsibility of generating an appropriate motor response (Lockery, 1990). Intracellular recordings from such a network reveal the activity of only a fraction of the cells that are involved at any one time leaving the experimenter to resort to a mosaic approach, piecing together activity that occurs at different time points. Multisite techniques provide a method of gaining a complete snapshot, but because of noise constraints, are best applied to neurones in culture. The number of active neurones in a single ganglion at any one time, also suggests simplification via cell culture. Based on multisite optical recordings for example, it has been estimated that 300 to 400 of the 1000 or so neurones in the abdominal ganglion of *Aplysia* are activated by touching the

skin of the siphon alone (Zecevic *et al.*, 1989). Twenty seconds worth of recordings from a mere 128 channels (sampled at 8 bits once every 0.7 ms) can generate over twenty million bits of information (Grinvald *et al.*, 1981a). Yet with such widespread activity, each channel may be monitoring the excitability of at least 3 neurones, making the identification of active cells a Herculean task, even before attempting to interpret the detailed interactions. Such an analysis is further exacerbated by complications that arise as a result of the action of neuromodulators and infringing activity from overlapping networks, both of which may transform the activity of a circuit on a moment to moment basis (a property called "polymorphism": for reviews see Getting, 1989; Harris-Warrick & Marder, 1991; Meyrand *et al.*, 1991). Clearly, a small reconstructed network *in vitro* would alleviate, if not eliminate, all these difficulties.

Kleinfeld *et al.* (1990) have grown the simplest of "networks" in culture (consisting of two identified cells from *Aplysia*), and shown them to have properties which resemble the electronic "flip-flop" circuit. The two cells are mutually inhibitory, so that activity in one cell restricts activity in the other. If the active neurone is silenced by an experimentally-imposed external stimulus, then the dormant cell gains the upper hand and inhibits any further activity from occurring in its previously dominant partner. *In vivo,* the same two identified cells types are not connected, so the behaviour in culture appears to be an artefact. However, mutual inhibition is believed to be an important mechanism *in vivo* for generating rhythmic activity, and confirmation that two cells in isolation can form such a relationship is an important finding.

A three cell network, using identified cells belonging to the central pattern generator that controls the respiration rhythm of *Lymnea*, has also

been studied *in vitro* (Syed *et al.*, 1990). Two of the cells were connected by mutual inhibition in a similar fashion both to the interactions found between these cells *in vivo* and to the cells of the previous example. The third cell was dopaminergic and when added to the network, generated alternate bursting: an effect that could be mimicked by the phasic application of dopamine. The network is the most complex reconstructed so far, and is useful in explaining the mechanism which generates breathing behaviour. It also offers insight into the subcellular mechanisms which allow its construction. For example, these experiments suggest that networks can operate with a fair degree of morphological independence. Yet, theoretical predictions of an inter-dependence between morphology and processing (Rall, 1981) have been loosely supported by experimental observations (e.g Jansen & Nicholls, 1973; Macagno *et al.*, 1987). A detailed analysis of networks in culture may reveal morphological similarities that are essential for the function of the three cell network. Alternatively, other cellular properties (such as synaptic strength) may counteract the effects of differing morphology. A third possibility, may be that morphological influences are too subtle to influence the overall behaviour. Whatever the reason, it seems that a culture approach may be instrumental in the elucidation of the relationship between morphology and function.

Another notable network grown in culture was a reconstruction of an *in vivo* three cell circuit found in *Aplysia* (Rayport & Schacher, 1986). This circuit participates in generating and modulating gill withdrawal reflexes. Modulation is believed to result from either synaptic depression or synaptic facilitation between a sensory neurone and a motor neurone. In culture, depression occurs in the amplitude of epsp's in the motor neurone following repeated stimulation of the sensory neurone. However, facilitation at this

synapse requires the presence and the activity of a third neurone which is serotoninergic. A similar effect could be induced by adding serotonin (5-HT) to the culture medium. This modulation appears to be presynaptic, as 5-HT increases the breadth of spikes in the sensory neurone resulting in a consequential increase in transmitter release (Klein *et al.*, 1980).

These basic networks illustrate how simple cell interactions can give rise to patterned, modulated activity. The usefulness of a culture approach to investigate more complex network properties is limited only by the difficulty of isolating and culturing larger networks of identified neurones. Technical improvements are eagerly awaited.

Pairs of neurones have also been cultured to investigate the formation and function of synaptic "building blocks". The main advantages are the accessibility of synaptic sites, the elimination of other synaptic inputs that are not being investigated and the possibility of monitoring and manipulating synaptogenesis. Cultured leech neurones have played an important role in these studies (discussion of which is deferred until Section 1.6 after the leech nervous system has been introduced), as have cultured *Aplysia* and *Helisoma* neurones. Hadley *et al.* (1983) demonstrated that synchronised neurite outgrowth was required for the formation of a novel[3] electrical synapse between two identifiable *Helisoma* neurones (designated B5 and B19). In a separate study, Haydon (1988) juxtaposed the cell bodies of the same two cell types and found that novel chemical synapses, in which B19 was postsynaptic, formed reliably after 3 days in culture. When the neurones

---

[3]A "novel" synapse refers to one which is normally not seen *in vivo*. B5 will however form both chemical (Haydon, 1988) and electrical (Hadley & Kater, 1983) synapses with B19 *in vivo* on regeneration after axotomy, as they do in culture.

were maintained separately for 3 days and then juxtaposed, chemical synapses formed as early as 10 seconds following contact, indicating that continuous contact was not required for the development of a "transmitter release capability" in B5. A recent study has shown that B19, when acting presynaptically, may behave rather differently (Zoran *et al*, 1991). Unlike B5, no novel synapses have been reported with B19 as the presynaptic element. Further, action potential-induced release of transmitter only occurs after a long period of contact with the appropriate, postsynaptic cell (a cultured muscle fibre). Elevating the level of intracellular calcium in B19 enhanced transmitter release only if contact was made with the appropriate target. This again is in contrast to B5, in which elevated Ca^{2+} *always* enhances transmitter release. These results suggest that not only would there appear to be rules which govern the assembly of synaptic building blocks, but the rules restrict the possible synaptic combinations in a cell type dependent manner.

Each of these elegant experiments would be very difficult to perform *in vivo* where accessibility is reduced and the possible effects of many other factors would have to be accounted for. A large number of studies have made use of these advantages to tackle the properties of single neurones.

A cell culture approach seems particularly suited to determine the electrical properties of neurones. Experiments performed *in situ* indicate that a single recording from the cell body may provide a sufficient record of excitability for only a limited number of cell types (see Cohen & Wu, 1990). Optical recordings using Ca^{2+} sensitive dyes injected into cerebellar Purkinje cells have localised regions of the dendritic tree which have distinct calcium influxes during activity (Ross *et al*, 1990). In other neurones processing may occur in regions that operate in complete independence (Laurent & Burrows, 1990). A cell culture approach not only maximises the prospect of recording

the excitability of small processes, but also allows the experimenter to contemplate using methods capable of controlling neurite morphology (see Chapter 5). Balanced against these advantages is the possibility that isolating neurones seriously effects their electrophysiological properties (see Chapters 2 & 3).

The aim of this thesis was to investigate the electrophysiological and morphological properties of single isolated leech neurones, with a view to explore neuronal information processing in small cultured network, of controlled design using extracellular electrode arrays.

1.3. Introduction to the leech nervous system

The central nervous system (CNS) of the medicinal leech, *Hirudo medicinalis*, is located on the ventral side of the gut and is housed within a blood sinus. It consists of a chain of 32 ganglia which almost spans the entire length of the animal. The ganglia communicate by way of paired connectives and a smaller bundle (Faivre's nerve) that runs from one end of the chain to the other. A pair of nerve roots emerge from both sides of most ganglia, connecting the CNS with the periphery (Figure 1.3).

On anatomical grounds, an anterior grouping of four fused ganglia can be regarded as the brain, although there is also a specialised region at the other end of the chain where the last seven ganglia are fused. The 5th and 6th ganglia are also different, innervating the segments that contain the reproductive organs and each comprising over 700 neurones (Macagno, 1980). The remaining (mid-body) ganglia are virtually identical, each containing about 400 neurones.

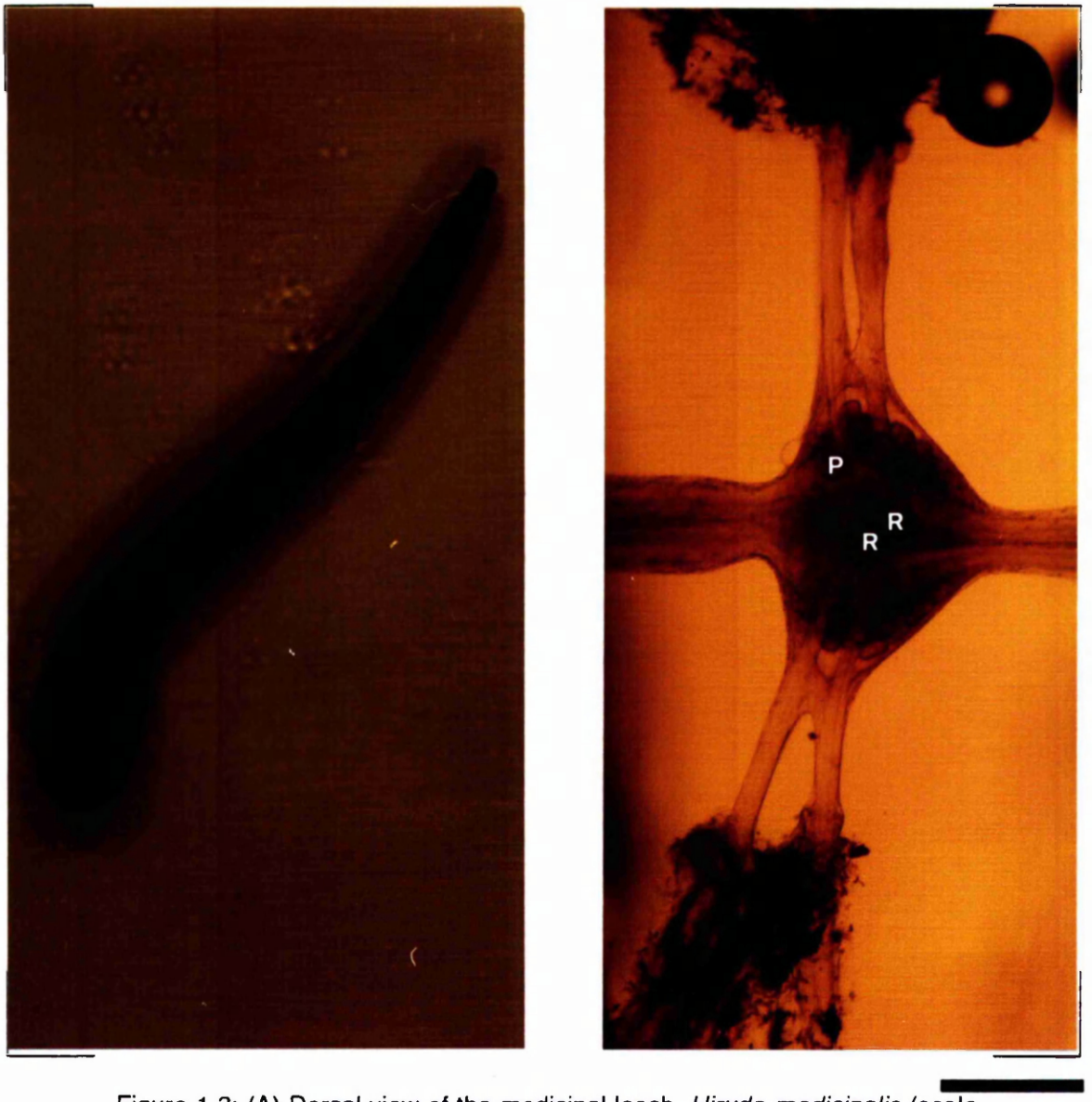

Figure 1.3: (A) Dorsal view of the medicinal leech, *Hirudo medicinalis* (scale bar: 1.6 cm), and (B) a ventral view of a single ganglion. The anterior half of the ganglion is to the right; Connectives are horizontal, nerve roots are vertical (scale bar: 400 µm). 'R' indicates a Retzius neurone, 'P' indicates a P cell.

The cell bodies of the neurones in each of the segmental ganglia are arranged into six packets, each enveloped by a single glial cell and located next to the outer wall (or capsule) of the ganglion. Two further glial cells are located centrally, encapsulating the labyrinth of processes that project from the surrounding neurones.

The margins of the packets can be used as landmarks along with the size of the cells to identify many of the neurones, from ganglion to ganglion, and from animal to animal. Other criteria can also be used, including the shape of the action potential and on intracellular dye injection, the morphology of the processes. The ability to locate the same cell from experiment to experiment, and the relatively small number of neurones in each ganglia, has led to a detailed structural and functional description of several central circuits (e.g. Lockery & Kristan, 1990). In many other systems, such a detailed study seems an impossibility.

1.4 The Retzius neurone

When viewed from the ventral side, the central packet of a mid-body segment ganglion is dominated by two large cells, the Retzius neurones (see Figure 1.3). Typically the neurones have a diameter of between 60-80 μm and originally were known as the "Kolossal" cells (Retzius, 1891). The ease with which Retzius neurones can be identified, allows theirs properties to be thoroughly investigated.

Retzius neurones fire spontaneously with overshooting action potentials recorded in the cell body (Nicholls & Baylor, 1968). These action potentials have an amplitude of around 50 mV and have durations of 2-5 ms (Kerkut *et al.*, 1967). There is now abundant evidence (e.g Kerkut *et al.*, 1967; Stuart *et al.*, 1974; Lent *et al.*, 1979) that the Retzius neurone contains serotonin, or 5-Hydroxytryptamine (5-HT), localised in dense-core vesicles (Yaksta-Sauerland and Coggeshall, 1973). The activity of cells in both the periphery and the central nervous system is affected by the experimental application of 5-HT (described below). It is assumed that these effects mimic the release of 5-HT by Retzius neurones, although there are at least 5 other

cells per ganglion that are also likely to contain 5-HT (Marsden & Kerkut, 1969).

In the periphery, application of 5-HT to body wall muscle causes an increase in Cl^- conductance, resulting in hyperpolarisation of muscle membrane (Walker *et al.*, 1968; Mason *et al.,* 1979). This has two effects: it causes a decrease in the longitudinal muscle tension and accelerates the rate of relaxation following contraction (Schain, 1961). Retzius neurones are the only 5-HT containing cell in any one ganglion to innervate the periphery of the same segment. (If other 5-HT containing cells do not innervate the periphery of *neighbouring* segments via the interganglionic connectives then the Retzius cell may well be the *only* 5-HT containing cell to innervate the periphery; Lent, 1981.) In addition, dense-core vesicles of the type seen in Retzius cells are present in terminals that are closely apposed to the body wall muscle cells (Yaksta-Sauerland and Coggeshall, 1973).

Taken together, this evidence implies a role as an inhibitory neurone. A study by Lent (1973) however, failed to correlate the activity of Retzius neurones with the occurrence of either inhibitory post synaptic potentials (ipsp's) or increased rates of relaxation of muscle in the body wall (Lent, 1973). These results conflict with a later study which showed that a volley of action potentials in a Retzius neurone can reduce tension and increase the rate of relaxation, but only 5-25 s after the onset of the burst (Mason *et al.*, 1979). The recovery time was also long, lasting up to 15 min. A slow ramping hyperpolarisation lasting many seconds with a long recovery period would be more difficult to detect than fast ipsp's, and therefore may have gone unnoticed by Lent (1973). With these time periods, the role of the Retzius cell on the muscle would best be described as neuromodulatory.

Not only do Retzius cells influence the state of muscles but they also

appear to cause the secretion of mucus from large unicellular glands in the body wall (Lent, 1973). Mucus release was assayed by adding carmine red to the medium bathing the body wall. After fifteen minutes the bathing solution was replaced and the mucus, which apparently adsorbs carmine red, was collected. The amount of carmine red absorbed was measured colorimetrically, and taken to be proportional to the amount of mucus released. Using this assay Lent (1973) claimed that the activity of Retzius neurones, or the direct application of 5-HT to the body wall, caused an increase in the amount of mucus released. Increasing the Mg^{2+} in the bathing medium eliminated the effect of activity in the Retzius cell but not the effect of directly applying 5-HT. This evidence implies that secretion is mediated by the Ca^{2+} dependent release of 5-HT from the nerve terminals of Retzius neurones located close to the mucus glands.The relationship between this neurosecretory function and the putative role as a muscle tone neuromodulator has not yet been clarified. Further clues to the function of the Retzius neurone come from the CNS studies described below.

A striking feature of a Retzius neurone's central connections, is the strong non-rectifying[4] electrical synapse made with the other Retzius neurone in the same ganglion (Hagiwara & Morita, 1962; Eckert , 1963). The degree of coupling varies from ganglion to ganglion, but is frequently sufficient to allow an action potential in one cell to initiate an action potential in its neighbour. This was one of the phenomena that led Eckert (1963) to put his head above the parapet and state that:

"*...[the] one-to-one transmission suggests that these [Retzius] cells may be concerned with bilateral coordination of an effector system having a rapid action*"

---

[4]Non rectifying electrical synapses allow current to flow equally in both directions.

A tight bilateral coordination of mucus secretion seems unnecessary whereas the bilateral coordination of body muscle could be achieved more rapidly by entraining motor neurones in the CNS. Indeed, a central circuit may well be the effector system that requires such strong, yet variable coupling.

Noxious stimuli (of either a pinch with forceps or salt) applied to the skin at the anterior end of the animal initiates a burst of action potentials in the Retzius neurones along the entire length of the CNS (Eckert, 1963). Mucus secretion may help a leech to escape from, or at least alleviate, the effects of such a stimuli. Swimming away would also be a good strategy. Interestingly, the level of 5-HT in the blood seems to be correlated with the likelihood of and time spent swimming. In addition, 5-HT perfusion greatly increases the likelihood of activating the swim motor program in the isolated nerve cord (Willard, 1981), an effect mirrored by the direct stimulation of a Retzius neurone. The cellular basis of this response may involve a large number of pathways leading to a general increase in the synaptic inputs onto the two interneurones (called 204 and 205) that initiate swimming. It would seem then, that the firing of Retzius neurones following noxious stimuli could be a primary step in eliciting an escape response, perhaps overriding other motor programs by modulating the activity of a large number of neurones through the non specific release of 5-HT.

The only central synapse in which the presynaptic element appears to be serotoninergic, having 50-60 nm granular vesicles and exhibiting glycoxylic acid-induced histofluorescence, is located within the connectives (Muller, 1981). Retzius neurones are known to have projections in the connectives (Mason & Leake, 1978) and may be the presynaptic cells, although Muller (1981) has issued the warning that the cell involved has not

yet been identified. However, the relevance of this connection to the function of Retzius cells remains: Retzius neurones are electrically coupled to all the other homoganglionic 5-HT-containing cells (Lent & Fraser, 1977). Therefore, if the Retzius cell is not the presynaptic cell it may be connected indirectly via another 5-HT containing cell. Since the post synaptic cell (called the S-cell) innervates cell 205 (capable of initiating and changing the phase of the swim program) it is likely that a multi-synaptic pathway between the Retzius cell and the swim initiating neurone does exist. Thus, the activity of Retzius cells may produce highly specific alterations to the motor program, as well as having the more general effect associated with the release of endogenous 5-HT.

The Retzius neurones would appear to be self modulating. Consider the following two observations. Firstly, the coupling between Retzius neurones decreases on application of 5-HT (and dopamine), apparently by directly reducing junctional conductance (Columbaioni & Brunellil, 1988). The second observation involves the spontaneous firing frequency of these cells which also decreases with 5-HT application (Kerkut *et al.*, 1967). *In situ*, both forms of negative feedback are likely to stabilise the activity of Retzius neurones, having the knock-on effect of controlling the amount of 5-HT released. The endogenous supply of 5-HT and the widespread, probably extrasynaptic, distribution of its receptor (Wallace, 1981) suggests that the electrical synapse may provide a mechanism of adjusting the *amount* of 5-HT released, rather than the distribution.

1.5 The P cell

The amplitude of the action potentials from the mechanosensory neurones that respond to touch (the T cells), pressure (the P cells) and

noxious stimuli (the N cells) applied to the body wall, are the largest to be found in the leech, being of at least 60 mV (Nicholls & Baylor, 1968). They overshoot by more than 15 mV, and the N and P cells have prominent undershoots. A further electrophysiological characteristic shared by these three cell types is the long-lasting hyperpolarisation that follows trains of impulses. An electrogenic Na^+/K^+ pump and a prolonged Ca^{2+} dependent increase in K^+ conductance have been implicated (Jansen & Nicholls, 1973). The three cells differ in their dependence on these two mechanisms, the hyperpolarisation in the P cells for example is a product of both components, whereas in the T cell the electrogenic pump alone is responsible. Although these properties could be used to identify the cells, in practise more discernible criteria are available. The P cells can be distinguished electrophysiologically from the other mechanosensory neurones, as they have larger and broader (4 ms compared to 2 ms) action potentials than the T cells, do not burst during sustained depolarisation like the T cells, show no signs of spontaneous activity and have smaller action potentials than the N cells (i.e. less than 100 mV).

There are four P cells in each segmental ganglion, two on either side, with both pairs located in the posterior half. The most lateral cell on either side innervates the dorsal body wall by way of the dorsal branch of the ipsilateral posterior nerve root. The medial P cells sends projections through both ipsilateral nerve roots innervating the ventral body wall. This innervation pattern has been confirmed electrophysiologically, each cell having a receptive field centred in a different quadrant with little overlap (Nicholls & Baylor, 1968).

As well as being stimulated by pressure applied to the skin, P cells receive inputs from other neurones. Serial sectioning techniques reveal that

at certain sites within the neuropil, the P cell appears postsynaptic (Muller & McMahan, 1976). In addition, the soma is also sensitive to neurotransmitters when applied by iontophoresis: acetylcholine and 5-HT depolarise the P cell whereas dopamine causes hyperpolarisation (Sargent *et al.*, 1977). Axosomatic contacts have been observed *in vivo* and synaptic interaction has been shown electrophysiologically, although no conventional synapses have been observed with the electron microscope (French & Muller, 1986).

P cells synapse onto a large number of neurones both within the ganglia in which they are located (see Lockery *et al.*, 1990) and in adjacent ganglia. Two connections that have received particular attention are the mixed electrical and chemical synaptic inputs onto L motor neurones which innervate the longitudinal musculature that mediates shortening (Nicholls and Purves, 1972) and onto AE motor neurones (responsible for causing erection of annuli). The synapses made by a single P cell onto these two motor neurones are distinct both in strength and dynamics. Thus, the synapse onto the AE neurone is weaker, but shows the strongest facilitation and unlike the synapse with the L neurone, reducing temperature does not cause depression. In addition, an AE cell may occasionally have small inhibitory potentials when a P cell is active (Muller & Nicholls, 1974).

By making use of the fact that P cells also innervate the AE and L neurones in neighbouring ganglia, the P cell has been used as a model to study the specificity of neuronal regeneration *in vivo*. If the axon of the P cell in the ipsilateral connective is severed, it will reinnervate the adjacent ganglion and there re-establish inputs onto the AE and L neurones. However, the amplitude of the inputs failed to return to the previous level (after 4 weeks) and occasionally, novel synaptic connections were formed with cells that are not usually innervated by the P cells (Jansen *et al.*, 1974).

1.6 Leech neurones in culture

Cultured leech neurones have been used in a variety of studies to investigate the properties of single neurones. The properties investigated include: the influence of substrate molecules in determining neurite outgrowth (e.g. Grumbacher-Reinert, 1989), intrinsic properties that influence morphology (Acklin & Nicholls, 1990), the characteristics of membrane channels (Stewart *et al.*, 1989), their distribution (Garcia *et al.*, 1989) and the distribution of receptors (Pellegrino & Simonneau, 1984). Another use of cultured leech neurones has been in the investigation of synaptogenesis.

1.6.1 Synaptic interactions between Leech neurones in culture

The type of synapse formed between two identified neurones depends on the type of cell used (Arechiga *et al.*, 1986). For example, Retzius neurones will form non-rectifying electrical synapses with other Retzius neurones, but not with P cells. P cells do not form electrical synapses with each other, but will make rectifying electrical synapses with Anterior Pagoda (AP) neurones (Davis, 1989). Similarly, a Retzius cell will chemically synapse onto a P cell *in vitro* but not vice versa. However P cells do form chemically synapse onto Retzius cells *in vivo* . P cells also fail to synapse onto L motor neurones in culture, whereas a strong chemical synapse occurs *in vivo.* The reason for these differences is likely to be a result of a complex interaction between cells. For example, isolated P cells do not lose the ability to form the presynaptic element of chemical synapses. This is demonstrated by a chemical component which is superimposed on the rectifying electrical synapse formed with an AP cell (Nicholls *et al.*, 1990). Synapses also occur in culture that are not seen *in vivo.* Thus, the Retzius cell forms strong electrical synapses with L and AE cells in culture but not *in situ* (Arechiga *et*

al., 1986).

The chemical synapse that forms between the Retzius neurone and the P cell in culture has been thoroughly investigated (e.g Henderson, 1983;. Drapeau & Sanchez-Armass, 1988; Drapeau *et al.*, 1989). Both cells have two types of receptors that respond to 5-HT. They function by increasing either Cl^- conductance causing hyperpolarisation or by a monovalent cation conductance giving rise to depolarisation (Drapeau & Sanchez-Armass, 1988). When a synapse is formed between a Retzius and a P cell, the Retzius neurone releases 5-HT and the P cell (but not the Retzius cell) loses the 5-HT dependent monovalent cation conductance. Surface contact is sufficient to induce this disappearance (Drapeau *et al.*, 1989). Taken together these observations suggest that surface contact, and not transmitter type, is the chief component in determining synaptic specificity (Nicholls *et al.*, 1990).

The importance of the site of synaptic interaction has also been investigated (Liu & Nicholls, 1989). The sequence of synapse formation is dependent on the configuration in which the cells are juxtaposed. Thus, electrical synapses precede the appearance of chemical synapses for both axon to axon and cell body to cell body pairs, whereas the opposite is true for stump to stump and stump to cell body configurations. A second effect which is dependent on the site of contact is the rate of synpase formation. Electrical synapses form between cell bodies only after a lag of a few days, whereas electrical synapses between the tips of axons occur after only a short delay of several hours indicating that the tips of the processes represent preferred sites for synapse formation (Liu & Nicholls, 1989). This conclusion is supported by studies of single isolated cells in which receptor concentration was charted, the highest values being located at the tips of the processes (Pellegrino & Simonneau, 1984). Electrophysiological data obtained using

extracellular electrode arrays (reported in Chapter 3) suggests that action potentials *in vitro* originate from this region, and the photographs presented in Chapters 2, 4 & 5 show that this region is also specialised in terms of its ability to generate new outgrowth.

1.7 The scope of this Thesis

This thesis considers the electrophysiological and morphological properties of single isolated leech neurones using both conventional techniques and microfabricated devices. The purpose of this study was to assess the prospect of using planar extracellular electrode arrays to investigate information processing in small cultured networks of identified neurones of controlled design. Specifically, Chapter 2 describes some of the electrophysiological properties of isolated Retzius neurones that can be determined from the cell body using intracellular electrodes. This is a necessary "first-step" before more complex properties can be fully investigation. The use of extracellular electrode arrays to determine the direction of propagation and the conduction velocity of cultured leech neurones is reported in Chapter 3. These properties are likely to be fundamental to the information processing of even the simplest of networks. Thus, the first half of this Thesis leads the way to the next electrophysiological step: that of recording from two or more identified neurones using extracellularly electrode arrays.

The use of extracellular electrode arrays to investigate information processing would be enhanced if the morphology of cultured networks could be controlled. One approach to this problem is to use properties of the substratum to guide regenerating processes. A better understanding of how the substratum influences morphology will no doubt lead to improved

methods of controlling the morphology of outgrowth *in vitro.* Thus, in Chapters 4 and 5 the effects of the substratum topography and the substratum coating (i.e. the substrate) on the morphology of single cultured neurones is examined.

CHAPTER TWO:

The isolation of leech neurones and the effects on electrical properties

SUMMARY: The conventional method of culturing leech neurones is described, along with two modifications which allow neurones to be extracted with very long processes. The modifications had no apparent effect on the morphology of new outgrowth generated by Retzius neurones cultured on Concanavalin A (see Chapter 4). Characteristic electrical properties were also preserved, as assessed by the shape of the action potential recorded intracellularly from the cell body. However, as a result of isolation, input resistance increases and an abnormal voltage response is observed during the application of hyperpolarising currents.

The average length constant of extracted processes was estimated from the specific membrane resistance (R_m) calculated from measurements made with intracellular electrodes. Two techniques were used. One derived R_m by used the average membrane time constant measured from cell bodies along with a value for the specific membrane capacitance. The other technique uses the assumption that input resistance decreases as surface area increases. R_m was determined by making a comparison between the input resistance and the surface area of cells with different lengths of process. Although the relationship between surface area and input resistance was found to be weak, the value determined for R_m is comparable to a previously published estimate.

1 Introduction

2.1.1 Methods of isolating leech neurones

The technique for isolating and culturing leech neurones has been steadily evolving for over 15 years. The removal of identified neurones was

first performed by Sargent (1977) in order to determine the activity of choline acetyltransferase in different cell types. Cells were isolated by using a loop of thin copper wire to lasso the initial axonal segment and pull the cell body free. This technique was used to good effect in the pioneering work of Ready and Nicholls (1979) who grew leech neurones in culture for the first time (nylon thread was used instead of copper wire). An enzyme treatment (using a mixture of collagenase and dispase) was later introduced by Dietzel *et al.* (1986) to reduce the mechanical force required to extract neurones. Others have used collagenase alone (e.g. Drapeau *et al.*, 1990). Enzymatically treated cells can be aspirated using a fire-polished pipette and have greater viability. Once a neurone has been extracted it is then transferred into medium containing 2% foetal calf serum (FCS), primarily to remove the encapsulating glia which would otherwise reduce adhesion during plating. Cells extracted by these methods can be voltage clamped more readily due to a large increase in input resistance, believed to be caused by the removal of processes during dissection (Dietzel *et al*, 1986). Cells extracted without processes have also been used to determine the structure of synapses which form between cultured neurones. With just the cell bodies juxtaposed, the number of serial sections required to locate synapses is greatly reduced (Henderson *et al*, 1983).

A further adaptation to the method which delivers neurones with longer processes has been reported. The enzyme treatment was facilitated by swirling, which probably improved the digestion of the connective tissue that holds the processes in place. Cells extracted by this method have been studied using the patch clamp technique to explore membrane channel distribution (Garcia *et al.*, 1989).

Here, the viability and outgrowth of Retzius neurones dissected using

collagenase/dispase was found to be highly variable (the method used was identical to that of Dietzel *et al*, 1986). Work was undertaken to reduce this variability, resulting in a modified enzymatic procedure for the extraction of leech neurones with very long processes (see Section 2.2.2).

2.1.2 Electrical properties of single isolated neurones

Balanced against the huge advantages of culturing neurones is the possibility that the properties of the cells are either irreversible altered by the extraction process, or undergo modification owing to the different environment. Most leech neurones retain their distinctive shaped action potentials when extracted using collagenase/dispase and grown in culture. Here, the modified enzyme treatment is assessed for an effect on the shape of the action potential of Retzius neurones. The rising phase was chosen as the criterion for analysis, as it is likely to be one of the most important components in dictating the conduction velocity of action potentials (measured for cultured neurones in Chapter 3).

Another set of parameters that can be measured from the cell body using intracellular microelectrodes are those that relate to passive electrical properties, namely the input resistance (R_N) and the membrane time constant (τ_m). Fuchs *et al.* (1981) have measured the input resistance of Retzius neurones before and after isolation. It was reported that immediately after isolation the normal input resistance of Retzius neurones (given as 22 MΩ *in vivo*) fell by more than 50% but soon recovered to over 70 MΩ. In their study, four neurones had an average input resistance of 129 MΩ after three days in culture. High input resistance was attributed to removing all the processes, and severing the electrical synapse that links a Retzius cell to its contralateral neighbour. However, these effects may be partly offset by the

removal of any closely associated glial membrane which would contribute to a higher input resistance *in vivo*. The possibility that isolation results in an increase in membrane resistance per unit area (R_m) was not ruled out (Fuchs *et al.*, 1981).

In order to facilitate the comparison with cells *in vitro*, measurements were made of the input resistance of cells in acutely dissected ganglia (from which the nerve roots and connectives had been removed). In the ensuing comparison, this should have minimised any error attributable to the length of the processes of the cells in dissected ganglia.

2.2 Material and Methods

The advances presented in this thesis come in part from the method of extracting cells with very long processes. This Section is highly detailed in order that the technique may be readily copied. See Figure 2.1 for a diagrammatical summary.

2.2.1 Dissecting the segmental Ganglia

Medicinal leeches, *Hirudo medicinalis*, were obtained from Biopharm (UK) Ltd. (Dyfed, UK) and Ricarimpex (Audenge, France), maintained in copper-free water at room temperature and fed when necessary on pig's blood[1].

Leeches were anaesthetised with 10% ethanol in copper-free water at 4°C for 10 min, before being washed in autoclaved leech Ringer (see

---

[1]The author would like to express immense gratitude to Scott Arkison, for cleaning and feeding the leeches

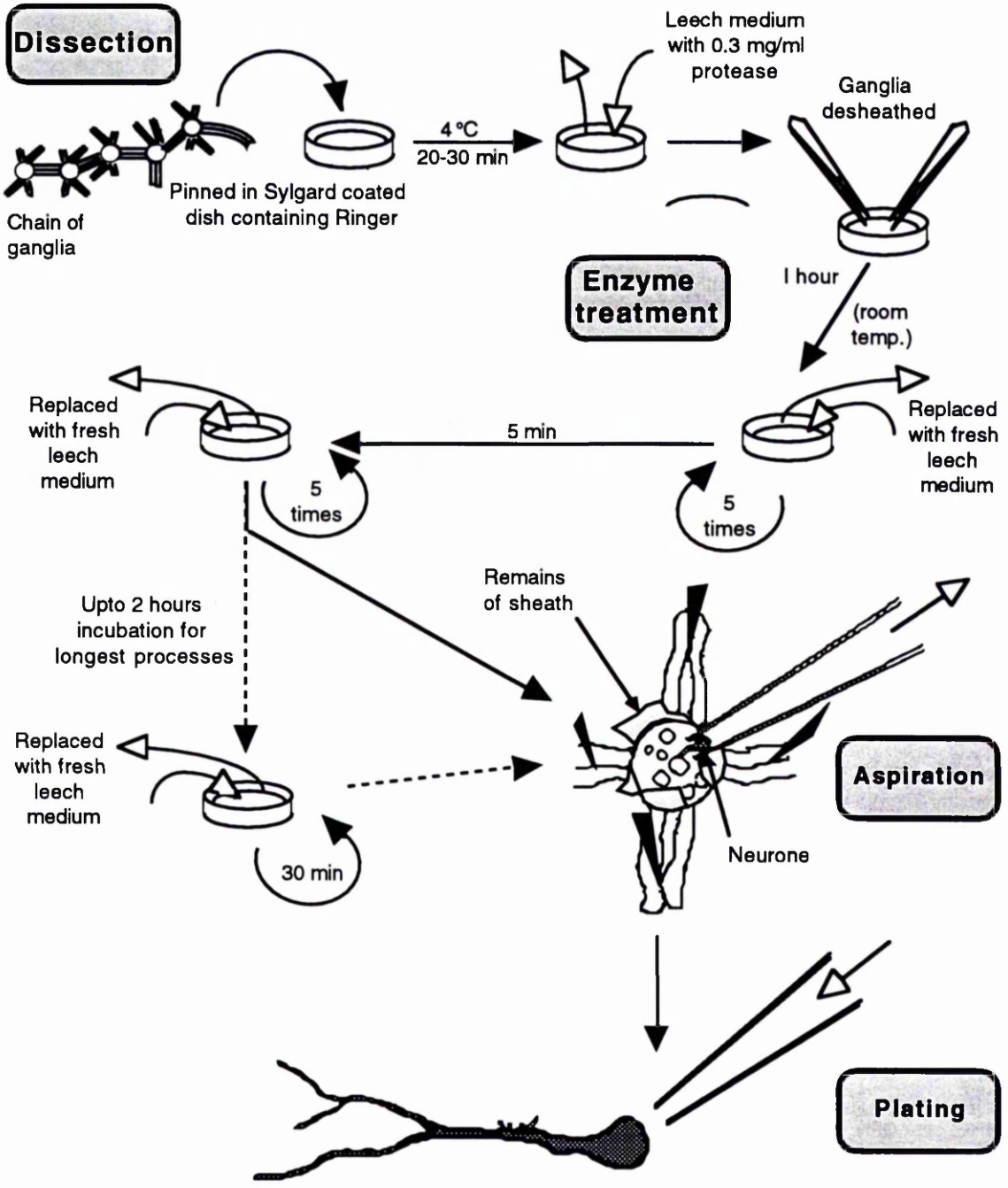

Figure 2.1: Summary of the method used to isolated leech neurones. See text for details.

Appendix 1). Leeches were pinned ventral side up, aseptically when necessary, in Ringer. A longitudinal incision exposed the chain of segmental

ganglia. The connective "stocking" surrounding the chain was cut longitudinally on the exposed ventral side with fine scissors (John Weiss & Son Ltd., London). The remaining stocking was chopped off on the anterior and posterior side of each ganglion (Figure 2.2). The body wall around the nerve roots was cut with a sharp scalpel, so that the chain could be removed with long lengths of nerve roots intact. The nerve roots were severed with the fine scissors, and the chain gently teased out and pinned in a 35 mm culture dish lined with Sylgard 180 (Dow Corning, Barry, UK), under Ringer. A similar procedure was used to obtain the acutely dissected ganglia,

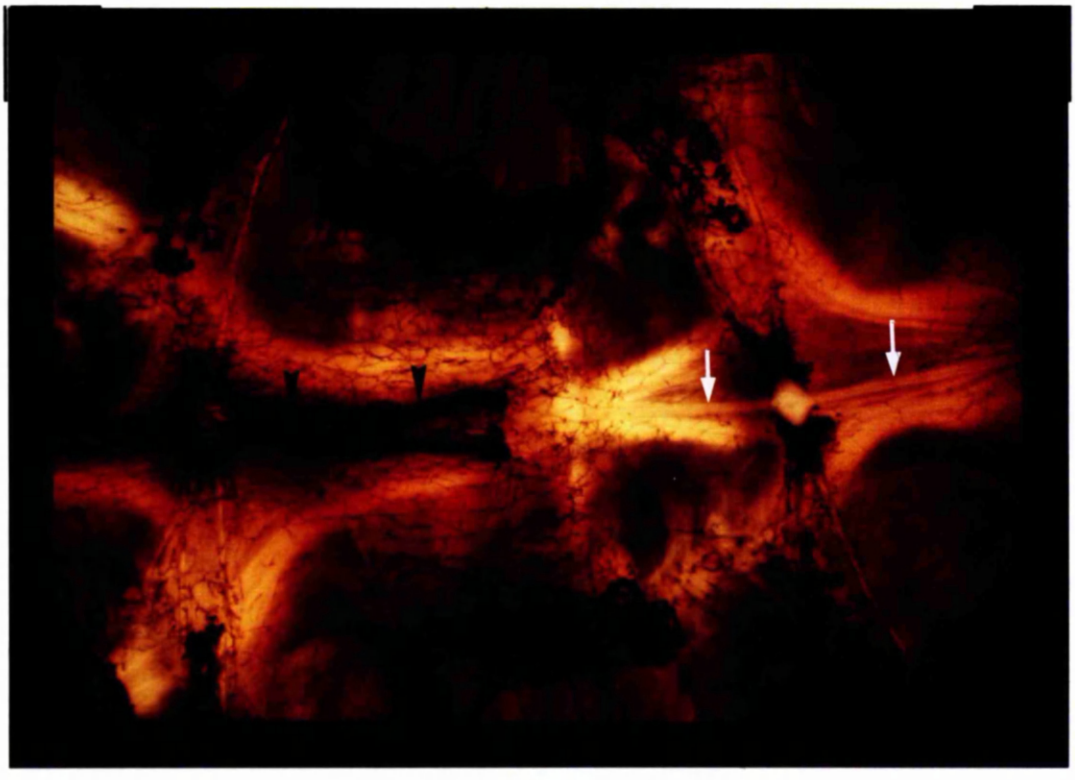

Figure 2.2: Photograph showing the initial steps of the dissection. The leech was pinned ventral side up. Following a longitudinal incision of the body wall, the nerve cord can be seen (running left to right and indicated by the arrows). The body wall was also cut laterally on either side of the nerve roots. To the right of the photograph, the connective tissue stocking was dissected from the ganglion and connectives (white tissue indicated by the white arrows).This was achieved by cutting the stocking longitudinally, and then laterally on either side of the ganglion. Scale bar: 1 mm)

except that individual ganglia were pinned through the shortest length of nerve root possible, and then trimmed of all the remaining nerve roots and connectives. Ganglia from the sex segments, identified by the small size of their Retzius neurones and the different packing arrangements, were not used (see Glover & Mason, 1986).

2.2.2 Enzyme treatment

Previously, 2 $mg.ml^{-1}$ of collagenase-dispase in leech medium (see Appendix 1 for constituents) was applied to each ganglionic chain for 1 h at room temperature (Dietzel *et al.*, 1986).

In a departure from traditional techniques the dish containing the ganglionic chain was left at 4°C for 20 to 30 min. On returning to room temperature, the ganglia looked slightly opaque in comparison to ganglia maintained at room temperature over the same period. The Ringer was replaced with sterile leech medium containing $^1/_3$ $mg.ml^{-1}$ of freshly made protease (type XXV; Sigma, UK) at room temperature. The capsules (indicated by the arrows in Figure 2.3) were opened with sharpened No. 5 forceps, and after one hour the enzyme-containing medium was carefully replaced by leech medium. As no FCS was used until after the first signs of outgrowth the ganglia require extensive washing with leech medium. 5 changes of medium followed by a 5 min soak and a further 5 changes was considered to be the minimal regime. Cells removed at this stage were the most viable and had long processes. However, if really long processes (up to 1 mm; see Figure 2.7) were required, extraction was delayed for up to two hours, with the medium replaced every 30 min.

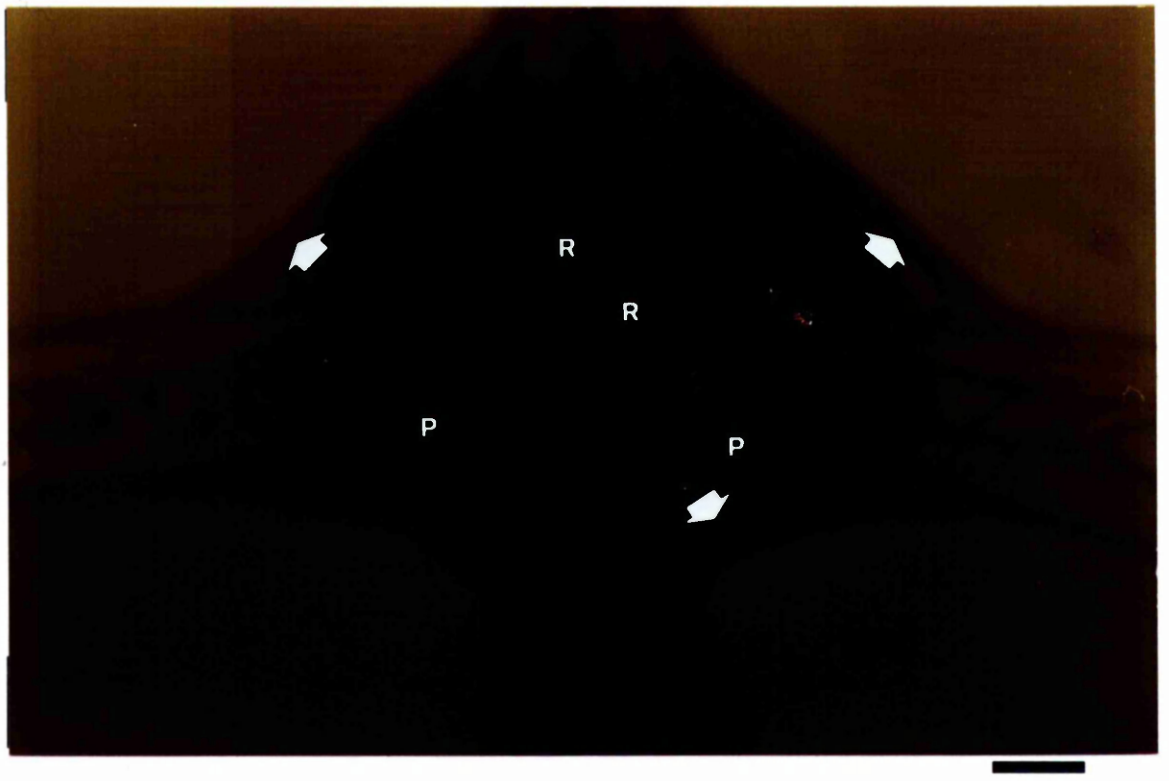

Figure 2.3: High power view of the ventral side of a leech ganglion showing the capsule (indicated by the arrows) which encases the ganglion. Anterior side is up (scale bar: 70 μm). 'R' and 'P' indicate Retzius and P cell respectively.

2.2.3 Aspiration

Suction pipettes were prepared from glass microelectrodes pulled from 1.2 mm capillary tubing (Clark Electromedical Instuments, UK). The tip of the microelectrode was broken off on one of the pins that restrain the ganglia so as to produce an orifice which was slightly larger than the diameter of the cell to be removed. The tip of the pipette was then fire polished by rapidly passing it through a flame. The other end was inserted into a length of P.V.C. tubing (internal diameter 0.8 mm; Altec, Hampshire, England). Medium was sucked by mouth into the pipette (via the tube), and then the tip was positioned over the desired cell. The cell body was sucked in and the pipette withdrawn, applying slight leverage on the process. As the process emerged, the cell body was sucked further into the pipette and more

leverage was applied. The procedure was repeated until the process snapped.

2.2.4 Plating

Occasionally during aspiration the glial fragments that surround the neurones could be seen to slide off, in which case the neurone was plated immediately. More usually the glial debris remained, giving an opaque appearance to the neurone. These cells were left for two to three minutes on the non-adhesive Sylgard floor of the dissecting dish. After very gentle trituration (during which very long processes are at high risk) the glial debris falls away. Cells were transfered to the culture dish, or to an electrode array (Chapter 3), and positioned in the desired location by gentle currents generated by applying positive or negative pressure through the pipette.

2.2.5 Concanavalin A coating

Substrates were coated with Concanavalin A (Type IV; Sigma, UK) by incubating in a solution containing 1 $mg.ml^{-1}$ in double distilled water. (Occasionally, a 2 $mg.ml^{-1}$ solution was used, but no consistent difference in adhesion, survival or outgrowth morphology was observed). The substrates were then sterilised by washing in 70% ethanol, and then rinsed thoroughly with sterile double distilled water. A final rinse with leech medium completed the coating procedure.

2.2.6 Electrophysiology

To determine the effects of isolation on the shape of action potentials, it was first necessary to determine the relationship between the shape of action potentials and temperature in dissected ganglia. Ganglia were pinned in a dish under leech medium and cooled to 4°C in a refrigerator. On returning to room temperature, the temperature of the medium rapidly

increased. To reduce the rate of increase a reservoir of liquid nitrogen was placed under the glass stage on which the dish was placed during impalement. A thermocouple connected to a digital display (Jenway, Essex, UK) was used to assess the temperature of the medium which was allowed to increase at an average rate of about 1.5°C every 5 min.

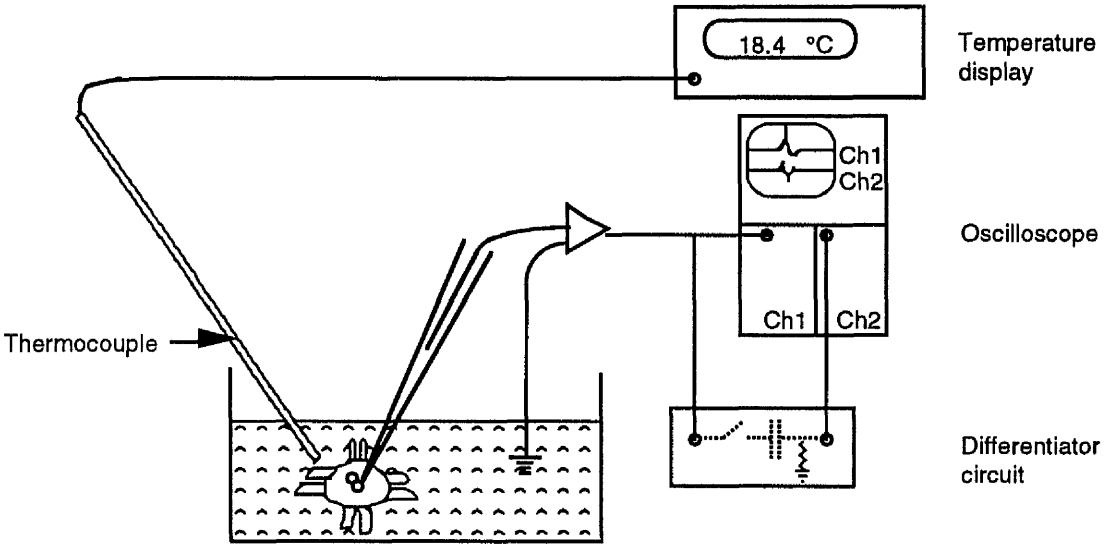

Figure 2.4: Recording arrangement to assess the effects of temperature on the shape of action potentials. A ganglion was impaled by a single microelectrode whilst a thermocouple monitored the temperature. Action potentials and their differentials were displayed simultaneously on the screen of an oscilloscope.

The recording arrangement is illustrated in Figure 2.4. Glass microelectrodes were pulled from 1.2 mm capillary tubing (GC120 TF; Clark Electro-medical Instruments, UK) and filled with 3M KCl to give electrodes which had impedances of 15-20 MΩ. Recordings were made via a Neurolog DC amplifier (Digitimer, UK), the output of which was displayed directly on to a two channel oscilloscope. The differential of the signal (produced by a simple circuit consisting of a capacitor and a resistor) was displayed on the second channel.

The input resistances of neurones were measured using the

technique described by Fuchs *et al.* (1981). This technique also provided the information required to calculate the membrane time constant, allowing the specific membrane resistance to be estimated.

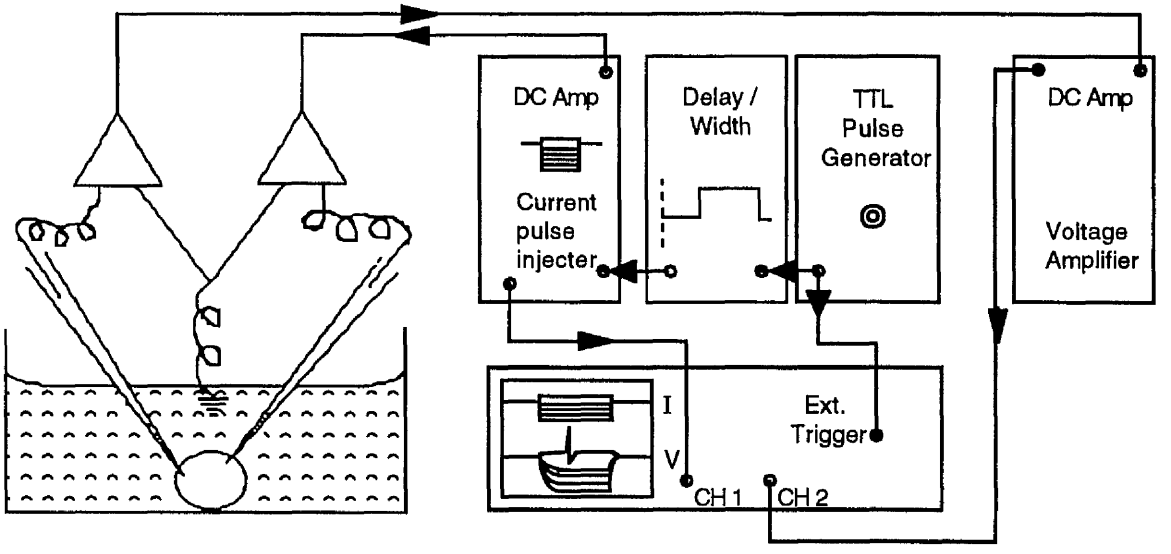

Figure 2.5: Recording setup for measuring the input resistance of neurones using two intracellular electrodes. The electrode on the right of the diagram was used to inject current pulses 400 to 500 ms in duration. The electrode on the left was used to inject a constant current sufficient to hold the resting potential at -50 mV, and to record the membrane potential.

Each cell was impaled with two electrodes simultaneously. Both electrodes were connected to Neurolog DC amplifiers (Digitimer Ltd., UK): one electrode was used solely to inject current pulses, the other was used firstly to record the resulting changes in membrane potential and secondly, to inject a steady hyperpolarising current capable of holding the resting potential at -50 mV. A TTL pulse was used to trigger a 511A storage oscilloscope (Tektronix, Heerenveen, The Netherlands) and a Neurolog delay-width generator. The delay-width generator controlled the delay and the length of the current pulse injected by the DC amplifier. Figure 2.5 shows the recording setup. The magnitude of the injected current pulse and the resulting changes in membrane potential were measured from Polaroid

photographs of the oscilloscope screen.

2.2.7 Measuring a cell's input resistance (R_N) and the membrane time constant (τ_m)

Changes in membrane potential were plotted against the size of the injected current. The total cellular input resistance (R_N) was taken as the tangent to the curve as it passed through the origin. Thus, R_N is determined by the smallest of the membrane potential responses.

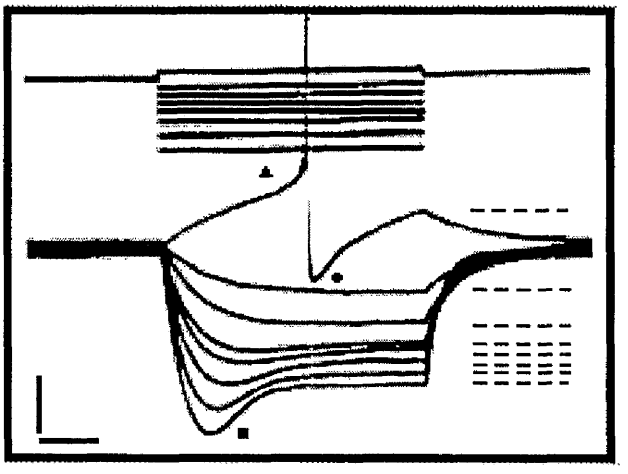

Figure 2.6 Recording of a Retzius neurone in culture to show how voltage measurements were made. The picture consists of 8 superimposed sweeps (horizontal bar: 100 ms). Each sweep consists of a record of the current injected into the cell (upper set; vertical scale bar: 1 nA) and the effect on the membrane potential (lower set; vertical bar: 10 mV). The resting potential of the membrane was held at -50 mV, by the injection of a constant hyperpolarising current through the voltage recording electrode. The current step was applied through a second electrode. Large current steps usually caused a *negative-going transient* (a short-lived increase in the level of hyperpolarisation illustrated by the solid square). These transients last for about 200 ms and are followed by a steady level of polarisation (indicated by the dashed lines). Note that the smallest two responses to hyperpolarising current steps do not show the transient. The filled triangle and the filled circle indicate the foot and the undershoot of the action potential respectively.

Frequently, during the first 200 ms of a large hyperpolarising current injection, the membrane potentials become highly polarised before settling at a less polarised level (as illustrated in Figure 2.6). The smallest membrane potential responses are immune from these *negative-going*

transients, and so the calculation of R_N is unaffected.

A different plot was used to calculate the membrane time constant (τ_m). The photographs of the oscilloscope screen were enlarged by 230%. The gradient of the tangent to the voltage trace (dV/dt) that peaks nearest to -65 mV was evaluated at different times (t) after the onset of the current step as described by Rall (1960). Membrane hyperpolarisations in the region of -65 mV do not display the type of transient that sometimes occur at more hyperpolarised levels (see Figure 2.6)

If a neurone consists of just a soma (without any processes), its passive electrical properties can be approximated to those of a sphere. According to this model, current injected into the soma would charge the *whole* surface area evenly as the internal resistance of the cytoplasm is much lower than the resistance of the membrane. The time course of the change in membrane voltage at any one location (in response to a current onset) depends on the membrane properties at that location (assuming the properties are constant over the entire surface area). Thus ln(dV/dt) when plotted against t is expected to yield a straight line, indicating that the change in membrane potential can be equated to a simple exponential (Rall, 1960; Gorman & Mirolli, 1972). The negative reciprocal of this gradient gives the membrane time constant, τ_m.

When a neurone has a more complex morphology, additional exponential components come into play. Consider a neurone which has a cell body and a single process. During a sustained current injection the cell body is isopotential (if charge is still spread evenly over its surface). The process however, has a significant longitudinal resistance owing to its small diameter. This creates an internal longitudinal potential gradient which is dependent on both the membrane resistance of the process and the

axoplasmic resistance. This gradient is constant when the level of injected current is constant. However, immediately after the onset of a current step the gradient is much steeper owing to the time taken for the passive spread of current along the process. When the gradient is steep, the process acts as a strong sink to the charge that is spread evenly over the surface of the cell body. As the current spreads down the process, the gradient is reduced, and the sink becomes weaker. Thus, the change in membrane potential recorded from the cell body, is dependent not only on the membrane properties of the cell body, but also on the dynamics of the longitudinal potential gradient. This can be expressed as a series of exponentials (Rall, 1969). If ln(dV/dt) is plotted against t, the effect of the additional exponentials is particularly apparent immediately after the current onset when t is small and when the magnitude of the longitudinal potential gradient is greatest. The later part of the curve is least affected and can still provide a reasonable estimate of τ_m. When processes make a significant contribution to the electrical properties of the cell body, a better estimate results when a compensatory factor ($\sqrt{t}$) is introduced (Rall, 1960). Accordingly, for each cell the function:

$$\ln\left(\frac{dV}{dt}\cdot\sqrt{t}\right) \qquad (2.2)$$

was plotted against t. A best fit line was drawn through all but the first few points, and the negative reciprocal of its gradient was taken as τ_m. A similar procedure was performed for each cell using ln(dV/dt) generating a different set of τ_m's. A third set was also considered, in which the two previous sets were combined according to the length of processes of each cell.

2.2.8 Measuring the cell surface area

Photographs were taken of each neurone and of a stage micrometer using the same optics. The negatives were then used to project images at high magnification, from which measurements were made. The diameter of the cell body was taken to be the average of the parallel and perpendicular diameters (relative to the initial process). The apex of an arc, determined by the curvature of the cell body, was drawn across the image of each stump and used to define the start point of the initial process. The initial process was modelled as a cone that tapered to the beginning of the primary process. The distinction between these two components was occasionally vague, but for most cells was highly distinctive, warranting the joint inclusion of these two parameters. The primary process reaches as far as the major branch point, followed by secondary processes. The diameters of processes that followed the initial segment were treated as uniform along their length. Appendix 2 gives a diagrammatical account of the dimensions measured and includes the equations used to approximate the total surface area.

2.2.9 Estimating the specific membrane resistance (R_m) and the length constant (λ).

Given the dimensions of a cell, the input resistance (R_N) and the time constant (τ_m), the specific membrane resistance per unit area (R_m) can be estimated. Two methods were used. Both treat R_m as being uniform over the entire cell, and both require that the leak caused by the electrode (G_{shunt}) is negligible. One makes use of τ_m and assumes a value for the specific membrane capacitance (C_m), which was taken to be 1μF/cm^2 (Hille, 1984). R_m can then be determined by the relationship:

$$R_m = \frac{\tau_m}{C_m} \qquad (2.2)$$

The other approach is based on the assumption that input resistance decreases as surface area increases. According to this assumption, R_m can be calculated from Equation 2.3. The cellular dimensions were measured and used to plot the reciprocal of surface area against the input resistance. The gradient of the (best fit) line represents (an approximation to) the specific membrane resistance:

$$R_m = \left(\frac{R_N}{\left(\frac{1}{Area}\right)}\right) = \frac{\Omega}{\left(\frac{1}{cm^2}\right)} = \Omega.cm^2 \qquad (2.3)$$

The accuracy of this second approach is likely to be dominated by two factors. One is the discrepancy between the calculated surface area and the actual area of membrane. The other is the length of intervening process that is required to make a patch of membrane electrically distant from the cell body. This factor leads to the prediction that the best estimate can be achieved by comparing plots in which the area of the cell body is lumped to that of different proportions of the process. The use of this prediction is discussed below.

An estimate of R_m, together with a value for the diameter (d) of a process and the longitudinal axoplamic resistance (R_i, assumed to be similar to other invertebrates (Hodgkin & Rushton, 1946) and assigned a value of 100 Ω.cm,) allows an approximation of the length constant (λ), since:

$$\lambda = \sqrt{\frac{d}{4} \cdot \frac{Rm}{Ri}} \qquad (2.4)$$

2.3 Results

2.3.1 The morphology of isolated Retzius neurones

Retzius neurones extracted with protease had long, bifurcated processes which occasionally exceeded a millimetre in length (see Figure 2.7).

Figure 2.7: Photograph of Retzius neurone extracted using the new protocol described in Sections 2.2.1-2.2.3. The cell was fixed in 2.5% glutaraldehyde immediately after plating, and stained with kenacid blue. Arrow indicates unshed glial debris. Scale bar: 80 μm.

Fine processes which emerge from the primary process were present on about half the cells extracted. These were highly adherent to the Con A-coated surface of the tissue culture dish, but sometimes degenerated within the first 12 h. Similar processes, branching from the primary processes of sensory neurones and innervating the neuropil, have been observed *in vivo* (Muller & McMahan, 1976). It seems likely that these processes would have been rich in synaptic sites.

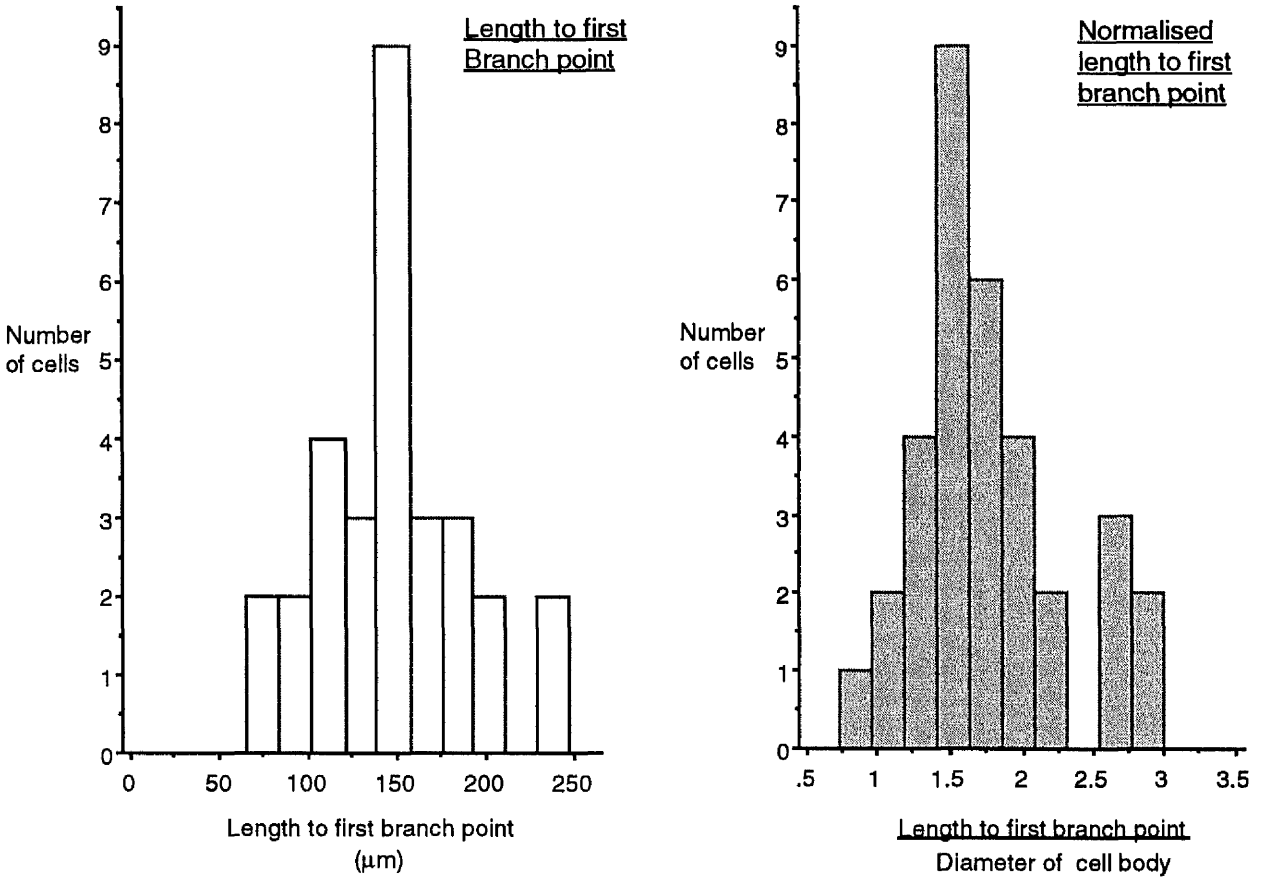

Figure 2.8: Variability in the distance between the cell body and the first branch point (n=30). Left: Histograms showing that the length between the cell body and the first branch point varies by more than 220 µm. Right: length to the first branch point corrected for differences in the size of cells (by dividing by the diameter of the cell body giving normalised units).

It became clear that the distance between the cell body and the bifurcation varied. The average length of the process between the cell body and the bifurcation of 30 neurones taken from different animals was 147 µm, with a standard deviation of 40.5. A histogram of this sample can be seen on the left hand side of Figure 2.8. It would seem that the length varied evenly about the mean. However, when the lengths were normalised with the diameter of the cell body the variability persisted and the distribution appeared to be multimodal. Since the normalisation procedure should reduce the variability that results from differences in the size of animals,

these results suggest that either different branch points from cell to cell were used for measurements or alternatively Retzius neurones can be classified into two populations according to morphology. The latter explanation is favoured because of the difficulty of mistaking the major bifurcation from subsequent branch points.

A second equally intriguing observation was that the cell bodies were sometimes non-spherical, having a large bulb (e.g. see arrows in Figure 4.4d & e). The extent to which these two observations reflect true variability in Retzius neurones, as opposed to being artifacts from stretch and deformation resulting from aspiration, is discussed below.

2.3.2 The shape of action potentials in culture and in ganglia

The shapes of action potentials of most isolated Retzius neurones were virtually identical to those of Retzius neurones in dissected ganglia (with a few exceptions; see below) judged by the presence of an overshoot and the shape of the undershoot (e.g. compare Figure 2.11 with Figure 2.13). Here, particular concern was centred on the rise time of the action potential, as this dimension is likely to be the most important in determining the rate of action potential propagation. As the rise time (and the rate of propagation) of action potentials in other preparations varies according to temperature (e.g. Hodgkin & Katz, 1949), a temperature calibration curve was required. Thus, the half-width of the differential, which was used as an index of action potential rise time, was plotted against temperature for cells in dissected ganglia (Figure 2.9). The resulting curve shows that the half-width decays exponentially with temperature, levelling off at very high temperatures. Eight out of a sample of nine Retzius neurones isolated with long processes had action potentials in which the half-width of the differential (a

measurement equivalent to the total rise time) fell within the standard error of the value found for cells in dissected ganglia at the same temperature.

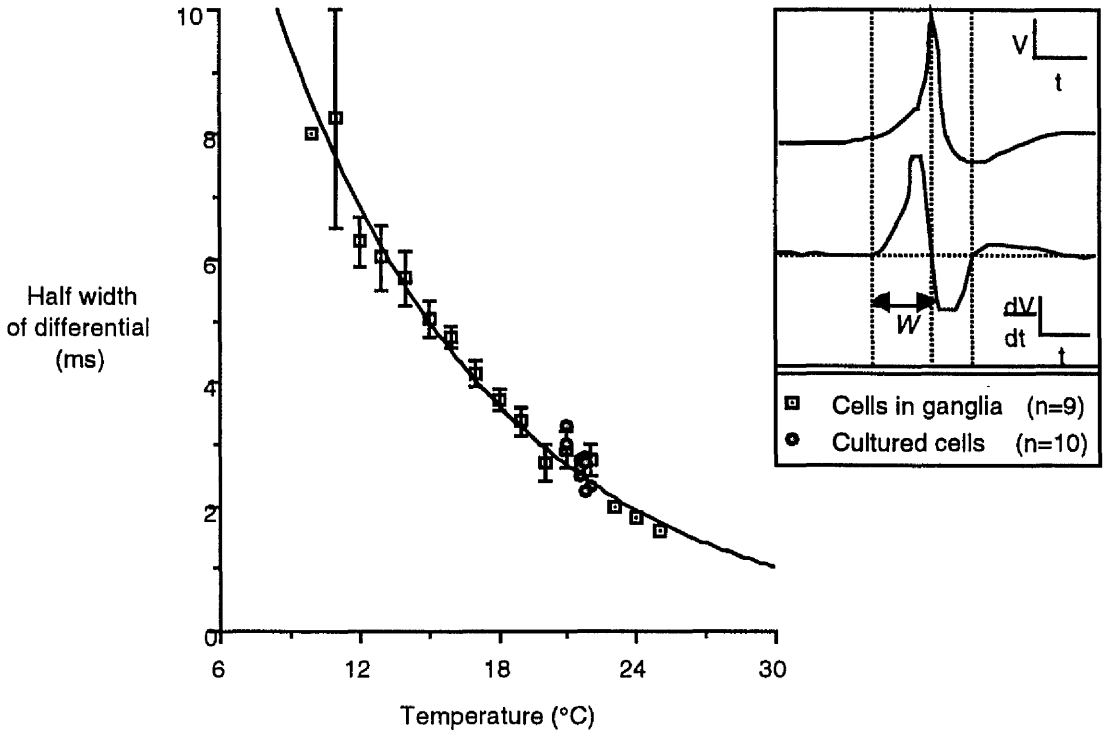

Figure 2.9: A comparison between the shape of Retzius neurone action potentials in acutely dissected ganglia and 1 h after isolation. The graph shows the pooled data of the half-width of the differential (*W*; see inlay) from 9 cells in acutely dissected ganglia at different temperatures (squares with dots). The curve can be compared with the single measurements from 9 cells, 1 hour after isolation, at room temperature (between 21 and 22°C; filled circles). Bars indicate standard errors.

A Retzius neurone extracted with a very short process (and not included in the above analysis) fired a burst of action potentials during depolarisation that differed from those normally seen in dissected ganglia. A photograph of this cells can be seen in Figure 2.10. The first action potential had an amplitude of a mere 30 mV. The second action potential began before the membrane potential had fully recovered and as the burst proceeded, the height of the action potentials decreased. How the length of the process may effect the pattern of activity is discussed in Section 2.4.2.

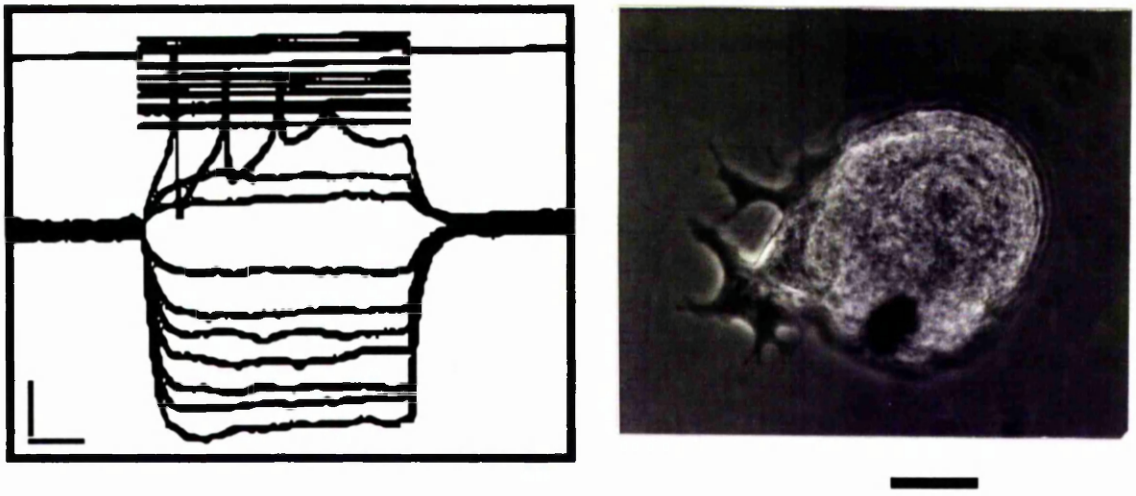

Figure 2.10: Shape of action potentials of a Retzius neurone with a very short stump 1-2 h after isolation. Left: current injected (upper set; vertical scale bar 1 nA) and correspond voltage response (lower set; vertical scale bar: 10 mV). Horizontal scale bar: 100 ms. Right: photograph of the cell using phase-contrast. Note the rapid outgrowth. Scale bar: 25 µm.

2.3.3 The current-voltage relationship of Retzius neurones in acutely dissected ganglia

A bridge balance circuit is required when the same electrode is used to inject current and record the resulting change in membrane potential. This circuit corrects for the additional voltage that results from the current across the tip resistance. Although this is a standard technique (Fein, 1966), it has both theoretical (Jack *et al.*, 1975) and practical difficulties. An alternative solution, which was used by Fuchs *et al.* (1981) and adopted here, is to use two electrodes simultaneously in the same cell: one electrode to inject current and the other to record changes in the membrane potential.

Using two electrodes has the advantage that a constant current can be injected through the recording electrode to hold the resting potential of the cell at a certain level. Cells were held with a resting potential of -50 mV. However, a disadvantage of this technique is the additional damage that

may occur during a second impalement. Indeed, occasionally a 5 mV depolarisation was observed with the first electrode, during the second impalement. The trace from the second electrode did not reveal this change. Within a few minutes the membrane usually returned to its previous resting potential, otherwise the data from the cell was not used. Other criteria adopted for a clean impalement were the the magnitude of the resting potential, which had to be greater than -35 mV, and the size and shape of action potentials. (One exception was made for a recording discussed in Section 2.4.2.) A recording from a Retzius neurone which typifies the standard required can be seen in Figure 2.6.

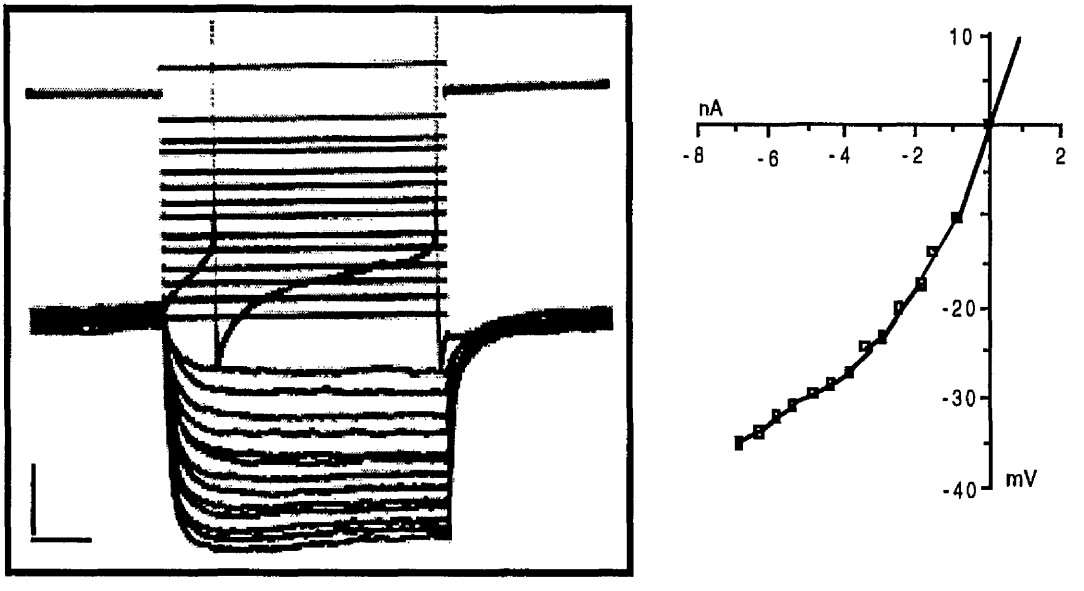

Figure 2.11: Recording and corresponding IV curve of a cell in an acutely dissected ganglion. Left, superimposed sweeps (horizontal bar: 100 ms) during current injection (top set; vertical bar: 2 nA) and the resulting effect on the membrane potential (bottom set; vertical bar:10 mV). Right, the resulting current voltage plot. The ordinate represents deviation from the holding potential of -50 mV. Input resistance was taken as the gradient of the straight line portion that passes through zero.

The recording shown in Figure 2.11 is from a Retzius neurone in an acutely dissected ganglion. Unlike the recording of the Retzius cell *in vitro*, illustrated in Figure 2.6, the recordings are not dominated by the negative-going *transient* that occurs during large hyperpolarising current injections. Within the first 200 ms of current injection, the amplitude of the largest hyperpolarisation reaches a maxima which is followed by a slightly less negative steady level. The difference between the maximum and the steady level is less than 2.5 mV. 3 out of a further 6 Retzius neurones, investigated in acutely dissected ganglia (n=7), gave similar results.

The Retzius neurone recorded in Figure 2.11 had an input resistance of 12.7 MΩ. The 7 Retzius neurones investigated in acutely dissected

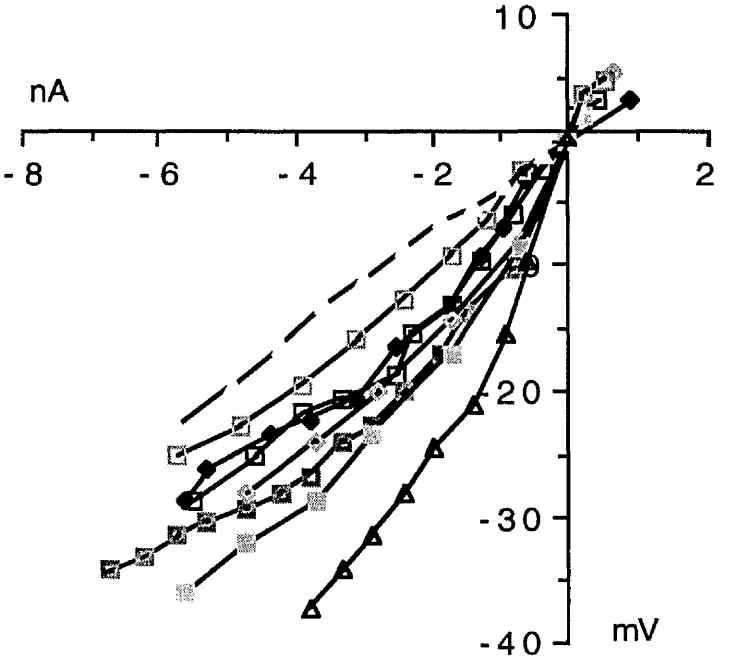

Figure 2.12: Current-voltage plots for Retzius cells in acutely dissected ganglia (n=7). The ordinate represents deviation from the holding potential of -50 mV. Note that in several cases the effect of current injection begins to diminish when the level of membrane hyperpolarisation exceeds -70 mV.

ganglia had an average input resistance of 12.29 MΩ (S.E.M.±1.15)[2].

The current-voltage plot in Figure 2.11 shows that as the level of hyperpolarising current increases, the effect on membrane potential is reduced. Thus, the input resistance decreases as the polarisation of the membrane increases. Most of the cells had a similar non-linear current-voltage relationship (as can be seen from individual plots in Figure 2.12). This property is known as inward-going rectification.

2.3.4 The current-voltage relationship of isolated Retzius neurones

The voltage recordings following the onset of large hyperpolarising current pulses are dominated by a negative-going transient. 13 out of the 15 Retzius neurones, studied 1 h after isolation, exhibited this property. One of the two not to show the property 1 h after isolation, did so when re-impaled after 12 hours. The difference between the peak hyperpolarisation and the steady level was much larger than for cells in acutely dissected ganglia, ranging up to 6 mV. Transients became apparent when the steady state level of membrane polarisation reached an average value of -79 (S.D.±5) mV, 1 h after isolation (n=13).

Input resistance after plating

The average input resistance of the 15 cells 1 to 2 h after plating was 35.3 MΩ (S.E.M ±3.1). A recording and the corresponding IV curve of a representative cell can be seen in Figure 2.13. This cell had an input

---

[2]S.E.M.: Standard Error of the Mean- used to determine the accuracy of the sample mean (i.e of a statistic) as an estimate of the population mean, rather than the inherent variability of the population as a whole (Colquhoun, 1971).

resistance of 31.6 MΩ 1 h after isolation. As with cells in acutely dissected ganglia, as the magnitude of the injected current increases, the relative effect on the steady level membrane potential decreases. The individual IV curves of several isolated cells can be seen in Figure 2.14(A). The majority of cells show this non-linearity. Figure 2.14(B) shows a comparison between the input resistances of isolated cells (n=15) with that of the 7 cells studied in acutely dissected ganglia.

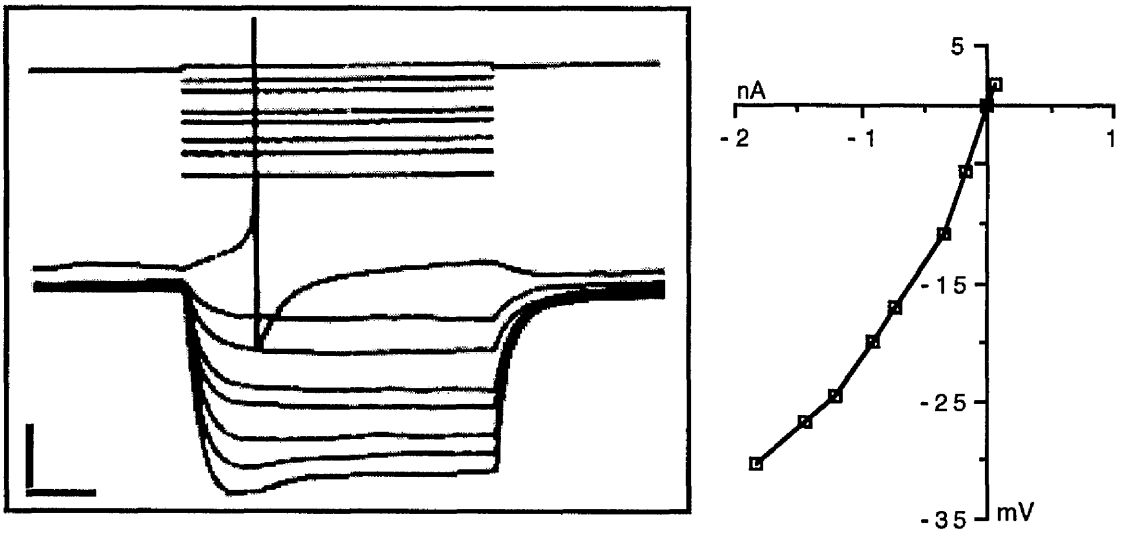

Figure 2.13: Recording and a plot of the corresponding current-voltage relationship of a Retzius neurone, one hour after isolation. Left, super imposed sweeps (horizontal bar: 100 ms) during current injection (top set; vertical bar: 1 nA) and the resulting effect on the membrane potential (bottom set; vertical bar:10 mV). Note the prominent negative-going transient in the lower two sweeps. Right, the resulting current voltage plot. The ordinate represents deviation from the holding potential of -50 mV. Input resistance was taken as the gradient of the straight line portion that passes through zero.

Change in input resistance with time in culture

A previous study (Fuchs *et al.*,1981) reported that the mean input resistance of isolated neurones continues to rise over a period of days, reaching 129 MΩ (S.E.M ± 36; n=4) after 3 days. Here, the input resistances

measured from six cells impaled 1 and 12 h following isolation show no clear trend. This is demanding work as it requires repeated impalements of the same cell. As measuring high input resistances becomes increasingly dependent on the quality of the impalement (a poor impalement giving lower input resistance) the possibility of artifact can not be ruled out. However, both the size of the trend reported by Fuchs et al. (1981) and the quality of the impalements obtained here would argue that other factors are involved.

An isolated Retzius neurone with a relatively short stump had an input resistance of 65.4 MΩ, 54.6 MΩ and 12.9 MΩ after 1, 12 and 24 h respectively (Figure 2.15). Other cells with longer stumps than the cell shown in Figure 2.15, had lower input resistances but again showed no trend towards increasing values with time. Out of seven cells examined, four showed a slight decrease in input resistance with time, one was unchanged and the remaining two showed a slight increase.

One possible explanation as to why cells did not show an increase in input resistance with time in culture might be that the cells reported here suffered long term physiological damage from previous impalements. Three observations weaken this hypothesis. Firstly, the resting potential of the neurone pictured in Figure 2.15 remained healthy, ranging between -42 and -48 mV. Secondly, the magnitude and form of outgrowth was equivalent to non-impaled cells (compare with the neurone in Figure 2.16) and thirdly, a low input resistance of 17.1 MΩ was measured in a cell which was first impaled after $3^1/_2$ days (86 h; see Figure 2.16). This cell also appeared healthy as it had produced extensive outgrowth, had a high resting potential (-40 mV) and fired with the characteristic action potentials of healthy Retzius neurones. If the input resistance of Retzius neurones does increase with time in culture, this cell might be expected to have had a much larger input resistance.

(A)

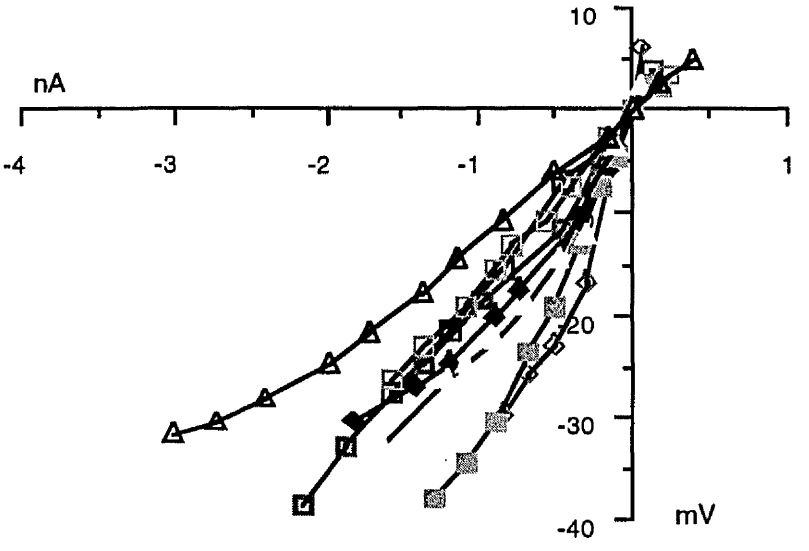

(B)

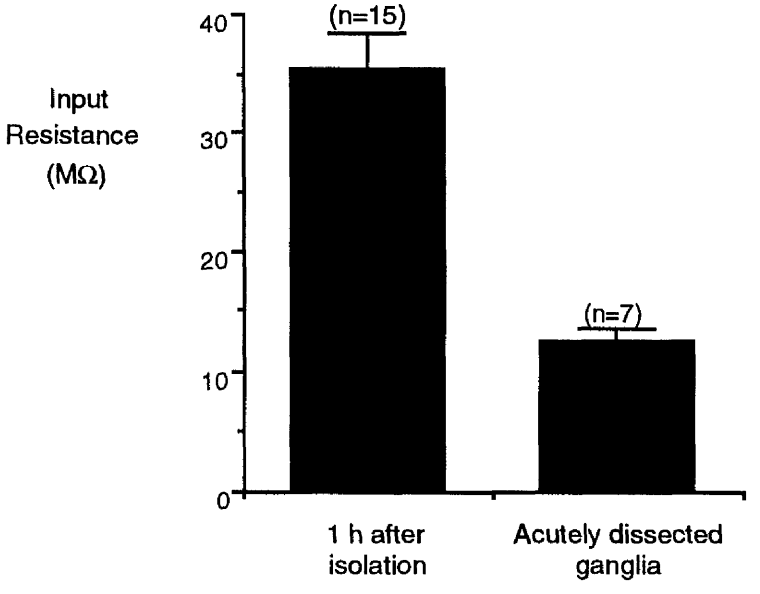

Figure 2.14: Effect of isolation on the input resistance of Retzius neurones: (A) composite of current-voltage curves 1 h after isolation; (B) Comparison between the input resistances of isolated neurones with neurones in acutely dissected ganglia (Bars show S.E.M.).

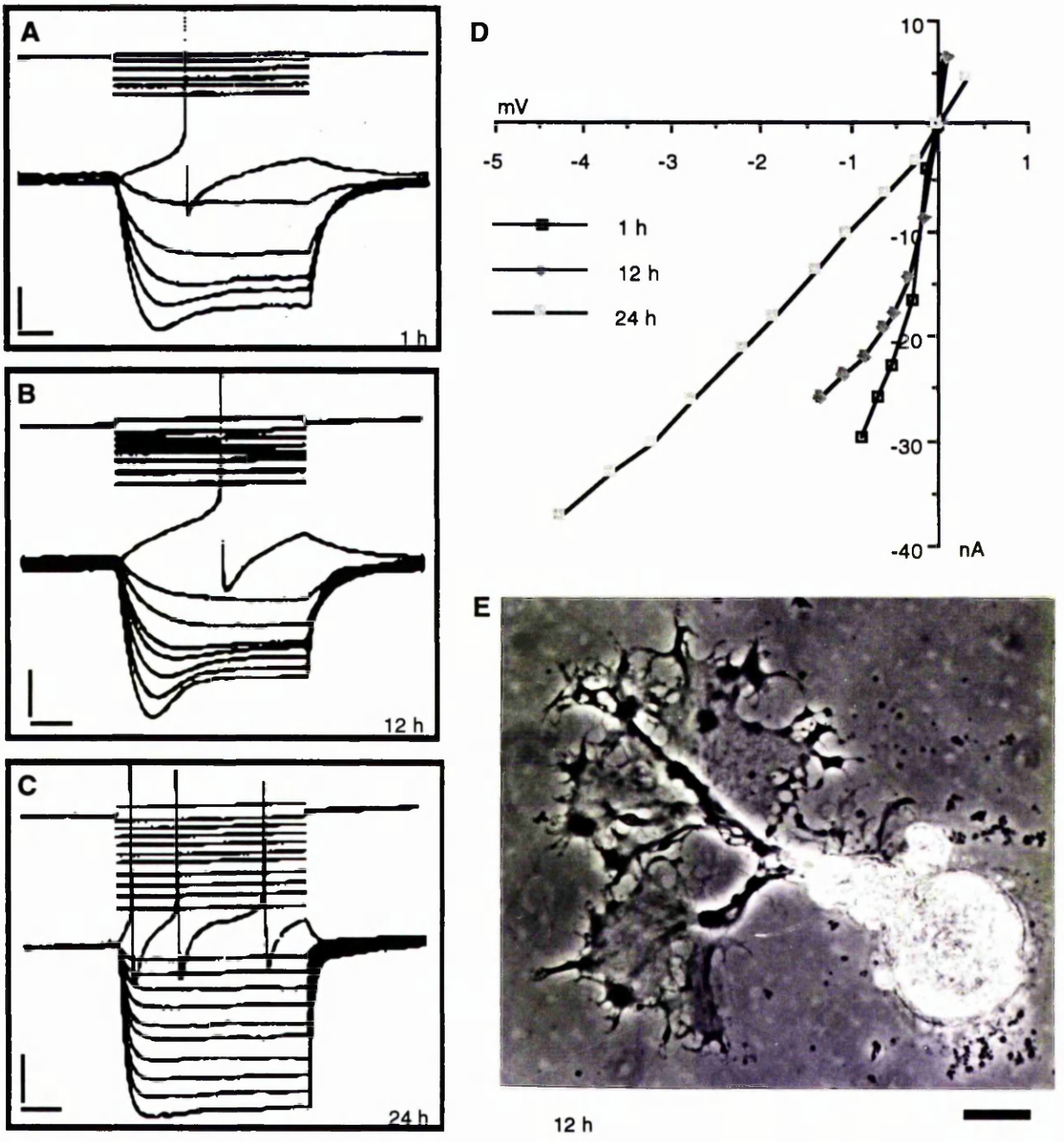

Figure 2.15: Input resistance vs. time in culture of the isolated Retzius neurone photographed in part E after 12 h in culture (scale bar: 33 µm). Recordings were made after: (A) 1 h, (B) 12 h, and (C) 24 h. (A), (B) and (C) are separate sets of superimposed sweeps (horizontal bar equivalent to 100 ms). The upper set of traces represent the current injected (vertical bar represents 1 nA, except in (C) where it represents 2 nA). The lower set of traces are recordings of the corresponding membrane potential response (vertical bar: 10 mV). The current voltage (steady state measurement) plots in (d) illustrate a decrease in input resistance with time.

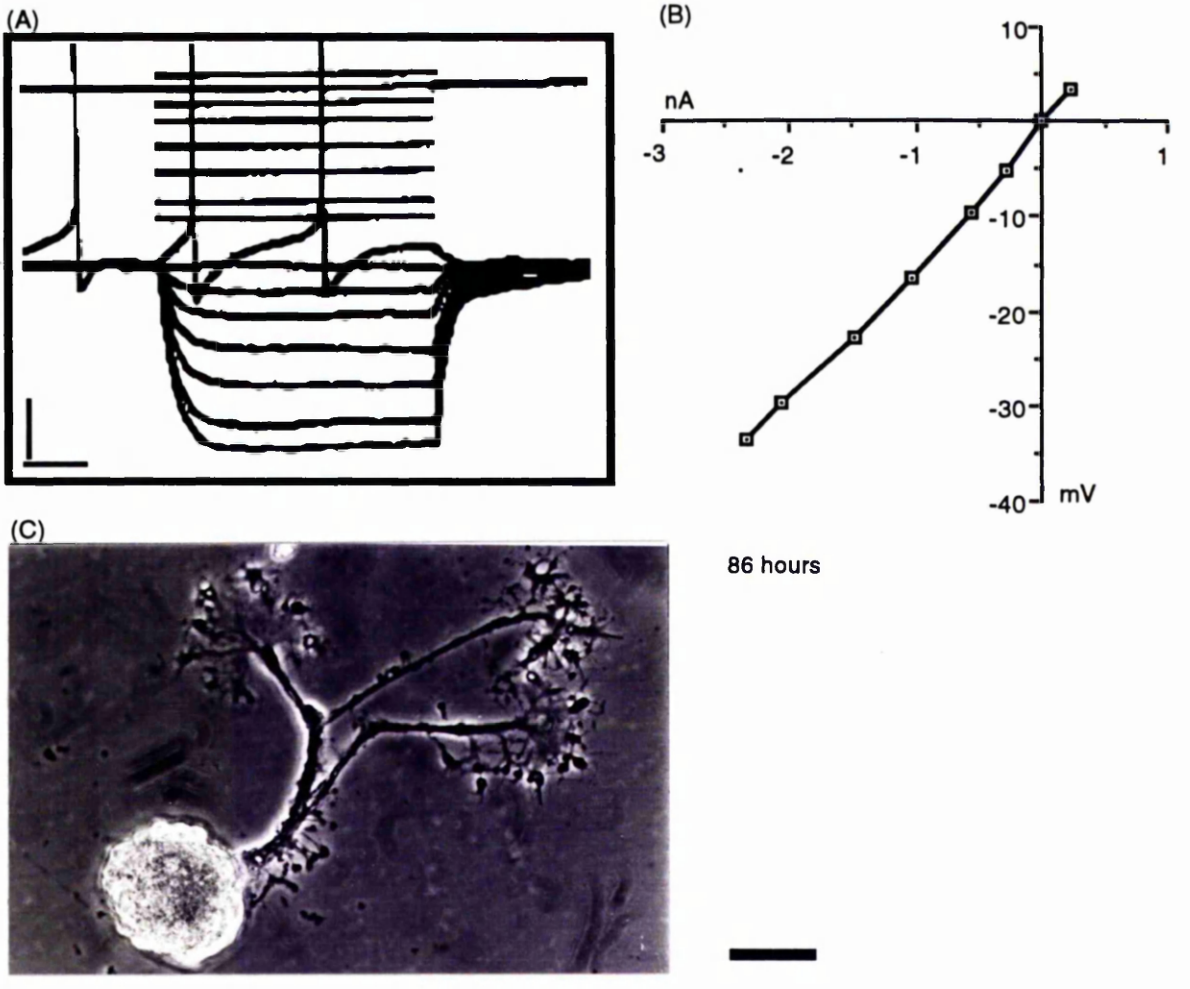

Figure 2.16: Single measurement of input restistance after 86 h (A) and current voltage plot (B) of a Retzius cell (C) impaled once after 86 h in culture. (A) shows superimposed sweeps (horizontal bar: 100 ms) representing current injected (upper set; vertical bar: 1 nA) and membrane potential response (lower set; vertical bar: 10 mV). Scale bar in (C): 50 µm.

The effect of morphology on input resistance

In order to derive a value for the specific membrane resistance (R_m) without using the time constant, the 15 isolated neurones were deliberately extracted with different lengths of process. An enlarged image of each cell

was divided into segments, and the corresponding surface area of each segment was calculated (see Appendix 2 and 3).

If the longitudinal resistance of the processes is very high, the input resistance will be a function dominated by the surface area of the cell body. Variations in the size of the cell body should account for the difference between the input resistances of cells. If however, the longitudinal resistance is very small, then the entire membrane of the process will make a major contribution to the input resistance measured at the cell body. Plotting the surface area of the cell body against the input resistance would result in a large amount of scatter, in which case the data may be better fitted by a plot of total surface area against input resistance. When the longitudinal resistance takes an intermediate value the membrane of the process near the cell body will make a large contribution whereas the contribution of very distant membrane will be very small. In this case, neither of the preceding plots would accurately describe all the cells (assuming a constant R_m). A compromise plot that considers variation in area over a shorter length of process may be more appropriate.

Figure 2.17 shows the area of the cell body plotted against the input resistance (points on the graph) for each of the isolated Retzius neurones. The exponential which best fits these points is also shown (hashed curve). Best fitting exponentials were also drawn for points (not shown) of the area of the cell body combined with different lengths of process against input resistance.

When the area is converted into cm^2 and the data re-plotted as 1/area v. input resistance, the gradients of the best fitting straight lines have units of $\Omega.cm^2$ (according to Equation 2.3) and can be regarded as estimates of the specific membrane resistance, R_m. The best estimate for R_m, determined by

comparing the Spearman's correlation coefficient of each data set (see Snedecor & Cochran, 1967), was the value obtained using the combined area of the cell body and initial segment. This gave a value for R_m of 51,300 $\Omega.cm^2$. However, the Spearman's correlation coefficient of this data set was low ($R^2<0.4$), comparable to that of other weak biological relationships (such as the inheritance of height; Snedecor & Cochran, 1967). One explanation for this may be that the variation in input resistance of cultured neurones is dominated by variation in the specific membrane resistance and not surface area. Alternatively, the value of the correlation coefficient may reflect large *variations* in the difference between the measured surface area (defined in Appendix 2) and the actual surface area of isolated neurones.

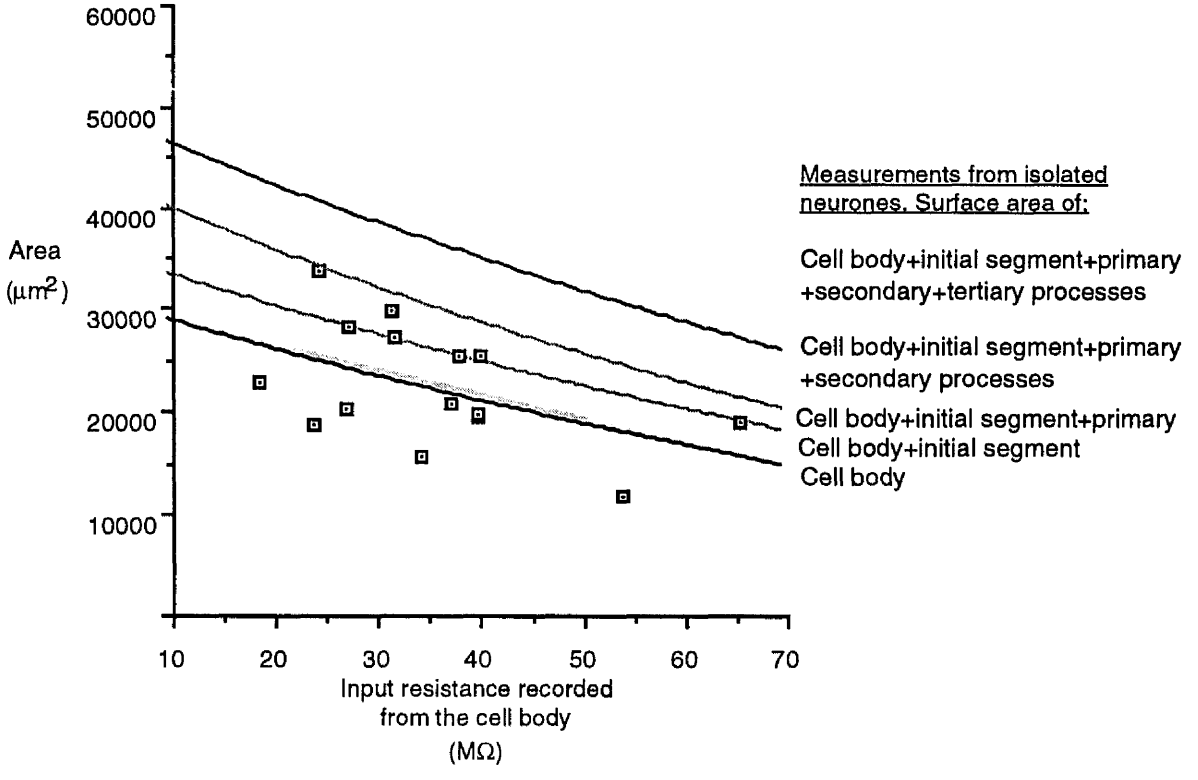

Figure 2.17: Cell membrane of isolated neurones that contributes to the input resistance measured at the cell body. The points show the relationship between the surface area of the cell body and input resistance. The hatched curve is the best fitting exponential to the points. The other curves were plotted using the area of the cell body combined with progressively larger segments of process (individual points not shown).

Membrane time constant

As described in Section 2.2.8, a value for R_m can also be derived using the membrane time constant. For each of the 15 isolated cells dV/dt was measured for the voltage transient that peaked nearest to -65 mV at short intervals following the onset of a current pulse. The lower set of points in Figure 2.18 represent values of dV/dt plotted against t (note the ln units). The curve which describes the points (not shown) deviates from a straight line when t (the time after the onset of the current pulse) is less than 30 ms. If the latter part of this curve is used to calculate the time constant it gives a value of 51 ms. Since the cell had a long length of process, extending beyond the first branch point, a more accurate estimate of the time constant may be achieved by using √t corrected dV/dt values (see Section 2.2.7 for explanation). The gradient of the line which best fits (the latter of) these points gives a slower time constant of 84 ms.

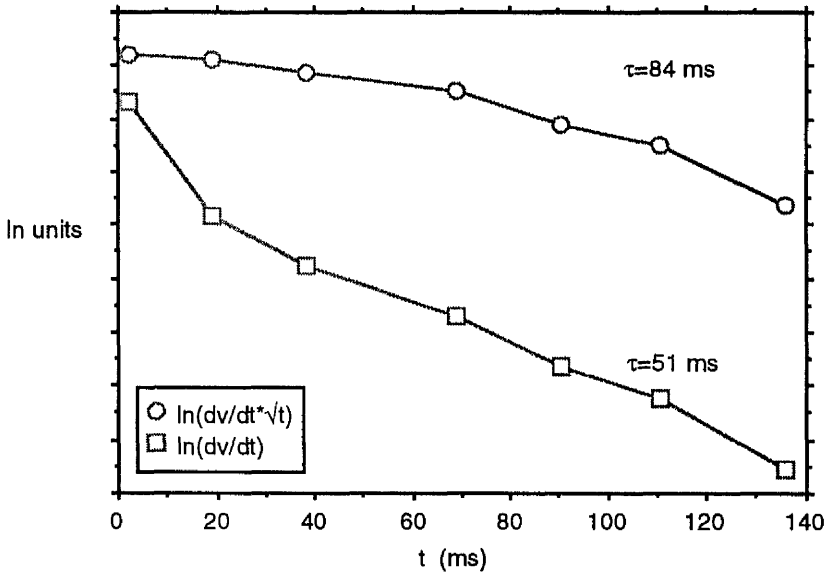

Figure 2.18: The change in dV/dt (squares) of the voltage response of an isolated neurone following the onset (t=0) of a current pulse. The points are joined by straight lines. The gradient of the line of best fit (not shown) through the latter points gives an estimate for the time constant (51 ms). For cells with processes, a better estimate may be made by plotting √t corrected dV/dt against t (circles). This gave the much slower time constant of 84 ms.

As the contribution made by the processes to the electrical properties of the cell body are unknown, the correct choice of estimate can not be made *a priori.* Three sets of time constants were generated, the first set uses the uncorrected dV/dt's. The second set included the correction and the third set was a combination of the two, depending on cell morphology. The mean time constants (in ms) for each set were 114.2 (S.E.M.±40) for the uncorrected set, 97.6 (S.E.M.±20) for the corrected set and 128.0 (S.E.M.±38) for the combined set. When used in Equation 2.2 (assuming C_m to be constant at 1μF/cm^2) these values give average R_m's of 114,200, 128,000 and 97,600 Ω.cm^2 respectively. Thus, R_m's calculated by this method are about a factor of two greater than the estimates made using the method that makes use of cell surface area.

Length constant

Estimates of the length constant were calculated by substituting the experimentally determined estimates of R_m into Equation 2.4, using a value of 100 Ω.cm for R_i and taking the average diameter of processes (d) as 10 μm. Using an R_m of 51300 Ω.cm^2 (from Table 2.1) gives a length constant of 0.358 cm. An R_m of 128000 Ω.cm^2 (combined set using a constant C_m) gives a value of 0.565 cm.

2.4 Discussion

2.4.1 The morphology of isolated Retzius neurones

The new technique for isolating leech neurones facilitates the extraction of very long processes that extend beyond the first major branch point. The distance between the cell body and this branch point was found to differ from cell to cell, the variation being centred around a single mean. This suggests that the same branch point of each cell was used to make the measurements. There are two possible explanations for the variation. Firstly, the variation seen in isolated neurones is a reflection of the morphology of cells *in vivo*, in which case cell geometry may differ either within or between animals, perhaps as a consequence of the size or age of the animal. In support of this possibility, the diameter of the cell bodies also varied. However, normalising the variation in length with the diameter of the cell body did not irradicate the difference between cells. Perhaps the difference in Retzius neurones reflects a left/right asymmetry.

A second possibility for the variation may be that it is a consequence of the extraction process. The force and (presumably the stretch) imposed during isolation varied from cell to cell and from animal to animal. To measure accurately the length of the process between the cell body and the bifurcation *in vivo*, and so determine which of these possibilities is correct, would require the use of three dimensional imaging techniques such as confocal microscopy.

As well as differences between the size of isolated cells, variation was also found in the shape of the cell body: some had a large bulb to one side. When viewed with phase-contrast optics, at 320x magnification, the membrane of the cell body appeared healthy (i.e it was not blebbed). A

simple explanation would be that the bulb results from distortion of the cell body during aspiration. This possibility can not be ruled out, despite the fact that the mouth of the aspirating pipette was larger than the cell body.

2.4.2 Affect of isolation on the electrical properties of Retzius neurones.

Ready and Nicholls (1979) showed that mechanosensory neurones (T, P and N cells) and the Retzius neurone retain their characteristically shaped action potentials in culture. However, the membrane properties of certain neurones are modified. The action potentials of cultured L motor neurones for example, are larger than those found *in situ* and current-voltage plots show a novel rectification (Fuchs *et al.*, 1981). Owing to the use of a new enzyme treatment it was necessary to re-evaluate the effects of isolation on electrical properties.

Shape of the action potential

Retzius neurones with long processes had action potentials that were similar in shape to those recorded in dissected ganglia. This was assessed by first considering the effect of temperature on the rising phase of Retzius action potentials in dissected ganglia. The resulting curve showed an exponential decay with increasing temperature. Action potentials from other preparations show a similar temperature sensitivity (e.g the giant axon of the squid, Hodgkin & Katz, 1949; the median giant nerve fibre of the earthworm, Lagerspertz & Talo, 1967; and a crayfish stretch receptor, Winters, 1973). The rise time of action potentials recorded at room temperature (21 to 22°C) from isolated Retzius neurones with long processes fell within the standard error of the value predicted from the curve.

On the other hand, a Retzius neurone extracted with a very short process fired a burst of action potentials during the injection of depolarising

current that differed significantly from those normally seen in dissected ganglia (Figure 2.10). The difference is unlikely to be the result of a bad impalement since the membrane potential returns to the holding potential at the end of the current pulse. It is also unlikely that these differences resulted from use of protease alone, as cells with longer processes are apparently uneffected. Closer examination of the published recordings of cultured Retzius neurones extracted using the lasso method, provides further reassurance that the enzyme treatment was not responsible for the unusual response (see Figure 10 & 11 in Fuchs *et al.*, 1981). Some of the recordings from cultured Retzius neurones presented by Fuchs *et al.*, (1981) had action potentials which resembled those in Figure 2.10, despite the fact that the lasso method was used instead of an enzyme treatment. These cells had also been extracted with very short processes, probably amounting to a fraction of the initial segment. This suggests that the unusual response is a result of a short process.

Patch clamp studies of cultured Retzius neurones reveals that the distribution of sodium channels over the surface of a cell is non-uniform. Specifically, in isolated Retzius neurones consisting of only a cell body and an initial segment, there appears to be a concentration of sodium channels at the broken tip of the initial segment (Bookman *et al.*, 1987). However, when Retzius neurones include a long length of 'axon', sodium currents are not detected in the membrane of either the cell body or initial segment (Garcia *et al.*, 1989). Presumably action potentials recorded in the soma of most Retzius cells invade passively from membrane containing voltage gated channels located in the process. If this supposition is correct it is surprising that cells with very short stumps have action potentials at all. Perhaps redistribution during extraction or the recruitment of new channels

is responsible (Brismar & Gilly, 1987; Titmus & Faber, 1986). Redistribution or recruitment of new channels may occur in regions distant from the cell body when cells are extracted with long processes. If these mechanisms do occur at the end of long processes they may not influenced the shape of action potentials recorded in the cell body, as changes in membrane potential at the cell body are likely to be dominated by the voltage sensitive channels of the intervening membrane. Garcia *et al.* (1989) have shown that even axons of cultured Retzius neurones several hundred micrometers in length terminate in a region of high sodium channel density. In measuring the conduction velocity of cultured leech neurones (see Chapter 3) it is assumed that the region of high channel density is confined to a small area near the tip of the process: the channel properties of the intervening membrane are treated as being similar to those found *in vivo*. These assumptions are not totally unfounded as suggested by Figure 2.10. The somatic action potentials of cells isolated with long processes had similar rise times (as assessed by the half-width of the differential) to somatic action potentials recorded in dissected ganglia at the same temperature.

Anomalous rectification

A second difference between Retzius neurones *in vitro* and in dissected ganglia is the prominence of a hyperpolarising transient (labelled in Figure 2.6), a property known as anomalous rectification (Marmor, 1971). The published recordings of Retzius neurones extracted using the lasso technique also show this property (see Figure 9 in Fuchs *et al.*, 1981), although this is not discussed by Fuchs *et al.*, (1981).

The most likely explanation is that the level of hyperpolarisation imposed by the current pulse (i.e. the peak of the transient) is reduced by the

flow of ions through a channel that is slow to activate (i.e. at about the time of the peak). The transients observed here appear when the membrane potential reaches -79 (S.D.±5) mV and increase with further polarisation. It is instructive to note that -79 mV is close to the value of -85 mV determined for the potassium equilibrium potential (E_k) when the external [K^+] is 4 mM (concentration in normal Ringer; Nicholls & Kuffler, 1964). Hyperpolarizing the cell membrane beyond E_k would cause the driving force on K^+ to reverse, potassium would enter the cell making it more positive, and membrane potential would fall (providing the membrane contains a population of open K^+ channels). Further increases in hyperpolarisation, would increase the driving force on potassium and makes the size of the transient larger.

Stewart *et al.* (1989) using voltage clamp techniques have demonstrated the presence of two slowly activating K^+ currents in cultured Retzius neurones, designated I_{k1} and I_{k2}. These are the only K^+ currents that were identified with activation kinetics sufficient to explain the delay to the peak hyperpolarisation observed here. However, these are both outward currents and are activated by *depolarisation*, not hyperpolarisation. The possibility that other potassium channels exist in the leech can not be excluded.

Anomalous rectification has been identified in a number of vertebrate (e.g. Czeh *et al.*, 1977; DiFrancesco & Ojeda, 1980; DiFrancesco, 1981; Bader *et al.*, 1982; Halliwell & Adams, 1982; Mayer & Westbrook, 1983; Constanti & Galvan, 1983) and invertebrate neurones (e.g. Marmor, 1971; Hagiwara, S. & Takahashi, 1974; Miyazaki *et al.*,1974). Cultured mouse dorsal root ganglion neurones for example, respond with a slow inward current when the level of hyperpolarisation during voltage clamp is stepped

from a holding potential of -50 mV to -60 mV (Mayer & Westbrook, 1983). When the extracellular [K^+] was raised the inward current increased, suggesting that it is mediated by a potassium conductance. However, reducing the extracellular [Na^+] concentration *also* has an effect, causing a reduction in the inward current. In this and several other cases, it would appear that both sodium and potassium currents are involved (Bader *et al.*, 1982; DiFrancesco & Ojeda, 1980; DiFrancesco, 1981; Halliwell & Adams, 1982). In other preparations the total block of the inward current by the Ba^{2+}, and a close relationship between the size of the current and an experimentally manipulated $V-E_k$ (the difference between the membrane potential and the potassium equilibrium potential), suggests that only potassium currents may be involved (Hagiwara *et al*, 1978; Constanti & Galvan, 1983).

The anomalous rectification recorded in mouse dorsal root ganglion neurones in culture (Mayer & Westbrook, 1983) is matched by that seen *in vivo* (Czén *et al.*, 1977). For Retzius cells anomalous rectification increases by a factor of two when cells are placed in culture. This increase may represent an unmasking of properties which are hidden in the ganglion. Given the large number of excitable cell types which possess anomalous rectifying properties, this phenomenon is likely to have an important function.

One suggestion for the role of anomalous rectification is that the inward current acts to stabilise the resting potential, preventing it from becoming over-polarised (Fain & Lisman, 1981; Mayer & Westbrook, 1983). In the mechanosensory neurones of the leech (but not in the Retzius neurone), periods of activity are followed by a long-lasting after hyperpolarization (Jansen & Nicholls, 1973). For such cells it is tempting to speculate that anomalous rectification may be part of the mechanism which

limits this hyperpolarization to a certain level, since at least one of the cell types, the N cell, appears to be capable of anomalous rectification (see Figure 8 of Fuchs *et al.*, 1981). Caution is required however, since the hyperpolarization has been shown to *result* from an increased potassium conductance (triggered by the depolarisation) causing a larger *outward* flux (Jansen & Nicholls, 1973).

In the Retzius neurone, the role of anomalous rectification is equally unclear. One can speculate that it may relate to the autoregulation of 5-HT release. Since 5-HT causes a reduction in the firing rate of Retzius neurones (Kerkut *et al.*, 1967), it is likely to hyperpolarise the membrane. It is noteworthy that when Retzius neurones synapse onto P cells in culture, the inhibitory post synaptic potentials seen in P cells results from an increase in chloride conductance (Fuchs *et al.*, 1982) which is mediated by the release of 5-HT (Henderson, 1983). If the equilibrium potential of this ion (which in other preparations ranges from -20 mV upto -90 mV; Miles, 1969) exceeds the threshold necessary for anomalous rectification, the effect of large increases in Cl^- conductance may be short circuited by inward potassium conductance. One expectation arising from this hypothesis is that 5-HT causes inhibitory potentials (caused by chloride entry), which depolarise with a time course that contains a component with a shape similar to the depolarisation seen during anomalous rectification[3]. The depolarising phase of the inhibitory potentials induced in P cells by the application of 5-HT do consist of dual exponential components (see Drapeau & Sanchez-Armass, 1988: Figure 1 & 4). It would be interesting to determine the

[3]Note that anomalous rectification (and inhibitory post synaptic potentials) consist of an initial hyperpolarising phase followed by a depolarising phase.

application of 5-HT to Retzius neurones (and N cells) causes an inhibitory potential with an appropriate depolarising time course. Secondly, whether anomalous rectification in Retzius neurones can be blocked by caesium (a blocker of monovalent cation channels that blocks anomalous rectification in other preparations; Constanti & Galvan, 1983) and if so whether or not it causes a change in the shape of the depolarising phase of inhibitory potentials in P cells. Thirdly, whether isolated P cells also have anomalous rectifying properties and finally, whether E_{Cl} is significantly higher *in vivo* than the calculated value of -48 mV) for P cells after 7-10 days in culture (Drapeau & Sanchez-Armass, 1988).

A second hypothesis for the role of the anomalous rectifyer channels has been put forward by Fuchs & Evans (1990). They observed that: firstly, the resting potentials of chick hair cells correlate with the degree of inward rectification, cells with the largest inward rectifying currents having the most negative resting potentials; and secondly, that the resting potential could be depolarised by 8 mV by the addition of Ba^{2+} to the bathing medium. Both observations were taken to imply that the K^+ channels responsible for inward rectification are open at the resting potential and have a role in *maintaining* the level of negativity. In this regard it is interesting that not only do leech neurones in culture show anomalous rectification (as reported here), but also their resting potential increases (Fuchs *et al.*, 1981). As E_k is more negative than the resting potential the open channels would cause an *outward* K^+ current. This would be more difficult to identify (in Figure 2.6) than the inward K^+ current that occurs when the membrane potential exceeds E_K. Ba^{2+} would be expected to reduce the membrane potential of cultured neurones more than their *in vivo* counterparts: an intriguing project for the future.

Increase in input resistance

A third difference between the electrical properties of Retzius neurones *in vitro* and within an isolated ganglion was an increase in average input resistance following isolation (a trend observed previously; Fuchs *et al.*, 1981) from 12.3 MΩ (n=7) to 35.3 MΩ after 1 h (n=15).

Several values for the average input resistance of Retzius neurones in dissected ganglia have been published: 20.7 MΩ (n=4; Fuchs *et al.*, 1981), 16 MΩ (n=7; Stewart *et al.*, 1989), 7.2 MΩ (n=12; Kuffler & Potter, 1963), 7.4 MΩ after staining with neutral red (n=3; Stuart *et al.*, 1974) and for Retzius cells in the duck leech, *Macrobdella decora,* 5.7 MΩ (n=6; Kleinhaus & Prichard, 1977). Bearing in mind the use of acutely dissected ganglia to facilitate the comparison with cultured neurones, an average value of 12.3 MΩ is not unreasonable.

The work of Fuchs *et al.* (1981) also provides a yardstick to judge the values obtained for the input resistance of Retzius neurones in culture. They found that one cell (impaled 1 h after isolation) had an input resistance of 72 MΩ. This is about twice the average input resistance of the 15 neurones reported here. Two differences in protocol may explain this discrepancy. Firstly, the neurones here were plated on Concanavalin A-treated dishes, not polylysine-coated collagen. Concanavalin A supports rapid outgrowth whereas polylysine-coated collagen does not (Chiquet & Acklin, 1988). Some cells show signs of outgrowth after one hour and this could result in a lower input resistance, accounting for some of the difference. The second factor is the use of protease, which could affect the membrane resistance directly. However, this seems unlikely considering the similarity between the action potentials of cells extracted by the lasso technique and those

extracted enzymatically (see above). Thus the voltage-dependent channels which participate in generating action potentials and *a priori* are likely targets for protease, appear not to have been affected. A more satisfactory explanation for the lower input resistance of the cells extracted here is the difference in the length of processes. Nearly all the cells extracted with protease had a complete initial segment, the area of which can amount to a third of the area of the cell body. On the other hand, the photographs in the study of Fuchs *et al.* (1981) show cells which appear to have been extracted without the initial segment. These cells would be expected to have a higher input resistance as a result of having a smaller surface area.

2.4.3 Change in input resistance with time in culture

Unlike the study of Fuchs *et al.* (1981) no clear trend toward an increase in input resistance with time was observed. On the contrary, in the majority of the 7 cells tested a drop in input resistance over the first 12 h was apparent. The input resistance of a cell impaled for the first time after $3^1/_2$ days was below 18 MΩ, suggesting that the absence of the expected trend was not a consequence of sustained damage from earlier impalements. The healthy outgrowth of the cells pictured in Figures 2.15 and 2.16 not only support this view but also provide an alternative explanation. The factors that bring about an increase in the input resistance of neurones plated on polylysine-coated collagen (a substrate on which the first significant outgrowth is not seen for 5 days) may be offset by the rapid outgrowth of lamellipodia-like processes that occur on Concanavalin A. The synthesis and/or unfolding of membrane which these processes represent is likely to cause a significant decrease in a cell's input resistance.

2.4.4 The specific membrane resistance of isolated Retzius neurones

The relationship between the input resistance of Retzius neurones and the size of the cell body can be seen in Figure 2.17. Although a general trend towards increasing input resistance with area of the cell body is apparent, there is also a great deal of scatter. There are at least three explanations for this. One is the difficulty of precisely measuring the cell area. If the cell bodies vary in the degree to which they match a sphere, then the accuracy of the area measurement will also vary. Similar arguments apply to the surface areas measured for other parts of the cell. Another explanation is that differences in the quality of impalements may lead to inaccurate measurements of input resistances. A third explanation is that variation arises because membrane in addition to that of the cell body contributes to the input resistance. As a result of this possibility, the input resistance was plotted against several different measures of area (see Section 2.3.3).

It should be noted that for idealised cells that differ only in the length of their processes, plotting input resistances against whole cell surface areas would be sufficient to derive the specific membrane resistance. The expected curve would show the input resistance to decrease exponentially with increasing surface area. As the curve levels out, further increases in the length of the process fail to reduce the input resistance. Unfortunately, the Retzius cells studied here differ from the idealised case in that their dimensions, and therefore the surface area of their cell bodies, varied. Since the membrane of the cell body is close to the site of current injection and presumably isopotential, slight variations in the size of the cell body between cells may have a far greater effect than equivalent variations in the length of

processes. This being the case, one would expect a large amount of scatter when the area to be plotted includes the contribution made by very long processes.

The curve with the least scatter was obtained for the plot of input resistance against the sum of the areas of the cell body and initial segment. This suggests that the presence of a process makes only a minor contribution to the input resistance (assuming detection is not limited by the resolution of the recordings). This conclusion is loosely supported by the plot of $\ln(dV/dt.\sqrt{t})$ against t in Figure 2.18. If conductance into the processes was sizable, then this curve should begin with a rising phase (when t is small) that rapidly reaches a maximum and is followed by a falling phase (Gorman & Mirolli, 1972). This would appear not to be the case, although for certainty the sampling frequency at which $\ln(dV/dt.\sqrt{t})$ was calculated would have to be high.

The process nearest the cell body is likely to have the greatest effect on input resistance measured in the soma (compared with other more distant processes). Thus, the lack of a strong correlation between the input resistance and the length of processes suggests that the higher input resistance of isolated neurones can not be explained solely by the removal of the majority of the processes during isolation. This in turn suggests that the specific membrane resistance may be affected directly.

When the data was replotted as input resistance against 1/area, the gradient of the line of best fit gave a specific membrane resistance of 51 300 $\Omega.cm^2$. This was less than half the value obtained using Equation 2.2. with the uncorrected set of membrane time constants. When the average of the combined set of time constants is used (allowing for the possibility that the

processes when present do have an affect) the discrepancy is worse.

Once again, the pioneering work of Fuchs *et al.* (1981) is called upon for a comparison. Using the input resistance of a single cell they give lower and upper estimates of R_m as 40 000 and 100 000 $\Omega.cm^2$ respectively. Thus the value calculated for the change in input resistance with cell area is within these bounds, whereas the value calculated from the averaged time constants is higher. Some other invertebrate neurones also have high input resistances. *Aplysia* neurones may have a specific membrane resistance of up to 690,000 $\Omega.cm^2$ (Graubard, 1975) whereas for the giant cell in the mollusc *Anisodoris nobillis*, R_m may be as much as 1 $M\Omega.cm^2$ (Gorman & Mirolli, 1972). Both these values were calculated taking into account the degree of membrane invagination. Invagination may be far more extensive in *Aplysia* neurones than in leech neurones (Parsons *et al.*, 1989). However, invagination is almost certainly a factor in cultured leech neurones as is suggested by scanning electron microscopy of the cell surface (see Chapter 5). Transmission electron microscopy of serial sections can be used to refine the calculation (Gorman & Mirolli, 1972). By ignoring this factor, the estimates of the specific membrane resistance of leech neurones is likely to be lower than the true value.

2.4.5 An estimate of the length constant of isolated Retzius neurones

In the previous Section, the measurements of input resistance were interpreted as being virtually independent of the processes. Thus, the estimate of the specific membrane resistance of isolated cells may apply only to the membrane of the cell body and initial segment. In order to estimate the length constant of a process, it was necessary to treat the membrane properties over the whole cell as being constant. Evidence

discussed in Section 2.4.2 suggests that the membrane of the cell body has a different population of channels from the process (Garcia *et al.*, 1989). This may cause slight differences in the specific membrane resistance of these two membranes and lead to an inaccurate estimate of the length constant.

2.5 Conclusions

- A new enzymatic treatment for isolating leech neurones was presented, that allows the extraction of neurones with very long processes. The major process usually included a bifurcation.
- The distance between the cell body and the bifurcation of the main process of Retzius cells varied. It is not clear whether this variation was a consequence of within or between animal variation, or whether it was an artefact of the isolation procedure.
- The half-width of action potentials of Retzius neurone in dissected ganglia was shown to decrease exponentially with increased temperature. Neurones extracted with long processes had action potential with half-widths similar to their counterparts in dissected ganglia when measured at the same temperature.
- Recordings made from a Retzius neurone *without* a long process revealed a strikingly different pattern of activity from neurones with long processes. This difference supports previous evidence which points to a non-uniform distribution of sodium channels over the surface of cultured leech neurones.
- The average input resistance of isolated neurones is more than twice that of cells in acutely dissected ganglia. This may be a result of a change in

membrane properties, as apposed to the removal of processes during dissection.

• Unlike a previous report, an increase in input resistance with time in culture was not observed. This may be a consequence of the substrate on which the cells were plated.

• Isolated Retzius neurones also differed from their counterparts in acutely dissected ganglia in that they show marked anomalous rectification. Isolated Retzius neurones may offer a preparation in which this poorly understood phenomenon can be readily investigated.

• A novel technique was used to estimate the specific membrane resistance of isolated neurones. The technique uses the input resistance along with measurements of the surface area of different parts of the cell lumped to that of the cell body. Although the relationship between surface area and input resistance was poor, the values obtained for the specific membrane resistance were comparable to estimates derived using a more conventional approach.

CHAPTER THREE:

Planar extracellular electrode arrays

SUMMARY: This Chapter surveys the use of extracellular electrodes in electrophysiology, and then introduces a more recent development: microfabricated planar extracellular electrode arrays. Originally these devices were used to make *in vivo* recordings but they are now being used increasingly to record from cells *in vitro*. Unlike optical recording techniques, electrode arrays are virtually non-toxic allowing the activity of excitable tissues to be monitored over very long periods (e.g. five weeks; Droge *et al.*, 1986).

Unfortunately, electrode arrays have several disadvantages (see Section 3.4). One is that the spatial resolution is low. This has previously limited recordings to one per cell. This Chapter reports the first multisite extracellular recordings from single cells using microfabricated planar electrode arrays. The conduction velocity of action potentials of isolated leech neurones was measured, and the origin of the action potentials determined. This Chapter also demonstrates that extracellular electrodes can be used to record the action potentials that result from stimulation by planar extracellular electrodes. Thus, these devices are unique in having the capacity to both record and entrain the long term activity of cultured neurones. These properties are likely to be useful in experiments designed to investigate the properties of neuronal networks constructed in culture.

3.1 Introduction

3.1.1 Historical perspective

Metal extracellular electrodes pioneered early experimental attempts to understand how nervous tissue functions (e.g. Edes, 1892). With

improved methods of recording rapid electrical events, extracellular electrodes were employed to study the electric fields surrounding skeletal and active heart muscle (Craib, 1927; 1928). Subsequent studies analysed the distribution of extracellular action potentials from a variety of preparations, both *in situ* (e.g. Rosenfalck, 1957; Furshpan & Furukawa, 1962; Rosenthal *et al.*, 1966) and *in vitro* (e.g. Tasaki, 1950; Krnjevic & Miledi, 1958).

These studies were limited in that they used a number of single electrodes which had to be individually positioned to make multisite recordings. Subsequently, multi-electrode devices were designed and manufactured. One of the first commercially available multi-electrodes consisted of a bundle of insulated platinum-iridium (90:10) wires, each with a diameter of about 90 μm. A small area of insulation was removed from each wire to produce an electrode which was then platinised to reduce impedance (Ray, 1965). This type of device was easy to manufacture and inexpensive. However, the electrodes tended to have large areas (0.09 mm^2) giving poor spatial resolution. Further more, the spatial relationship *between* electrodes was limited, imprecise, and difficult to reproduce.

To avoid these problems many workers have turned to microfabricated structures, manufactured with technology developed by the microelectronics industry. A large number of devices for *in vivo* use have been reported (see Pickard, 1979, for an early review). These have been designed as probing devices (Pickard & Welberry, 1976; BeMent *et al.*, 1986; Urban *et al.*, 1990; Rutten *et al.*, 1991; Najafi & Hetke, 1990;) and as neural/prosthetic interfaces (Edell, 1986).

In vitro studies have also been performed using microfabricated extracellular electrodes arrays. A typical device is illustrated in Figure 3.1.

Multisite extracellular recordings have been made from hippocampal slices (Jobling *et al.*, 1981) and *Aplysia* abdominal ganglia (Novak & Wheeler, 1986) placed over planar electrodes. The power of this approach however, is better illustrated by experiments on cultured neurones. Such preparations are likely to be more susceptible to toxicity, providing a better test for the biocompatibility of the devices. In addition, the cultures are virtually two dimensional, complimenting the planar nature of the electrodes.

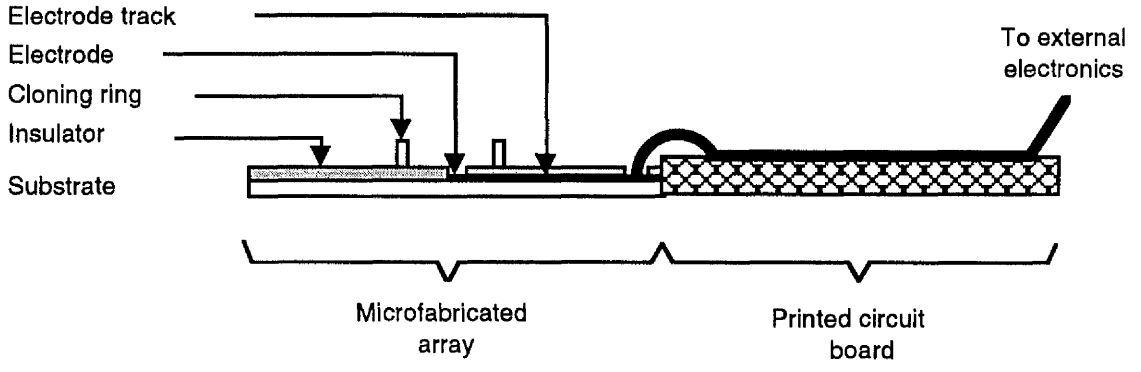

Figure 3.1: Cross section through a typical planar electrode device, designed for work *in vitro*. Cells are plated in the cloning ring above the electrodes. Insulated electrode tracks diverge and are bonded to a printed circuit board. Tracks on the circuit board fan out to connections on a scale suitable for connecting to commercially available amplifiers.

A variety of vertebrate and invertebrate neurones have been cultured on substrates which incorporate planar electrode arrays. Extracellular recordings from, and stimulation of, dissociated neurones from neonatal rat superior cervical ganglia have been reported (Pine, 1980). Gross & Hightower (1986) have performed similar experiments on monolayers of mouse spinal cultures, and were able to observe spontaneous activity which included rhythmic bursting that persisted for over 12 hours. Three to five weeks after seeding, simultaneous recordings from different electrodes revealed synchronised in-phase bursting at multiple sites. Invariably, the composition of bursts recorded from different electrodes suggested that each

electrode recorded the activity of a different electrically active 'unit'. Occasionally antiphasic bursting at different electrodes was also observed, illustrating that randomly seeded spinal circuits can exhibit a variety of organised activity (Droge *et al.*, 1986).These are important experiments in their own right, but they also show that electrode arrays can be used to make multisite long term recordings that would be virtually impossible using the currently available alternatives (see Section 1.1).

The use of cultured invertebrate neurones with extracellular electrode arrays provides two highly desirable refinements. Firstly, identified cells can be used which have well defined electrical properties and characteristic synaptic partners. Secondly, single cells can be individually manipulated (owing to their large size), allowing precise positioning over electrodes. The importance of this follows from the fact that reducing the distance between a neurone and an extracellular electrode increases the size of the recorded signal. In addition, by individually placing cells the experimenter may ensure that recordings can be made from every neurone which contributes to network properties.

Although networks of identified cells have yet to be constructed over planar electrodes, recordings have been made from the cell bodies of single identified *Aplysia*, *Helisoma*, *Hirudo* (Regehr, 1988; Fromherz *et al.*, 1991) and *Lymnaea* (L.Breckenridge, personal communication) neurones. Single site recording from axonal stumps have also been made (Regehr, 1988), but no simultaneous extracellular multisite recordings from single isolated neurones have previously been reported.

3.1.2 Parameters important for the design of planar electrode arrays[1]

There are a number of design criteria that must be satisfied for the successful application of electrode arrays:

(a) Ease of manufacture. The number of devices available for experimentation depends on the number and reliability of the steps involved in manufacture. Several groups that use electrode arrays have sacrificed high performance for speed of manufacture. For example, photoresist has been used as an insulator despite poor mechanical and electrical properties (Thomas *et al.*, 1972; Loeb *et al.*, 1977).

(b) Biocompatibility. All the materials used should be as non-toxic as possible. They should also stand up to experimental wear and tear, sterilisation protocols and long term exposure to saline solutions.

(c) Insulator. Ideally, the insulator should provide a uniform, pinhole-free surface so that it can be readily sterilised. In addition, the insulator should be durable so that devices can be used repeatedly. Silicon dioxide (SiO_2) and silicon nitride (Si_3N_4) fulfil these requirements. However, SiO_2 is permeable to Na^+ and K^+ ions, reducing its performance as a long term insulator in saline conditions (Prohaska *et al.*, 1986). Several types of insulating material have been used previously, as can be seen from Table 3.1.

---

[1]The designers of the electrode arrays used in this thesis were Prof.A.S.G.Curtis , Dr. P.Connolly, Dr. J.A.T.Dow & Prof. C.D.W.Wilkinson. The author has participated in discussions concerning recent modifications only.

Insulator	Key Properties	Reference
Silicon oxide (SiO_2)	Readily available technology, but Si wafer is not transparent and is permeable to Na^+ and K^+ reducing insulating properties.	Wise *et al.*, 1970. Mercer and White, 1978. Pine, 1980. Fromherz *et al.*, 1991.
Photoresist	Poor biocompatibility, easily damaged.	Thomas *et al.*, 1972. Loeb *et al.*, 1977. Israel *et al.*, 1984.
Isocyanoacrylate	-	Pickard & Welberry, 1976.
PTF teflon	-	Pickard *et al.*, 1979.
Silicon nitride (Si_3N_4)	Blocks ion diffusion leading to low conductivity (10^{13} $\Omega^{-1}.cm^{-1}$ for signals at 10 Hz).	Prohaska *et al.*, 1986. Connolly *et al.*, 1990.
Polyimide	Easily damaged but can be spun on, and photosensitive form available.	Novak and Wheeler, 1986.
Polysiloxsane	Spin application of 1-2 μm thick has low shunt impedance (10 MΩ at 1 KHz), additional insulator required.	Gross & Hightower, 1986. Droge *et al.*, 1986.

Table 3.1: Selection of materials used as insulators in microfabricated electrode devices.

(d) Electrode spacing. Photolithography can be used to define structures with features down to 1 μm, although at this resolution dust particles and interference patterns (which are highly dependent on the exact thickness of the photoresist) make the manufacturing process more haphazard. Theoretical considerations also limit electrode spacing. One constraint is the necessity of minimising cross-talk between neighbouring electrode tracks. The amount of cross-talk is dependent on the quality of the insulator used and the separation of the tracks. The separation in turn is determined by the spacing between the electrodes and the degree of divergence of the tracks. Note that the greater the density of electrodes the smaller the possible degree of divergence. The cross-talk capacitance between a pair of 10 μm wide tracks, running in parallel on a planar surface with a separation of 10 μm and insulated with a layer of silicon nitride has been estimated at 0.03 $pF.mm^{-1}$ (Prohaska *et al.*, 1986). This value was considered acceptable for tracks up to about 20 cm long providing the

electrodes had impedances below 1 MΩ (Prohaska *et al.*, 1986). The electrodes in the devices used here also have tracks 10 μm wide and are insulated by a layer of silicon nitride. However, where the tracks run in parallel the cross-talk capacitance is likely to be less than the above estimate as the separation is at least 90 μm, and cross-talk capacitance decreases with the logarithm of the separation (Offner,1967). The cross-talk capacitance is further minimised by limiting the length over which the tracks are in parallel (to ≤300 μm) by rapid divergence (see Figure 3.3).

As well as reducing the pickup between tracks, the insulator also serves to reduce the capacitive leak to the overlying medium and shields the tracks from activity occurring at sites other than in the immediate vicinity of the electrodes. These factors maintain the signal amplitude and minimising noise.

(e) Electrode Impedance. As a first approximation the electrode-electrolyte interface can be modelled as a capacitor and a resistor in series (Geddes, 1972). The impedance (Z) of such a component is made up of a resistive (R) and a reactive (X) component (for an introductory text see Offner, 1967):

$$Z=\sqrt{R^2+X^2} \tag{3.1}$$

Reactance diminishes the flow of alternating currents, analogous to the effect of resistance on direct currents. Capacitors have a reactance as the insulator between the two plates hinders the flow of current. The capacitance (C) is proportional to the area (A) of the two plates divided by the separation (*g*):

$$C \approx \frac{A}{g} \tag{3.2}$$

Since the capacitance between a pair of plates decreases as the thickness of the insulator increases, reactance is inversely proportional to the capacitance. This inverse relationship also applies to the area of the plates and the frequency (f) of the alternating current (since both these parameters are directly proportional to capacitance). The inverse relationship between reactance and frequency can be appreciated when one considers that frequency determines the rate of the voltage change between the plates that is responsible for current flow. Capacitive reactance (X_c) is given by the relationship:

$$X_c = \frac{1}{2\pi fC} \tag{3.3}$$

When equation 3.3 is substituted into equation 3.1, it becomes apparent that electrode impedance is dependent on frequency. Therefore, in order to make a comparison between the impedances of different electrodes, measurements must be made at the same frequency. A suitable standard which has been adopted in the literature is 1 KHz, which corresponds to the main frequency component of vertebrate action potentials.

Combining the above equations also demonstrates that the impedance of an electrode will be inversely proportional to its surface area. Several authors have reported modifying the surface of planar electrodes with techniques which are likely to increase the surface area. Edell (1986) for example, reduced the impedance of smooth gold electrodes by 2/5^{ths} by sputter-coating with gold. The electrodes at the end of transparent tracks made of indium-tin oxide have been modified in this way (Gross and Hightower, 1986). Electrolytically deposited gold has also been used (Prohaska *et al.*, 1986; Kim *et al.*, 1985). Although it is less biocompatible

than sputter-coated gold (Loeb *et al.*, 1977) it avoids the need for additional microfabrication steps. A third method of reducing the impedance of an electrode is to use platinium black (e.g. Thomas *et al.*, 1972; Israel *et al.*, 1984; Regehr *et al.*, 1988). Platinium black reduces impedance more than either sputter-coated or electrolytically-deposited gold. It is used here despite the fact that it may be less biocompatible (Robinson *et al.*, 1961).

Electroplating and sputter-coating probably reduce impedance by adding to the microroughness of the electrode and thus increasing the surface area. Edell (1986) has considered the theoretical consequence of changing the size of electrodes directly. He predicts that the peak-to-peak noise decreases rapidly as the diameter of the electrode is increased, levelling off as the electrode radius exceeds 10 μm (~310 μm^2). He also points out however that the cost of increasing electrode size is a loss of signal selectivity. The compromise favoured by the designers of the array used in Glasgow is electrodes with diameters of 10 μm. The arrays used here had slightly larger electrodes (≈100 μm^2) and were made by etching a 10 μm groove through the insulator perpendicular to 10 μm wide electrode tracks.

3.2 Material and Methods

3.2.1 Planar electrode arrays

Photolithography is used in the fabrication process (for an introductory text see Gise & Blanchard, 1979; or White *et al.*, 1983). The first step is to produce a chrome mask of the desired pattern. This can be achieved by photographically reducing a giant prototype.

Glass slides were ultrasonicated for 5 min in a fresh solution of 1 part H_2O_2 in 9 parts H_2SO_4. They were then washed thoroughly (including a further 5 minutes ultrasonication) with double-distilled water. The slides were blow-dried, and heated in an oven at 90°C for 5 min to remove residual moisture. After cooling, a layer of positive photoresist (S1818, Shipley, UK) was spun onto each slide. The appropriate mask was placed on top of the photoresist, and the assembly irradiated with ultraviolet light (Figure 3.2a).

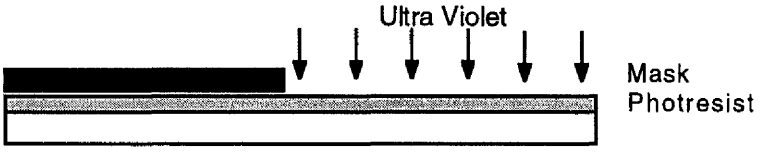

Figure 3.2a

The slides were developed (Shipley developer, UK), washing away the exposed area of photoresist, and a nichrome-gold (60 nm thick)-nichrome sandwich was evaporated over the entire slide (Figure 3.2b). The nichrome enhances the adhesion of the gold to the glass, and subsequent layers to the gold.

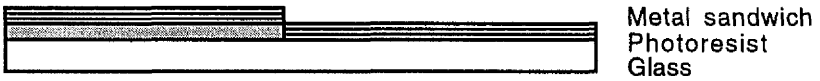

Figure 3.2b

By chemically dissolving away the remaining photoresist with acetone, the unwanted regions of the metal sandwich were lifted off, leaving intact the electrode tracks (Figure 3.2c).

Figure 3.2c

The next step involved depositing a 0.5-2 mm layer of silicon nitride (Si_3N_4) onto the slide to form the insulator). This was achieved by using plasma chemical vapour deposition (CVD)[2].

The final task was to bore through the insulation, at predetermined positions, to form electrodes. A layer of nichrome was evaporated onto the insulator, which was then followed by a layer of positive photoresist (Shipley S1818). The photoresist was patterned using another mask (Figure 3.2d) and developed.

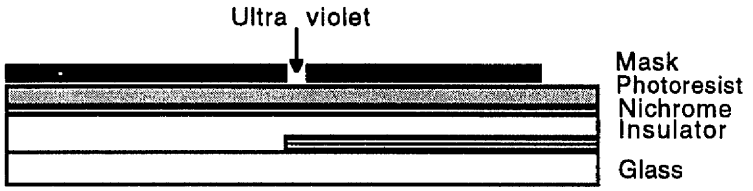

Figure 3.2d

The areas of nichrome uncovered during the development of the photoresist were removed by wet etching with an 80% solution of HCl. (Figure 3.2e).

Figure 3.2e

The remaining nichrome (which was shielded from the wet etch by the photoresist) acts as a mask, selectively protecting the underlying insulator from a subsequent C_2F_6 plasma etch[2]. On completion of the plasma etch, the residual photoresist was removed with acetone, and the remaining nichrome removed by wet etching (Figure 3.2f).

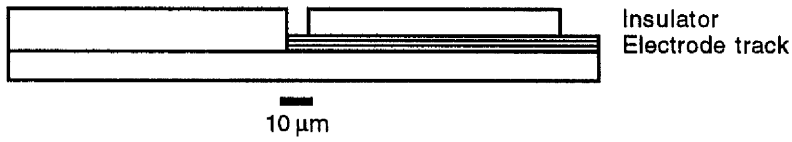

Figure 3.2f

[2]The CVD and C_2F_6 plasma etch steps were performed by Bill Monaghan.

An aerial view of the microfabricated electrode array can be seen in Figure 3.3a. A glass cloning ring is placed over the electrode array and glued in position with a silicone elastomer resin (Sylgard 184; Dow Corning, Barry, UK). The free end of each electrode track was bonded to a printed circuit board with fine gold wires[3]. The printed circuit board extends the electrode tracks to a 'D' plug which facilitates the attachment of pre-amplifiers. A completed structure can be seen in Figure 3.3b.

A large planar gold reference electrode was incorporated in arrays designed for long term experiments. This electrode was also bonded to the printed circuit board. Arrays used for short-term experiments (in which the importance of maintaining aseptic conditions was reduced) were made without the reference electrode, since its large area made it susceptible to damage during washing. A platinum wire placed over the edge of the cloning ring was used as an alternative.

Once a device had been assembled, the gold electrodes were platinised. The cloning ring was filled with a solution containing 1% chloroplatinic acid in 0.0025% HCl and 0.01% lead acetate. The tip of a platinum wire was placed in the solution and used as an anode, with each planar electrode in turn making up the cathode. A 100 nA current was sufficient to form a black deposit at the end of an electrode track within the first few seconds. The process was observed under a dissection microscope, and the current was turned off when the deposite began to extend beyond the rim of the window etched through the insulator

---

[3]The author would like to thank Mary Robertson for enduring many hours bonding the electrode tracks to printed circuit boards.

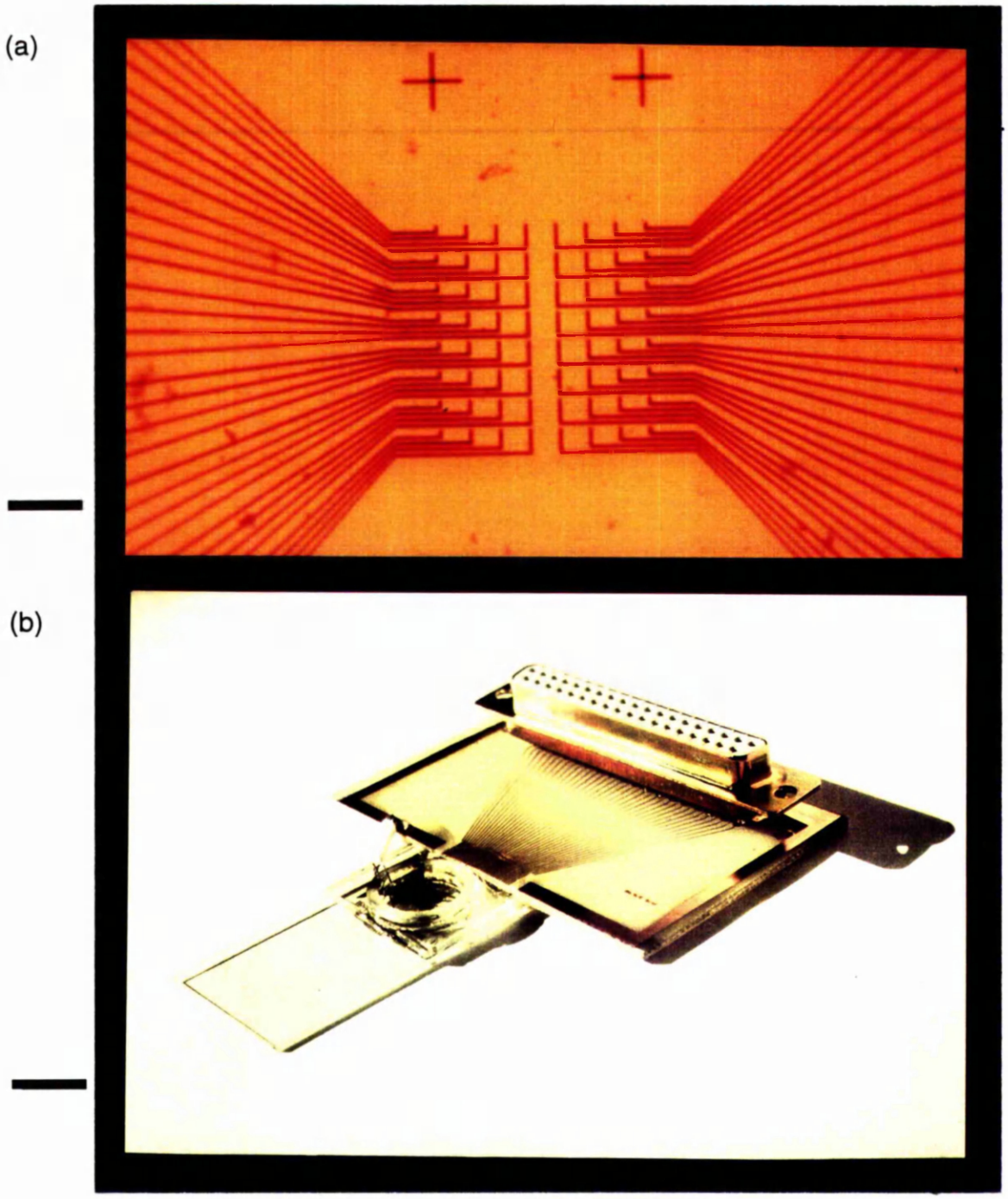

Figure 3.3: Photograph of a planar electrode array. (a) High power view of 64 electrode tracks (scale bar:100 μm). The insulator was removed at the central terminal of each track (giving an 8x8 array of electrodes) or in a line across the tracks as they diverge (producing one or two 32 member linear arrays). Insulator was also removed at the ends of the tracks where the tracks were fully diverged to allow bonding to a printer circuit board. (b) Low power view showing the relationship between the microfabricated device (inside the cloning ring) and the printed circuit board that facilitates the connection of external electronics, via the 'D' plug (scale bar~1.5 cm).

Electrodes arrays were washed extensively with distilled water after platinising. The cloning rings were then filled with Hepes saline (Departmental stocks) and the impedance of each electrode was measured using a specially designed circuit[4].

3.2.2 Cell Isolation

Before each experiment, the arrays were washed in Decon 90 (Decon Lab. Ltd., UK), rinsed thoroughly and left to soak for 12 h in double-distilled water. To enhance adhesion of leech neurones the arrays were coated with Concanavalin A as described in Section 2.2.5. Cells were isolated with long processes using protease (described in Section 2.2) and plated along a row of electrodes with impedances below 500 kΩ. Survival of the processes was enhanced by laying sheets of the capsule which surrounds each ganglion (see Figure 2.3) over the neurones.

3.2.3 Electrophysiology

The electrophysiological setup is illustrated in Figure 3.4. Recordings were made at room temperature, on an air table, in a Faraday cage.

Pairs of planar extracellular electrodes were connected to AC amplifiers (Neurolog NL104; Digitimer, UK) used differentially. Neurolog AC-DC filters (NL125; Digitimer, UK) were used as notch filters to remove 50 Hz interference. The amplifier and filter combination had a low frequency cut-off of 10 Hz and a high frequency cut-off of 5 KHz. The recordings were displayed on Gould two-channel oscilloscopes, digitised at 7 kHz (PCM-4; Medical Systems Corp., Greenvale, N.Y.) and stored on video cassettes. A CED 1401 with Massram (Cambridge Electronic Design Ltd., UK) provided a computer interface for multichannel display. Intracellular recordings from the cell bodies were made using a DC preamplifer (NL102)/AC-DC amplifier

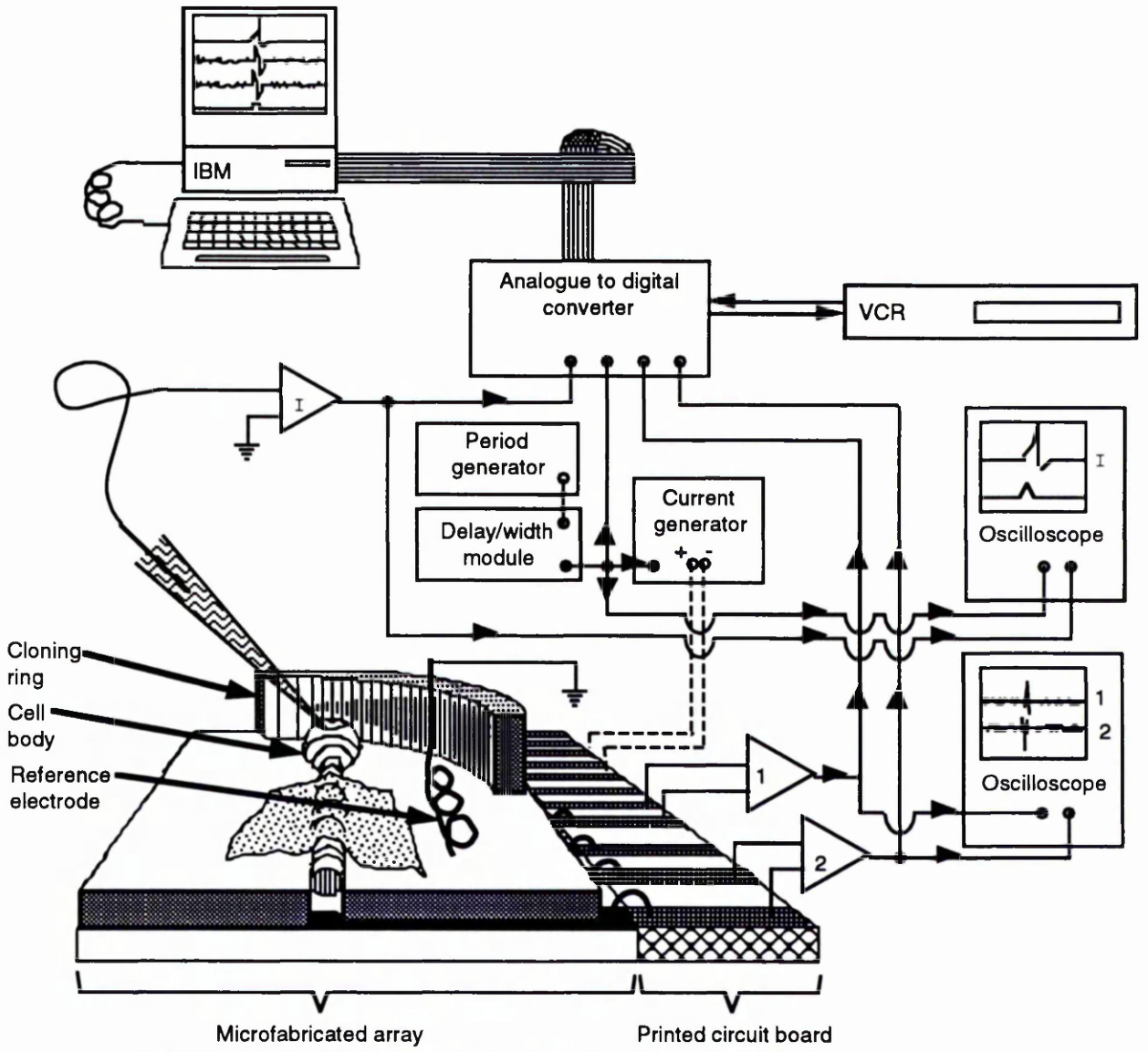

Figure 3.4: The setup used to record from, and stimulate the processes of leech neurones. A section of an array with part of a cloning ring is shown. Processes were plated along the groove in the insulator which exposes the electrode tracks and defines the location of the electrodes. An intracellular electrode (I) was used to record action potentials in the cell body. Extracellular recordings were made using differential amplifiers which subtract the output of one electrode from that of another. Intracellular and extracellular traces were displayed on oscilloscopes, digitised and stored on video cassette. Extracellular stimulation was performed by passing current between two planar electrodes as illustrated. The TTL pulse used to trigger the current injection was stored alongside the intracellular and extracellular recordings on the video tape.

(NL106) combination (also from Digitimer, UK.) with 15-20 MΩ glass microelectrodes (Clark Electromedical Instruments, UK) filled with 3M KCl. The electrodes were driven by either motorised or manual micro-manipulators (DC-3K; Leitz, Germany). The intracellular recordings were displayed and stored as above.

To stimulate through the extracellular electrodes a circuit was used[4] which took a TTL pulse, produced by a Neurolog Delay-width module (NL403) driven by a Neurolog period generator (NL304), and produced a constant current output for the duration of the pulse. The current produced by the circuit could be varied from between 100 to 900 nA.

3.2.4 Measuring conduction velocity

The conduction velocity of action potentials were measured at room temperature by plating the primary process of each neurone along a row of extracellular electrodes. An intracellular electrode was used to verify that the extracellular spikes used for the measurement were true action potentials. For P cells the intracellular electrode was also used to stimulate action potentials as these cells did not fire spontaneously. The time difference between the first extracellular spike that occurred on each channel was taken as the delay in propagation between the electrode pairs.

A photograph was taken of each cell and was used to project a highly magnified image. The negative of a photograph taken of a stage micrometer using the same optics provided calibration. The length of the process between the centres of the electrode pairs was measured (as illustrated in Fig. 3.5) and divided by the propagation delay to give the conduction velocity.

---

[4]Circuit built and designed by Julian Dow

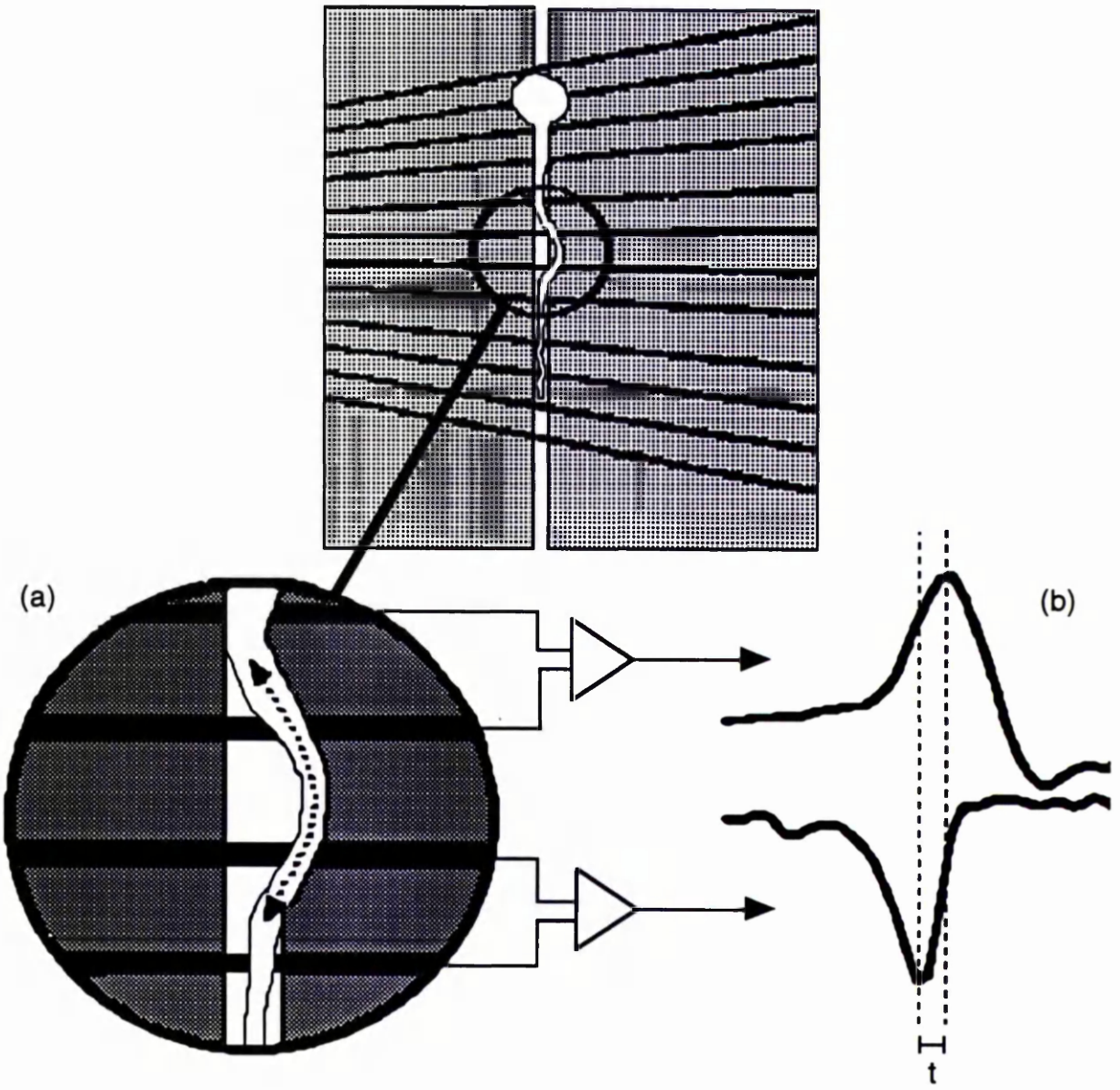

Figure 3.5: Method used to measuring conduction velocity. The length of process between the centres of the two electrode pairs (indicated by the dashed line in part a) was taken as the distance over which the action potential propagated in time t (indicated in part b).

3.3 Results

3.3.1 Optimal spacing of electrodes when using a differential amplifier

Extracellular electrodes monitor the potential fields in their environment. One source of a potential field is the current created by ionic fluxes across the membrane of excitable tissue. Thus, a single extracellular electrode monitors a cell's excitability in terms of the rate of current flow across the membrane, *not* the membrane potential *per se*. Extracellular recordings of action potentials have been shown mathematically and experimentally to be proportional to the second derivative of the membrane potential recorded intracellularly (Geddes, 1972). If an extracellular recording is made by combining the output of two extracellular electrodes (i.e. differentially) the resulting waveform is complicated by the propagation of the action potential between the recording sites. First consider the case of a single electrode.

An amplifier connected to a single signal electrode and a large ground (or reference) electrode, amplifies the difference between the signal voltage and the 'reference' voltage of the ground electrode. Unfortunately, noise constraints limit the use of 'single ended' recordings: electromagnetic interference causes fluctuations in the ground voltage which are superimposed on the signal voltage. This problem can be overcome by making differential recordings using two signal electrodes simultaneously. In this mode, the amplifier subtracts the common components in the two signals and amplifies the difference. Thus, fluctuations common to both electrodes (such as fluctuations in the reference voltage) are eliminated. Note that if the 'output' of each electrode in response to cell excitability was

the same, then the signal would also be eliminated. However, the electrodes occupy slightly different locations and therefore the electrical field (generated by a point source) experienced by the electrodes is slightly different. Increasing the spacing between the electrodes would serve to increase the difference in the electric field experienced by each electrode and could increase the size of the signal. On the other hand, if the spacing is too large, any increase in the size of the signal would be offset by the increase in noise associated with electrodes experiencing slightly different electromagnetic interference.

The above discussion suggests that it might be possible to increase the size of the signal-to-noise ratio by optimising the electrode spacing. During the course of this work, it was observed that if the electrodes were of similar impedance, then the best signal to noise was obtained by using neighbouring electrodes. The spacing of the electrodes used here ranged up to 300 μm. The following experiment suggests that this value may exceed the optimal spacing. Simultaneous intracellular and extracellular recordings were made from a Retzius neurone (without a process) plated over an extracellular electrode. During an attempt to withdraw the electrode at the end of a recording session the cell detached from the surface but remained impaled and continued to fire action potentials. The electrode was used to crane the cell above the surface (see Figure 3.6), using the graticule of the micromanipulator to measure the relative height of the tip of the intracellular electrode (assumed to be equal to the absolute height of the cell above the extracellular electrode). A graph was then plotted of the size of the extracellular signal (normalised to the size of the corresponding intracellular action potential) against the distance of the cell above the extracellular

electrode (Figure 3.6)[5].

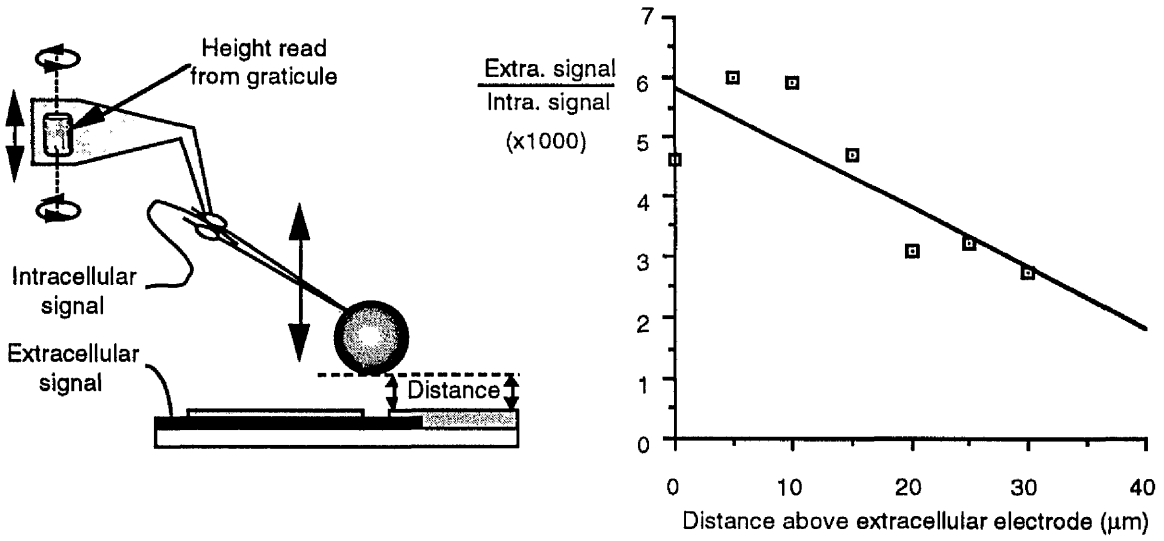

Figure 3.6: Graph of distance of a cell above an extracellular electrode versus the size of the extracellular signal (normalised with the size of the action potential recorded intracellularly). A Retzius neurone, plated over an extracellular electrode was impaled intracellularly. The intracellular electrode was used to crane the cell off the extracellular electrode and the distance was measured from the graticule on the micromanipulator. (Line fitted using Cricket graph.)

Figure 3.6 was produced with data obtained from a single cell. Attempts to repeat the experiment were confounded by the difficulty of lifting a neurone off the substrate whilst maintaining a good impalement. Bearing in mind this cautionary note, the graph suggests that the size of the extracellular signal decreases rapidly with the distance of a cell from an extracellular electrode and predicts that the action potential of a Retzius neurone more than 60 μm from an extracellular electrode would not be

[5]Immediately after lifting the cell off the extracellular electrode the rise time of the action potential recorded intracellularly decreased (presumably the movement *improved* the intracellular impalement). This may explain why the point at distance=0 has a *lower* intracellular/extracellular ratio than the recordings that follow. The width of the action potentials of all the other recordings appeared to be approximately constant.

detected. If the cell body distorted or slipped around the electrode during lifting then the results *over-estimate* the distance over which extracellular signals can be detected. This suggests that the optimal spacing of two extracellular electrodes, to record the activity of a point source using a differential amplifier, may be less than 60 μm.

For an action potential propagating along a process which overlies two extracellular electrodes the optimal spacing may be quite different. In this case the output of the differential amplifier will no longer be the second derivative of the membrane potential. Rather the output will be a result of an interaction between two second derivatives (one from each electrode). The amount of interaction will depend on the time delay between the occurrence of the second derivatives that is a consequence of the propagation of the action potential between the two electrodes. If the conduction velocity is infinitely fast or the spacing between the electrodes is infinitesimally small (and the two electrodes had identical properties) then the two second derivatives cancel. If the conduction velocity is very slow or the electrode spacing is very large then the output of the differential amplifier would consist of two distinct second derivatives, one of which would be inverted. In this case, the delay between a point on each waveform could be used as the delay from which the conduction velocity can be calculated.

For the spacing of the electrodes used here, an intermediate state is likely in which the output of the amplifier consists of a more complex interaction: some of the peaks in the second derivatives may combine whereas others may cancel. Unfortunately, no two points on such a waveform can be used to determine the delay required to calculate the conduction velocity as it becomes impossible to categorically identify two equivalent points as coming from separate second derivatives.

The waveform of the extracellular recordings obtained here were either biphasic or triphasic (intracellular action potentials were biphasic; Figure 3.11).

3.3.2 Multisite extracellular recordings using two or more amplifiers

Initial attempts to make multisite recordings from neurones failed because processes plated along the grooves containing extracellular electrodes tended to degenerate. This problem was overcome following the observation that the processes of cells plated on tissue culture plastic also degenerated *if* the amount of contact made between the process and the substrate was poor. This lead to the possibility that processes degenerated owing to the poor contact made with the sides of grooves. Survival of processes was improved by providing an additional surface for contact from above, in the form of a sheet of ganglion capsule, as illustrated diagrammatically in Figure 3.7 and photographed in Figure 3.9(b). Although not tested quantitatively, the sheet of ganglion capsule may also act as a biocompatible insulator, reducing the current flow to ground and thus increasing the signal to noise ratio.

A comparison between the waveforms from each differential pair reveals the conduction delay associated with the propagation of an action potential. This delay allows the conduction velocity to be calculated but also provides a means of verifying the cellular origin of extracellular spikes. Thus the presence of a time delay alleviates the need for an intracellular electrode in cells that fire spontaneously, and allows the effect of intracellular impalement on the firing frequency of cultured cells to be determined.

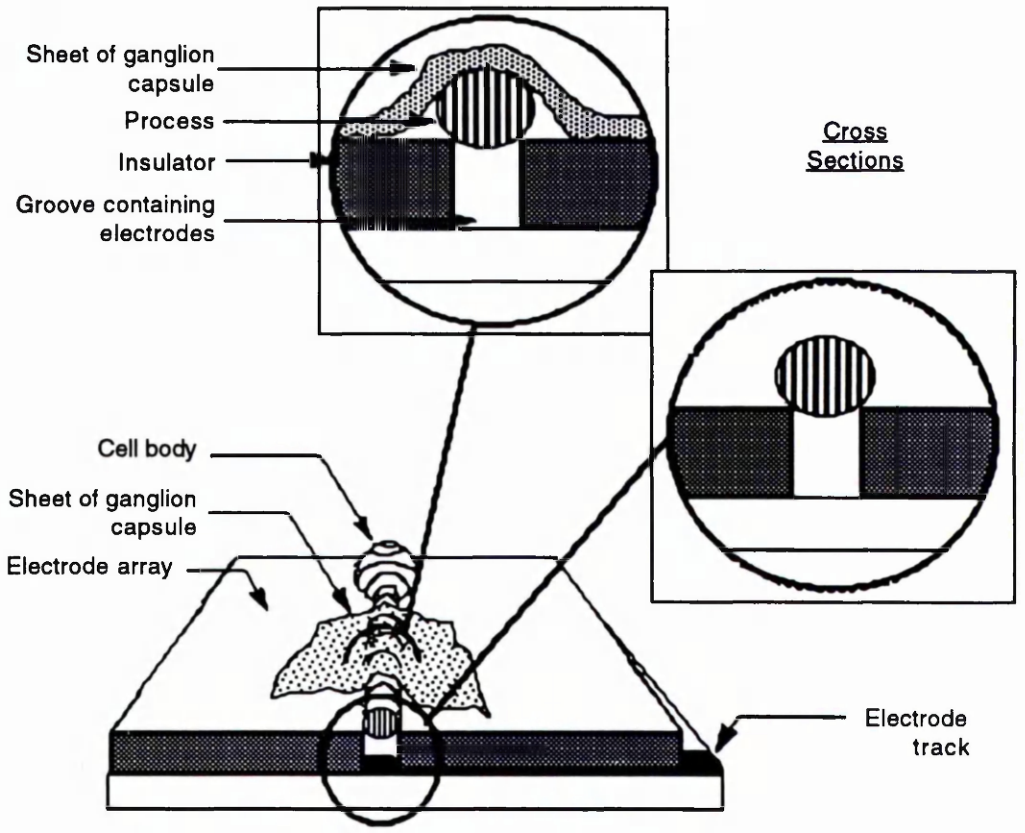

Figure 3.7: Using a sheet of ganglion capsule to increase the contact area of a processes plated along a groove. Lower diagram shows the cell body and process plated along the groove in the insulator which exposes the electrode tracks. Inlays show drawings of the cross sections through the process with and without a sheet of ganglion capsule. Long processes plated along a groove usually degenerated without the sheet.

Effect of intracellular impalement on firing frequency

Figure 3.8 shows inter-spike histograms of spontaneous activity recorded extracellularly from a cultured neurone. One set of recordings were made before inserting a glass microelectrode, the other set was made after it's withdrawal. One second *after* withdrawal it can be seen that the firing frequency has increased to almost twice that recorded prior to impalement.

As well as the increase in firing frequency, Figure 3.8 also suggests that the variability of the interval between spikes is reduced following the removal of the intracellular electrode from the cell. This probably indicates that the frequency of firing following the removal of the intracellular electrode

was limited by the refractory period of the action potentials.

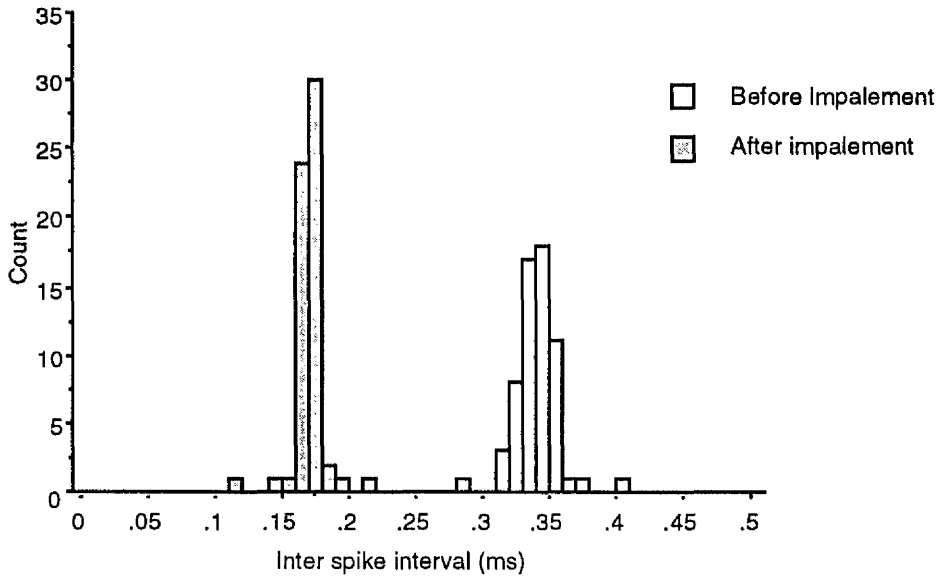

Figure 3.8: Effect of impalement on firing frequency. Inter spike histogram of extracellular recording from a single Retzius neurone before (dots) and after impalement (stripes) with an intracellular electrode.

Conduction Velocity

Figure 3.9 shows a photograph of an isolated P cell, along with an intracellular recording from the cell body and two differential extracellular recordings from the process of the same cell. The intracellular trace is typical of P cells with a single action potential occurring shortly after the onset of a depolarising current injection. The intracellular action potential had a peak-to-peak amplitude of about 80 mV. This can be compared to the extracellular spike recorded differentially from electrodes 30 and 29. This spike had a peak-to-peak amplitude of about 120 μV, only 0.15% of the intracellular signal. The trace has about 30 μV peak-to-peak noise, giving a signal-to-noise ratio of 4:1.

Both extracellular signals are biphasic, but one of the traces appears to be inverted. One explanation for this occurrence is that the site of action potential initiation lies between electrode 27 and electrode 29. The action

action potential would then be expected to propagate in both directions away from the site of initiation. In this case, it would traverse the two pairs of differential electrodes in opposite directions giving similar outputs but with different signs. However, cells in other experiments probably had different spatial relationships with the two pairs of differential electrodes, yet in all cases the inverse relationship between the extracellular traces persisted. In addition, spikes caused by turning on and off the motorised micromanipulator were common to both extracellular recordings and also differed in their sign. Thus a more likely explanation is that one of the amplifiers was wired in a way which inverted the output.

The time delay between the peaks of the two extracellular traces was 168 μs. The section of process which spans the centres of the two electrode pairs was 348 μm long. Hence the conduction velocity of action potentials in the process of this cell was calculated to be 2.07 $m.s^{-1}$.

(a)

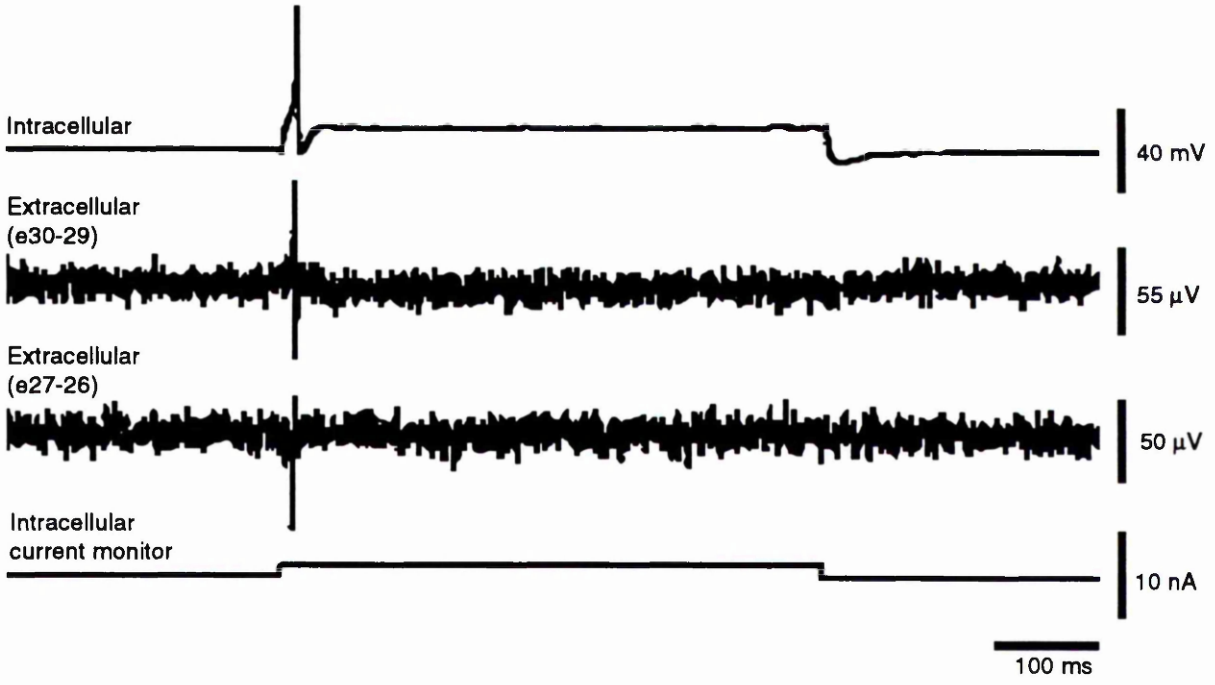
Intracellular
40 mV
Extracellular
(e30-29)
55 µV
Extracellular
(e27-26)
50 µV
Intracellular
current monitor
10 nA
100 ms

(b)

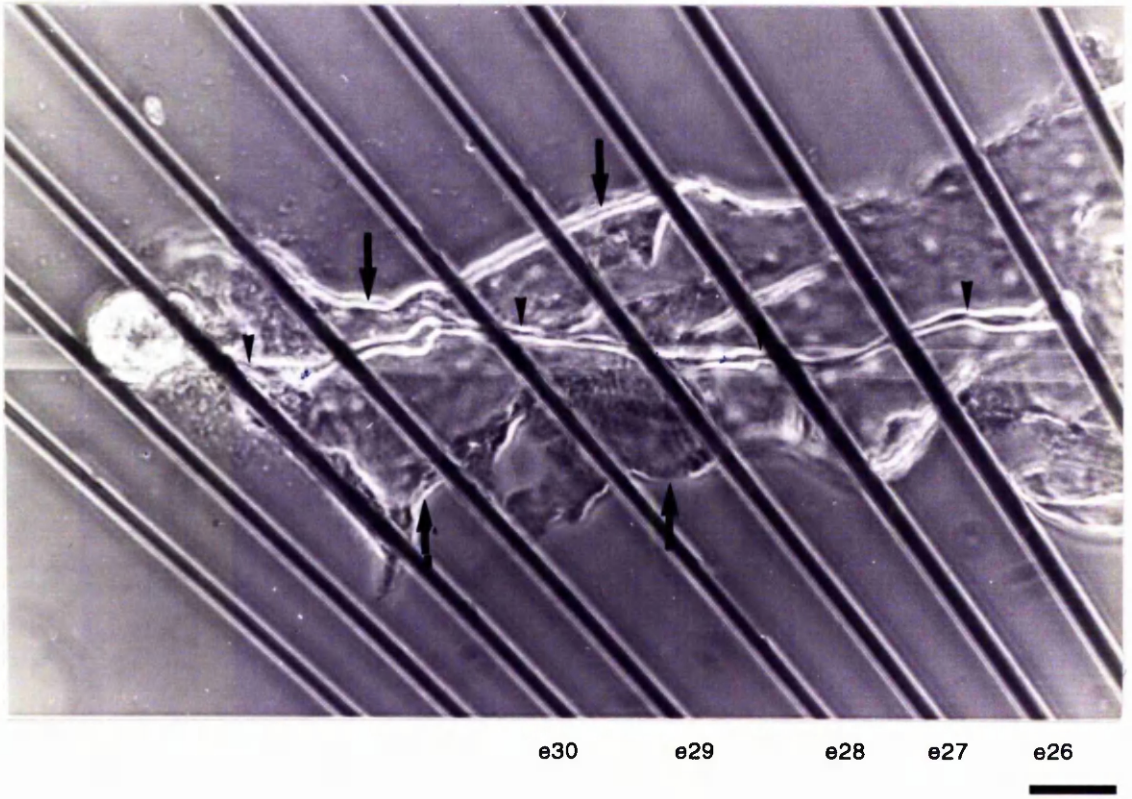
e30
e29
e28
e27
e26

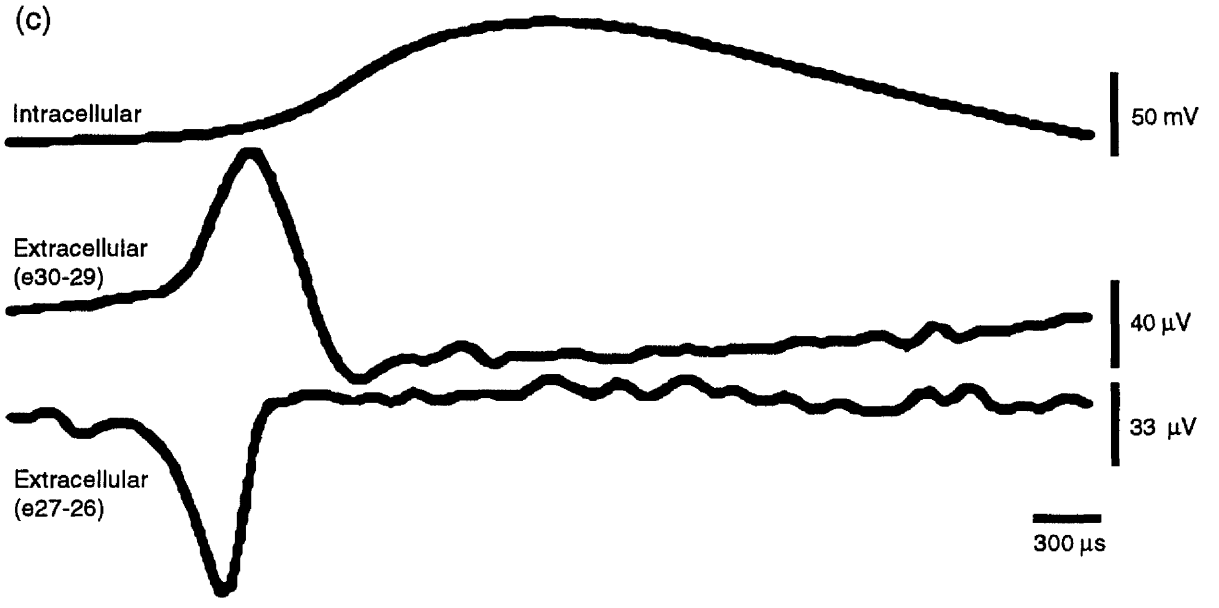

Figure 3.9: Simultaneous multisite extracellular recordings from the process of a P cell using a planar extracellular electrode array. (a; *previous page*) An intracellular electrode (top trace) was used to inject depolarising current (lower trace) into the cell body to initiate an action potential. Differential recordings were made from the process using two pairs of electrodes (middle traces). The location of the electrodes in relation to the cell can be seen from the photograph on the previous page (b; scale bar: 60 µm). The small arrow heads point to the location of the process, whereas the larger arrows indicate the margin of a piece of ganglion capsule which was laid over the plated neurone. (c) Same action potential as in (a) with an expanded time base. Note the time delay and the order of the extracellular spikes.

Considerable difficulties were encountered in positioning the processes of P cells along grooves, perhaps reflecting the smaller diameter and greater flexibility of their primary process (Muller & McMahan, 1976; Mason & Leake, 1978). Despite these difficulties, the conduction velocities of four P cells were determined. The mean conduction velocity of this sample was 1.45 (S.E.M. ±0.36) $m.s^{-1}$. The primary process of Retzius cells have larger diameters and are less flexible, making positioning slightly easier. The conduction velocity of six Retzius neurones was measured, giving an average value of 0.19 (S.E.M. ±0.05) $m.s^{-1}$. A graphical comparison between

the conduction velocities of Retzius and P cells is shown in Figure 3.10. The speed of action potentials in P cells would appear to be almost an order of magnitude faster than the conduction velocity of Retzius neurones. The rise time of P cell action potentials is shorter than that of Retzius neurones. This difference could account for the faster conduction velocity in P cells (Pearson *et al.*, 1970) and may reflect a higher density of sodium channels.

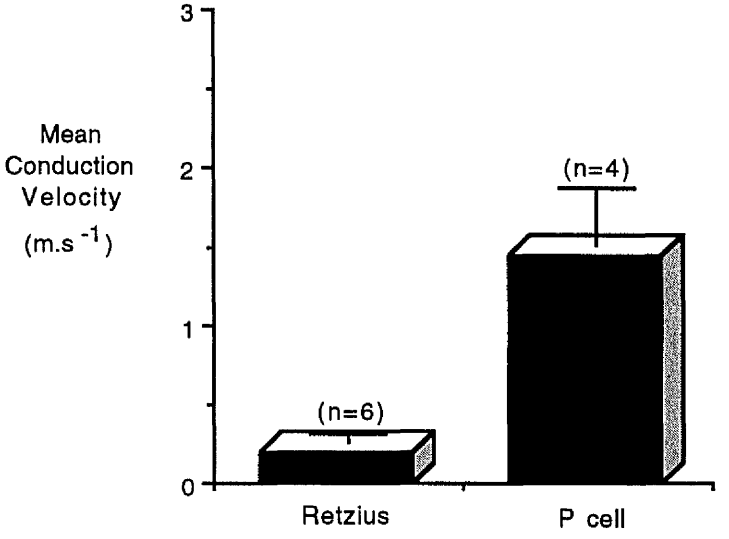

Figure 3.10: The conduction velocity of action potentials from Retzius and P cells. Bars reflect standard errors.

Calculation of the length constant (λ) from the conduction velocity (θ)

In Chapter 2 the length constant was calculated from the value of R_m derived from the input resistance, the diameter of a process and an estimate of the axoplasmic resistance, R_i (see equation 2.4). According to Jack *et al.* (1975) the time constant of the foot of the action potential (τ_{foot}) can be expressed in terms of the length constant (λ), the conduction velocity (θ) and the membrane time constant (τ_m):

$$\tau_{foot}=\frac{(\lambda/\theta)2}{\tau_m} \qquad (3.4)$$

Rearranging equation 3.4 to make the length constant the subject gives:

$$\lambda=\theta\sqrt{\tau_{foot}.\tau_m} \qquad (3.5)$$

The τ_{foot} of six Retzius neurones was calculated from six action potentials using plots of ln(dV/dt) against time[6]. The average value was 18.4 (±1.52 S.E.M.) ms. Using this value for τ_{foot}, the upper and lower estimates for the membrane time constant of isolated Retzius neurones calculated in Section 2.3.4, and the average conduction velocity gives an upper and lower estimate for the length constant. The lower estimate is 8.0 mm and the upper estimate is 9.2 mm. These are approximately twice the values obtained in Chapter 2 using equation 2.4.

Origin of the Action potential

The delay between extracellular spikes allows the conduction velocity to be measured whereas the *order* of the spikes indicate the direction of propagation. In Figure 3.9 the distal pair of electrodes (i.e. e27 & e26) experienced the field effects caused by the action potential before the more proximal pair (i.e. e30 & e29). Thus it seems highly probable that the action potential propagates from the tip of the process towards the cell body. The action potentials of all the other neurones examined (both P cells and Retzius neurones) shared the same direction of propagation (see part (c) of Figure 3.11 for an example of multisite recordings from a Retzius neurone).

---

[6]τ_{foot} was calculated for each cell from measurements made using two intracellular electodes. One was used to inject a depolarising current just sufficient to initiate an action potential, which was recorded using the second electrode. At different times (t) after the current onset the slope (dV/dt) of the prepotential (or foot) of the action potential was measured. τ_{foot} was taken as the gradient of the line of ln(dV/dt) plotted against t (see section 2.2.7 for more details on this approach).

3.3.3 Stimulation

In addition to making multisite recordings, extracellular electrodes can also be used to non-invasively stimulate the processes of neurones. Previous attempts to stimulate neurones using planar extracellular electrodes have successfully generated action potentials (Pine, 1980). However, this success was offset by the disturbance at the electrode-medium interface caused by the injected current. The disturbance is sufficient in amplitude and duration to make the likelihood of using a single gold extracellular electrode to stimulate and then to record the resulting activity remote. By having a number of electrodes located under the same cell this problem can be avoided: one extracellular electrode can be dedicated to the task of stimulation, whilst the others can be used solely as extracellular recording electrodes. This approach could provide a means of verifying the production of action potentials during experiments which involve long term stimulation.

Figure 3.11 shows recordings made during the extracellular stimulation of a process belonging to an isolated Retzius neurone. Although there is an increase in spontaneous activity, the size and shape of intracellular action potentials that follow the extracellular current pulse are unaffected. However, the intracellular spike initiated by stimulation differs from a normal action potential in that it lacks a prepotential. Presumably, the potential field generated at the tip of the extracellular electrode was sufficient to cause a virtually instantaneous activation of a large number of voltage activated sodium channels. The number of channels opened may be equivalent to the maximum number that opens during a spontaneous action potential (the rising phase of the intracellular record in Figure 3.11d can be


(a)
Intracellular
20mV
e14-e13
100µV
100 msec
e11-e10
50µV
e12
100 nA

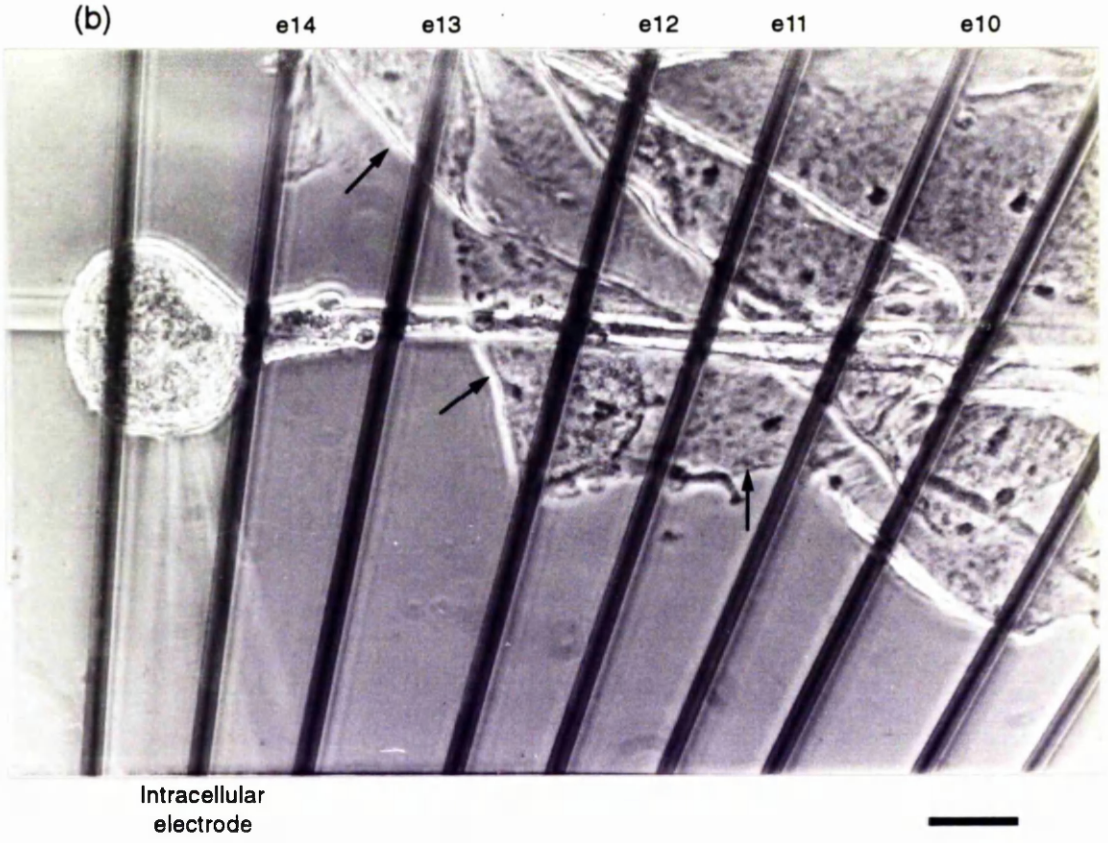
(b)
e14
e13
e12
e11
e10
Intracellular
electrode

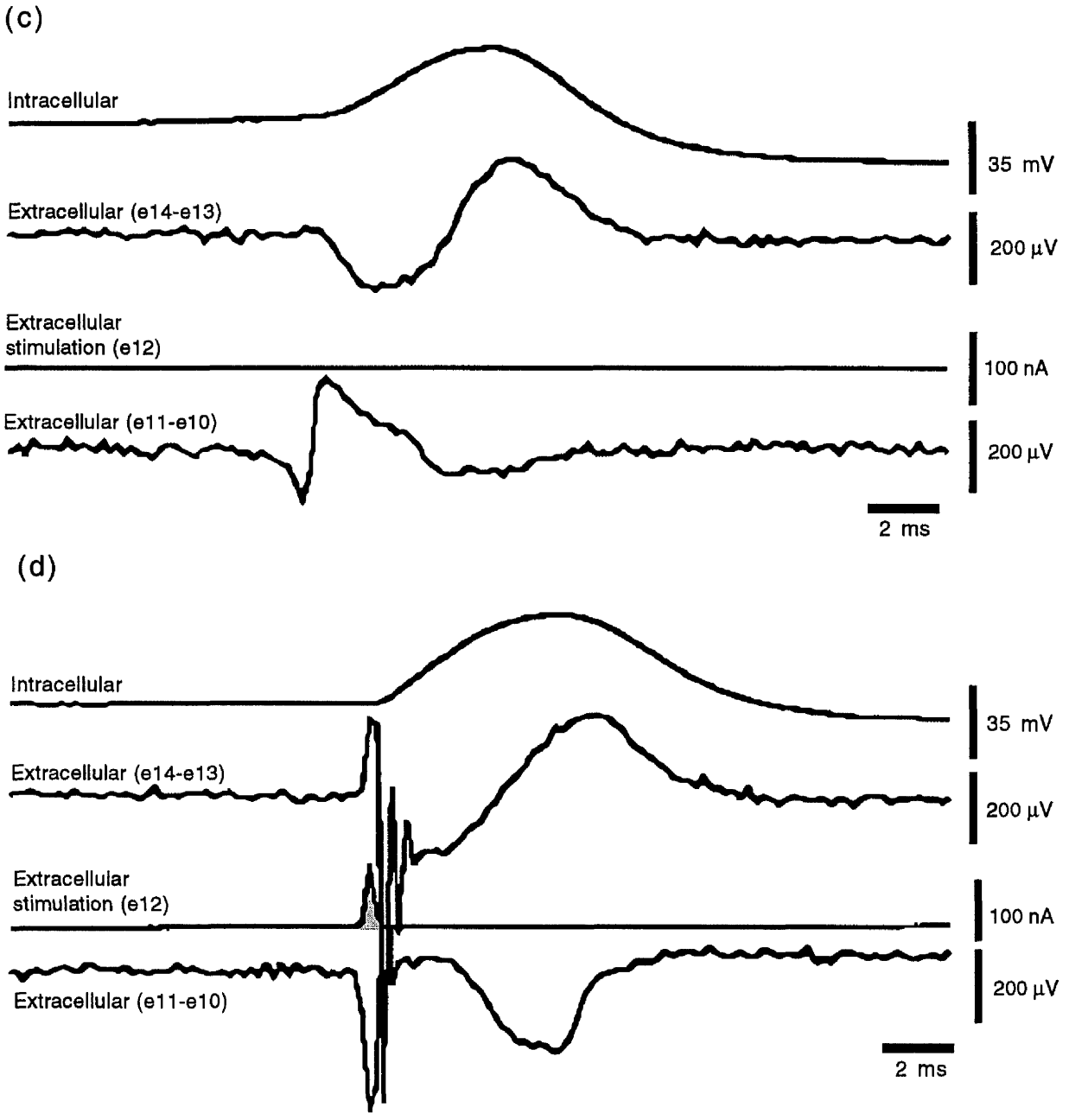

Figure 3.11: Simultaneous multisite recordings from a Retzius neurone during the extracellular stimulation of the process using a planar extracellular electrode array. (a; *previous page*) Intracellular recording from the cell body and differential extracellular recordings from a proximal section of process (e14-e13) and a more distal section (e11-e10). The intervening trace shows the TTL signal used to generate the current pulse which was injected through electrode 12 (scaled in the Figure to the magnitude of the injected current). The relative position of the electrodes to the cell can be seen from the photograph on the previous page (b; scale bar: 40 µm). Note the overlying sheet of ganglion capsule (indicated by the arrows). The shape of the extracellular signature produced by a spontaneous action potential (c) can be compared with the signature of an action potential (from the same cell), stimulated by passing current through electrode 12 (d).

described by a straight line, not an exponential as in Figure 3.11c).

The extracellular traces show that action potentials produced by extracellular stimulation can be resolved using extracellular recording electrodes. Unfortunately, the initial part of the signal waveform from each extracellular amplifier is distorted by the stimulus artifact. The rest of the waveform, however, is similar to extracellular traces produced by spontaneous action potentials (compare the extracellular traces of Figure 3.11c with those of Figure 3.11d).

Comparing the intracellular recording with the extracellular recordings during a spontaneous and an extracellular-stimulated action potential reveals a subtle difference. Consider the peak of the intracellular action potential in Figure 3.11c and Figure 3.11d, with the positive peaks of the extracellular recordings made differentially between electrodes 14 and 13. In Figure 3.11d the delay between these intracellular and extracellular peaks is more substantial than in Figure 3.11c. Thus the difference between the onset of the downward peak of the extracellular recording and the intracellular action potentials is likely to be less when extracellularly stimulated. One way to interpret this difference is that the action potential in the cell body (recorded by the intracellular electrode) occurs sooner in relation to the extracellular action potential when activity is initiated by extracellular stimulation (i.e. in Figure 3.11d). Note that the action potential in the process still propagates towards the cell body as judged by the order of the peaks in the two differential extracellular recordings.

In summary Figure 3.11 shows that action potentials induced by extracellular stimulation can be detected by other extracellular electrodes under the same cell. The sequence of events recorded both intracellularly from the cell body and extracellularly from the process provides information

about the pattern of activity. Comparing the recordings of Figure 3.11 parts c & d suggests that the extracellular stimulation instantaneously reduces the membrane potential to above threshold over a larger proportion of the cell than spontaneous activity originating at the tip of the extracted process.

3.4 Discussion

3.4.1 Conduction velocity

The conduction velocity of an action potential is dependent on a number of factors. These include the temperature (Hodgkin & Katz, 1949), the extracellular resistance (Hodgkin, 1939), the axoplasmic resistance (Baker *et al.*, 1962) and the diameter of the process (discussed below). Most of the variation between the conduction velocities of neurones from different animals (see Table 3.2) may be explained by species-specific differences in these parameters. However, differences in the conduction velocity of different neurones from the same animal have also been reported (e.g. Gasser & Erlanger; 1927). These differences have been attributed to variation in axon diameter. Hursh (1939) for example showed that the conduction velocity of myelinated cat neurones was directly proportional to the diameter of the axons. A linear relationship between conduction velocity and fibre size has also been demonstrated for non-myelinated fibres of mammalian peripheral nerve (Gasser; 1950) and for squid giant fibres (Hodes; 1953). However, two reports suggest that the conduction velocity of squid neurones is proportional to the *square root* of axon diameter (Pumphrey & Young, 1983; Burrows *et al.*, 1965). Furthermore, a

Cell type	Conduction velocity ($m.s^{-1}$)	Diameter (μm)	References
Squid giant axon	25	500	Katz (1948)
Crab axon	4.5	30	Katz (1948)
Non myelinated Parallel fibre in skate cerebellar slices (dye with diode array)	0.13	2?	Konnerth *et al.*, 1987.
Pyramidal cells in the CA1 region of hippocampus slices (Dye with diode array)	0.1	2?	Grinvald *et al.*, 1982c.
Axons innervating deep extensor abdominal muscle of Rock Lobster	2.8-3.5	50	Parnas *et al.*, 1991.
Mouse neuroblastoma (N1E-115). Recorded from soma & process.	0.4	6	Grinvald *et al.*, 1981.
Fibres in the nerve of a cat	6D	D	Hursh, 1939.
Dendritic branches and axons of rat and kitten cerebella cultures using microelectrodes	0.02-0.05	<2?	Hild & Tasaki,1962.
Cultured *Aplysia* abdominal ganglia neurones	0.1	1-2	Stepnoski *et al.*, 1990.

Table 3.2: The conduction velocity and diameter of a selection of different cell types. Question marks indicate that the diameter of the axons were not published with the estimate of the conduction velocity. D's stand for diameter.

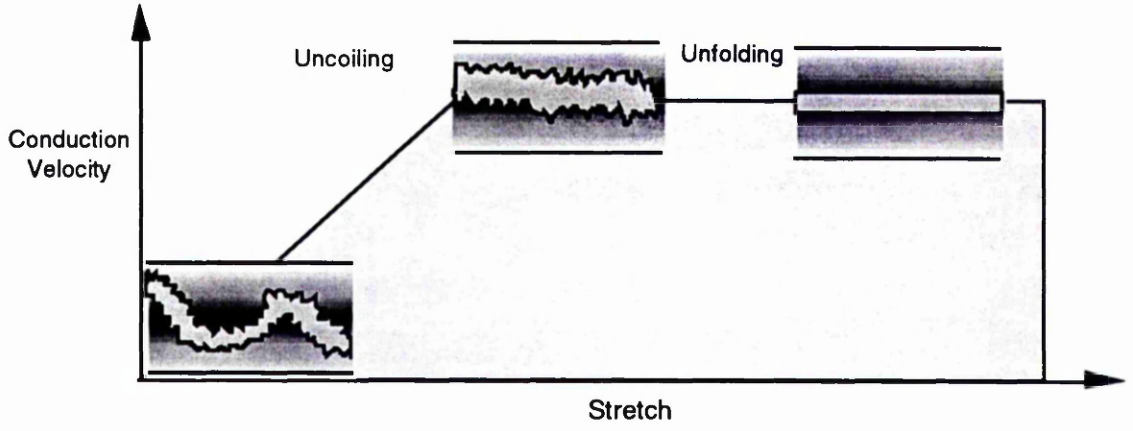

Figure 3.12: Conduction velocity and membrane invaginations. When a nerve is stretched from zero tension the conduction velocities of axons increase, this is correlated with uncoiling. Further tension causes unfolding of invaginations and a reduction in the diameter of axons, but does not cause a further increase in conduction velocity.

mathematical analysis also predicts a non-linear, square-root relationship (Hodgkin & Huxley, 1952).

If axon diameter directly affects conduction velocity, then one would expect the conduction velocity to decrease if the the axon was stretched longitudinally. This type of experiment has been performed on the median giant fibre in the ventral cord of *Lumbricus* (Bullock *et al.*, 1950) and on single nerve fibres within the pleuro-visceral connective of *Aplysia* (Goldman, 1961). In both cases initial stretch (from zero tension) caused an increase in conduction velocity. This phase correlated with, and can be explained by, the uncoiling of the fibre within the connectives (Figure 3.12). Subsequent stretch caused the apparent diameter of the fibres to decrease but no further change in the conduction velocity was observed. During this phase the membrane of the fibres may be unfolding, which would reduce the membrane capacitance 'per apparent' unit area whilst increasing the conductance 'per apparent' unit area. These effects may cancel, leading to no net change in conduction velocity (see Goldman, 1961). It should be noted that this does not imply that the conduction velocity is independent of the diameter or the degree of infolding. Rather, the effect of reducing the infolding may balance the effect of reducing the diameter.

The above discussion justifies the approach used here to measure the conduction velocity. Firstly, the length of process between the recording sites can be accurately measured. This avoids the under-estimate which may otherwise result from the coiled structure of a process within a connective. Secondly, if the process is stretched during extraction then the estimate of conduction velocity may still be an accurate one, as conduction velocity is unaffected by stretch.

Of the two types of neurone used here, the P cell had the faster

conduction velocity (by almost an order of magnitude), despite the fact that processes of Retzius neurones had slightly larger diameters. Obviously, another factor must account for the difference. A likely candidate is the density of voltage dependent sodium channels. A high density would decrease $\tau_{foot,}$ and (from equation 3.5) would lead to a faster conduction velocity. The faster rise time of P cell action potentials can be seen by comparing the intracellular traces of Figure 3.9 with those of Figure 3.11.

Recently, another group has also produced an estimate of the conduction velocity of cultured leech Retzius neurones (Fromherz, personal communication). Their value for the conduction velocity (measurement using voltage sensitive dyes) is almost half that reported here (0.1 $m.s^{-1}$ compared to 0.19 $m.s^{-1}$). However, some difference would be expected on the grounds that the processes in which the action potentials were measured differed in diameter. Fromherz *et al.* made their recording from a process grown on leech extracellular matrix. This substrate supports the outgrowth of thin processes which were probably less than half the diameter of the extracted processes used here (see Section 4.3.2; Chiquet & Acklin, 1986). The substrate may also affect the degree of infolding, which may also give rise to some of the difference.

Another factor which may explain the differences in the measured conduction velocity of leech Retzius cells is the difference in the enzyme treatment used for their extraction. Enzyme treatment may irreversibly affect the electrical properties of the neurones. For example, the enzyme treatment used by Fromhertz may have *reduced* the conduction velocity. In the present set of experiments no evidence was found for a change in the half-width of action potentials recorded from the cell body of Retzius neurones

isolated using protease (see Section 2.3.2). A remote possibility is that the protease *increased* the conduction velocity of the process without affecting the electrical properties of the cell body.

Finally, the discrepancy between the estimates of the conduction velocity of action potentials in Retzius neurones could be explained if the membranes of new and extracted processes differ in their channel distribution. Optical recording techniques have revealed that calcium influxes associated with intracellular somatic stimulation were absent from *newly formed* processes grown on Concanavalin A (Ross *et al.*, 1987) but not from newly formed processes grown on leech extracellular matrix. If the extracted processes plated here were stripped of a small proportion of their calcium channels the membrane would be slightly more resistive during an action potential, increasing the membrane time constant (τ_m) and hence reducing dV/dt. This would tend to reduce the conduction velocity. A more likely alternative to changes in the calcium channel distribution of extracted processes, is that new outgrowth has an abnormally high sodium channel density. Garcia *et al.* (1989) have provided direct evidence in support of this hypothesis by mapping channel densities in leech neurones using the loose-patch clamp technique (see Section 2.4.1).

Invasion of the action potential into the cell body

When an action potential invades the cell body, it is likely that a delay occurs as a result of the additional expanse of cell membrane that has to be charged (Khodorov & Timin, 1975). If the delay could be measured it could be used to refine the value of variables determined in the previous Chapter or to calculate the values of new parameters such as the degree of membrane invagination.

Unfortunately there are considerable problems in making an accurate measurement of the invasion delay. One of the most serious is the difficulty of comparing intracellular with extracellular traces. If extracellular recordings were made with a single signal electrode the second derivative of the intracellular trace would be all that is required for the comparison. The delay between the two waveforms could then be corrected to account for the delay that results from the propagation of an action potential from the extracellular recording site to the place where the process joins the cell body, leaving the delay associated with invasion into the cell body. However, the use of differential a.c. amplifiers complicates the waveform of extracellular recordings (Section 3.3.2) and makes a comparison with a derivative of the intracellular electrode highly risky.

No attempt at the measurement was made here, but in Section 3.4.5 a modification to electrode arrays is discussed which avoids the need for differential recordings. This adaptation may be of considerable value in determining the delay of action potential invasion into the cell body.

3.4.2 Direction of propagation

In vivo, action potentials of mechanosensory neurones such as the P cells, are likely to propagate towards the CNS (Nicholls & Baylor, 1968). On the other hand action potentials in Retzius neurones appear to cause the release of 5-HT from terminals associated with the body wall (Mason *et al.,* 1979). Therefore, the action potentials of Retzius neurones are likely to propagate away from the CNS. The results show that *in vitro* the action potentials of both cell types propagate towards the cell body.

In Figure 3.9 and Figure 3.11 it is apparent that action potentials propagate from the distal end of the process towards the cell body. This is

true for action potentials stimulated by depolarising the cell body using an intracellular electrode (Figure 3.9), for action potentials initiated by extracellular stimulation of the process and for spontaneous action potentials. In all these cases the site of initiation is likely to be located at the terminal of the process. This supports and extends the conclusion of Bookman *et al.* (1987) and Garcia *et al.* (1989) who suggest that the tip of the extracted process is rich in voltage-sensitive sodium channels. It would appear that not only is this site rich in sodium channels, but it has the highest density to be found anywhere on extracted neurones.

When the intracellularly injected and extracellular generated currents initiate action potentials, they mostly do so by passive spread from their site of origin (the cell body and process respectively) to the broken stump. This electrotonic potential must be below the threshold of the intervening membrane but above the threshold of the region of high channel density at the stump. Thus, either the difference between the threshold at the stump ($V_{Th(stump)}$) and that of other regions ($V_{Th(other)}$) is very large, or alternatively the length constant of the process must be very large. Thus:

$$V_{Th(stump)} - V_{Th(other)} \propto \frac{1}{\lambda} \qquad (3.6)$$

3.4.3 Extracellular stimulation

Extracellular stimulation was sufficient to stimulate action potentials as recorded both intracellularly and extracellularly. The direction in which these action potentials propagate along the process is the same as the direction of propagation of spontaneous action potentials. However, in one cell extracellular stimulation of the process reduced the delay between the action potentials recorded extracellularly in the process and the action potential in the cell body recorded with an intracellular electrode.

Spontaneous action potentials are triggered by a cascade of channel openings. Initially, a slow depolarisation (for example produced by the slow kinetics of voltage sensitive calcium channels) causes the opening of additional channels, which increases membrane depolarisation, opening a greater number of channels, and so on. This cascade takes time owing to the kinetics of the channels, the membrane time constant and the lateral spread of charge (see Chapter 2). During extracellular stimulation this cascade is short-circuited (the membrane potential during the rising phase of the intracellular action potential increases linearly). Yet despite the short circuit the action potential in the process occurs before that of the cell body, thus the time courses of the two action potentials must be quite different. Specifically, the time constant of the foot of an action potential (see the filled triangle in Figure 2.6) in the process must be shorter than that measured in the cell body. Equation 3.4 can be used to evaluate the τ_{foot} providing the membrane time constant and the length constant (both calculated from measurements made from the cell body) are accurate and applicable to the process. Using the upper limit for the membrane time constant calculated in Section 2.3.4 and the corresponding length constant gives the value for τ_{foot} as 6.91 ms. This is considerably faster than the value of 18.4 ms obtained from measurements of the action potential recorded from the cell body.

If the τ_{foot} of an action potential in the process is shorter than that measured in the cell body it would explain some of the discrepancy between the length constants calculated from equation 3.5 (which makes use of the conduction velocity) and the values calculated from equation 2.4 (which uses the estimate of the specific membrane resistance). This in turn means that the difference between the threshold at the broken end of the process and the threshold of the rest of the membrane is far larger than the difference

that would be expected using the length constant derived from the conduction velocity.

3.4.4 Improving performance

This Chapter demonstrates that problems arising as a result of the comparatively low spatial frequency of extracellular recordings can be overcome. Several problems remain, including the difficulty of recording from very thin processes and the problems of detecting subthreshold events. These two problems are related in that they both require the detection of a very small perturbance in the electric field which surrounds the electrode. Attempts to improve the recordings made by planar electrode arrays can be divided into at least three classes.

One class includes attempts to build devices which incorporate electronics on the substrate that supports the electrodes. Originally, only buffer amplifiers were included (Bergveld, 1968; Wise and Angell, 1975). More recently, multiplexers have been added (Jobling *et al.*, 1981) and the most advanced devices include circuits to test the impedance of the recording sites so that electrode characteristics can be readily monitored (BeMent *et al.*, 1986).

In terms of the effect on signal-to-noise ratio, the built in amplifiers are the most interesting aspect of this development. In the most extreme cases the recording sites double as gate electrodes for underlying Metal-Oxide-Semiconductor Field Effect Transistors (MOSFETs; Jobling *et al.*, 1981; Fromhertz, 1990). When used in the source-follower mode, these behave as self-biasing buffer amplifiers. Thus, they eliminate "passive" conducting tracks which are prone to electrostatic pick up. This is particularly important for recordings made *in vivo*, where the distance between electrodes and

external electronics may be large. In the recordings reported here, the signals were virtually free of electrostatic pickup[7]. This was eliminated by shielding the preparation using a Faraday cage and employing differential amplifiers. Although differential amplifiers give good signal-to-noise ratios they require two neighbouring signal electrodes per amplifier, effectively halving the spatial resolution of the recordings. In addition, for action potentials propagating along a process, differential recordings are difficult to decipher in terms of changes in membrane voltage. If MOSFETs replace planar electrodes, it may be possible to measure the time it takes for action potentials to invade the cell body, and determine directly the shape of action potentials in processes. Further more, improving the spatial resolution of recording devices may enable experimenters to determine whether action potentials propagate uniformly.

The second approach used to improve recordings is to form a high resistance seal between neurones and electrodes. This has two consequences. Firstly, the signal to noise ratio is dramatically improved. Ratios of 100:1 have been reported (Regehr *et al.*, 1988) and 5 mV peak-to-

---

[7]The remaining noise can be divided into several categories. One is thermal (or Johnson) noise caused by the random motion of electrons and is proportional to the square root of electrode resistance and frequency band width. 10μV rms of noise would be expected from this source with a 1 MΩ resistor and a sampling frequency of 10 KHz. A second source of noice is shot noise which describes the random motion of electrons from a cathode to an anode. This is probably of the same order of magnitude as thermal noise (Buckingham, 1983). A third source of noise is biological in origin, and consists of perturbations caused by movement of the cell. Convection currents may have a similar effect.

peak signals have been obtained (L.Breckenridge, personal communication). Secondly the recordings show a greater sensitivity to slow changes in membrane potential. This can be seen qualitatively by considering Figure 3.13. When charge enters the "patch" (formed when a cell forms a high resistance seal over an electrode pit) it causes a voltage change at the interface of the underlying electrode which is proportional to the flux through the cell membrane. Reducing the seal (as in Figure 3.13b) causes some of the charge produced by a flux to leak from the patch. Rapid ionic fluxes from the cell will still "flood" the electric field around the electrode, but the voltage across the electrode will diminish rapidly as the charge dissipates from the pit. This reduces the likelihood of detecting small, slow ionic fluxes from cells when seals are not formed over electrodes.

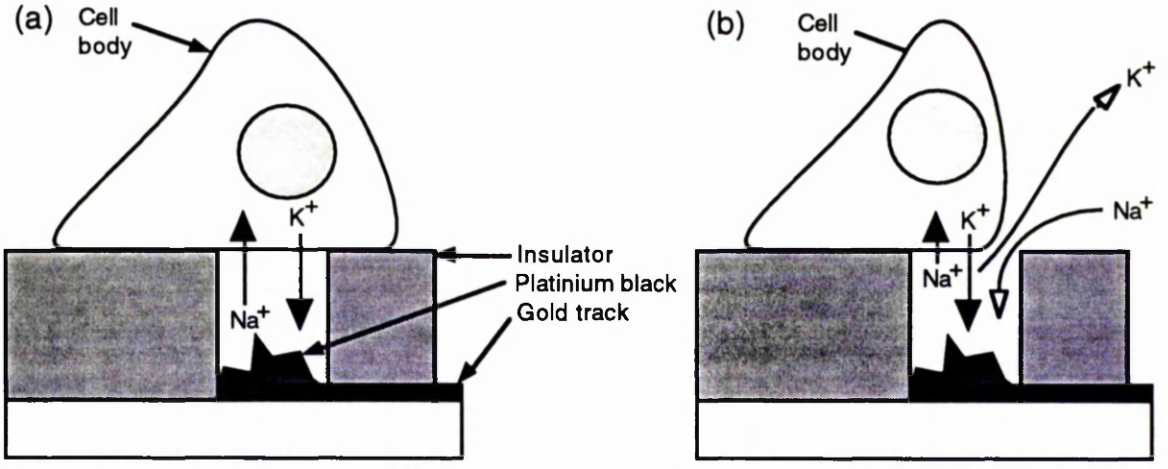

Figure 3.13: The effect of a cell sealing over an extracellular electrode. Field effects caused by ionic fluxes in (a) will be long lasting as the current paths to ground are reduced. In (b) the seal is insufficient to prevent the escape of current or ionic redistribution. Rapid ionic fluxes will be detected, however the resulting field effects will rapidly diminish as ions equilibrate and charge escapes to ground.

High seal recordings have been reliably obtained from cell bodies of *Helisoma* neurones using a microfabricated "diving board" electrode (Regehr *et al.*, 1988) and from the cell bodies of *Helisoma* and *Lymnea* neurones using planar electrodes (Tank *et al.*, 1986; L.Breckenridge, personal communication). In addition, Fromherz *et al.* (1991) have recently succeeded in making similar recordings from the cell bodies of leech neurones by using MOSFETs coated with polylysine. If this type of recording can be achieved reliably, then it may be possible to make continuous long term recordings of synaptogenesis and synapse-induced modifications of network function.

It would seem probable that as the diameter of cells decrease their maximum spread area also decrease. Thus, it is likely that sealing cells over electrodes becomes increasing difficult the smaller the diameter of the cell. Vertebrate neurones have been tried with limited success (Regehr *et al.*, 1988), and it seems unlikely that this technique can be refined sufficiently to record from very fine, cylindrical processes. However, sealing electrodes with larger processes may be possible: in the following Chapter interference reflection microscopy is used to show that extracted processes of leech neurones do spread to a certain degree.

A third approach may be more universal. Recently, a computer simulation has predicted that the placement of recording electrodes at the bottom of a deep groove may improve the signal-to-noise of extracellular recordings by a factor of 10 (Lind, 1991). Preliminary results, using heart myoblasts, support this view (Lind, 1991). The walls of the grooves confine the current paths around the electrode, increasing the size of the signals. Similarly, extracellular insulation may have been provided by a glial monolayer which was reported to cover vertebrate neurones recorded with

extracellular electrode arrays (Gross & Hightower, 1986). The use of deep grooves has several advantages over the use of glial sheets. Firstly, the glia hinder experimental accessibility, which might be important in a post-recording morphological or histochemical analysis. Secondly, experimentally imposed changes in the ionic and pharmacological nature of the culture medium may be buffered by the glia in the small volume of liquid under the glial sheet. Thirdly, deep grooves provide strong topographical features that are likely to align neurite outgrowth by means of contact guidance (see Chapter 5). This would not only ensure that processes cross consecutive electrodes but it also gives rise to the possibility of recording from networks of neurones in which the morphology of, and the interaction between, cells is under experimental control.

3.5 Conclusions

• This Chapter demonstrates for the first time the use of extracellular electrode arrays to make multisite recordings from the processes of single neurones. This was achieved by exploiting the method described in Chapter 2 for extracting leech neurones with very long processes.

• It is necessary to verify that extracellular events relate to cell excitability. Intracellular recordings can be used for this purpose, but a more satisfactory solution is to use a property inherent in the extracellular recordings. The propagation of an action potential between two points on a cell necessitates a delay. By making multisite recordings this delay can be used as a criteria to identify events caused by cell excitability.

• The conduction velocities of action potentials of two cell types (Retzius and P cells) were ascertained. The P cells had the fastest conduction velocity and the fastest rising action potentials. However, they also have the thinner processes. The conduction velocity of Retzius neurones was used to calculate the length constant.

• The order of the extracellular traces revealed the direction of propagation. For both cell types the action potentials propagate from the distal end of the process towards the cell body. This direction of propagation was apparent for both spontaneous and stimulated action potentials and indicates that the distal end of the process contains a zone with the lowest threshold.

• Extracellular stimulation of individual processes is sufficient to initiate action potentials that can be recorded both intracellularly and by other extracellular electrodes. The time course of intracellular and extracellular events following the extracellular stimulation of one cell suggests that the action potentials in the processes have faster rise times than those that are

recorded in the cell body. A similar conclusion can be drawn by comparing the time constant at the foot of the action potential (recorded intracellularly from the cell body) with a value derived from the conduction velocity of the process.

• Extracellular electrode arrays can be used to make non-invasive, multisite recordings from single cells or networks over very long periods. With the improvements discussed in Section 3.4.4, extracellular electrodes may also be able to detect subthreshold activity and more readily provide recordings that resemble intracellular traces. These improvements would open the way to new experimental approaches and would lead to the more widespread use of extracellular electrode arrays.

CHAPTER FOUR:

The influence of the substrate on morphology

SUMMARY: Previous findings have shown that the morphology of cultured neurones depends on the type of substrate on which they are plated (Chiquet & Acklin, 1986; Gunderson, 1987). This suggests that the composition of the extracellular matrix (ECM) may influence neuronal morphology *in vivo*. One possibility is that the morphology depends solely on the adhesive properties of the substrate. Alternatively, the substrate may instigate morphological change by a receptor-mediated mechanism. This Chapter addresses this issue by examining the relationship between outgrowth morphology and cell-substratum adhesion using leech neurones cultured on different substrates.

The results reported below confirm that Retzius neurones plated on planar surfaces coated with either leech ECM extract or the plant lectin Concanavalin A (Con A) produce outgrowths with distinct morphologies (e.g. Chiquet & Acklin, 1986). Interference reflection microscopy is used to extend these results, demonstrating that the nature of the substrate determines the type of contact made by leech neurones with the substratum. Specifically, the lamellar type outgrowth produced by Retzius neurones plated on Con A interacts with the substratum by a continuous region of close contact. This type of interaction can be explained by either simple adhesion or a receptor-mediated mechanism. In contrast the neurites produced by cells plated on ECM extract were characterised by a series of very close but intermittent contacts, suggesting a mechanism involving signal transduction. Thus either one or both of the morphologies produced on these two substrates would appear to be receptor-mediated.

4.1 Introduction

4.1.1 Rationale for using identified neurones in culture

The control of neuronal morphology has been attributed to various factors. Some of the factors may be intrinsic to specific cell types, such as branching pattern and growth cone morphology (e.g. Acklin & Nicholls, 1990; Haydon *et al.*, 1985); others factors can be directly related to electrophysiological behaviour, such as the response of growth cones to electric fields and the retraction of filopodia following the application of neurotransmitters (e.g Fields *et al.*, 1990; Haydon *et al.*, 1987). A third factor which also influences morphology is the nature of the substratum (considered in this and the following Chapter).

Investigating any one of these factors *in vivo* is made problematic by the complexity of the environment. For example several of these factors may act simultaneously to determine the morphology of a growing neurone (e.g. Haydon *et al.*, 1987). An alternative approach is to use identified neurones in culture as a model for developing and regenerating neurones *in vivo*. This approach has several advantages: (1) the morphology of different neurones can be compared under virtually identical conditions allowing intrinsic properties to be investigated (e.g. Acklin & Nicholls, 1990) or (2) intrinsic variability can be reduced by using a single type of identifiable neurone; (3) the environment can be manipulated to investigate each non-intrinsic factor independently, and (4) the accessibility of cultured neurones allows a wider range of experimental techniques (e.g. IRM).

This Chapter describes the use of identified leech neurones to investigate the mechanism by which the molecular composition of the substrate influences neuronal morphology.

4.1.2 Rationale for using interference reflection microscopy

There are at least two possible explanations for the difference in morphology of outgrowth between Retzius neurones cultured on Con A and leech ECM extract (e.g. Chiquet & Acklin, 1986). One is that the difference may be a direct result of differences in surface adhesive qualities (Section 4.3.1). A second explanation is that one or both of the component molecules may provide signals that initiate receptor-mediated biochemical pathways capable of inducing fundamental changes in the properties of new outgrowth. These two possibilities need not be mutually exclusive.

A survey of the contacts between the underside of the cell and the substratum may shed light on which of these explanations is most valid. For example, if the broad, flat outgrowth induced by Con A results solely from strong adhesion then one might expect a large area of membrane to be in close apposition to the Con A-coated substratum. Furthermore, if the outgrowth-to-substratum contacts produced by neurones plated on Con A and ECM are identical, then one might conclude that one or both of these substrates instigates outgrowth by way of a signal-mediated mechanism (so as to explain the difference in outgrowth morphology). Intermittent surface contacts may also signify a signal-mediated mechanism, the maintenance of the intermittent stretches being independent of adhesion. Although the broad outgrowth produced by Retzius neurones plated on Con A can be explained in terms of adhesion, the results presented below suggest a receptor-mediated mechanism may best explain the neurites produced on ECM.

4.1.3 The Extracellular Matrix

Neuronal migration, growth and regeneration occur on a molecular

scaffold consisting of macromolecules which protrude from the surface of cells or reside in an extracellular matrix. This matrix may have a loosely woven structure or, as is the case of the basement membrane, it may be dense and impervious (Martin & Timpl, 1987). Until recently the loosely woven ECM in the bulk of the CNS has defied rigorous experimental investigation (Fessler & Fessler, 1989), so interest has centred on basement membranes which underlie endothelial and epithelial cells, surround muscles and encase peripheral nerves (Kleinman & Weeks, 1989).

Component	Structural homologues present in:	Approx. Mol. Wt. (kD)	Binding properties
Laminin	Vertebrate Invertebrate	850	RGD (Cell binding) & EGF motifs; binds to Type IV Collagen, Heparan sulphate proteoglycan, entactin and itself.
Entactin (Nidogen)	Vertebrate Invertebrate	150	Collagen & Calcium binding. Glutactin, EGF.
Collagen (TypeIV)	Vertebrate Invertebrate	550	RGD domain and binds to itself thus likely to be a major structural and functional component.
Fibronectin	Vertebrate Invertebrate	230	Contains RGD motifs; binds with other ECM components (e.g.collagen).
Heparan sulfate proteoglycan Low density: High density (low protein content):	Vertebrate	 600-700 ›1000	Occur in basement membrane & cell membrane. Laminin, hyaluronic acid, & lectin binding. Also contains EGF repeats.
Thrombospondin	Vertebrate	450	RGD, EGF motifs.
Hyaluronic acid	Vertebrate	›1000	Unlike other glycosaminoglycans in that it is not covalently linked to a core protein.
Tenascin (cytotactin)	Vertebrate Invertebrate	1000	RGD, EGF; Remains enigmatic, but probably not adhesive to neurones. Dimeric and Trimeric homologues to tenascin have been identified.

Table 4.1: ECM components of the nervous system. Compiled from Reichardt & Tomaselli (1991), Martin & Timpl (1987), Sanes (1989) and Erickson & Bourdon (1989).

The molecular platform provided by the basement membrane lends mechanical support, but many of the component molecules (listed in Table 4.1.) have also been suggested to have an active role in neural differentiation, elongation and regeneration (Martin & Timpl , 1987).

4.1.4 Leech extracellular matrix

A Triton X100 (detergent) treated homogenate of the CNS of the leech provides a substrate conducive to rapid and extensive neurite outgrowth from identified neurones grown in culture (Chiquet & Acklin, 1986). Furthermore, if the homogenate is treated with 4M urea (or 10 mM EDTA) the extracted component retains its neurite promoting ability when adsorbed on to a substratum. The neurites produced by Retzius neurones grown on this material are reported as being longer with fewer branches than would usually be expected for neurones grown on Con A (a plant lectin that also supports neurite outgrowth; Chiquet & Acklin, 1986; Acklin & Nicholls, 1990). By examining the morphology of neurites which extend across boundaries between regions of a culture dish coated with either Con A or ECM extract, Grumbacher-Reinert (1986) has demonstrated that these differences appear to be mediated by local interactions between the substrate molecules and the neurites. In this Chapter, the influence of the substrate on morphology is further characterised by using interference reflection microscopy (IRM) to assess the surface contact made by cells plated on these two substrates.

Further purification of the neurite promoting factors has revealed that a sizeable proportion of the activity is accounted for by a large molecule with a cruciform shape that is made up of three subunits weighing 340, 220 and 160-180 kD (Chiquet *et al.*, 1988). Immunofluorescence staining of leech CNS with antibodies raised against this molecule have shown that it is concentrated in regions with basement membrane-like material. This is particularly true of the endothelial basement membrane, located on the outer surface of the ganglion capsule (Chiquet *et al.*, 1988). The neurite

promoting ability, the size, the structure and the distribution of this molecule are similar to that of vertebrate laminin.

Structural homologues to vertebrate laminin have also been purified from other invertebrate species including the fruit fly (Fessler *et al.*, 1987) and the sea urchin (McCarthy *et al.*, 1987). Although the molecular weight differs from vertebrate laminin the differences are not large, as can be seen from table 4.2. In addition, the sequence of *Drosophila* laminin is similar to that of the mouse (45% overall homology; Kleinman & Weeks, 1989) with regions of 50-55% match (domains III and V; Fessler & Fessler, 1989). To what degree leech laminin shares this sequence homology is as yet unknown.

Source of laminin	Size of subunits (kD)			Reference
Vertebrate:				
Englebreth-Holm-swarm tumor	400	210	200	Martin & Timpl, 1987
Invertebrate:				
Leech (*Hirudo medicinalis*)	340	220	160-180	Chiquet *et al.*, 1988
Sea urchin (*Sphaerechinus granularis*)	480	230	205	McCarthy *et al.*, 1987
Fruit fly (*Drosophila melanogaster*: Kc cell line)	400	215	185	Fessler *et al.*, 1987

Table 4.2: The size of laminin subunits from different sources;

Other components of leech ECM

Although the majority of the neurite-promoting activity of the leech CNS extract is accounted for by the presence of laminin, a small amount of outgrowth persists in extracts from which laminin has been immunologically removed (Chiquet *et al.*, 1988). Molecules which are structurally homologous to vertebrate tenascin and to collagen IV have been detected in the neurite-promoting fractions of leech extract using rotary shading (Masuda-Nakagawa, 1988; for a review on the structure and function of

tenascin in vertebrates see Erickson & Bourdon, 1989). However, neurite outgrowth from cultured leech neurones is not supported by a surface coated in the purified collagen IV-like molecules. In addition, it has been reported that no change occurs in either the extent or morphology of outgrowth when leech neurones are plated on surfaces coated with fractions that contain both the tenascin-like molecules and leech laminin (Masuda-Nakagawa, 1988).

Leech extracellular matrix may be contaminated by other components that can influence neurite outgrowth, such as cell surface molecules. In vertebrate CNS, a recently discovered class of molecule that protrudes from myelin membrane (Caroni *et al.*, 1988) and posterior somites (Davies *et al.*, 1990) causes the collapse of growth cones following filopodial contact. Although it is too early to reject the possibility that there are invertebrate equivalents, they are likely to be either less widespread or less potent. The vertebrate CNS, which usually fails to regenerate, can be made to do so by the injection of antibodies against the myelin-associated glycoproteins. This suggests that these molecules are responsible for inhibiting regeneration. Invertebrate CNS neurones on the other hand, regenerate *in vivo* (e.g. Baylor & Nicholls, 1971; Macagno *et al.*, 1985; Bannatyne *et al.*, 1989) and thus the CNS is unlikely to contain such a potent neurite inhibitory component. Of course, the presence of a sparsely distributed or milder form of such molecules can not be ruled out.

Cell adhesion molecules that can promote neurite outgrowth have been identified both in vertebrates and invertebrates. When leech neurones are plated on a polylysine-treated substratum, they grow preferentially over the lower surface of the neighbouring cell with only limited outgrowth occuring on the cell free areas of the polylysine (Fuchs *et al.*, 1982). The

processes that do form are highly fasciculated (Ready & Nicholls, 1979). As the membrane belonging to the cell bodies and processes of neurones within intact ganglia are not stained with antibodies against leech laminin it is conceivable that molecules other than laminin are involved (Chiquet *et al.*, 1988).

Molecules have been identified on the surface of axons (using monoclonal antibodies) which may influence neurite outgrowth (e.g. Zipser & McKay, 1981; Chang, *et al.*, 1987; Harrelson & Goodman, 1988). For example, Fab fragments to two antigens (designated G4 & F11) present on the surface of chick sympathetic axons reduced the average length of fasciculated sympathetic neurites on axons from sympathetic explants. However, these Fab fragments did not affect the length of outgrowth on uniform laminin substrates (Chang, *et al.*, 1987). In the leech, antigens have been found which are localised to functional groups of identified neurones (Zipser & McKay, 1981). One example is the Lan2-3 antigen which is part of a carbohydrate motif present only on the surface of peripheral sensory neurones. The axons of these neurones form a fascicle in the nerve roots suggesting that they recognise one another. This is substantiated by the observation that regenerating sensory axons in the nerve roots grow preferentially along well defined tracts, which coincide with the distribution of the Lan2-3 antigen (Peinado *et al.*, 1987). If these molecules are involved in recognition between different sensory neurones then one must conclude that the peripheral sensory neurones also have a Lan2-3 binding protein. Recently it has been shown that blocking or cleaving the site containing the Lan2-3 antigen prevents the normal defasciculation of developing peripheral sensory axons as they enter the CNS (Zipser & Cole, 1992). Thus if Lan2-3 is involved in recognition, then molecules in the CNS must

compete for the binding site. An alternative hypothesis is that Lan2-3 binding proteins are not present on the axons of other peripheral sensory neurones, but are located solely within the CNS. This hypothesis could explain why cleaving the antigen later on in development causes the refasciculation of axons which have defasciculated normally (Zipser & Cole, 1992). If the Lan2-3 antigen was involved in recognition between the different peripheral sensory neurones then one would not expect cleavage to result in refasciculation, since the information required for this reorganisation would be lost.

4.1.5 Nonphysiological substrates

Two nonphysiological substrates have been used to culture leech neurones. The first to be used was polylysine, either in combination with collagen (Ready & Nicholls, 1979; Fuchs *et al.*, 1981) or applied directly to tissue culture plastic (Fuchs *et al.*, 1981). Leech neurones adhere strongly to these highly charged surfaces but only start producing outgrowth after a delay of a few days (Chiquet & Acklin, 1986). In contrast, neurones isolated from other preparations including chick dorsal root ganglia (DRG; Gunderson & Park, 1984) and *Aplysia* (Burmeister & Goldberg, 1988) are capable of rapid outgrowth on polylysine-treated surfaces providing that serum or haemolymph is present in the medium. For both these cell types the effect may be partly mediated by the adsorption of neurite-promoting substances from the serum on to the substratum. For example, skeletal muscle-conditioned medium is less effective in promoting the adhesion and outgrowth of DRG neurones if it is first left standing in a polylysine-coated vessel (Burmeister & Goldberg, 1988). Although serum increases the survival of leech neurones in culture (Fuchs *et al.*, 1982), it does not appear

to facilitate the extension of neurites on polylysine (as judged by the length of the delay before the first neurites appear; Chiquet & Acklin, 1986). In addition, leech neurones differ from DRG neurones in that they do not extend neurites when plated on surfaces coated with purified vertebrate laminin (Chiquet *et al.*, 1988). It would be interesting to determine whether a substratum coated with purified vertebrate laminin is capable of supporting the rapid outgrowth of neurites from *Aplysia* neurones. It has been suggested that the delayed outgrowth of leech neurones plated on polylysine is a result of the neurones conditioning the substratum (Chiquet and Nicholls, 1987).

Leech neurones also strongly adhere to surfaces coated with the plant lectin Concanavalin A, which binds specifically to methyl α-D mannoside residues. On this substrate the first signs of outgrowth occur shortly after plating with little or no lag (Chiquet & Acklin, 1986). The neurite outgrowth of neurones isolated from other animals is also influenced by Con A. For example, both DRG and *Aplysia* neurones produce neurites more rapidly on Con A than on polylysine (DeGeorge, 1985; Lin & Levitan, 1987). Neurites are produced by DRG neurones and small *Aplysia* neurones in the absence of serum (or conditioned medium) when grown on Con A but not when grown on polylysine[1]. Both the DRG and the *Aplysia* neurones cultured in the presence of Concanavalin A are characterised by normal filopodia and large lamellipodia as summarised by Lin and Levitan (1991). The same authors report that leech neurones are distinct, in that they lack large lamellipodia, a view not supported by the results presented in this

---

[1]Large neurones from *Aplysia* can grow on polylysine in the absense of serum or conditioned medium.

Thesis. An analysis of the literature reveals that some reports contain photographs of Retzius neurones grown on Con A which are dominated by structures that resemble processes (e.g. Chiquet and Acklin, 1986; Chiquet & Nicholls, 1987). However, these are balanced by other reports in which Retzius neurones appear to produce large lamellipodia (Ross *et al.*, 1987; Ross *et al.*, 1988). The results reported below show that the morphology of Retzius neurones grown on Con A varies within these two extremes. The outgrowth of most cells is dominated by lamellipodia, although occasionally neurones are seen that produce well defined processes when cultured on Con A.

4.1.6 The theory of Interference reflection microscopy

Following the introduction of Interference Reflection Microscopy (IRM) by Curtis (1964), it has been used extensively in cell biology as a means of gauging the spatial relationship between the underside of cultured cells and the substratum to which they adhere and spread (reviewed by Verschueren, 1985; for a practical guide see Lacey, 1989). The cellular structures that are closest to the substratum appear darkest, whereas more distant structures appear brighter. This is brought about by the following:

Reflection occurs whenever light is shone at an interface between two substances which differ in their refractive indices (n). The greater the difference the greater the reflection. When two interfaces are separated by a gap (*g*), the light reflected from one interface combines with light reflected from the other interface to produce an interference pattern. The nature of the interference pattern depends on the optical path difference, Δ, between the light reflected from the two surfaces:

$$\Delta = 2.n_{medium}.g.\cos\theta \qquad (4.1)$$

where n_{medium} is the refractive index of the medium and θ is the angle of refraction of light in the medium. When the optical path difference is a multiple of the wavelength of light (λ):

$$\Delta=N\lambda \quad \text{where } \{N=0,1,2,...\} \tag{4.2}$$

the two sources of reflected light retrain their phase relation and undergo constructive interference producing a bright image (see Figure 4.1). On the other hand when the optical path difference causes a difference in phase of half a wavelength, i.e.:

$$\Delta=(N+1/2)\lambda \quad \text{where } \{N=0,1,2,...\} \tag{4.3}$$

then the resulting destructive interference between the two sources of reflected light produces a dark image.

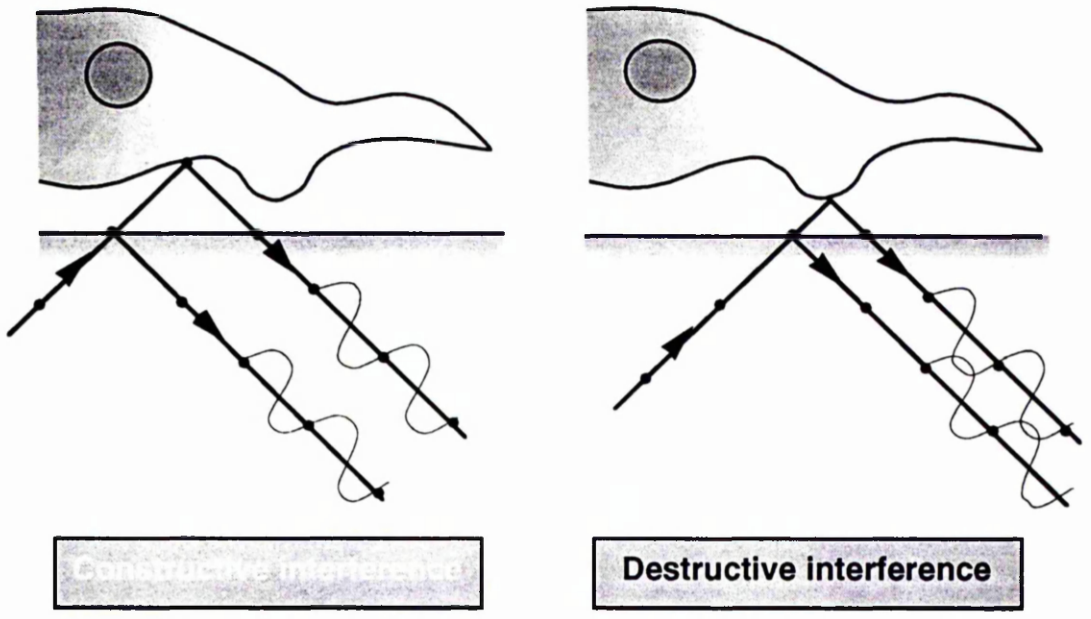

Figure 4.1: How IRM images relate to cell contact with the substratum. Cells were plated on glass coverslips and viewed with an oil immersion lens with a high numerical aperture. Areas of a coverslip without an overlying cell appear light grey as a result of the light reflected from the glass/medium interface. A brighter image occurs when the light reflected from this first interface is reinforced by light reflected from a second interface. The lower membrane of a cell and the underlying medium can provide this interface if the membrane is sufficiently distant from the substratum (a). In areas where the cell membrane is in very close contact with the glass coverslip the interference between the light reflected from the two interfaces is destructive resulting in a dark image (b).

The integer N in equations 4.2 and 4.3 designates the order of interference. According to equations 4.2 a bright interference fringe would occur whenever the gap between the two interfaces is a multiple of the wavelength of light. This property has been exploited in studies of the surface contours of motile fibroblasts (Izzard & Lochner, 1980). However, interference fringes produced by gaps of different dimensions makes interference reflection images difficult to interpret in terms of cell-substratum contacts. Using a lens with a high NA limits this problem, giving images which contain only the zero order interference, discussed further in Section 4.3.3 (Izzard & Lochner, 1976; Gingell & Todd, 1979).

In this Chapter IRM is used qualitatively to determine the relationship between neuronal outgrowth and substratum contact. The results presented below demonstrate that ECM extract and Con A affect not only the gross morphology of outgrowth from Retzius neurones, but also determine the nature of the contacts made between the outgrowth and the substratum. The different sorts of contact suggest that the two types of morphology may be produced by different mechanisms.

4.2 Material and Methods

4.2.1 Extracellular matrix extract

Chains of segmental ganglia were dissected (as described in Section 2.2.1) and stored on ice in leech Ringer. Once eight chains had been dissected they were Dounce homogenised and extracted overnight at 4°C in 2% Triton X-100/10mM Tris/HCl (pH 7.4) supplemented with a cocktail of protease inhibitors consisting of 2mM phenylmethylsulfonyl fluoride, 5 mM

N-ethylmaleimide (solubilised in DMSO) and 2 mM EDTA (all from Sigma, UK). The membranous fragments were pelleted using a microcentrifuge at 13 000 rpm and washed three times in double-distilled water. Two approaches were employed to solubilise the protein components, both were performed at 4°C. One approach was to subject the pellet to a solution containing 150 mM NaCl, 10 mM EDTA and 10 mM Tris-HCl (pH 7.4) for 12 h. 50 µl of this solution was used per ganglionic chain (Chiquet et al,1988). The other approach used a urea solution followed by dialysis. Specifically, 100 µl of 4 M urea in 10 mM Tris-HCl buffer (pH 7.4) was added per ganglionic chain. After 24 h the solution was centrifuged and the resulting supernatant was dialysed against 10 mM Tris-HCl for 12 h (Chiquet & Acklin, 1986).

Any remaining membrane fragments were removed from the solutions containing the solubilised proteins by centrifugation. The supernatants were used immediately when possible, or aliquoted into eppendorfs and stored at -70°C.

Glass coverslips were exposed to dimethyldichlorosilane vapour and then incubated at 120°C for 10 min. A 50 µl drop of the solution containing the solubilised ECM was then applied for 2 h, followed by three washes in double-distilled water and one wash with leech medium. A similar procedure was employed to coat glass substrata with Con A. Note that both of these procedures result in protein attachment by adsorption. Neurones were extracted using the protease treatment described in Section 2.2.2. To facilitate the attachment of cells to the ECM extract cells were incubated overnight in leech medium containing 2% FCS. This procedure removes the last traces of glial debris maximising cell adhesion. Cells were plated in FCS free medium and observed after 24 h.

4.2.2 Other substrates

Aminosilane

3-aminopropyltriethoxysilane (aminosilane) was bound to glass coverslips using the recipe described by Kleinfeld *et al.*, (1988). Briefly, glass coverslips were cleaned by placing in a fresh solution of 90% H_2SO_4 and 10% H_2O_2. The coverslips were then rinsed in deionized water followed by 1M NaOH to neutralise any remaining acid. The NaOH was in turn removed by thoroughly rinsing in deionized water.

3-aminopropyltriethoxysilane was attached to the surface as follows. The coverslips were baked at 130°C for 60 min and allowed to cool, before being soaked for 10 s (with agitation) in a solution containing 95% ethanol, 1% 3-aminopropyltriethoxysilane (Sigma, UK) adjusted to pH 5 with acetic acid. Excess aminosilane was washed off with three changes of ethanol. The coverslips were then baked at 120°C for 10 min.

Neurones were cultured on the aminosilane-coated coverslips, or alternatively, glutaraldehyde was attached to the amino groups and used as a cross-linker to bind Con A (see below).

Covalently bound Con A

Glutaraldehyde was coupled to the amino groups of the glass-bound aminosilane by soaking the coverslips for 1 h in PBS containing 1% glutaraldehyde (EM grade; TAAB Lab. Equipment. Ltd, UK) and 40 mM sodium cyanoborohydride (Sigma, UK). The coverslips were washed in PBS and then soaked for a further hour in a solution containing 25 $\mu g.ml^{-1}$ of Con A and 40 mM sodium cyanoborohydride (in PBS). The final step in the processes was to wash the coverslips in PBS. This method was kindly provided by Enrique Perez (Dept. of Cell Biology, University of Glasgow).

To ensure that no Con A was attached by adsoption, the coverslips were incubated for 10 min in 4M urea (in PBS). Following this incubation the coverslips were washed thoroughly in PBS and used immediately.

4.2.3 Interference Reflection microscopy

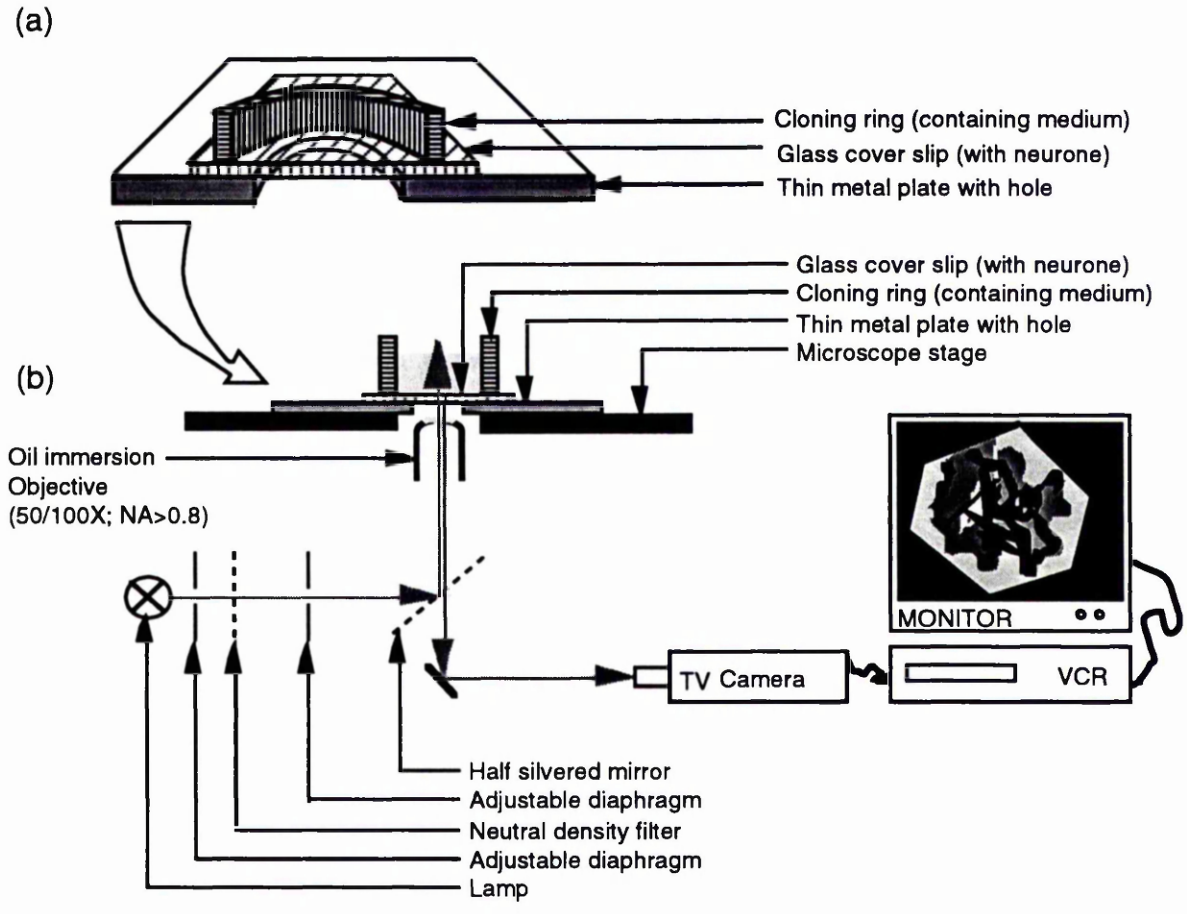

Figure 4.2: The method used to obtain IRM images. (a) A glass coverslip was sealed to the bottom of a cloning ring to form a culture chamber. The chamber was then glued over a hole in a metal plate. (b) Cells were cultured in the chamber for 24 h. An inverted microscope was used with an epi-illuminator. Light was provided by a mercury lamp. A half-silvered mirror separated the illuminating light from the reflected light. The reflected light was captured by a TV camera and stored on a video cassette. Photographs were then made of contrast-optimised images played back through a TV monitor.

The arrangement used for IRM is summarised diagrammatically in Figure 4.2. Briefly, an inverted microscope (Diaphot; Leitz, Germany) was used with

an epifluorescence illuminator (Leitz, Gemany) and a 100x oil immersion lens (1.24 NA; Vickers, UK). A glass coverslip formed the bottom of the culture chamber (illustrated in part a of Figure 4.2). Illumination was provided by a mercury lamp and regulated by two adjustable field diaphragms and neutral density filters. The filter set in the epifluorescence illuminator was replaced by a single half-silvered mirror. The resulting images were monochromatic, suggesting that either illumination was monochromatic or the images contained only zero-order interference. The setup was carefully centred to ensure uniform illumination. Images were recorded using a standard TV camera (WV1850/B; Panasonic, Japan) connected to a video cassette recorder (Cameron S-VHS; Panasonic, Japan).

Photographs were taken from the screen of a television monitor. This approach was favoured over taking direct photographs as the contrast of the image could be enhanced by using the controls of the monitor. In principle, contrast could be further improved by using a video camera with a contrast enhancement device (Gunderson, 1988). A drawback of photographing the screen is the loss of detail that results from the scan lines. A high resolution monitor would alleviate this problem (Gunderson, 1988).

4.3 Results

4.3.1 Attachment of neurones to Con A and ECM extract

Con A and leech ECM extract differ in their adhesive properties to Retzius neurones as observed during plating. The cell bodies and processes of Retzius neurones attached immediately to Con A-coated substrates, provided that most of the encapsulating glial debris had been removed. This was readily achieved by using protease. Occasionally cell bodies detached within the first 12 h, perhaps as a result of shedding the last of the glial debris. These cells usually remained anchored to the substratum by membrane belonging to the initial segment, the extracted process and new outgrowth.

For neurones plated on ECM extract attachment was not immediate: cells could be rolled across the dish or coverslip with gentle currents blown through the mouth pipette. To maximise attachment it was necessary to ensure that the last remaining fragments of glia were removed. This was achieved by washing the neurones for 12 h in a culture dish containing leech medium supplemented with 2% FCS. During this time most of the cells failed to attach to the bottom of the dish (as a result of the FCS) and the extracted processes degenerated. When cells were plated on ECM extract weak attachment formed (if at all) within 10 min of plating, providing the dish containing the plated neurones was not disturbed. Attachment was mediated primarily by the tip of the initial segment. Despite the wash, cell bodies failed to adhere to ECM extract-coated substrates.

4.3.2 Gross Morphology

Outgrowth on Con A

Figure 2.10 and Figure 2.15 (in Chapter 2) show isolated Retzius

neurones grown on substrates coated with Con A. Typically, Retzius neurones grown on Con A have broad, flat expanses (as judged by their uniform appearance when viewed with phase-contrast optics). These broad expanses (which are referred to below as lamellae) are located basally, originating from the broken tips of the extracted processes.

In most cells the morphology of the outgrowth was dominated by the lamella which may have had an area in excess of 10 890 μm^2 (as in Figure 2.15). Occasionally however, the most prominent feature of the outgrowth was a series of finger-like structures along the distal edge. The reason for this diversity was unclear. Variations occurred in the extent of the finger-like morphology between Retzius neurones extracted from the same leech. This implies that variation between leeches was not primarily responsible. The morphology of neurones extracted with two or more processes (e.g Figure 4.3) suggests that the variation in the morphology of outgrowth results from factors that are specific to individual processes. The Retzius neurone photographed in Figure 4.3 was isolated with a bifurcated process and plated on tissue culture plastic coated with Con A. The two extracted branches had lengths of 127 μm and 345 μm. After 24 h in culture the longer branch had produced an outgrowth typical for Retzius neurones cultured on Con A, being dominated by a broad basal lamella (see part b of Figure 4.3). At the distal edge of the outgrowth, the lamella gave way to a phase dark region from which filopodia protruded. This morphology can be

Figure 4.3 (following page): Local influences of the substrate on outgrowth morphology (A) A Retzius neurone extracted using protease and culture for 24 h on a substratum coated with Con A (scale bar:50.5 μm). The outgrowth at the end of each process has a distinct morphology suggesting the influence of local factors (B& C; scale bars: 30.7 μm). Photographed using phase-contrast optics.

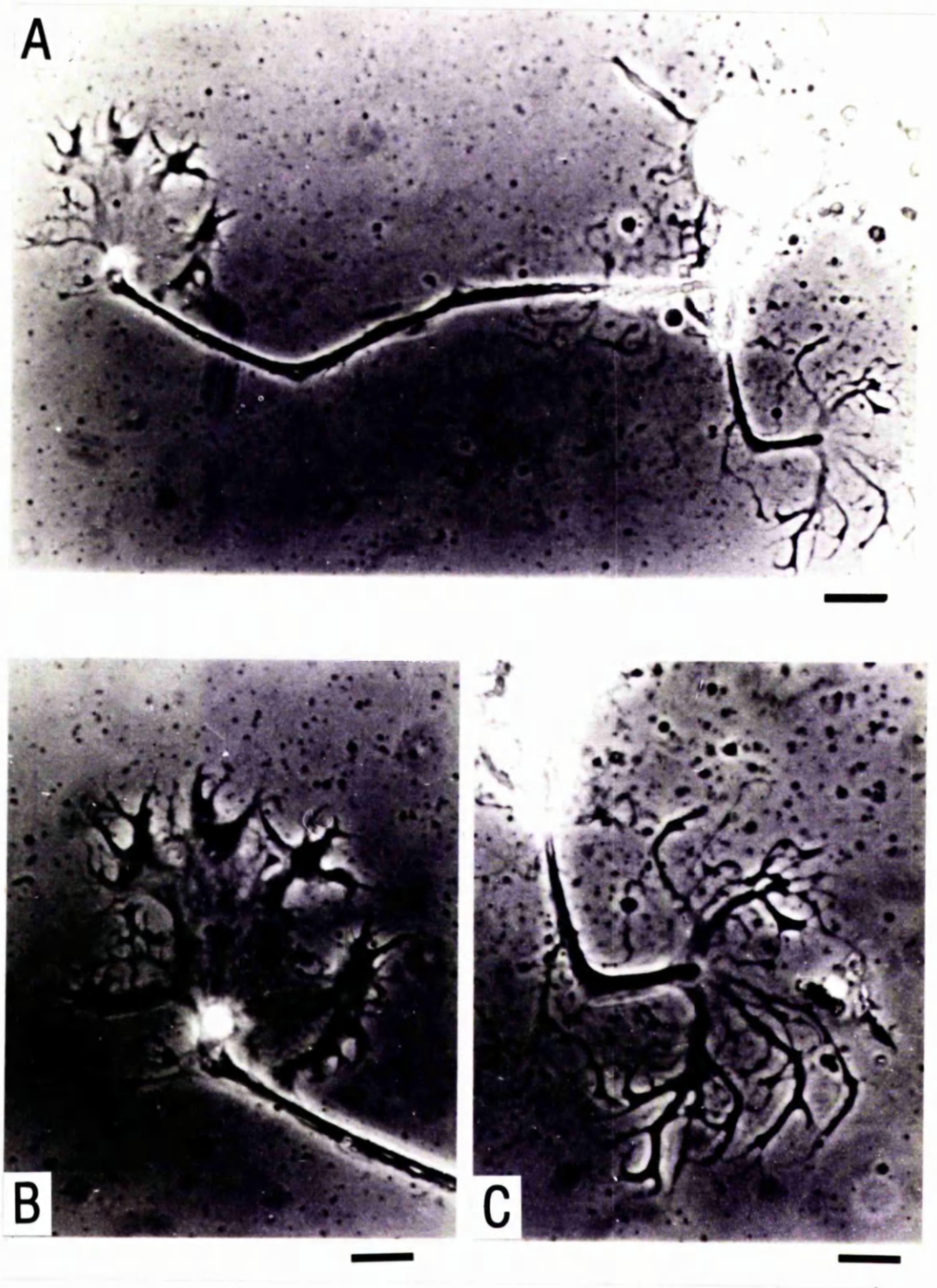
A
B
C

contrasted with that of the outgrowth produced at the end of the shorter branch (Figure 4.3b). At the tip of the extracted process the lamella was reduced to three or four narrow ribbons of membrane that rapidly divided up into neurite like structures. These had distinctive branch points and ended in fine filopodia. The morphology of this outgrowth shared similar characteristics to that of Retzius neurones grown on substrates coated with either ECM extract or with covalently bound Con A (see below). Although the outgrowths at the end of each process had a different morphology it is interesting to note that the total area occupied by each outgrowth was similar.

Outgrowth on leech ECM

The difference between the typical morphology of the outgrowth produced by cells plated on Con A and that produced by cells plated on leech ECM extract was striking (compare parts a-e with f in Figure 4.4). This confirms previous observations (Chiquet & Acklin, 1986). Retzius neurones cultured on ECM extract develop an elaborate network of fine, highly branched processes. The lamellae which typify the outgrowth produced on Con A were absent. Instead, the processes were well defined and had very distinctive branch points. The total length of the neurites in Figure 4.4a *exceeded* 1.3 mm. On average (n=6) the total length of neurites produced after 24 h was 1.00 (S.E.M±0.097) mm. These Figures are likely to underestimate the true extent of the outgrowth as many of the finer neurites were only just visible using phase-contrast optics.

Figure 4.4 (following two pages): Retzius neurones grown on leech ECM extract;. Cells cultured for 24 h on leech ECM extract (a-e; scale bars: 20 μm) can be compared to a cell cultured for the same period on Con A (f; scale bar: 30μm). Arrows in (d) & (e) indicate cell bodies with bulbs.

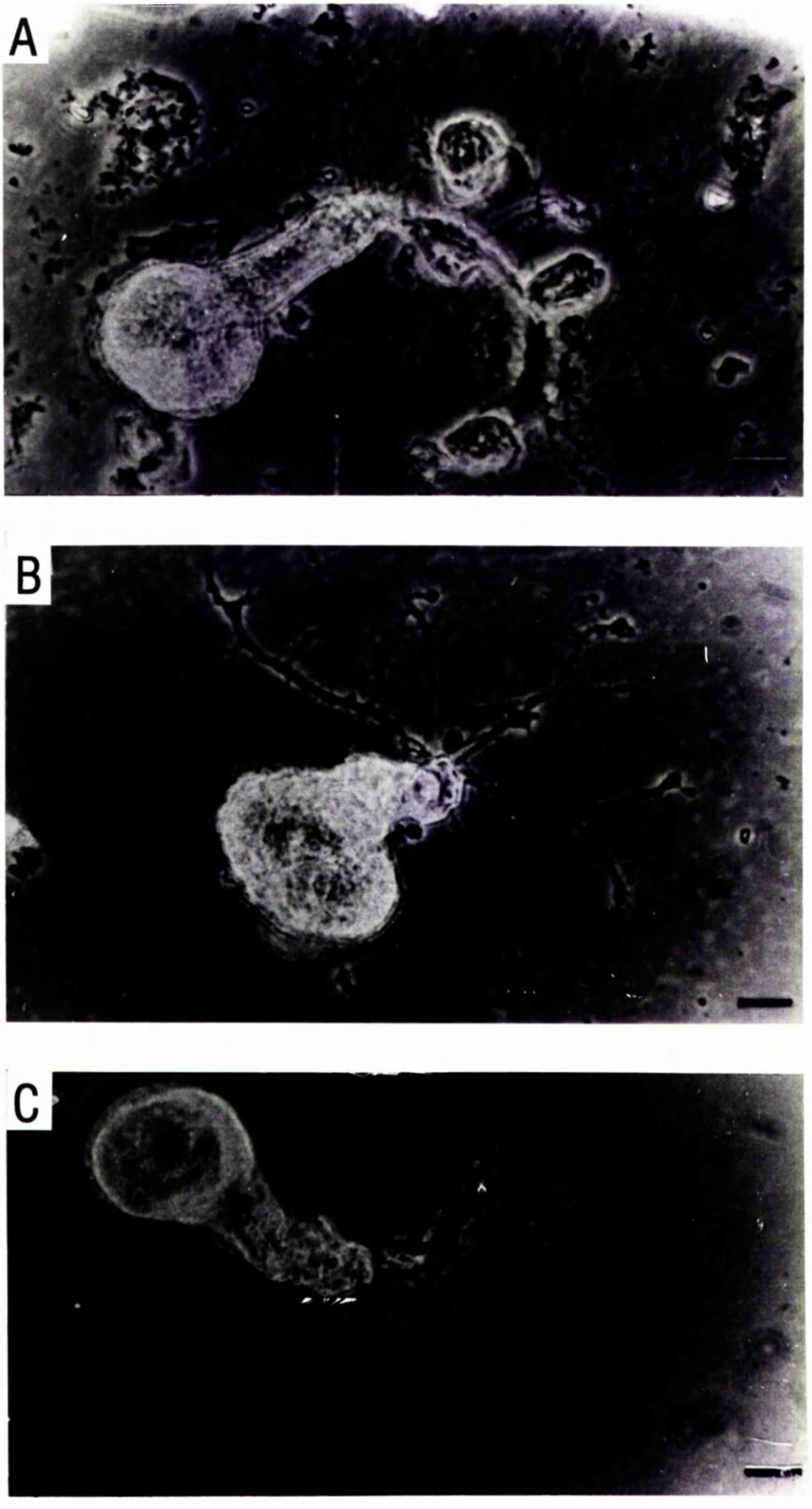
A
B
C

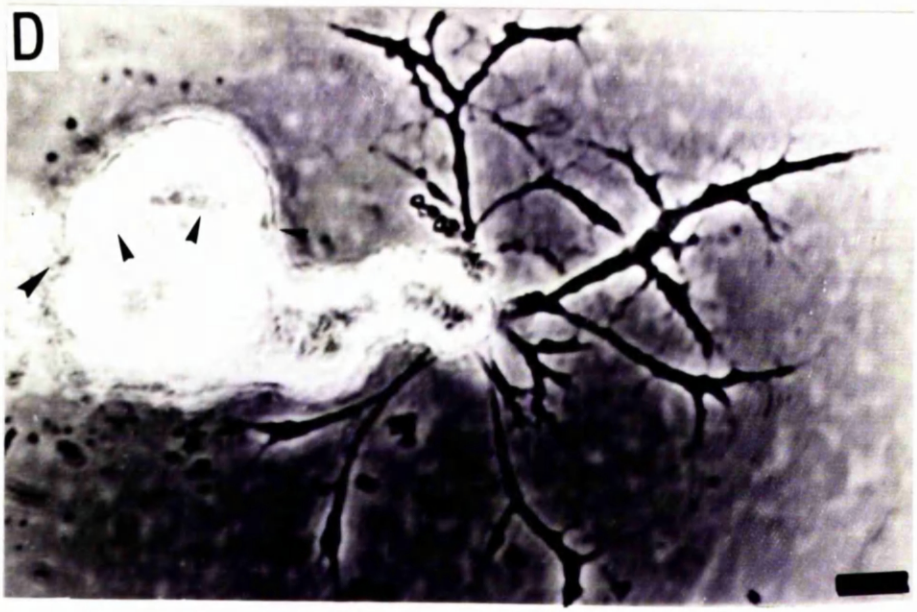
D

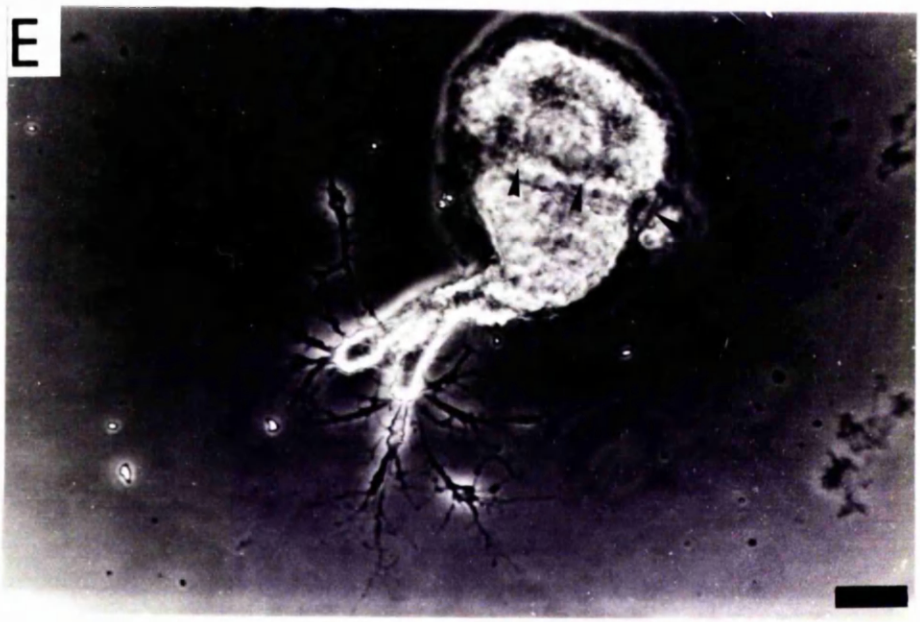
E

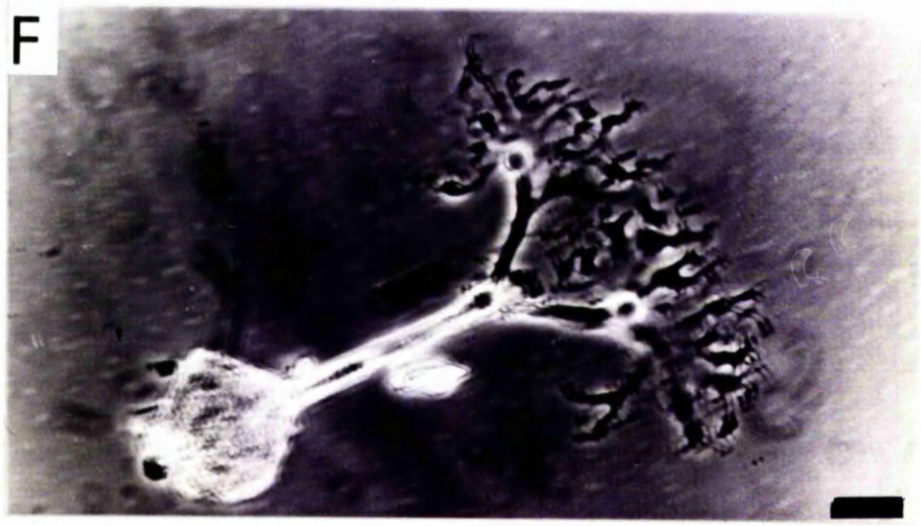
F

Only a few of the processes ended in a pronounced tip (e.g top left and bottom right in Figure 4.4e). The perimeters of these tips were phase bright and appeared to give rise to very fine filopodia. Classical growth cones which are believed to sense environmental signals and migrate accordingly, have a similar structure. It would be fascinating to determine whether the neurites which end with a phase bright tip are those which are actively elongating and thus whether the tips constitute true growth cones.

4.3.3 IRM of surface contacts

IRM of Retzius neurones cultured on Con A

Figure 4.5a shows a phase contrast micrograph of a Retzius neurone cultured for 24 h on a Con A-coated glass coverslip. The cell was extracted using protease and incubated for 12 h in 2% FCS before plating. Broad flat membrane can be observed in the vicinity of the extracted stump and is particularly apparent near to the cell body. The outgrowth became increasingly finger-like towards the distal edge and was marked by areas of phase dark membrane. A low-power IRM image of the same cell shows that the outgrowth was dominated by a lamella and not by filopodia. The out-of-focus bright area to the top of this photograph is caused by light reflected from the cell body. Figure 4.5c shows a composite of three high power IRM images of the outgrowth. There are several points to note. One is that the darkest areas of the image produced by the outgrowth are not distributed evenly over the entire lamella, but are instead concentrated towards the most distal edge of the outgrowth. It is tempting to speculate that these represent areas of close contact with the substratum (a similar conclusion was drawn with reservations by Gunderson, 1988). However an inherent drawback of IRM is the contribution to the image made by the upper surface

of the cell when the cytoplasm is very thin. Using a lens with a high numerical aperture reduces this problem providing that the specimen is illuminated with monochromatic light or contains only zero-order interference (Izzard & Lochner, 1976; Gingell & Todd, 1979). This may be a result of improved "optical sectioning", or the dampening of higher order interference fringes (leaving only the zero-order), with increasing NA (Beck & Bereiter-Hahn, 1981; Gingell & Todd, 1979). Unfortunately, even with a high NA the contribution of the upper cell membrane can remain acute in areas where the thickness of the cell is below 100 nm (Izzard & Lochner, 1976). The distal margin of a lamellipodia may well have a thickness of about this value (Heath, 1982). It is possible therefore that the dark areas at the distal edge of the outgrowth do not represent densely packed focal contacts (Verschueren, 1985).

Figure 4.5 (following page): The contacts made by a Retzius neurone to a Con A-coated substratum. (A) Phase contrast image of a cell isolated using protease, washed for 12 h in 2 % FCS and then plated on a Con A-coated substratum. Photographed after 24 h in culture (scale bar: 22 μm). (B) low power interference reflection micrograph (IRM) of the same cell (scale bar: 15 μm). (C) Composite of IRMs made using a high powered lens (scale bar: 5.6 μm). Dark regions represent areas where the cell is in close contact with the substratum.

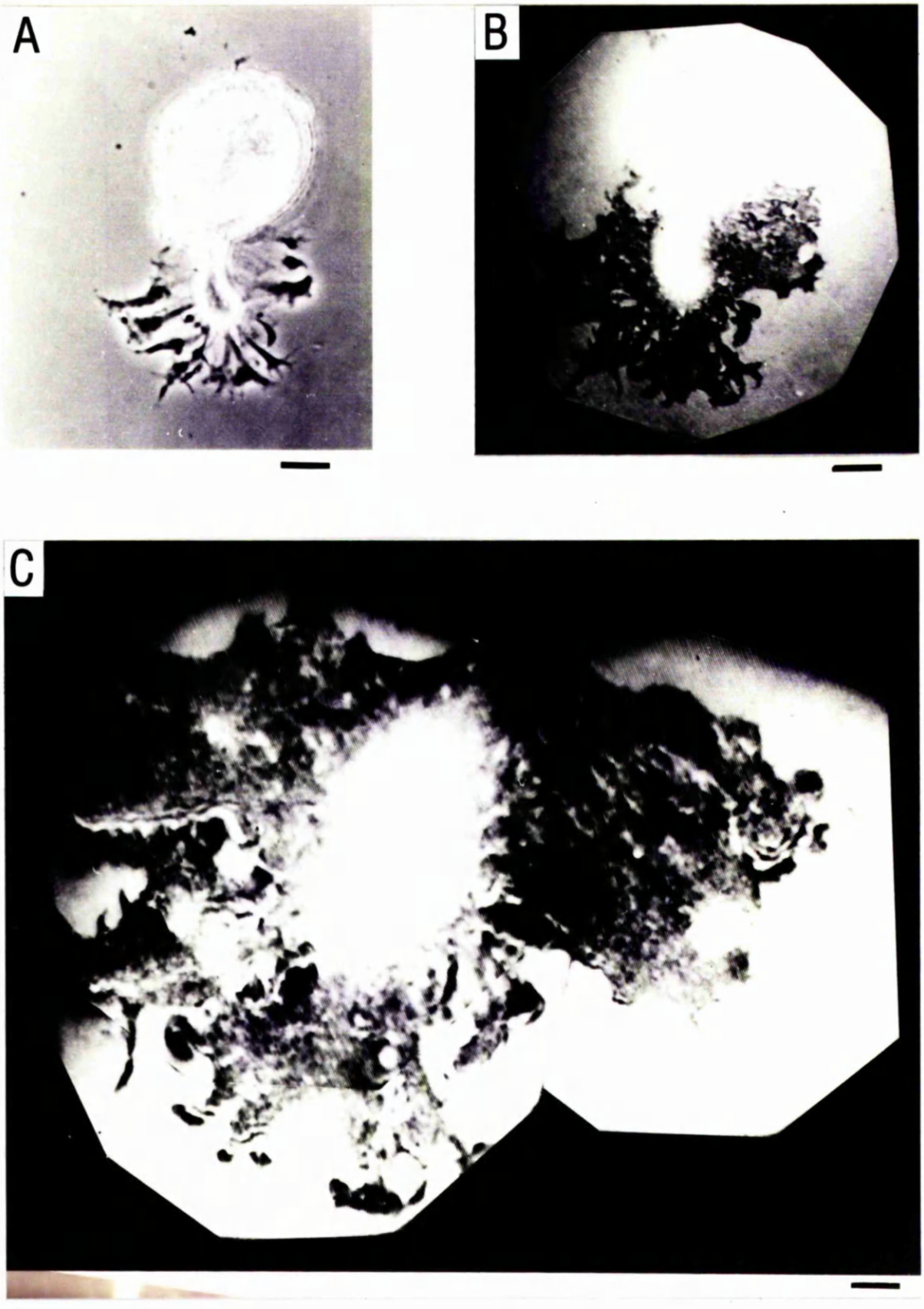
A
B
C

Another feature to note about Figure 4.5c is that the dark areas of the IRM image are frequently located close to very bright regions, giving a striated appearance to the distal edge of the outgrowth. These shift with change in focus indicating that they are produced by higher order interference[2]. Such an interference pattern could have resulted from a region of steeply angled membrane (Gunderson, 1988). The location of these patterns suggests that they may be formed by regions at the perimeter of the outgrowth which rise rapidly from areas of close contacts made with the substratum. Alternatively they may constitute regions where the thickness of the cytoplasm declines rapidly to form the distal edge of the lamella.

A further point to note about Figure 4.5c is that the internal region of the lamella appears to be fairly uniform. There are three main exceptions: the dark stripes to the right of the bright blob (caused by the stump of the extracted process) which probably represent clustered focal contacts and may be within 15 nm of the substratum (Izzard & Lochner, 1976; Heath, 1982); several white patches which could be small areas devoid of outgrowth and finally, a few white streaks which occasionally run in parallel (see the top right of Figure 4.5c). The white streaks are likely to be the only area of the outgrowth not associated with the substrate, possibly separated

---

[2]This can be explained as follows: for any one focal plane the image consists of the reflected light originating from membrane about that plane (plus the reflected light from the interface between the glass and the medium). The light from these different sources varies slightly in phase so that when the light is combined (i.e. in the image) a complex interference pattern is produced. The light which is added and removed as the focus is changed differs in phase causing an apparent shift in the interference pattern.

from the substratum by 150 nm. (Letourneau, 1979). The remaining area of light grey resembles an area of *close contact*, suggesting a separation from the substratum of about 30 nm (Izzard & Lochner, 1976; Heath, 1982). Close contacts are believed to be highly dynamic adhesions. For example, they form the entire underside of motile cells (see Verschueren, 1985). Close contacts can also be seen on the ventral side of classical growth cones, located discretely around areas of focal contact (Letourneau, 1979).

In summary, the majority of the outgrowth from the Retzius neurone in Figure 4.5 would appear to be in close contact with the substratum, forming what is likely to be a dynamic adhesion to the Con A substrate. Only a few dark area were identified. These may represent focal contacts where the cell strongly adheres to the substrate. However, the majority were located at the margin of the outgrowth were the cytoplasm is likely to be particularly thin. Thus the actual number of focal contacts may have been very small.

IRM images of a second cell cultured on a Con A-coated substratum can be seen in Figure 4.6. This cell was extracted using the protease treatment (described in Chapter 2) and plated without washing in 2% FCS. The outgrowth at the end of each of the three widest processes had different morphologies (although the difference was less striking than the difference between the outgrowths of the neurone in Figure 4.3). For example, the process that terminated to the left of the Figure (labelled "C") produced a broad flat outgrowth without any obvious filopodia. This can be contrasted with the outgrowth from the process that terminated at the top of the Figure (labelled "A") which consisted of a region to the right which was dominated by a large lamella *and* a region to the left which had several filopodia. Despite these differences the areas of these two outgrowths were similar (measured at 1723 and 1744 μm^2 using a tracing of their outlines and a

piece of graph paper). The third outgrowth was about 2/3 smaller having a measured area of 738 μm^2. Like the outgrowth of the cell in Figure 4.5 the perimeter of each outgrowth appears dark. However, the white band which is frequently associated with this dark outer rim is more extensive than any one of the striations that can be seen in the previous Figure. In Figure 4.6 the width of the white band of outgrowth "A" at the widest point is equivalent to 4.6 μm (measured from a larger print) . Thus, it is unlikely to be a striation caused by angled membrane, and probably indicates an area of the lamella that is not in contact with the substratum (separated by ≈150 nm). If the dark rims of the lamellae were produced by concentrated focal contacts it suggests that in places the cytoplasm rose almost vertically until it was about 100 nm above the substratum. Alternatively, if the dark rim was produced by a thin margin then it implies that sections of that margin were 150 nm above the substratum. If a very high power lens is used for IRM, it may be possible to eliminate one of these alternatives according to the focal plane of the margin.

Despite the differences in gross morphology between the outgrowths in Figure 4.6, the IRM images of the outgrowths conform to the main conclusion drawn from the cell in Figure 4.5: adhesion to the substrate was likely to be widespread and dynamic, if areas of focal contact did exist they were confined to the perimeter of the outgrowth.

Figure 4.6 (following page): The contact made by extracted processes on a Con A-coated substratum;. Top left: Phase-contrast image of a Retzius neurone cultured for 24 h on a Con A-coated substrate (scale bar: 47.6 μm). Collage: IRM images of parts of the same cell (scale bar for A-E: 15.4 μm; photographs in the region surrounded by the dashed box: 24 μm).

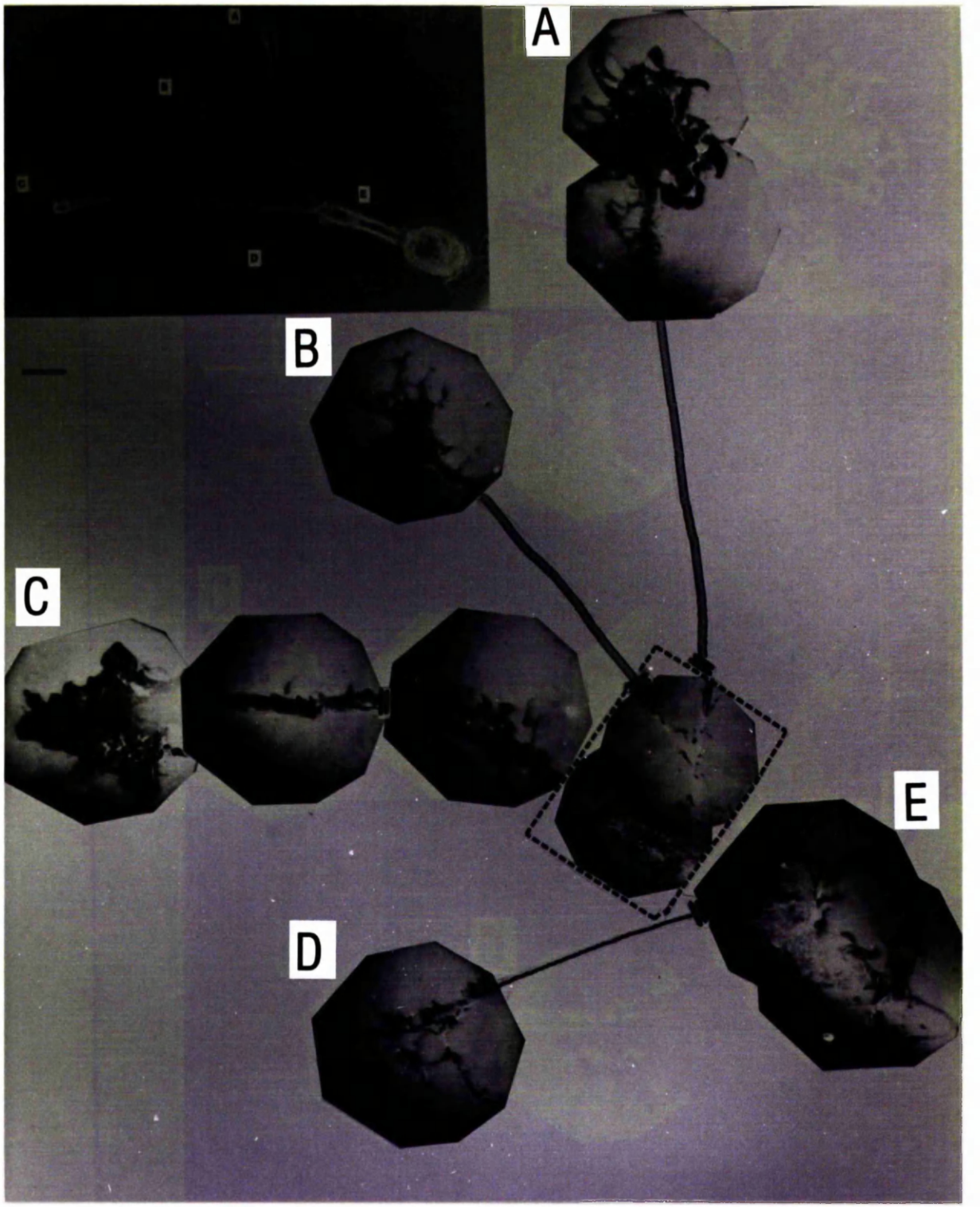
A
B
C
D
E

The collage in Figure 4.6 also demonstrates the association between the extracted processes and the substrate. The thick process which terminates with the outgrowth on the left of the Figure (labelled c) made a series of contacts with the substratum along its length. These were located at different points around the lower half of the process's circumference, but tended to be concentrated laterally. In the most extreme areas the contacts suggest that the shape of the cross section deviated from that of a cylinder, possibly as a result of the lateral outgrowth of new membrane. This observation raises the exciting possibility of forming high-resistance seals between extracellular electrodes and large processes (see Section 3.4.4) which would allow slow changes in membrane potential to be recorded extracellularly.

The finer processes (which probably innervate the neuropil in intact ganglia) also came into contact with the substratum. However, these contacts differed from those of the main processes in that they appeared very dark and are interspaced by regions which produced a bright IRM image (see for example D in Figure 4.6). Thus these processes would appear to have had a series of arches along their length which were not attached to the substrate. The arches may have resulted from the way in which the processes were plated.

IRM of Retzius neurones cultured on leech ECM extract

Figure 4.7a shows a Retzius neurone cultured on a substrate coated with leech ECM extract. Note the mass of fine neurites which typified the morphology of the outgrowth from Retzius neurones cultured on this substrate (see Section 4.3.2). When viewed with IRM neurites had long stretches which produced very dark images (see Figure 4.7 parts b & c for a

collage of IRM images; not the same cell as in part a). This suggests that neurites were in very close contact with the substratum for at least part of their length. The dark stretches which made up approximately 60% of the total neurite length were interspaced by very light sections. For the neurone in Figure 4.7a the average lengths of dark and light stretches were 8.56 (S.D. ±4.20) μm and 9.14 (S.D.±4.9) μm respectively (measured over a total neurite length of 1052 μm). The average lengths of the dark and light sections of the neurites from the cell in Figure 4.7b & c were about half that for the neurone photographed in part a (having values of 4.1 (S.D.±2.7) μm and 4.6 (S.D.±2.9) μm respectively).

The light sections indicate a neurite-substratum separation of around 150 nm (Letourneau, 1979).This separation may have arisen as a result of partial neurite detachment or alternatively, it may represent areas of the substratum that were spanned by neurites as a result of a different density or composition of adsorbed ECM extract. If the former is correct it suggests that 60% surface contact is sufficient to maintain neurites, whereas if the latter explanation is correct then one might conclude that neurites can elongate by more than 9 μm without surface contact. From the evidence presented here it is difficult to select or reject either of these hypothesis.

Note that part C of Figure 4.7 overlaps with the composite in part B, but is at a higher contrast. This enhances the view of the contacts made under the process which was the parent of many of the finer neurites in this

Figure 4.7 (following two pages): IRM of Retzius neurone cultured on a substratum coated with leech laminin; A: Photograph of a Retzius neurone after 24 h on an ECM-coated substratum (scale bar: 10.5 μm). B: Composite of IRM images of some of the outgrowth that can be seen in A. Note the process to the right of this field that had a length which appeared brighter than the background (indicated by the arrow) and was bordered on either side by stretches that were darker than the background. C: IRM which partially overlaps the field of view of A but with a different exposure. (Scale bars for B and C: 4.2 μm)

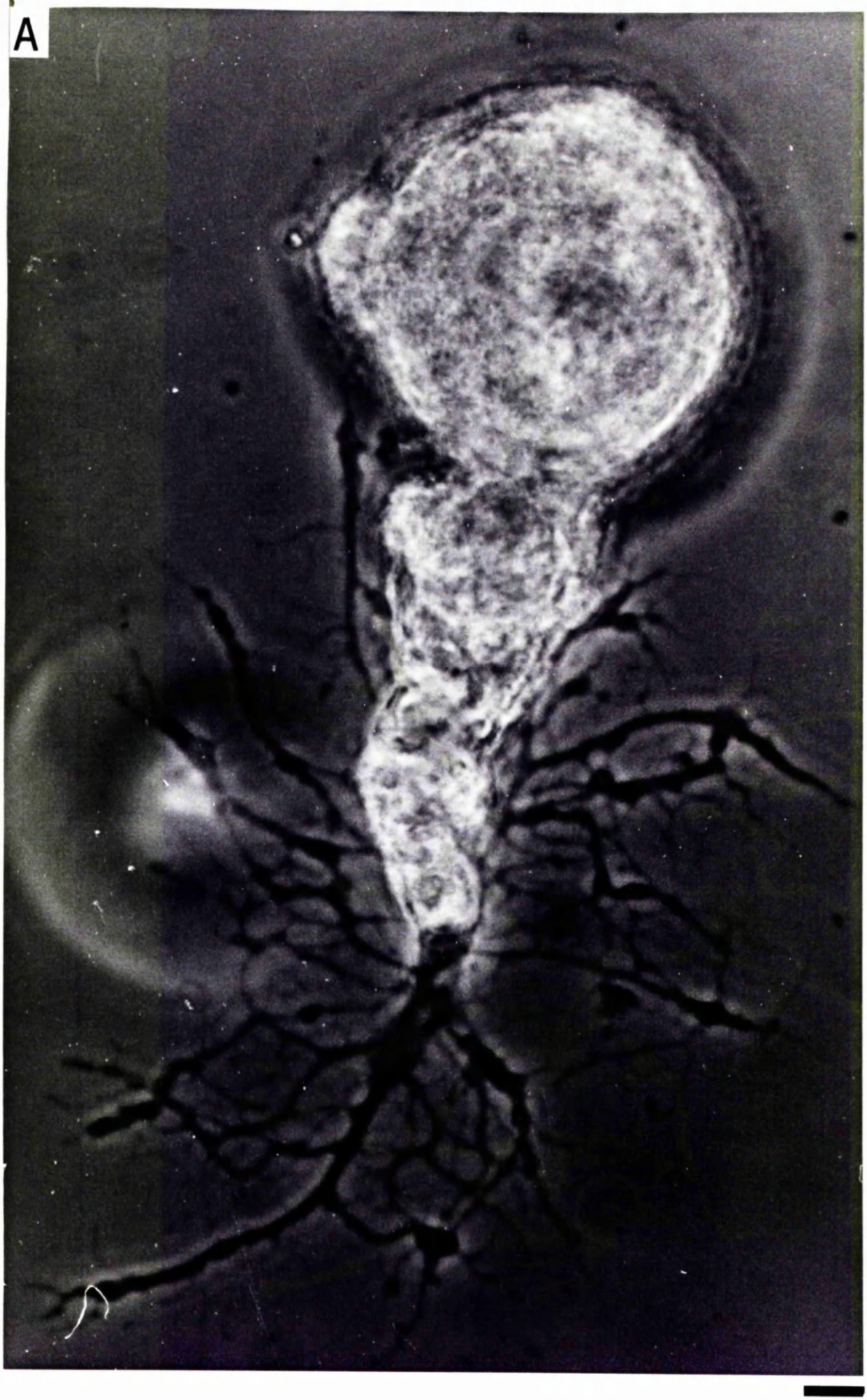
A

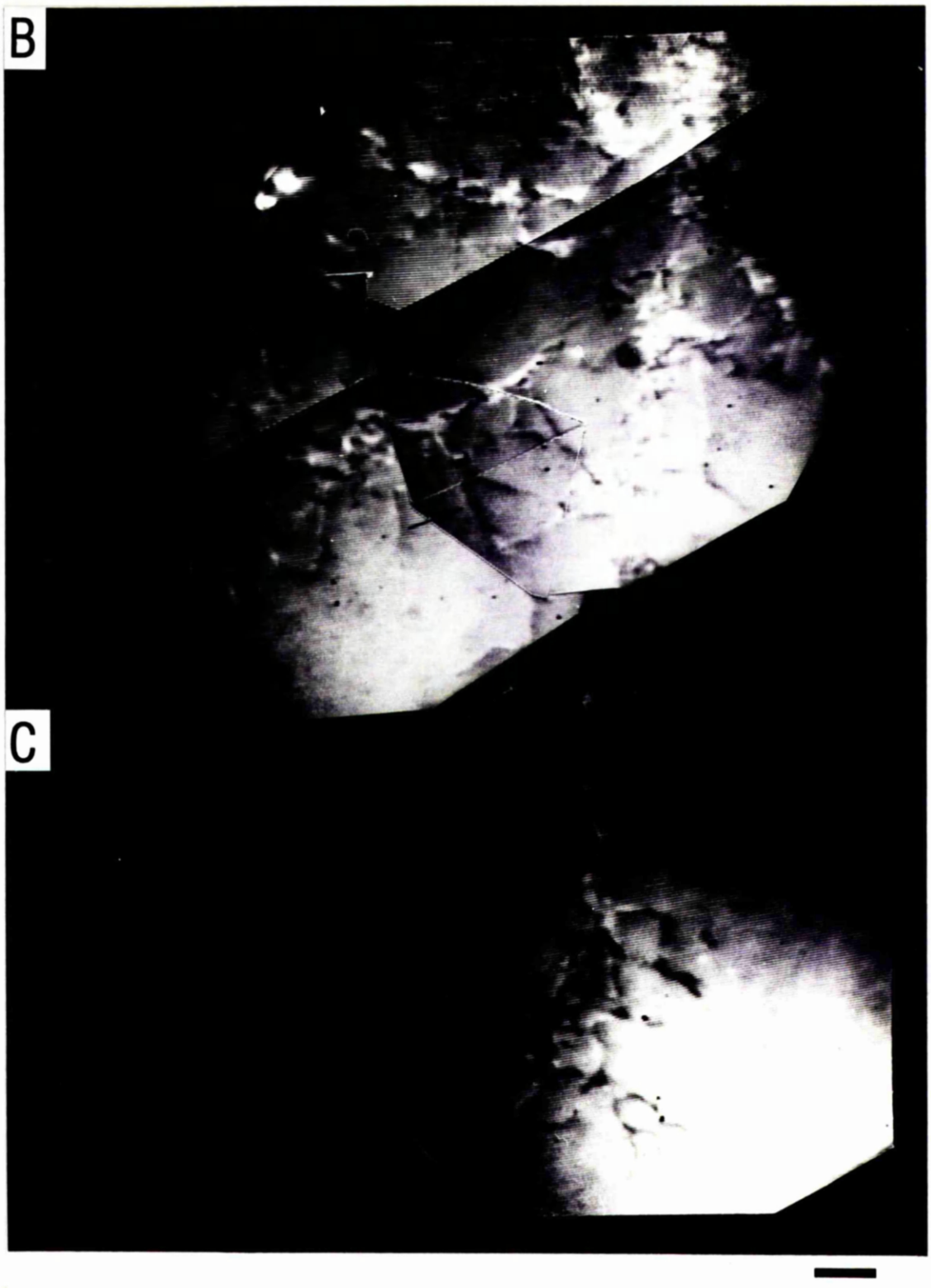
B
C

field. It is interesting that the contacts seem to be made by the initial sections of the finer neurites and not the parent process. This may represent differences in membrane properties.

4.3.4 Neurones plated on other substrates

Suppose that the morphology of outgrowth is dependent on a *signal* provided by the substance (i.e. the substrate) used to coat the coverslip (i.e. the substratum). If this were the case then one might expect morphology to be virtually independent of the strength of the bond between the coating substance and the substratum (a detached signal molecule would have the same effect as an attached molecule). If on the other hand the main determinant of morphology was the *physical adhesion* of the cell to the coating then one might expect the morphology of outgrowth to be highly dependent on the strength of this bond.

Figure 4.8 shows two Retzius neurones cultured on a glass coverslip to which Con A was covalently bound. This experiment was performed twice using one leech per experiment. The two neurones shown in Figure 4.8 were the only cells to show any signs of outgrowth, thus the possibility of toxicity can not be ruled out. On the other hand, both of the cells in Figure 4.8 look healthy: the cell bodies and the extracted processes were not blebbed and both cells had produced significant outgrowth. The outgrowths lacked the broad basal lamella which typified the outgrowth of Retzius neurones cultured on adsorbed Con A (see Section 4.3.1). Hence the results of this limited sample could be interpreted as showing that adhesive properties of the substrate were important in determining morphology.

Figure 4.8 (following page): Outgrowth of Retzius neurones on Con A covalently bonded to the substratum;(A & B) Phase-contrast micrographs of cells grown for 24 h on glass coverslips to which Con A had been covalently coupled (Scale bar: 21 μm).

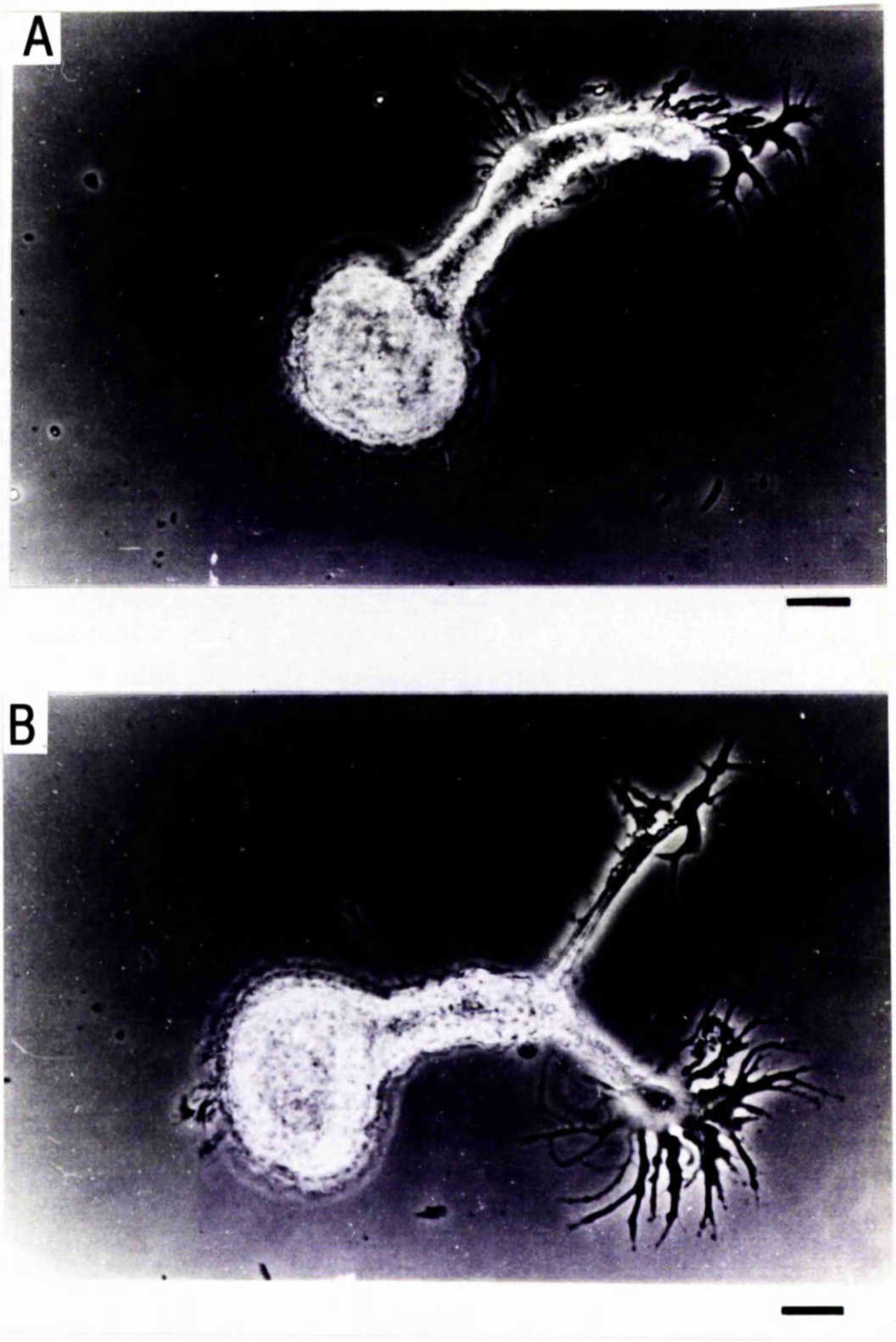
A
B

However, another interpretation is also possible. Since the amount of substratum-bound protein was not measured it is quite feasible that a difference in the concentration of Con A (when compared to substrata coated by adsorption) may be responsible for the variation in morphology (see Section 4.4).

Leech neurones were also plated on aminosilane-coated surfaces. This was a highly adhesive surface as judged by the rapid attachment of neurones. After 24 h the only outgrowth that was observed was a few short, fine processes. These appeared to terminate in very small growth cones (photograph not shown).

4.4 Discussion

The results reported here support earlier claims that the morphology of cultured leech neurones is dependent on the molecular composition of the substrate on which they are plated (Chiquet & Acklin, 1986). Profuse neurite outgrowth occurred from neurones plated on ECM extract-coated substrata. On the other hand Retzius neurones plated on a surface of adsorbed Con A typically produced broad flat lamellae. It was shown using IRM that the substrate also determine the nature of the contacts made with the substratum.

Cause of the variation In the morphology of outgrowth on Con A

The distal margin of the lamellae produced by neurones plated on Con A were finger-like and often gave rise to numerous filopodia. The degree of finger-like morphology and the number of filopodia varied not only from cell to cell but also between different outgrowths produced by the same cell (Figures 4.3 & 4.6). This suggests that local factors were responsible for the variable morphology. Two of the possible candidates are variations between the state of each individual extracted process and local differences in the properties of the substrate. The former candidate can not be rejected from the currently available evidence, although the fact that the total extent of outgrowth from two of the processes in Figure 4.3 (and in Figure 4.6) was similar may indicate that the terminals of the processes were equally healthy. In addition, it should be noted that outgrowths dominated by a large lamella occur from both long and short processes (compare Figure 4.5 with Figure 4.6). If the state of the process was involved then the length of the process might be expected to correlate with the morphology of the outgrowth.

The possibility that the variation is caused by local differences in the properties of the substrate is supported by two experiments which studied the morphology of neurones on patterned substrata (Gunderson, 1987; Grumbacher-Reinert, 1989). For example, it was reported that the morphology of leech neurites changes abruptly at the interface between areas of tissue culture plastic coated with either ECM extract or Con A (Grumbacher-Reinert, 1989). Could more subtle differences in surface properties account for the variation observed here? Two lines of evidence suggest that this may have been the case. One is the claim that the production of lamellipodia by DRG neurones is dependent on the concentration of Con A in the culture medium (Degeorge *et al.*, 1985). The other line of evidence comes from observations of leech neurones plated on Con A-coated substrata in medium supplemented with different concentrations of methyl α-D mannoside (a sugar which specifically binds Con A; Chiquet & Nicholls,1987). With high concentrations (50 to 100 mM) of the sugar the outgrowth was minimal, as presumably no Con A was available for cell binding[3]. However, low concentrations of the sugar *enhanced* "neurite outgrowth" indicating that morphology is dependent on the concentration of substratum bound Con A (Chiquet & Nicholls,1987)[4].

---

[3] 50 mM methyl α-D mannoside does not prevent the delayed outgrowth of leech neurones plated on polylysine, suggesting that the effect was a direct result of blocking Con A (Chiquet & Acklin, 1986).

[4]The paper reports that on Con A *neurite* outgrowth increases with the addition of small amounts of methyl α-D mannoside. Using the word "neurite" implies that lamellae were not produced, although this seems unlikely in view of the results reported in section 4.3. Thus the possibility exists that the only effect observed was an increase in neurite length.

These lines of evidence suggest that lamella-dominated outgrowth occurs in areas where the concentration of Con A available for cell binding is high. Finger-like morphology and the production of filopodia may indicate a lower concentration of Con A. Differences in the concentration of available Con A may arise as a result of non-uniform surface properties before coating with Con A (e.g. charge), or sporadic contamination after coating (e.g with bacteria, microglia or glial debris).

An explanation based on Con A concentration could also explain the difference between the morphology of Retzius neurones on adsorbed and covalently bound Con A. A demonstration showing that the concentration of Con A bound covalently was less than the concentration that attached by adsorption would corroborate this explanation. It would also be interesting to compare the morphology of leech neurones on substrates coated with different concentrations of adsorbed Con A. In both cases ^{125}I-labelling could be used as an assay for protein attachment.

The mode of action of Con A

As well as influencing morphology Con A affects other forms of neuronal behaviour (recently reviewed by Lin & Levitan, 1991). For example, in the presence of Con A the strength of electrical synapses formed between cultured *Aplysia* neurones from different ganglia is increased to the level expected for cultured neurones dissected from the same ganglion (Lin & Levitan, 1987; Carrow & Levitan, 1989). Also nanomolar concentrations of Con A are sufficient to block the desensitization of neuronal activity to long term glutamate exposure in a variety of cell types including locust skeletal muscle (Mathers & Usherwood, 1976) and mammalian hippocampal neurones (Mayer & Vyklicky, 1989). In

Aplysia and *Helix* Con A causes the majority of cells to be depolarised by glutamate as a result of a sodium current which is usually small or absent (Kehoe, 1978). These effects are likely to be mediated by Con A binding directly to membrane glycoproteins such as the glutamate receptor[5].

The glycoproteins which are responsible for the effects of Con A on the morphology of leech neurones have yet to be identified. An exciting possibility is that Con A binds to the sugar residues of a glycoprotein like Lan2-3, which is believed to have a role in determining the morphology of neurones *in vivo* (Zipser & Cole, 1992). Although Lan2-3 is only present on peripheral sensory neurones, competing for mannose binding sites with mannose conjugated to bovine serum albumin (BSA) inhibited defasciculation (as did blocking or cleaving the Lan2-3 antigen). If the action of Con A is also inhibited by mannose conjugated to BSA then it may indicate that the Lan2-3 antigen is involved in the morphological effects seen *in vitro*. Alternatively, Con A may bind to a functionally similar, but different glycoprotein with a more ubiquitous distribution. It is noteworthy that growth cones from neurones located in different parts of the vertebrate nervous system can also be distinguished by "a surface carbohydrate signature" (e.g. Pfenninger *et al.*, 1984).

Identifying the glycoprotein to which Con A binds, might help resolve the question as to how Con A-glycoprotein binding affects neural morphology. At present there would appear to be two possibilities. One is the possibility that binding a subset of membrane proteins to the substratum results in a direct alteration in cell adhesion. This "physiochemical"

---

[5]Supported by the dose response curves for the desensitization of DRG neurons to kainate (a glutamate agonist) in the presence and absence of Con A (Heuttner, 1990)

interaction could distort the cytoskeleton causing the initiation of wider morphological change (Letourneau, 1975). The other possibility is that the binding of Con A to a certain class of glycoprotein *instigates* morphological change by initiating or modulating a molecular pathway that alters the cytoskeleton. Since an instigated morphological change could lead to a change in adhesion, there is little direct evidence as to which of these two possibilities is correct.

Influence of outgrowth adhesion on morphology

Letourneau (1975) measured the adhesion of chick sensory neurone growth cones by applying a blast of air through a syringe needle. He found a strong positive correlation between a substrate's adhesiveness and its ability to support the formation and elongation of neurites. Other observations have strengthened this correlation. One example is the elongation of spinal cord neurites towards a source of skeletal muscle-conditioned medium, since skeletal muscle-conditioned medium was shown to increase neurite adhesion (Gunderson & Park, 1984). Another example is the guidance of elongating DRG neurites to patterns of substrate-bound NGF (to which the neurites strongly adhere; Gunderson, 1985). Similarly, DRG neurites are guided by paths of non-UV-irradiated laminin when bordered by UV-irradiated laminin (which is less adhesive; Hammarback *et al.*, 1985). It would appear that in each of these cases the neurites were guided by *differential adhesion* along the adhesive tracts.

In recent years a number of anomalies to Letourneau's (1975) correlation have emerged. One example is the findings of Gunderson (1987) who cultured dorsal root ganglia on substrates patterned with laminin against a background of Type IV collagen. The explanted ganglia produced

neurites which tended to be fasciculated in regions coated with Type IV collagen and unfasciculated in regions coated with laminin. The laminin-coated regions also stabilised growth cone protrusions and enhanced the rate of neurite elongation. However, despite the apparent preference for laminin, growth cones were shown to adhere more strongly to, and be in closer contact with, regions coated with Type IV collagen (Gunderson, 1987; Gunderson, 1988). To explain this "anomaly" Gunderson (1988) has turned the differential adhesion hypothesis on its head, along with Letourneau's (1975) correlation, believing that neurite outgrowth occurs preferentially on substrates of *lower* adhesion (see Figure 4.9). Clearly there is a need for an arbitrator to determine the relationship between DRG neurite elongation and growth cone adhesion.

Another anomaly to the differential adhesion hypothesis according to Letourneau (1975) comes from experiments using cultured leech neurones. Leech neurones adhere very strongly to substrates which do not support rapid neurite outgrowth, including polylysine (Chiquet & Acklin, 1986) and aminosilane (Section 4.3.4). In addition, the behaviour of leech neurones on Con A and ECM extract is similar to that of DRG neurites on Type IV collagen and laminin (as reported by Gunderson, 1987): the least adhesive substrate supports the fastest rate of neurite outgrowth. Thus in Section 4.3.1 it was pointed out that the initial attachment of leech neurones to Con A was far greater than the initial attachment to ECM extract. Nevertheless, the rate of outgrowth is reported to be slight faster for Retzius neurones on ECM extract than on Con A (Chiquet & Acklin, 1988; Acklin & Nicholls, 1990). Caution is required since initial attachment may not be related to the adhesion of outgrowth: the membrane of the new outgrowth may differ from that of the cell body and extracted processes. This warning is reinforced by

the observation that attachment of isolated neurones to ECM extract is mediated primarily by a small patch of membrane at the broken tip of the process (Section 4.3.1).

In this Chapter IRM was used to assess the outgrowth-to-substratum contacts of Retzius neurones plated on different substrates. The results presented in Section 4.3.3 showed that the neurites that elongated on ECM extract did have regions that were in very close contact with the substratum. However these regions were interspersed by considerable lengths of neurite that were not associated with the substratum. This suggests that either intermittent surface contact was sufficient for neurite outgrowth on ECM, or that neurites elongated and then partially detached. Both possibilities would seem to be indicative of poor surface contact. On the other hand, the underside of the outgrowths produced by cells plated on Con A was made up almost entirely of close contact. Thus, in terms of adhesion, Con A may to be the more effective of the two substrates.

If the behaviour of leech neurones falls outside the realm of Letourneau's version of the differential adhesion model does it comply with Gunderson's (1988) version? The experiments of Chiquet & Nicholls (1987) would suggest not, bearing in mind that they reported that optimal neurite elongation occurred when a low concentration of methyl α-D-mannoside was added to the culture medium. Low concentrations are likely to have reduced but not abolished the adhesion of the neurones to the substrate. Thus the differential adhesion hypothesis may need further modification: rapid neurite outgrowth occurs at an optimal level of adhesion, above or below which neurite outgrowth is seriously impaired. This modification is represented diagrammatically as the central region in Figure 4.9.

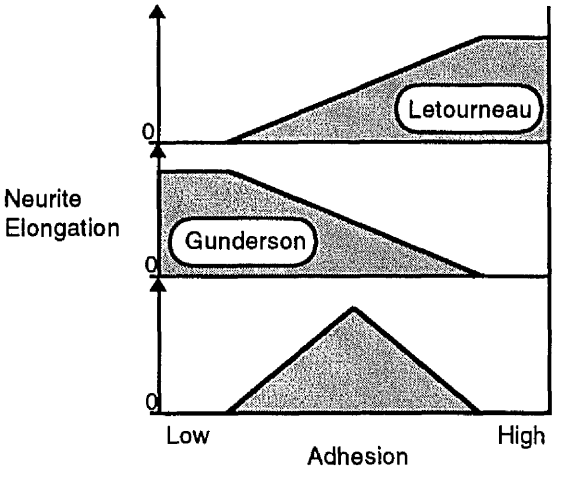

Figure 4.9: Three different versions of the differential adhesion hypothesis.

Letourneau (1975) found a positive correlation between increased neurite elongation and cell-substratum adhesion, whereas Gunderson (1987) found an inverse relationship. The area shaded in the lower graph represents a possible compromise in which optimal neurite elongation occurs as a result of intermediate adhesion (Chiquet & Nicholls; 1987)

Instigated morphological change

In a recent study aimed at resolving the issue as to whether adhesion was the cause or the product of morphological change Curtis *et al.*, (1992) applied fibronectin coated-beads (2.5 μm in diameter) to fibroblasts before the cells were plated on different substrates. They found that beads could stimulate the cells to attach more strongly to, and spread on, a substrate of absorbed haemoglobin if the beads were coated in fibronectin but not if they were coated in bovine serum albumin or Tris groups. Furthermore, IRM and scanning electron microscopy revealed that the beads were located on the dorsal surface of the cell and therefore did not take part in adhesion directly. These results are indicative of a pathway-mediated response to the fibronectin (Curtis *et al.*, 1992).

The outgrowth of leech neurones in response to substrate molecules may involve a similar mechanism. The intermittent substrate-contacts of neurites produced by Retzius neurones plated on ECM extract corroborates this view (Section 4.3.3). However, in the light of the evidence for the involvement of local factors in determining outgrowth morphology

(discussed above) the signal must be of short range. An interesting observation is that Con A-coated beads cause a *local* degranulation of mast cells around the area of bead contact (Lawson *et al.*, 1978). Similarly, experiments using cultured monocytes suggest that when fibronectin receptors are occupied by a ligand a local interaction occurs with nearby complement receptors (Wright *et al.*,1984). To account for these observations, Curtis *et al. (1992)* suggest that different signal molecules may operate over different ranges. Unfortunately, as the range of the signal decreases it becomes increasingly difficult to separate the site of adhesion from the site of the signal. Thus, a definitive demonstration that short range signalling is responsible for cell morphology is much more demanding.

4.5 Conclusions

• The typical morphology of the outgrowth produced by cultured Retzius neurones depends on the molecular composition of the substrate, confirming previous reports (e.g. Chiquet & Acklin, 1986).

• Neurones plated on Con A tended to produced broad lamellae. However the lamellae were often finger-like and gave rise to filopodia. Well-defined neurites which characterised the outgrowth of neurones plated on ECM extract were only rarely produced on Con A.

• The variability in the morphology of the outgrowth which was observed on Con A is manifest in the literature e.g. compare Chiquet and Acklin (1986) with Ross *et al.*, 1987. One possibility is that it may have arisen as a result of variation in the concentration of Con A adsorbed to the substrata. This explanation could account for the different morphology of outgrowth generated by cells plated on covalently-bound Con A.

• The outgrowths produced by Retzius neurones plated on either adsorbed Con A or ECM extract also differed in respect to the form of the contact made with the substrata. On Con A almost the entire underside of the outgrowth could be characterised by close contact with the substratum. In contrast the neurites produced on ECM extract made a series of intermittent, but very close contacts.

• These two different types of contact were discussed in terms of the differential adhesion hypothesis. The intermittent contacts that formed on ECM extract may be more reminiscent of a mechanism involving signal transduction.

CHAPTER FIVE

TOPOGRAPHICAL GUIDANCE

SUMMARY: This Chapter demonstrates for the first time that topography can influence the outgrowth morphology of large identified invertebrate neurones. Neurites were aligned by topographical features with dimensions similar to those required to align the neurites of much smaller vertebrate neurones. This Chapter also illustrates that the effect of topography is dependent on the type of outgrowth, since the lamellae which typify the outgrowth of Retzius neurones plated on a Con A substrate show only slight signs of alignment. Combining these results with those presented in the previous Chapter suggests a new hypothesis: the ECM may modulate the influence of topographical discontinuities on the behaviour of cells.

Another type of substratum non-uniformity, namely chemical heterogeneity, was also investigated. Baby hamster kidney fibroblasts (BHKs) produced numerous aligned processes when cultured on a planar substratum patterned with Con A stripes. In the most extreme cases the resulting morphology resembled a pair of back-to-back combs. Con A may mediate this response by reducing the filament organisation of the cytoskeleton. This may cause an increase in both the flexibility of the cytoskeleton and the persistence of microprotrusions lacking focal contacts. It is conceivable that a similar mechanism may explain the typical outgrowth morphology of Retzius neurones grown on Con A-coated grooves.

5.1. Introduction

During the course of migration in the developing cerebellum, neuroblasts are found in close proximity to a variety of cell types. It has been

suggested that contact may be an integral part of the mechanism by which the neuroblasts find their target (Das *et al.*, 1974). Similarly, it is tempting to speculate that the correlation between the orientation of extracellular matrix molecules and the direction taken by migrating neural crest cells over the medial face of somites is indicative of a substratum-associated guidance mechanism (Newgreen,1989).

The first clear evidence for such a mechanism was provided by Harrison (1911). Following experiments in which he cultured various explants on spiders' webs he stated that the *"surface of a solid...with a specific linear arrangement..."* could act to influence the form, direction of movement, and arrangement of cells (see Dunn, 1982). A similar conclusion was later reached by Weiss (1934) who coined the phrase "contact guidance". He examined the outgrowth from, and the interactions between explants and proposed that the structural (fibrillar) and ultrastructural (molecular) organisation of the substratum was responsible for cell alignment (Weiss,1934). Based on further observations he concluded that the substratum influenced cell migration and elongation by way of oriented surface molecules. Thus, although he rejected the hypothesis that topography directly affects cell behaviour, he was the first to recognise that cells could be influenced by a heterogeneous distribution of molecules on a substratum. In spite of Weiss' intention contact guidance is frequently used in relation to topographical influences only.

5.1.1 Chemical heterogeneity and haptic guidance *in vitro*

Exploiting advances in cell culture, Weiss performed an experiment which has since been repeated in many guises. A suspension of dissociated cells was plated over a glass substratum which had previously been

scratched with a series of parallel grooves (Weiss,1958). The subsequent elongation of cells along the scratches lead Weiss to deduce that the cells adhered more strongly to the scratches in the glass than they do to the surrounding surface.

The feasibility of this hypothesis was tested further by experiments using glass substrata streaked with silicone paste or cholesterol. Cells aligned between the streaks but failed to spread on the silicone paste or cholesterol (Weiss,1959). Since then a variety of techniques have been applied to pattern a range of substrates capable of aligning neurites including palladium, NGF, laminin, Con A and diamines (Harris, 1973; Gunderson, 1985; Hammerback *et al.*, 1985; Gunderson, 1987; Grumbacher-Reinert, 1989; Fromherz *et al.*, 1989; Kleinfeld *et al.*,1988).

These experiments demonstrate that cells can be guided by molecular heterogeneity either by some form of differential adhesion or by a more complex mechanism that may involve signal transduction (discussed in section 4.4). However, these experiments do not rule out the possibility that cells are sensitive to other properties of the substratum such as topography.

5.1.2 Topographical heterogeneity and steric guidance *in vitro*

Cells are strongly aligned to the long axis of fine rods made of glass and plastic (Weiss,1945; Dunn & Health,1976; Curtis & Varde, 1964), to fabricated surfaces with cylindrical profiles (Rovensky & Slavnaya,1974) and other topographical features (e.g. Clark *et al.*, 1987; Dow *et al.*, 1987; Wood, 1988). It is difficult to envisage how surface molecules could be distributed or oriented in a manner capable of explaining the alignment of cells on these substrata. Curtis and Varde (1964) concluded from their own investigations that the mechanism responsible involves the cells directly detecting the

shape of the substratum.

How cells transduce surface geometry has come under close scrutiny. The simplest type of topographical feature consists of the intersection of two planes at an angle (α in Figure 5.1a) to form a prism. Dunn & Heath (1976) showed that the angle at which two planes meet determines the success of cultured fibroblasts in crossing from one plane to the other. When the substratum was almost planar (or more specifically when the included angle between the two planes was greater than 176°) the topography had little or no effect. As the angle decreased (and the prism became more pronounced) the effect on the fibroblasts increased, reaching a limit below 148° when the cells became stranded on one of the two planes. This threshold angle matches the angle anticipated from an analysis of cytoskeletal geometry. The analysis considered a cytoskeletal microfilament sloping from the top of the nucleus to the basal membrane of the leading lamella. The angle of the slope was constant and the filament was considered to be inflexible. In the analysis, when the filament protruded over an angle greater than its slope anchorage failed and traction was impaired (Figure 5.1a). Thus, according to this model, the response to topography is due to "*...mechanical restrictions imposed on the locomotory system by the substratum*" (Dunn & Heath, 1976). The model predicts that filopodia explore the substratum, become oriented to the topography and align the cells accordingly (by contraction of microfilamentous components).

This model is successful in describing the behaviour of fibroblasts to topographies with different curvatures such as spheres (Dunn,1982) and spirals (Dow *et al.*,1987). However, observations of cells on grooved surfaces suggest an alternative hypothesis. Fibroblasts and epithelial cells are aligned by narrow grooves over which they bridge. If bridging is a

product of the ability of microfilaments to span the grooves, it suggests the grooves impose the minimum of mechanical restraint on the microfilament elements (Figure 5.1b). Ohara and Buck (1979) have proposed that the orientation of the focal contacts connecting microfilaments to the substratum is of key importance. These structures can be observed using interference reflection microscopy, appearing as elongated "feet" in contact with the

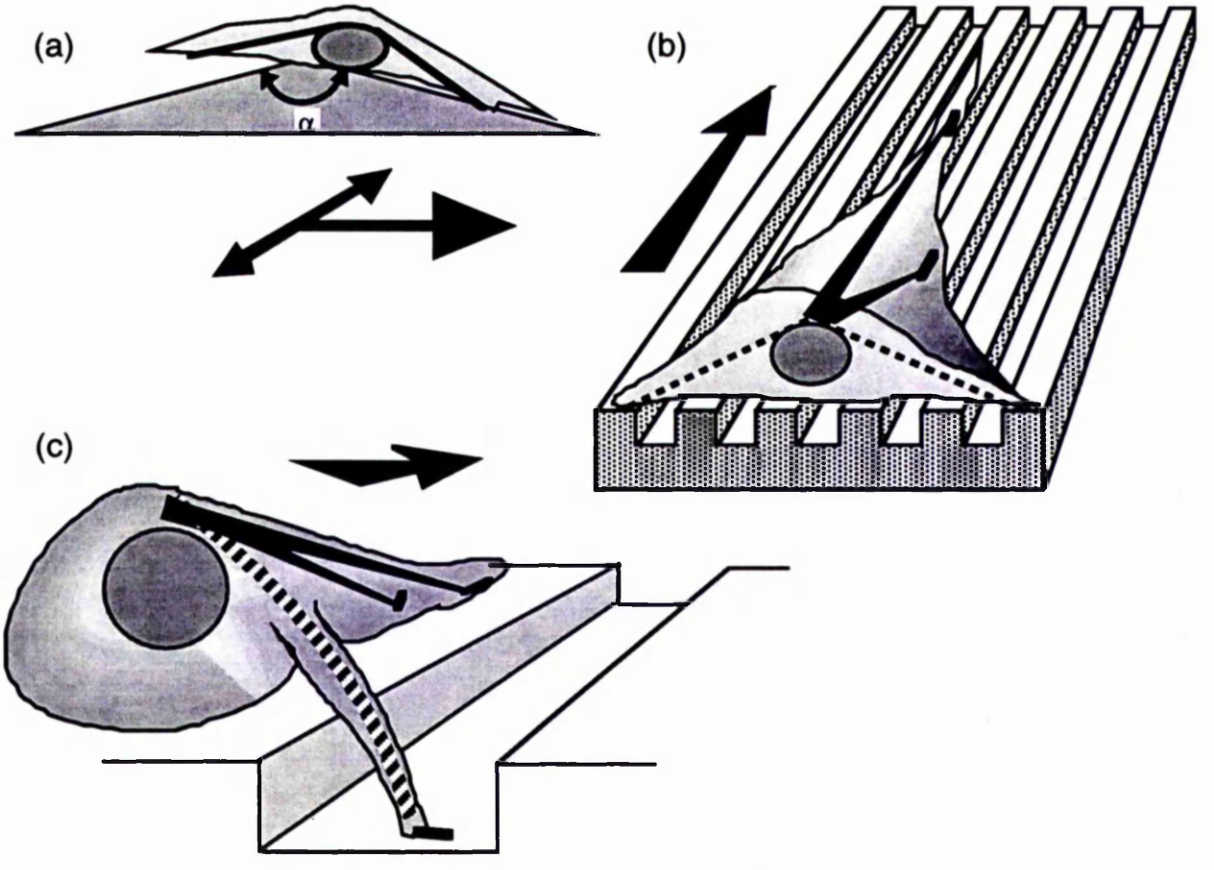

Figure 5.1: Constraints on cell alignment imposed by substratum topography (arrows indicate likely axis of alignment; solid and dashed lines show favoured and unfavoured orientations for microfilaments respectively). (a) Dunn & Heath (1976) showed that cells become stranded if plated one side of a prism if the angle of intersection (α) is below that of microfilament projection. However, Ohara and Buck (1979) proposed a different hypothesis to explain the alignment of cells to grooved substrata (b). They proposed that alignment was a consequence of oriented focal contacts. Dunn & Brown (1986) showed that the orientation of focal contacts in aligned cells could be distributed and observed focal contacts in the bottom of grooves. To account for these observations they concluded that alignment occurs in the direction which entails the smallest amount of distortion of the cytoskeleton (c).

substratum. As the orientation of the focal contacts coincides with the direction of microfilament polymerisation it is conceivable that it is the disruption to the formation of focal contacts that is important (Ohara and Buck; 1979). According to this hypothesis, cells would tend to align along the axis of topographical discontinuities owing to the comparative stability of the focal contacts aligned with this axis.

A detailed survey has been conducted to determine the distribution of focal contacts on grooved substratum (Dunn & Brown, 1986). Unlike Ohara and Buck's (1979) observations, cells were frequently observed making focal contacts with the floor of the grooves, a discrepancy that may be explained by the different method used to produce the grooves. Furthermore, the focal contacts on the ridges showed no obvious alignment and therefore invalidated Ohara and Buck's focal contact-based hypothesis. An additional observation made in this survey was that the actin bundles associated with focal contacts located in the grooves were nearly always oriented along the axis of the grooves. To account for these observations the key elements of the two models described above were combined to produce a third hypothesis (Dunn and Brown, 1986). Briefly, this hypothesis suggests that the restraints imposed on focal contact formation by topographical discontinuities are superimposed on the limitations caused by the inflexible nature of cytoskeletal components. Thus on a grooved substratum focal contacts are more *likely* to be aligned to the longitudinal axis of the grooves. Moreover, microfilaments anchored to focal contacts located within the groove will also tend to have a longitudinal orientation, since a perpendicular orientation would require curvature which would reduce the stability of the filaments (Figure 5.1c; Dunn and Brown,1986).

The alignment of neurites to topographical features may be mediated

by a similar mechanism. Interestingly the lamellae produced by Retzius neurones cultured on a planar substratum coated with Con A make few if any focal contacts (reported in Chapter 4). Instead the outgrowth is characterised by a large area of close contact, similar in appearance to the dynamic adhesions made by highly motile cells (see Verschueren, 1985) that show a relatively large resistance to topographical influences (Clark *et al.*, 1987). The results below show that unlike neurites, the lamellar-type outgrowth was only slightly influenced by the topography. This supports the suggestion that the nature of the adhesion made with the substratum (along with the flexibility of the cytoskeleton) may be of key importance in determining cell specific behaviour to topographical features (Clark *et al.*, 1987) and corroborates the hypothesis presented in the discussion that the influence of topographical discontinuities is modulated by the composition of the ECM.

5.2 Materials and Methods

5.2.1 Fabrication of grooves

A method of fabrication was adopted (summarised in Figure 5.2), capable of producing regular arrays of parallel grooves in perspex substrata (Clark *et al.*, 1990). Squares with sides of 20 mm, were cut from 4 mm thick perspex sheets. This thickness was preferred as it was less prone to warping.

The protective covering provided by the manufacturers (ICI, UK) was removed from each square which was then washed thoroughly by ultrasonication for 5 min in each of the following: liquid soap (RBS.25, Chemical Concentrates (RBS) Ltd.,UK), iso-propanol and double-distilled water.

An aluminium coat approximately 100 nm thick was evaporated onto the perspex in an Edwards vacuum coating unit at $4x10^{-5}$ Torr (Figure 5.2a). A uniform coat of positive photoresist (S400-31 Microposit, Shipley Chemicals, UK) was applied by spinning at 4000 rpm for 25 s, giving a typical thickness of 0.5 μm. The perspex square was then baked for 30 min in a fan oven at 90°C. The photoresist was selectively exposed to ultraviolet light through a chrome mask (Figure 5.2b), and developed with 50% Microposit developer (Shipley Chemicals, UK; Figure 5.2c). The length of the exposure and the time in developer required careful adjustment to ensure that the grooves and ridges in the photoresist had the correct ratio. A wet etch (Figure 5.2d) consisting of 80% concentrated phosphoric acid, 5% concentrated nitric acid and 15% water was used to remove the exposed aluminium, leaving areas of bare perspex (Figure 5.2e). The structure was then blanket exposed to ultraviolet light and developed to remove the remaining photoresist. The areas of aluminium on the surface of the perspex

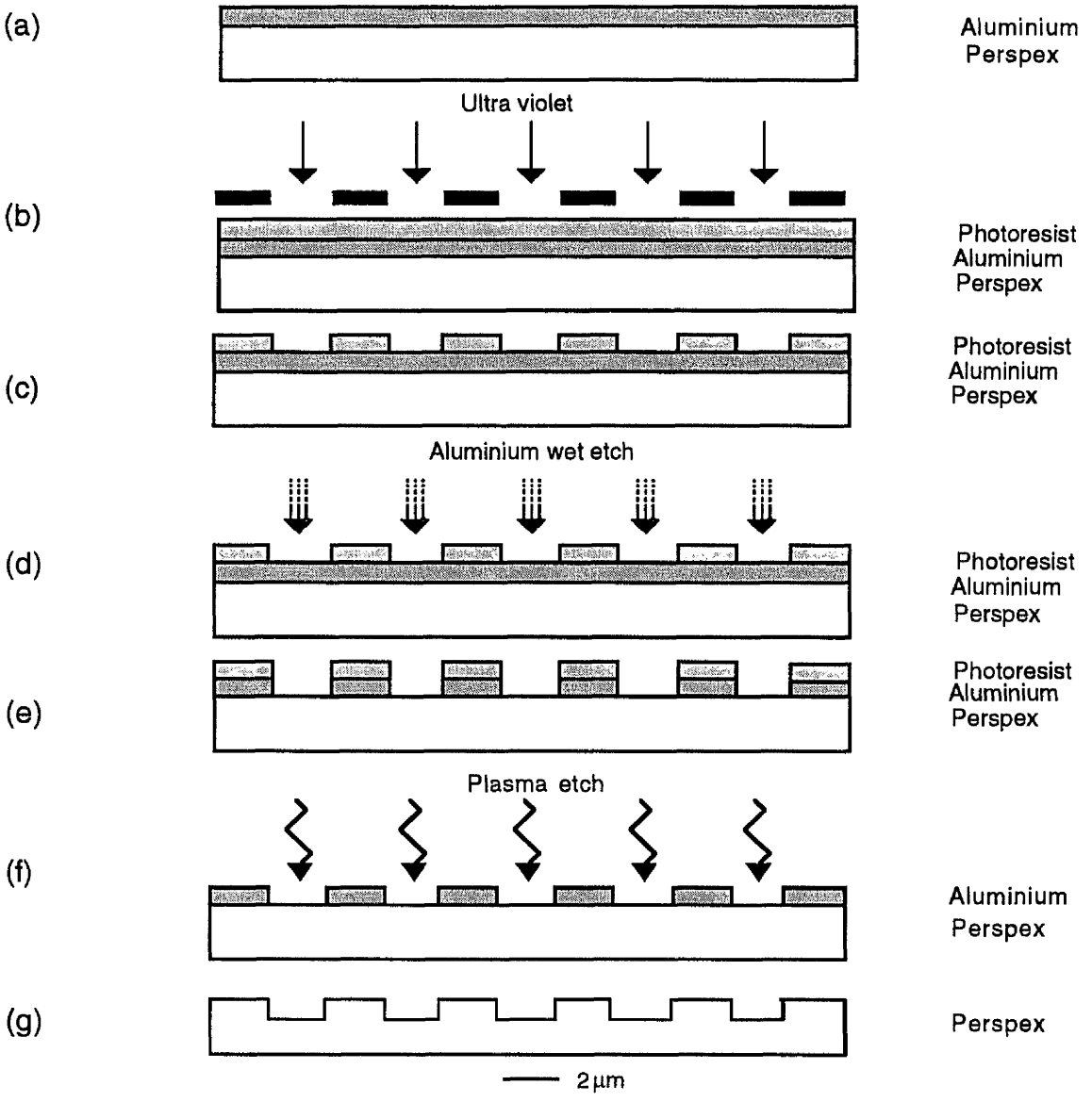

Figure 5.2: Microfabrication of grooved substrata. (a) Aluminium was evaporated onto perspex. (b) A layer of photoresist was spun onto the aluminium and then selectively exposed to ultraviolet light by way of a mask. (c) These areas were removed by developing, which made areas of the underlying aluminium susceptible to a subsequent wet etch (d). At this stage, the pattern of the mask was replicated on the perspex as areas of aluminium coated with photoresist (e). This pattern was transformed into a surface topography by etching the unshielded perspex using a plasma etch (f). The length of the etch determined the magnitude of the topography.Finally, the remaining aluminium was removed by a wet etch and the entire surface exposed to a brief plasma etch to ensure uniform surface properties (g).

replicated the pattern of the mask.

A topography was produced by dry-etching the bare perspex using an oxygen plasma, reactive ion etch system (System 80, Plasma Technology, UK; Figure 5.2f)[1]. The length of the etch was skilfully controlled to give a topography of the desired depth. The aluminium negative was removed by wet etching and then briefly blanket-etched to ensure surface uniformity.

The completed structures had parallel ridges separated by grooves of the same width (either 2 μm or 12 μm) of varying depths. Structures were sterilised before use with 70% ethanol and coated with Concanavalin A as described in section 2.2.5.

Neurones cultured on wide grooves could be observed with phase contrast optics. However, the morphology of neurones grown on narrow grooves was obscured by the phase interference produced by the topography of the substratum. Thus on narrow grooves cells were fixed in leech Ringer containing 2.5% glutaraldehyde (EM grade; TAAB Lab. Equipment. Ltd, UK) and washed in leech Ringer. Following fixation, cells were either stained for 30 min in a 1% solution of kenacid blue and photographed using bright field optics, or prepared for the scanning electron microscope by post-fixing in osmium tetroxide, freeze drying in liquid propane and then coating with a thin layer of evaporated gold.

5.2.2. Patterning of Proteins

Photolithography was used to define the dimensions of the small areas required. In view of the apparent delicacy of leech extracellular matrix extract, a method was developed for patterning which was likely to have

---

[1]This stage was very kindly performed by Bill Monaghan

minimised the possible damage to the component proteins. This method was successful in patterning Con A as judged by immunofluorescence and the alignment of BHK cells (see below).

Glass slides (BDH, UK) were scribed on one side with a 10 mm by 10 mm square, which was used to reference the patterned area. The slides were ultrasonicated in soap solution (RBS.25, Chemical Concentrates (RBS) Ltd., UK) for 5 min, rinsed under double-distilled water and then acid washed as follows. The slides were ultrasonicated for 5 min in a fresh solution of 90% sulphuric acid and 10% hydrogen peroxide. They were then washed in 20 changes of double distilled water, ultrasonicated in double distilled water, rinsed and air dried.

A coat of photoresist (S400-17 Microposit; Shipley Chemicals, UK), approximately 0.5 μm thick, was spun onto the unscribed surface of each slide at 4000 rpm for 25 sec. The slide was then baked for 30 min at 90°C in a fan oven. A chrome mask was used to selectively expose areas of the photoresist, centred about the scribed square. The exposed photoresist was developed using a solution containing 50% Microposit developer (Shipley Chemicals, UK).

The patterned photoresist was used to selectively shield protected glass from dichlordimethyl silane (Sigma, UK). This was applied as a vapour. A glass container with a loose-fitting lid was preheated to over 150°C on a hot plate in a fume cupboard. Slides were placed in the container with about 0.25 ml of dichlorodimethyl silane and the lid was closed. The same amount of dichlorodimethyl silane was added after 5 and 10 min, and the container removed from the heat after 15 min. The slides were washed in 3 changes of chlorobenzene to remove residual dichlorodimethyl silane and then immediately rinsed in double distilled water. Exposure to the chlorobenzene

was made as brief as possible to avoid over-hardening the photoresist.

The next stage in the process involved removing the remaining photoresist to reveal the untreated glass. Two methods were tried. One method was to over-expose and develop, the second was to rinse in acetone. Inspection, using reflection microscopy, revealed that neither of these methods reliably removed all the photoresist. Extensive ultrasonication (lasting up to 90 min) in acetone was found to be the best approach, but was not always successful, sometimes leaving highly fragmented strips of photoresist.

At this stage, the pattern was tested by wetting the slide. The bare glass was hydrophilic, but the area defined by the scribed square (scratched on the opposite side of the glass) was hydrophobic indicating that the preliminary stages were successful.

The bare glass was treated with aminosilane using the method developed by Kleinfeld *et al.* (1988). Slides were agitated for 10 s in a fresh solution containing 95% ethanol, 1% 3-aminopropyltriethoxysilane (Sigma, UK) and adjusted to pH 5 with acetic acid. The slides were rinsed in three changes of ethanol and then baked at 120°C for 10 min in a fan oven.

The chemistry in the following procedure was suggested by Prof. A.S.G. Curtis. The aminosilane pattern was used to couple polyserine (Sigma, UK), which has a high density of hydroxyl groups[2]. This was achieved by (1) coupling polyserine to N-hydroxysulfosuccinimide (Sulfo-NHS; Pierce, The Netherlands) dissolved in a solution containing dimethylformamide (DMF; Pierce, The Netherlands) and N,N-

---

[2]According to Curtis *et al.* (1986) cell adhesion is poor on surfaces with a high density of hydroxyl groups.

Dicyclohexylcarbodiimide (DCC; Pierce, The Netherlands) and then (2) reacting the Sulfo-NHS-polyserine complex with the amine groups on the surface of the glass. For the first step 5 mg of polyserine, 1 mM Sulfo-NHS and 1 mM DCC were added to 3 ml of DMF, and left standing at room temperature for 1 h. This solution was then added to 100 ml of PBS in a dish containing the slides. The cocktail was stirred for 12 h and then poured off.

The next stage in the process was to convert the remaining amino groups to hydroxyl groups, using dilute nitrous acid. 50 mg of sodium nitrite ($NaNO_2$; Hopkins and Williams, UK) was placed in a vessel containing the slides. 100 ml of 0.5M HCl was added to produce nitrous acid. After 30 s in the acid, the slides were washed thoroughly in Phosphate Buffered Saline (PBS).

The final step in the process was to incubate the slides for 1 h in 150 $\mu g.ml^{-1}$ of Con A in PBS. The slides were again washed extensively in PBS and used within a few hours.

5.2.3 Fibroblast assay of protein patterning

Baby Hampster kidney fibroblasts (BHK cells) were used as a bioassay to determine the success of the protein patterning technique.

Cells were originally obtained from departmental stocks, and grown to confluency at 37°C, in a 250 ml tissue culture flask (Greiner Labortechnik, Germany) containing BHK medium (known as HECT: Hepes Eagle Calf serum Trypose phosphate; see Appendix 1).

Flasks containing confluent cells were rinsed in Ca^{2+} and Mg^{2+} free, 20 mM Hepes buffered Hank's basic salt solution. 0.05% trypsin in 0.2 $mg.ml^{-1}$ EDTA was added, and the flasks were incubated at 37°C until the cells detached. The trypsin was inhibited by adding serum-containing

medium. The cell suspension was centrifuged at 4000 rpm for 6 min, the medium replaced, and the cells resuspended by trituration. After counting, a proportion of the cells was added to a new medium-containing flask for future use. The remaining cells were used for experiments.

The slides were placed in a 35 mm tissue culture dish with the patterned side uppermost. BHK cells were added to each dish in modified BHK medium containing 2% foetal calf serum, to give a plating density of approximately 1000 cells/cm^2.

12 h after plating the slides were gently rinsed in PBS and then fixed with PBS containing 2.5% glutaraldehyde for 15 min. Cells were either photographed using phase contrast optics, stained with a solution containing 2.5% Kenacid blue and photographed using bright-field optics, or used as described below.

5.2.4 Immunofluorescence staining of Concanavalin A patterning

In order to ensure that the BHK cells were aligning to the Con A stripes (and not the highly hydroxylated intervening areas), the absorbed Con A was stained using immunofluorescence.

Fixed slides were washed thoroughly by rinsing and soaking three times in a 2% solution of Tween 20 (Sigma, UK) in PBS. Non-specific absorption of antibody was prevented by an additional 30 min soak in a 2% solution of Tween 20 supplemented with 4 $mg.ml^{-1}$ Bovine Serum Albumin (BSA; Sigma, UK).

The slides were incubated with a 0.2% solution of Rabbit Anti Con A (Molecular Probes, US) in PBS for 1 h, and then washed extensively with three 30 min soaks in 2% Tween 20 solution. A second incubation (also 1 h) with a 0.2% solution of fluorescein-conjugated Donkey anti-Rabbit antibody

was used to immunologically label the first antibody. The slides were then washed as before.

The fluorescence was viewed using an epifluorescence microscope (Leitz, Germany), using fluorescein filters and a 50x water immersion lens (with a numerical aperture of 1.0).

5.3 Results

5.3.1 Topographical guidance

Alignment of neurites to grooves

A small proportion of the Retzius neurones cultured on grooved substrata (coated with Con A) produced neuritic outgrowth which lacked lamellae. Three of the cells were plated on grooves which had a depth, width and separation of 2 μm (e.g. Figure 5.3). The fourth cell was plated on slightly shallower grooves (1.5 μm deep) with a larger width and separation (both 12 μm). This small sample of cells demonstrates the potency of topographical features on neurite outgrowth.

As a whole the outgrowth of the cell in Figure 5.3 had a shape which was elongated in both directions along the axis of the grooves. The overall shape had a length:width ratio of 3.73, whereas the length:width[3] ratio of the outgrowth from 12 Retzius neurones plated on a planar substratum coated

[3]The length taken as the long side of the rectangle which best describes the shape of the outgrowth, NOT the axis defined by the process.

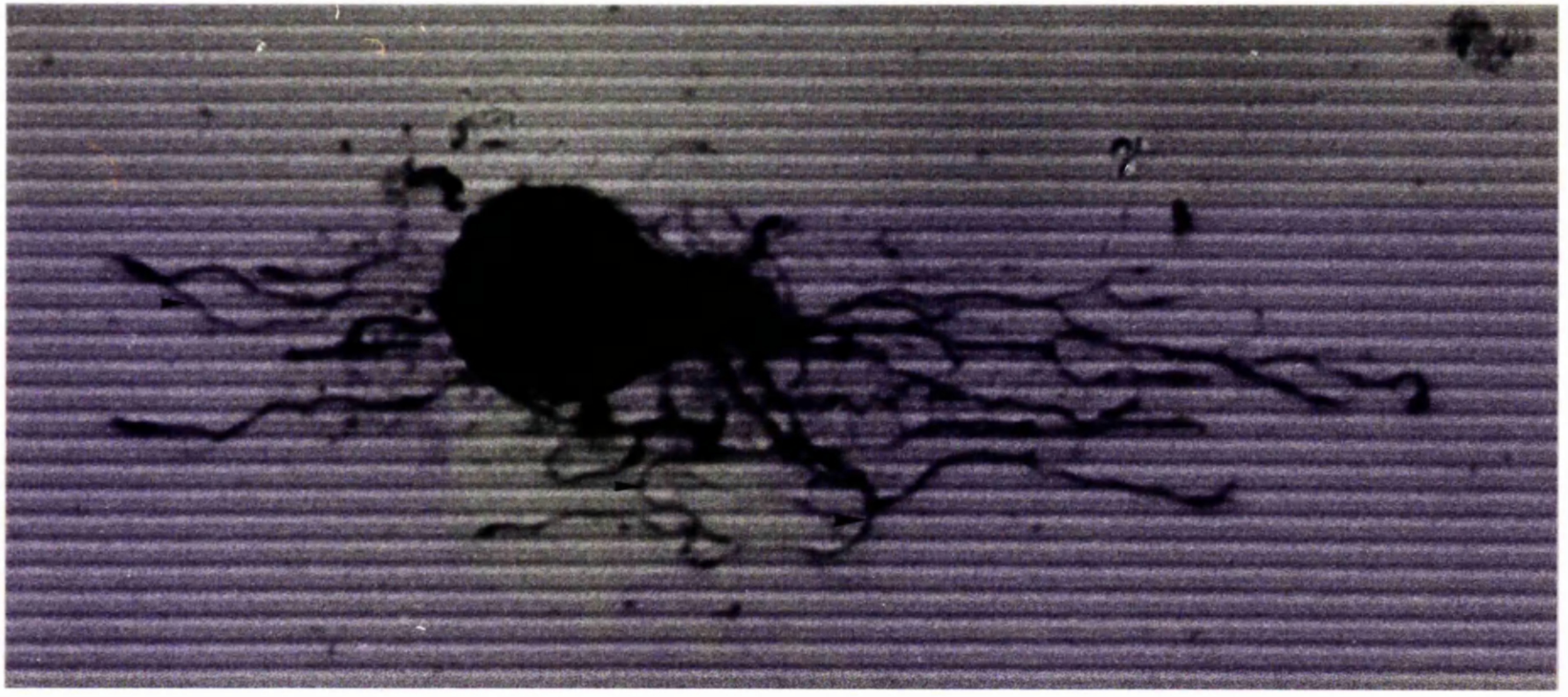

Figure 5.3: Topographical guidance of an identified leech neurone. The photograph shows a Retzius neurone plated on grooves with a depth,width and separation of 2 µm. The cell was cultured for 7 d and then was fixed in 2.5% glutaraldehyde and stained with a 1% solution of Kenacid blue. Arrows indicate neurites showing repeated disregard for individual topographical features. Scale bar: 10.6 µm.

with Con A was 1.43 (S.E.M.±.0.09) μm. The outgrowth appeared to be weighted in the direction of the stump. The outgrowth in this direction extended approximately 100 μm whereas the most distal point in the opposite direction was only 53 μm away from the cell body. Note however that if the neurites originated from only the axon stump then the outgrowth in both directions was approximately equal.

Most of the neurites showed strong alignment along their length, except in places where the alignment was briefly disrupted by short protrusions across the grooves. These protrusions may have been the result of small variations in the topography or the Con A coating. Alternatively they may have simply reflected the probabilistic nature of contact guidance (Clark *et al.*, 1987). A few processes which were elongated along the axis of the grooves appeared to disregard several of the individual topographical features (each of which can be regarded as a step; see arrows on Figure 5.3). Perhaps in these cases the angle of encounter with consecutive steps was too large or maybe the topographical influences were overridden by innate cytosketetal restraints associated with branch points (Acklin & Nicholls, 1990; Solomon, 1979).

The grooves in Figure 5.4 had a depth of 1.5 μm and a width and separation of 12 μm. These dimensions would appear to be less effective in elongating the overall shape defined by the perimeter of the outgrowth, since the ratio between the length and the width (perpendicular to the grooves) of the outgrowth from the cell in Figure 5.4 was approximately 1.33. However, a closer inspection reveals that several neurites had aligned along the axis of the grooves. Furthermore, the direction of elongation of most of the neurites was heavily influenced by each encounter with a topographical feature (or step).

The influence of each individual step was roughly quantified by dividing the total neurite length by the number of times the neurites crossed steps. This gave the average length of neurite between each step crossing, which was normalised with the separation between the steps:

$$\text{Influence of a single discontinuity (or step)} \approx \frac{\text{Total neurite length}}{\text{Number of crossings}} \times \frac{1}{\text{Step spacing}} \qquad (5.1)$$

A comparison between the neurones in Figure 5.3 and Figure 5.4 shows that the influence of each topographical feature was similar (Table 5.1). Thus the low value for the length:width ratio of the overall outgrowth in Figure 5.4 was likely to be a consequence of dispersion caused by the wide spacing between the topographical discontinuities, rather than a difference in the neurite-aligning capability of each step.

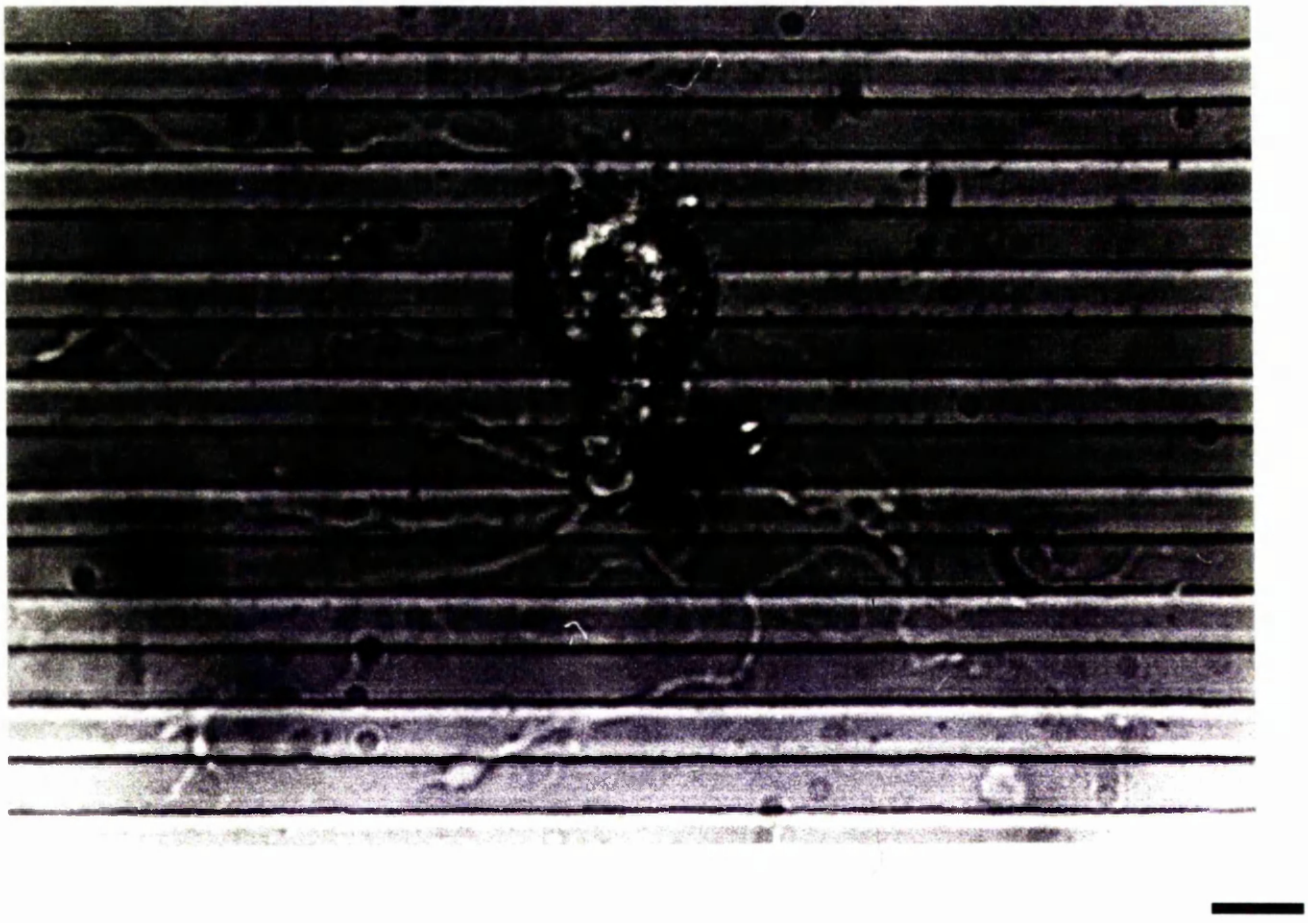

Figure 5.4:Phase contrast image of a Retzius neurone grown on Con A-coated grooves . The grooves had a depth of 1.5 µm, a width of 12 µm and a separation of 12 µm. Scale bar: 10 µm.

	Depth	Spacing of discontinuities (µm)	Total neurite length (µm)	Number of crossings	Normalised Influence ratio
Figure 5.3	2	2	1008	34	3.5
Figure 5.4	1.5	12	1273	143	3.12

Table 5.1: The influence of single topographical features on the neurites of two cells cultured on grooved substrata.

Alignment of lamella-dominated outgrowth

The vast majority of Retzius cells cultured on grooves coated with Con A produced broad flat processes which also typified the gross morphology of the outgrowth seen on planar Con A-coated substrata (section 4.2.3). These lamellae often covered several grooves (e.g. Figure 5.5); only the edge of the lamellae appeared to be influenced by the topography.

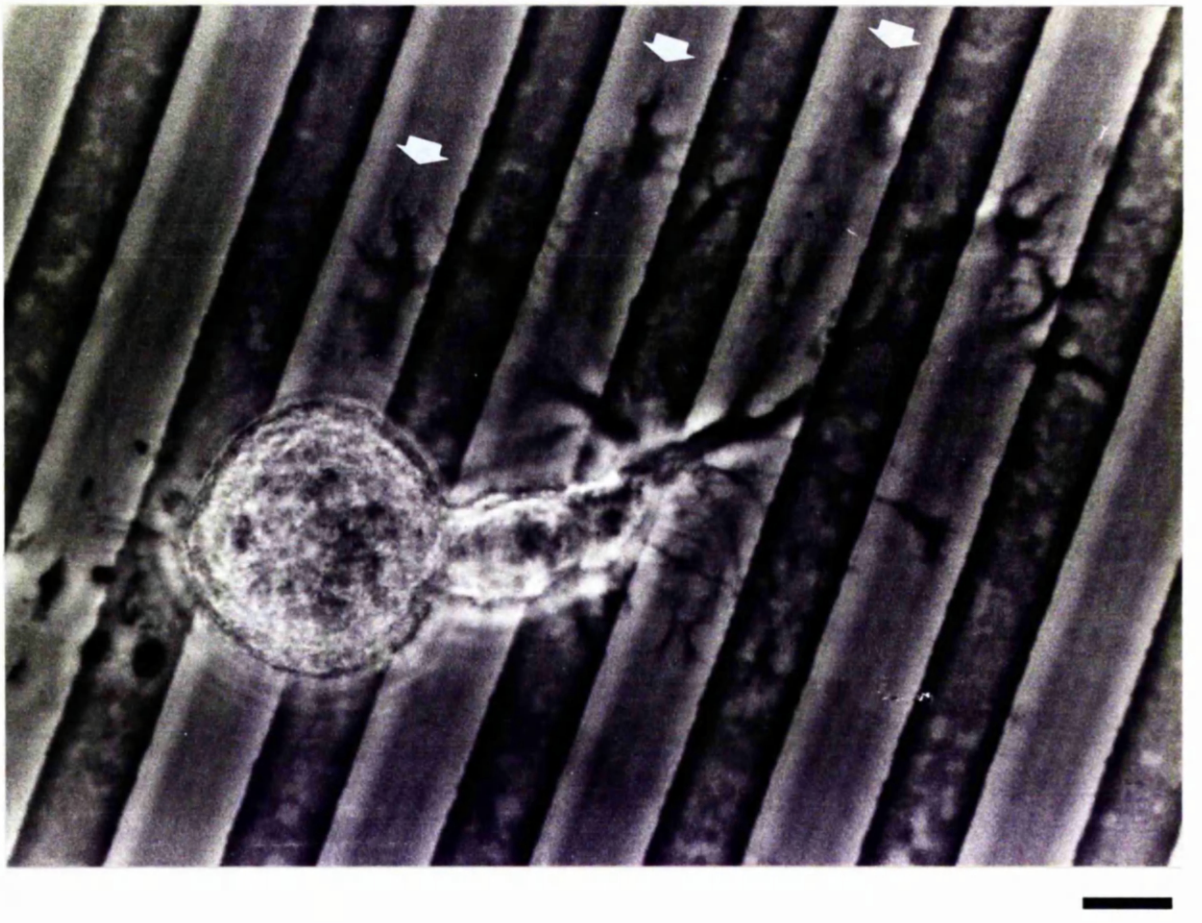

Figure 5.5: Response of a lamellar-type outgrowth to 1 µm deep Con A-coated grooves. The grooves have a width and separation of 12 µm. The photograph was taken after 12 h using phase-contrast. Arrows indicate finger-like structures in the distal margin of the lamella that appear to be aligned to the grooves. Scale bar: 11 µm.

The Retzius neurone in Figure 5.5 is representative of the results

obtained. The cell was cultured on grooves 1 μm deep that had a width and separation of 12 μm. To the right and to the left of the outgrowth the lamellae appeared to bridge two and three topographical discontinuities respectively. Only the finger-like structures at the distal edge of the lamellae seemed to be oriented along the axis of the grooves (marked by arrows in Figure 5.5).

On deeper, narrower grooves the alignment of the distal finger-like structures was more pronounced, but lamellae were still able to bridge individual grooves. For example, in Figure 5.6a a lamellar region can be seen spanning 3 of the grooves although finger-like structures did correspond to groove crossings (illustrating that the topography did have some effect on the formation of the lamella).

The effect of the topographical discontinuities on the filopodia was even less striking. The filopodia that can be seen in Figure 5.6b (which shows the central region of Figure 5.6a but at a higher magnification) demonstrated a variety of responses. Some of the filopodia were oriented along the axis of the grooves for part of their length, for example the four filopodia that ran side by side on the ridge that separates the middle and lower grooves in the photograph. However, when these filopodia reached the edge of the ridge they appeared to plunge down into the groove. At least one of them traversed the groove to the opposite wall but did not climb out, instead it was deflected back into the middle of the groove. Thus this filopodium was able to overcome the downward step but was restrained by the upward step on the opposite side of the groove. Other filopodia responded quite differently to step encounters. For example, the filopodium that began on the ridge at the top of the photograph encountered, descended and crossed the floor of a groove, but then climbed out on reaching the opposite wall. In both this and the previous example descending the walls of

the grooves appeared to cause a slight *reduction* in alignment. Another type of encounter can also be observed from the photograph. Three of the filopodia crossed the bottom groove in the photograph without descending. These bridging filopodia appeared to approach the grooves perpendicularly.

In both parts of Figure 5.6 there is evidence that outgrowth occurred preferentially on the Con A-coated surface as compared to on pre-existing membrane. For example, the group of four filopodia described above were not fasciculated despite the close proximity between neighbours. In addition, of the two filopodia from the four that can be clearly discerned on the floor of the groove, only one of them appears to have interacted with the opposite wall, yet both were deflected, suggesting that the inner of the two was deflected by the presence of the outer. Finally, in both cases where a fillopodia crossed other membrane it appears that membrane to membrane contact was minimised (and membrane to Con A contact was maximised) by perpendicular crossings.

In summary, the guidance of neurites by the grooves was pronounced. The closer the spacing of the grooves, the larger the number of interactions that occurred between the neurites and the topographical discontinuities, and the better aligned the overall outgrowth. The effect of the grooves on the lamellar type outgrowth of Retzius neurones was more subtle. The lamellae spanned several grooves, the only effect of the topography was to determine the position of the finger-like structures at the leading edge of the lamella.

Figure 5.6 (following two pages): S.E.M. of the distal margin of a lamella produced by a Retzius neurone plated on a Con A-coated grooved substratum. The grooves had a depth, width and separation of 2 μm, and appear dark in the photographs. The cell was fixed after 24 hours. Black scale bars in (a) & (b) are 5 μm and 2 μm respectively.

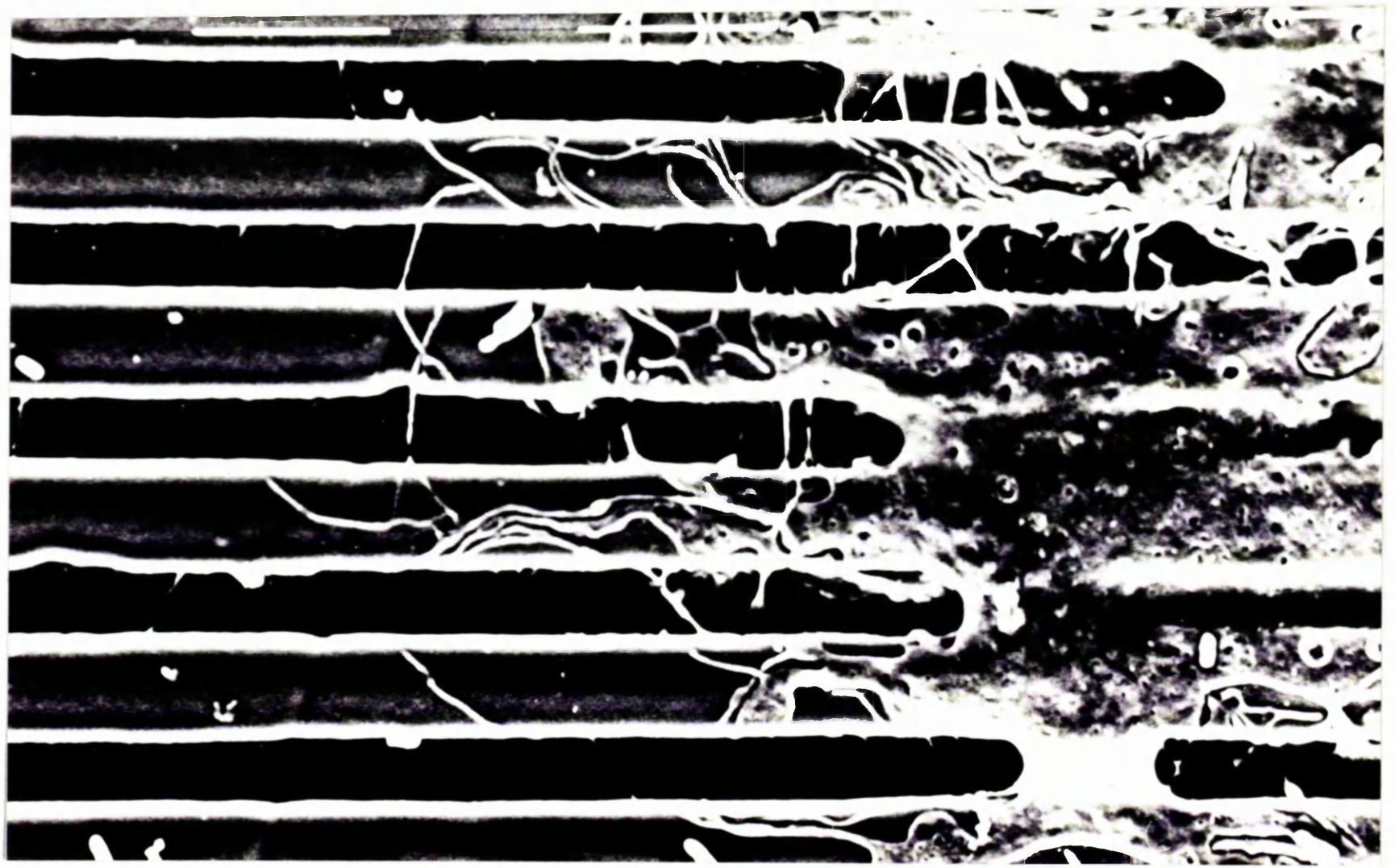

A

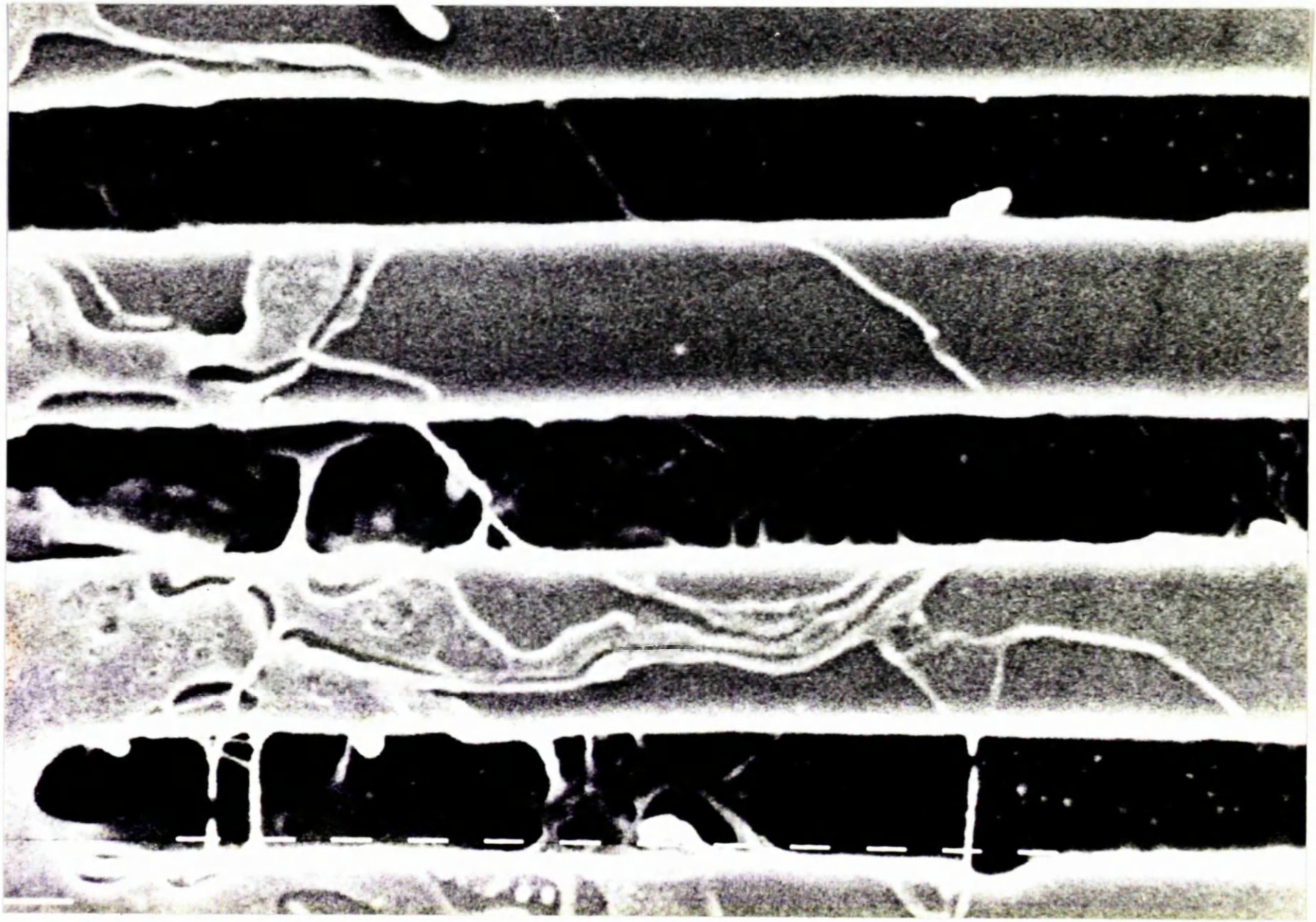

B

The interaction between the filopodia and the walls of the grooves was mixed. Bridging filopodia approached perpendicularly, those that descended into the grooves approached less acutely. Descending into a groove appeared to *reduce* alignment. Filopodial alignment was only enhanced when the filopodium were deflected by the walls of the grooves.

5.3.2 Protein patterning

BHK cells were used primarily to test batches of slides to ensure protein patterning was successful. However, the peculiar morphology of BHK cells on stripes of Con A may be of greater consequence.

On microscopic grooves over 1 μm deep and on submicroscopic (ultrafine) grooves[4] over 100 nm deep BHK cells are reported as being bipolar and highly elongated (Clark *et al.*, 1990; Clark *et al.*, 1991). As can be seen from Figure 5.7 the response of BHK cells to the putative Con A pattern was more complicated. The cells *were* elongated. For example, a random field of view of one slide contained 25 cells which had an average overall length to width ratio of 3.8 (S.D.± 2.4). However, the morphology was rarely bipolar (n=2 of the above sample) since the cells had processes which were aligned along neighbouring strips of Con A. The number of aligned processes varied between cells: the average number in the above sample

Figure 5.7 (following page): Alignment of BHK cells to substrata patterned with stripes of Con A. The cells were fixed and then stained with 1% Kenacid blue. Scale bar; (a) 20 μm; (b) 180 μm.

[4] The width and the separation of grooves were between 2 and 12 μm whereas the dimensions of the ultrafine grooves are in the order of 130 nm.

A

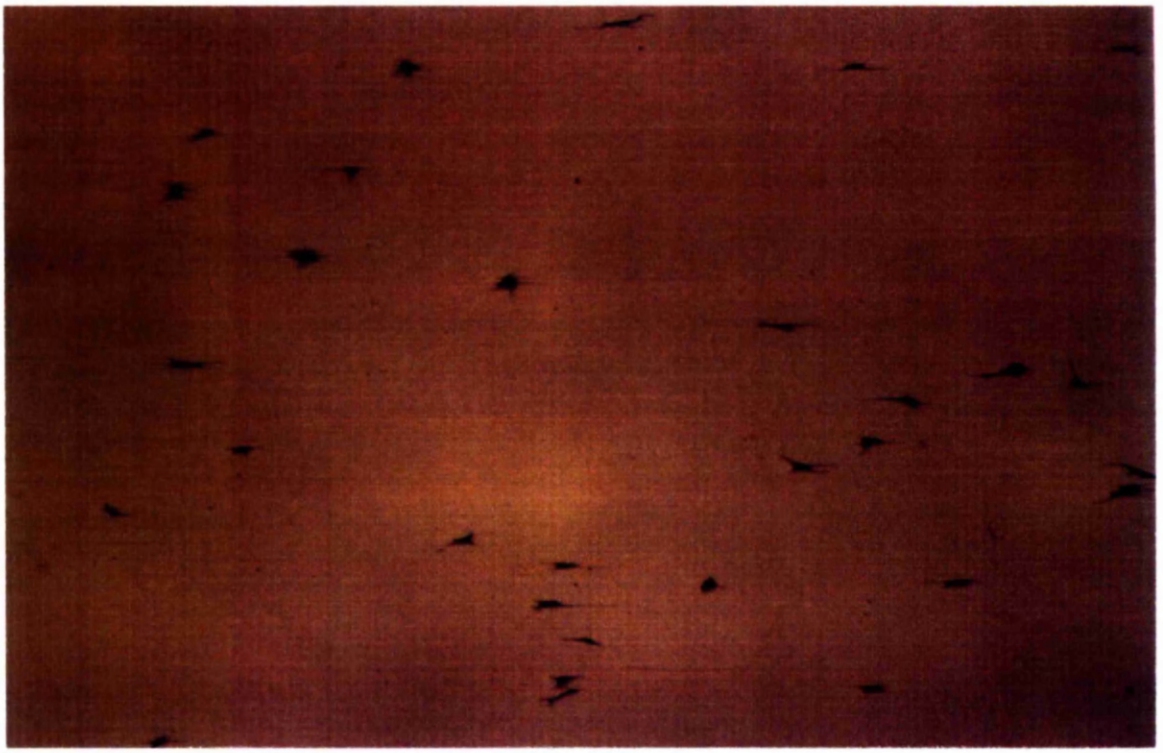

B

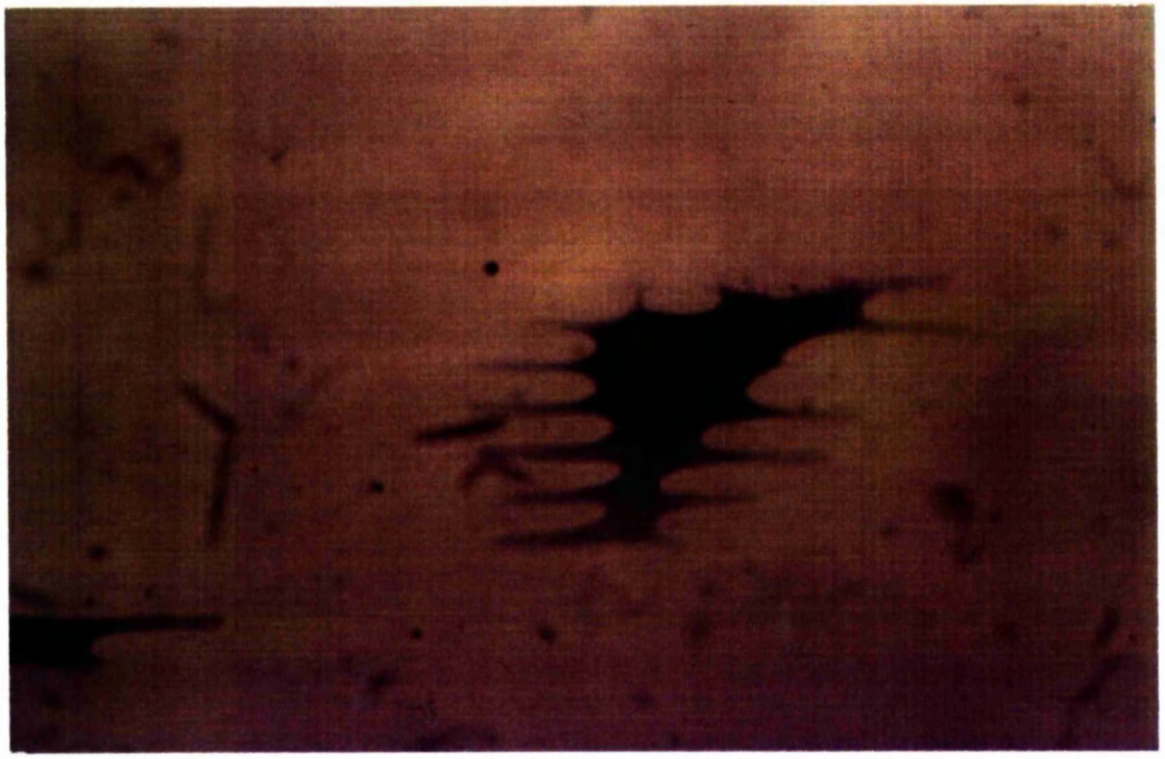

was 4.32 but the standard deviation was 1.93. The cell stained with Kenacid blue in Figure 5.7b had a length:width ratio of 1.7 yet had 11 processes which were oriented in the direction of the stripes. The processes on either side of the cell resembled a comb.

The processes of the BHK cells were correlated to fluorescently labelled strips which were visible following immunofluorescent staining. This suggests that not only was the Con A patterning successful but also that the alignment was to the Con A and not to the aminosilane or polyserine-treated areas.

Attempts to influence the morphology of the outgrowth of Retzius neurones with patterned Con A were less successful. Out of a total of 16 slides (made in 4 batches) on which 2-3 Retzius neurones were placed per slide only one cell showed any signs of alignment (Figure 5.8): the vast majority of the cells failed to attach or attached but failed to produce outgrowth. The outgrowth of the cell in Figure 5.8 was highly finger-like structures and the broadest of the narrow lamellae were oriented approximately in the same direction (within an average angle of 20° to the axis of the 2 μm wide Con A strips; n=5). If this does constitute alignment then it is conceivable that it may have been caused by properties other than a pattern of Con A since the cell in Figure 5.8 was plated in a region were a proportion of the photoresist remained. In addition, the cell body was surrounded by an area which appears to be contaminated with glial debris. The photoresist may contribute directly to the alignment by topographical guidance and the glia debris may influence one or both of the patterned substrata.

Two batches of slides (8 slides/batch) were used in an attempt to pattern leech laminin. Unfortunately, neurones failed to attach during plating

or attached but did not produce outgrowth.

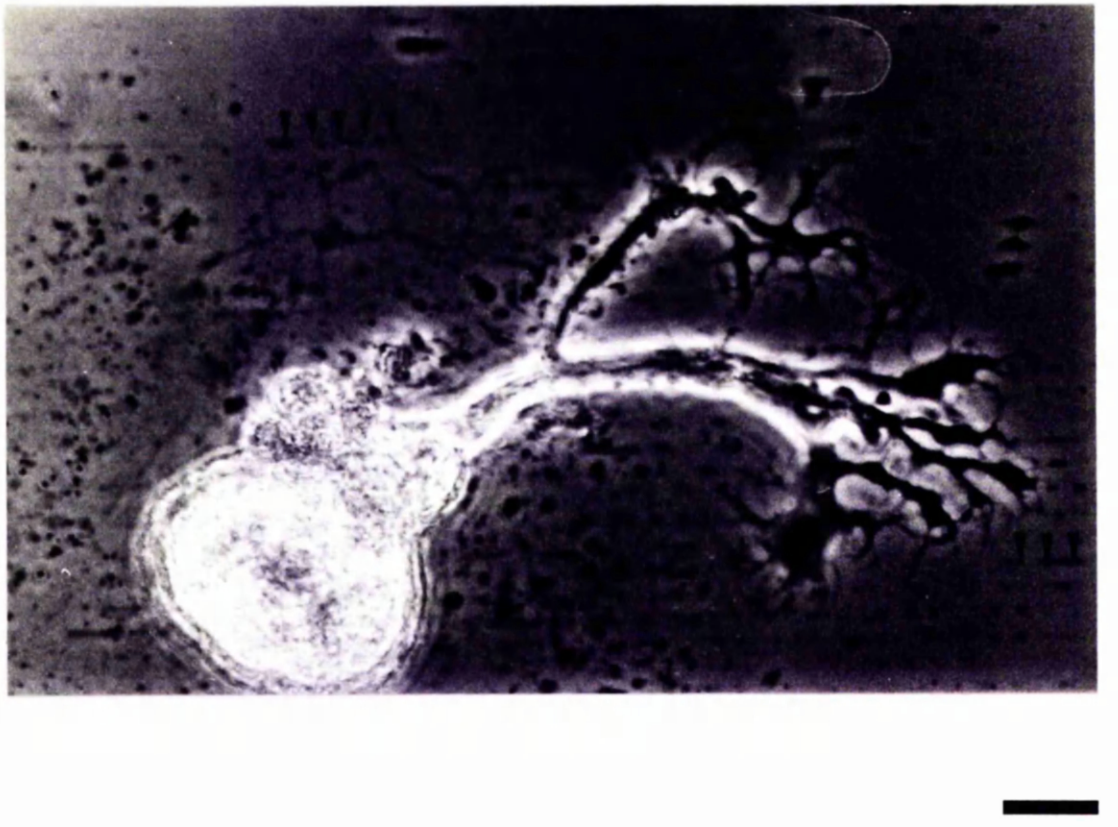

Figure 5.8: Photograph of a Retzius neurone cultured for 24h on a surface patterned with strips of Con A. Each strip was 2μm wide, with 2μm separations. Note the narrow bands of lamellar-type outgrowth which may have been slightly aligned to the patterned substrate. Also note however that the cell was plated on a region containing residual photoresist (indicated by the arrows). The photoresist may have provided topographical cues.Scale bar: 18 μm.

5.4 Discussion

The results in this Chapter provide the first demonstration that large invertebrate neurones are aligned by topographical discontinuities. Furthermore they show that the dimensions of the topographical features required to change the orientation of invertebrate neurites are similar to those required to align the processes of vertebrate neurones (Clark *et al.*, 1990). Despite the difference in the size of the cell body (and the average diameter of processes *in vivo*), the machinery influenced by topography is likely to share similar dimensions.

In light of these results the discussion considers whether topographical guidance plays a role in neuronal development and regeneration *in vivo*. It then presents the hypothesis that the nature of the ECM mediates the influence of topographical features.

5.4.1 Topographical guidance of regenerating leech neurones *in vivo*?

The morphology of the Retzius neurone in Figure 5.3 shows some similarities with the morphology of regenerating N cells within crushed connectives (described by Wallace *et al.*,1977). It was reported that the axon of the N cell began to branch profusely near to the site of the crush. The resulting neurites elongated along the axis of the connective, initially in both directions. Thus, within a crushed connective it seems that the main alignment cue provides no additional information as to which direction the previously innervated ganglion lies. Topographical cues could fill such a role, but they are not alone: uniform tracks of adhesive molecules could also produce bidirectional alignment. It is noteworthy that the outgrowth from cultured Retzius neurons has been guided by 10 μm wide tracks of patterned

leech laminin (Fromherz *et al.*, 1989). Attempts to guide neurones with finer patterns were unsuccessful, possibly because of toxicity (Section 5.3.2).

A second similarity between the outgrowth of the neurone in Figure 5.3 (see also footnoot '3' this Chapter) and regenerating N cells *in vivo* was the possible polarised elongation. Although new neurites grew in both directions along the axis of the connective, the longer neurites would appear to have extended in a direction similar to the course taken by the original axon. One possibility is that *in situ* additional long range cues provide the neurites with the directional information. Removing the ganglion at the end of a crushed connective had no effect on the morphology of regenerating neurites within the connective (Wallace *et al.*,1977). Thus, any additional cue that might be available, is not ganglionic in origin. The possible polarisation in the length of neurites seen *in vitro* may have reflected an intrinsic property of the cell. For example, the remaining cytoskeletal filaments may be polarised in the direction of the stump, and may define the axis of new filaments. Cultured leech neurons also show polarisation in forming synapses. Liu & Nicholls (1989) demonstrated that synapses form most readily between the stumps of two adjoining cells than between any other combination of locations. Presumably the stumps of extracted neurons and crushed axons are sites at which a high proportion of the cell's scaffold prematurely terminates. Proteins that are transported along the scaffold might become concentrated in this region, differentially promoting regeneration.

Finally, the neurites from both the N cell and the Retzius cell in Figure 5.3 occasionally undergo short perpendicular protrusions, which act to disperse the neurites within the regenerating connective and on the grooves. These breakdowns in alignment, may be due to the probabilistic nature of contact guidance (Clark *et al.*,1987), and/or the other cues involved. Slight

dispersion may not be detrimental, as it would act alongside branching frequency to increase the number of entry points into the next ganglion. This in turn would increase the number of cells contacted, which could be beneficial to those neurons which have a wide influence. The probability of topographical guidance does vary between classes of cells such as rabbit neutrophils and chick hemisphere neurons (possibly as a result of differences in cytoskeletal organisation and/or substratum adhesion; Clark *et al.*, 1987) and morphological differences in the outgrowth from different types of identified neurons plated on the same chemical substrate has been reported (Chiquet & Acklin, 1986). It would be interesting to compare the influence of topography on different identified neurones extracted from the leech. At the moment the issue remains as to whether the extent of dispersion is also neurone type dependent.

5.4.2 Topographical guidance of neurites in other animals

The appearance of channels or tunnels in developing tissues frequently coincides with periods of rapid axonal outgrowth (e.g. Singer *et al.*, 1979; Caudros & Rios, 1988; Silver and Sidman, 1980). For example, in mice pioneering axons from the retina navigate through a series of tunnels in both the retina and the optic nerve, on their way to the optic tectum (Silver and Sidman, 1980). These tunnels appear prior to the formation of ganglionic cell axons and extend from the marginal zone of the primitive retina into the optic stalk. Interestingly the spatial relationship between the tunnels is retained suggesting that they may be important in ensuring an ordered mapping of ganglionic cell axons onto the tectum.

A similar relationship between axonal outgrowth and channel formation has been reported (Woddington,1941) and experimentally

manipulated (Blair *et al.*,1985) in the developing wing of *Drosophila*. The wing develops from an epithelial sac, which inverts and flattens forming the dorsal and ventral surfaces. Gaps form between these two apposing sheets, producing a series of channels. The timing of these events is loosely related to the period when pioneering sensory neurones initiate outgrowth. The channels persist until a template of nerve bundles is in place, following which the wing inflates, and the channels are transiently lost. In order to determine whether the channels are required by pioneer neurones for axonal pathfinding, the epithelial sheets have been separated and placed in culture before the initiating of axonal elongation (Blair,1985). Dorsal pioneering neurones (ACV and TSM(1)) elongate and navigate appropriately, despite the absence of channels. Thus, if the channels do play a role, they do so in association with other locally available guidance mechanisms (Blair,1985).

Other substratum associated guidance mechanisms

The growth cones of dorsal pioneering neurones may navigate by means of cues that are present on the surface of the cells belonging to the epithelial envelope through which they migrate. This possibility is illustrated by a monoclonal antibody that has been raised against a small region of chick retina (Trisler, 1982). This antibody binds to a protein present on the surface of cells (from day 4 onwards) which has a concentration which varies continuously (from cell to cell) with distance around the circumference of the retina. Such a protein may encode position and could be used during pathfinding (Trisler, 1982). Some systems, including *Drosophila*, appear to make use of discrete positional markers. For example, in the limb bud of the grasshopper the axonal growth cone of the Ti1 pioneer neurone is closely associated with the basement membrane until it reached a proximal

Guidepost neurone to which it becomes highly fasciculated (Condic & Bentley,1989). Thus, a series of guidepost neurones may act like stepping stones determining the path of elongation. The presence of guidepost neurones does not exclude the presence of other cues. This has been illustrated in the isolated wing bud of *Drosphila* , where pioneering neurones have been shown to navigate appropriately in the absence of both guidepost neurones and channels suggesting that at least one other guidance cue is involved in the navigation of axonal growth cones (Blair *et al.*, 1985).

In *Caenorhabditis elegans* pioneering growth cones also navigate between the epidermis and the basal lamina. However, mesodermal cells that contact only the basal lamina, migrate in the same direction (Hedgecock *et al.*, 1990). Thus other guidance cues may be located in the ECM. For example, growth cones may extend up or down adhesive gradients. This possibility is illustrated by the discovery of a graded distribution of ECM molecules in the developing wings of the moth *Manduca sexta* which could influence axonal guidance (Nardi, 1983). However, cultured neurones show no preference in their direction of elongation or growth cone motility when grown on gradients of substratum-bound laminin (McKenna & Jonathan, 1988). A basement membrane preparation from the developing chick retina has been used to test directly the hypothesis that cells are aligned by cues that are inherent to the basement membrane (Halfter *et al.*, 1987). Explants from the retina placed over the basement membrane failed to show any basement membrane-induced effects on the orientation of axonal outgrowth despite apparently normal growth rates. It should be noted however that detaching the basal lamina from the epithelial sheet may have seriously disrupted the three-dimensional structure. Interestingly, in the grasshopper epithelium, the cells show an intrinsic polarity in that the proximal edge of

one cell overlaps the distal edge of the more proximal neighbour (Berlot & Goodman, 1984). Thus the pioneering growth cones could be guided by this "tiles on a roof-like" structure. In this light it is worth noting that a grid of microfabricated cell size hillocks was sufficient to orientate cultured fibroblasts (Dow *et al.*,1987). Perhaps the shape of the basement membrane reflects the contours of the underlying cells and acts in a similar way to orientate developing axons. The ultrastructural organisation of the basement membrane may also be important. For example fibroblasts have recently been shown to align to microfabricated grooves which approach molecular dimensions (Clark *et al.*, 1990) and axons are known to elongate along the axis of aligned collagen fibrils (Ebendal, 1976). Thus, it is possible that growth cone migration across basal lamina maybe sensitive to topographic features of cellular and subcellular dimensions. These cues in combination with the inherent properties of a neurone (Solomon, 1979; Acklin & Nicholls, 1990) could dictate both the axis and the direction of elongation.

5.4.3 Relationship between the ECM and topographical guidance

The Topographical Modulating Hypothesis

As well as providing topographical features the extracellular matrix may influence topographical guidance indirectly by altering the association between the substratum and the outgrowth. In Chapter 4 the relationship between outgrowth morphology and the composition of the substrate was considered. Two different substrates were shown to produce fairly distinctive types of outgrowths that differed in their association with the substratum. In this Chapter, the effect of topography was shown to be dependent on the type of outgrowth. Thus, it is at least conceivable that *different ECM molecules may modulate the importance of the topography* in determining neuronal navigation. This hypothesis is referred to below as the

topographical modulating hypothesis.

The hypothesis that the ECM controls the influence of the topography on the behaviour of cells can be seen as an extension to an earlier suggestion made by Clark *et al.* (1987). They proposed that cell type-dependent behaviour to topographical features may be accounted for by cell type-dependent differences in substrate adhesion. However, the topographical modulating hypothesis emphasises the possibility that a *single cell type* may be influenced by *similar* topographical features in *different* ways, according to the nature of a substrate which could be *homogeneous*.

Homogeneous and heterogeneous substrates

Clark *et al.*, (1987) showed that the probability of ascending a step was reduced if the top of the step was less adhesive than the lower surface. The substrate did influenced topographical guidance. In this case the effect was mediated by the *heterogeneity* in substrate adhesiveness, and not by the adhesiveness of the substrate *per se.* Thus Clark *et al.* (1987) highlighted the possibility of *interactions* between different substratum-associated guidance cues, namely topographical and chemical heterogeneities. This is in contrast to the hypothesis presented above which highlights the concept that a single guidance cue (i.e. topography) may be modulated by properties of the substrate which could be isotropic and homogeneous and need not entail guidance (see Figure 5.9).

In developing and regenerating nervous systems the hypothesis predicts that the influence of topographical guidance is increased or decreased depending on whether the topography agrees or conflicts with the desired pathway. This is achieved by controlling the molecular composition of the ECM which may or may not provide additional guidance cues.

Modulating the efficacy of topographical guidance would allow the nervous system to make full use of topographical features to increase the probability of correct guidance.

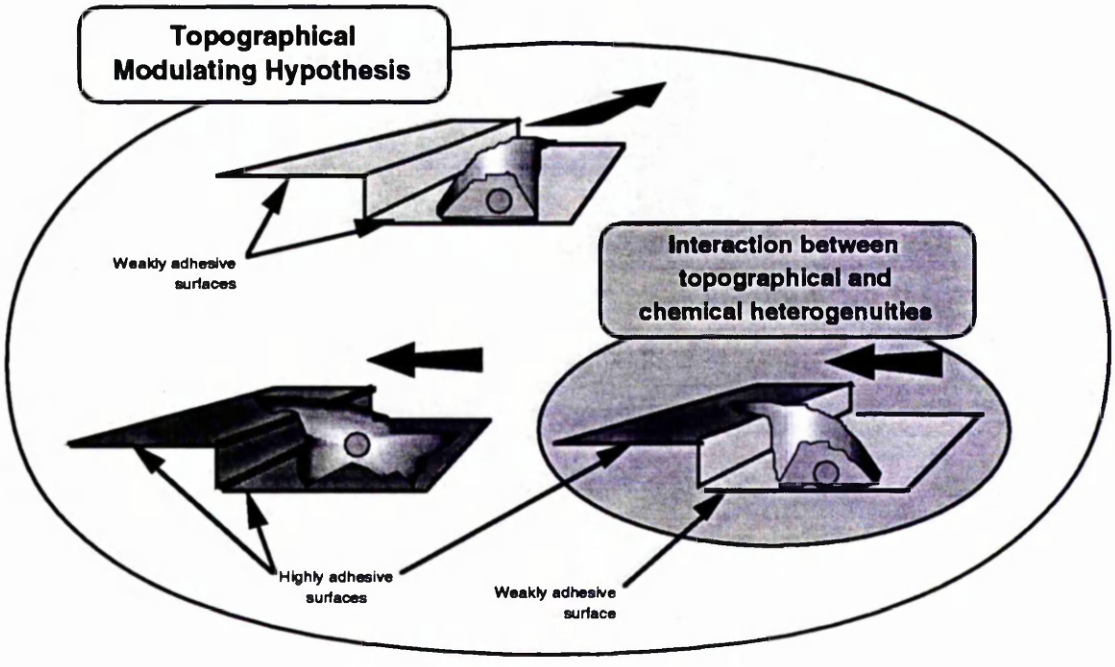

Figure 5.9: The topographical modulating hypothesis in relation to the interaction between topography and substratum coating. The probability of cells aligning along a step (represented by the diagram at the top) decreases if the top of the step is more adhesive than the bottom (diagram at the bottom right; Clark *et al.*, 1987). The influence of the difference in adhesion effectively overrides the effect of the topography on the behaviour of the cell. This is incorporated by the topographical modulating hypothesis. However, the topographical modulating hypothesis also accounts for the possibility that differences between chemically homogeneous substrates can modulate the effects of topography. For example, a substrate that increases the spread area of a cell may increase the probability of a cell crossing a step (represented by the diagram on the left hand side).

It would be fascinating to determine whether this hypothesis is generally applicable. For example, is the influence of topographical features on vertebrate neurones also dependent on the type of outgrowth? This question could be answered by comparing the alignment of DRG neurones plated on grooved substrata coated with laminin, fibronectin and collagen.

These substrates are particularly suitable since they are physiological and support neurites with distinctive morphologies when applied to planar substratum (Gunderson, 1987; Chamak *et al.*, 1989). Alternatively the comparison could be made between DRGs plated on grooves coated with Con A and polylysine. These artificial substrates also cause DRGs to produce distinctive outgrowth (DeGeorge *et al.*, 1985).

5.4.4 Alignment of BHK cells to stripes of Con A

BHK cells which are modulated by grooves (Clark *et al.*, 1990; Clark *et al;* 1991) or stripes of patterned fibronectin (P.Clark; personal communication) become elongated and bipolar. The peculiar comb-like morphology of the BHK cells plated on stripes of patterned Con A was also elongated, as was illustrated by the average overall length:width ratio which had a value of 3.8. Presumably elongation reflects the stability of projections along the axis of the discontinuity regardless of whether the discontinuity is a consequence of topography or chemical heterogeneity. According to the model proposed by Dunn and Brown (1986; described in section 5.1.2) projections in other directions are less stable because of the inflexible nature of the cytoskeleton and the restraints imposed on the distribution of focal contacts. The alignment of multiple processes on neighbouring stripes of patterned Con A suggests that one or both of these restraints is partially relaxed (allowing part of the cell to cross the area not coated in protein). If the flexibility of the cytoskeleton was not reduced it is unlikely that the cell would realign to neighbouring stripes since this entails a 90° bend. Similarly if the dependence on focal contacts was not relaxed then the crossing would not occur as focal contacts are very unlikely in the uncoated area.

In the previous Chapter IRM was used to show that the outgrowth of

Retzius neurones on Con A is characterised by a large area of close contact; focal contacts could not be identified categorically and may have been absent. Although caution is required in applying the results obtained with Retzius neurones to BHK cells the possibility that BHK cells spread on Con A without forming focal contacts cannot be rejected. If this were the case then the observed elongation conflicts with the Dunn & Brown (1986) model; a cell without focal contacts would be expected to spread ubiquitously on a planar surface.

A satisfactory way to account for the behaviour of the BHK cells on the Con A stripes is to postulate that morphology is a result of a mechanism, such as strong physical adhesion, that acts to maximise the contacts between cell and the substratum (whether close contacts or focal contacts). In accordance with the Dunn & Brown (1986) model, this mechanism is limited by cytoskeletal constraints which on other substrates (e.g. fibronectin) may be more severe (figure 10.5).

This account can also be used to explain the effect of Con A-coated grooves on the lamellar-type outgrowth of Retzius neurones. For example, the model predicts that the lamellae span grooves because of the flexibility of their cytoskeleton (note the curvature of the concave regions of cytoplasm which span the grooves in Figure 56a). This is supported by the observation that disrupting the microtubules of cultured Retzius neurones using nocodazole, a treatment which is likely to reduce the rigidity of the cytoskeleton, increases the production of lamellar-type outgrowth (Acklin & Nicholls, 1990). Further more, neutrophils which are regarded as having a flexible cytoskeleton are unaffected by steps which strongly align other cells (Clark *et al.*,1987). Clark *et al.* (1990) pointed out a similar relationship for transformed cells (e.g. Rovensky & Slavnaya, 1974).

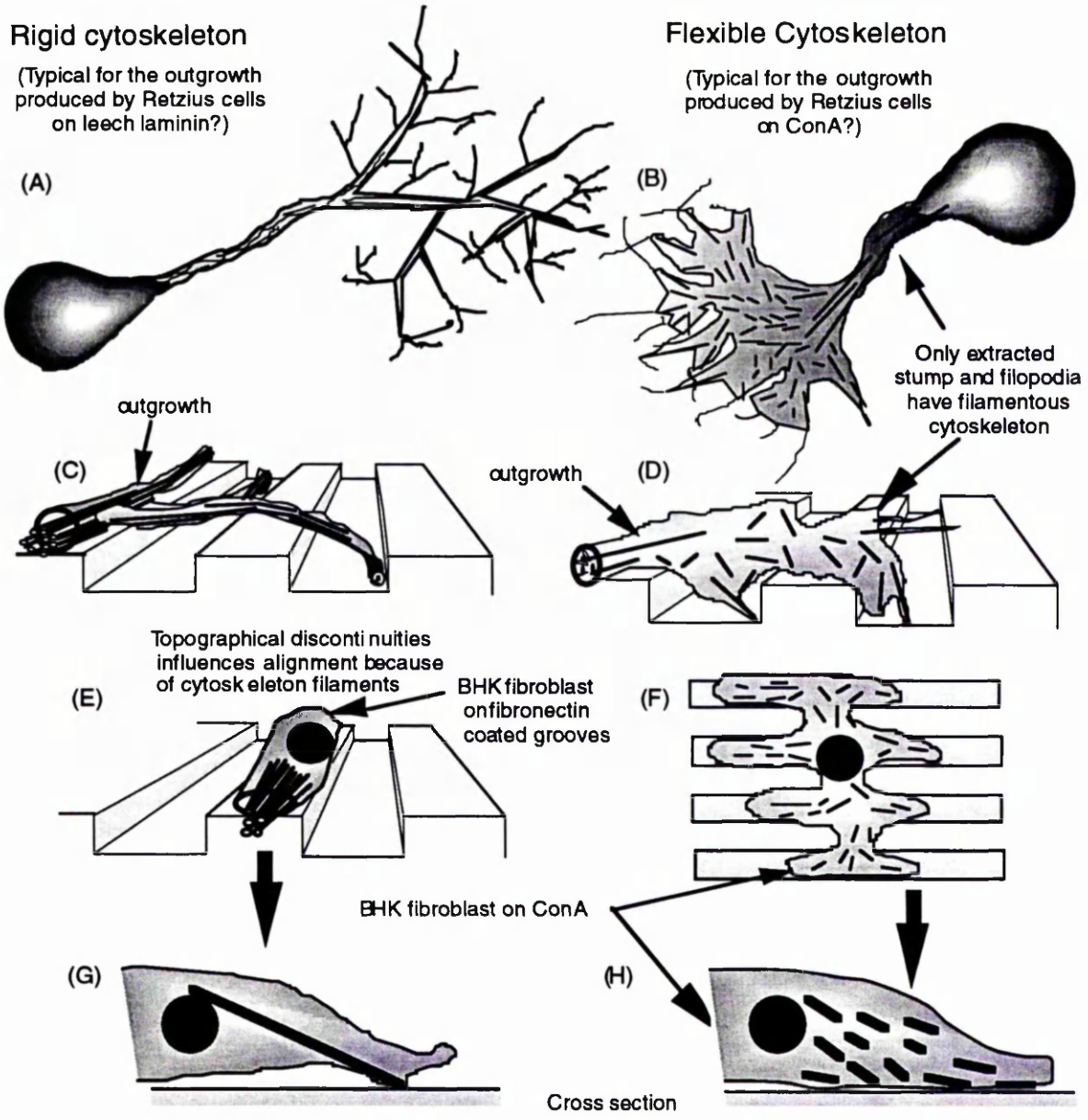

Figure 5.10: Cytoskeletal flexibility and the guidance of cells. The diagram explains how the rigidity of the cytoplasm might determine the response of cells to guidance cues. Physiological substrates such as ECM extract or fibronectin may enhance the filamentous organisation of the cytoskeleton (represented on the left hand side of the figure). Alternatively, Con A may support outgrowth with a poor filamentous organisation, giving rise to broad, lamellar-like structures (B). Such outgrowths may have greater flexibility than the outgrowth produced on physiological substrates and thus may be less affected by topographical discontinuities (C & D). A Reduction in cytoskeletal constraints only partly explains the unusual comb-like morphology of fibroblasts cultured on patterned stripes of Con A (compare E & F). The comb-like morphology also appears to maximise the contact between the cell and the Con A-coated regions. Thus, it seems likely that the cytoskeleton may impose restraints on morphology, possibly by limiting the contacts with the substratum (G & H). Generally, this is in accordance with the Dunn & Brown (1986) model.

Another prediction of the model is that the finger-like structures at the distal edge of the lamella coincide with the grooves because this morphology is more likely to increase the area that is in close contact with the substratum. It is interesting that neutrophils which also form close contact with the substratum, but not focal contacts were "unresponsive" to single steps but were "largely unaffected" by grooved substrata (implying a very small response; Clark *et al.*, 1990).

It was apparent that a proportion of the filopodia which emerged from the distal margin of the lamella disregarded some of the topographical features. The degree of flexibility demonstrated by these filopodia is not readily predicted by the model as these structures would be expected to have a largely filamentous (and inflexible) cytoskeleton. However, filopodial inflexibility is demonstrated by occasional bridges which result from perpendicular encounters with the grooves. Furthermore on at least one occasion an encounter with the wall of a groove caused a deflection in the direction of orientation. Disregarding topographical features may only have been possible when the angle of encounter was shallow.

5.5 Conclusions

- The results in this Chapter provide the first demonstration that the neurites of large invertebrate neurones can be aligned by topographical discontinuities.
- The dimensions of the topographical features required to align Retzius neurites are similar to those required to align the processes of vertebrate neurones.
- The lamellae which typify the outgrowth of Retzius neurones plated on a substratum coated with Con A show only the slightest signs of alignment, suggesting that the effect of the topography depends on the type of outgrowth.
- As the type of outgrowth depends on the nature of the substrate (see Chapter 4) it is conceivable that the ECM determines the influence of the topography (referred to as the topographical modulating hypothesis).
- Attempts to align Retzius neurones along fine stripes of Con A (or leech ECM extract) were generally unsuccessful. Better results were obtained using BHK cells.
- The response of BHK cells to patterned Con A was unusual in that cells developed a comb-like morphology, probably as a result of a Con A-mediated increase in the flexibility of the cytoskeleton and restraints imposed by the pattern on the distribution of cell-substratum adhesion.
- A Con A-mediated increase in the flexibility of the cytoskeleton may also account for the difference in response between the neurites and the lamellar-type outgrowth of Retzius neurones to topographical features.

References

Acklin, S.E. & Nicholls, J.G. (1990) "Intrinsic and extrinsic factors influencing properties and growth patterns of identified leech neurons in culture" *J.Neurosci.* **10**:1082-1090

Albowitz, B., Kuhnt, U. & Ehrenreich, L. (1990) "Optical recording of epileptiform voltage changes in the neocortical slice" *Exp. Brain Res.* **81**:241-256

Arechiga, H., Chiquet, M., Kuffler, D.P. & Nicholls, J.G. (1986) "Formation of specific connections in culture by identified leech neurones containing serotonin, acetylcholine and peptide transmitters" *J.Exp.Biol* **126**:15-31

Bader, C.R., Bertrand, D. & Schwart, E.A. (1982) "Voltage-activated and calcium activated currents studied in solitary rod inner segments from the Salamander retina" *J.Physiol.* **331**:253-284

Baker, P.F., Hodgkin, A.L. & Shaw, T.I. (1962) "The effects of changes in internal ionic concentrations on the electrical properties of perfused giant axons" *J.Physiol.* **164**:335-375

Bannatyne, B. A., Blackshaw, S.E. & McGregor, M. (1989) "New outgrowth elicited in adult leech mechanosensory neurones by peripheral axon damage" *J. Exp. Biol.***143**:419-434

Baylor, D.A. & Nicholls, J.G.(1969) "Chemical and electrical synaptic connexions between cutaneous mechanoreceptor neurones in the central nervous system of the leech" *J.Physiol.* **203**:591-609

Baylor, D.A. & Nicholls, J.G.(1971) "Patterns of regeneration between individual nerve cells in the central nervous system of the leech" *Nature* **232**:268-270

Beck, K. & Bereiter-Hahn, J. (1981) "Evaluation of reflection interference contrast microscopy images of living cells" *Microsc. Acta.* **84**:153-178

BeMent, S.L., Wise, K.D., Anderson, D.J., Najafi, K. & Drake, K.L. (1986) "Solid-state electrodes for mulitchannel multiplexed intracortical neuronal recording" *IEEE Trans Biomed. Eng. BME* **-33**:230-242

Bentley, D. & Keshishian, H. (1982) "Pioneer neurons and pathways in insect appendages" *TINS* **5**:354-358

Bergveld, P. (1968) "A new amplification method for in depth recording" IEEE Trans., *Biomed. Eng.* **14**:497

Berlot, J. & Goodman, C.S. (1984) "Guidance of peripheral pioneer neurons in the grasshopper adhesive hierarchy of epithelial-and neuronal surfaces" *Science* **223**:493-496

Bermeister, D.W. & Goldberg, D.J. (1988) "Micropruning: the mechanism of turning of Aplysia Growth cones at substrate borders in vitro" *J.Neurosci.* **8**:3151-3159

Blair, S.S., Murray, M.A. & Palka, J. (1985) "Axon guidance in cultured epithelial fragments of *Drosophila* wing" *Nature* **315**:406-409

Bookman, R.J., Reuter, H., Nicholls, J.G. & Adams. W.B. (1987) "Loose patch mappping of ion channel distribution in cultured leech neurons"*Soc.Neurosci.Abstr.* **13**:1442

Brauner, T., Hulser, D.F. & Strasser, R.J. (1984) "Comparative measurements of membrane potentials with microelectrodes and voltage-sensitive dyes" *Biochimica et Biophysica Acta.* **771**:208-216

Brismar, T. & Gilly, W.F. (1987) "Synthesis of sodium channels in the cell bodies of squid giant axons" *Proc.Natl.Acad.Sci. U.S.A.* **84**:1459-1463

Buckingham, M.J. (1983) *Noise in electronic devices and systems.* Ellis Horwood Ltd., Chichester.

Bullock, T.H., Cohen, M.J. & Faulstick, D. (1950) "Effect of stretch on conduction in single nerve fibres" *Biol.Bull* **99**:320

Burrows, M. (1987) "Parallel processing of proprioceptive signals by spiking interneurons and motor neurons in the locust" *J.Neurosci.* **7**:1064-1080

Burrows, T.M.O., Campbell, I.A., Howe, E.J. & Young, J.Z. (1965) "Conduction velocity and diameter of nerve fibres of cephalopods" *J.Physiol.* **179**:39-40P

Caroni, P., Schwab, M.E. (1988) "Two membrane protein fractions from rat central myelin with inhibitory properties for neurite growth and fibroblast spreading" *J.Cell.Biol.* **106**:1281-88

Carrow, G.M. & Levitan, I.B. (1989) "Selective formation and modulation of electrical synapses between cultured Aplysia neurons" *J.Neurosci.* **9**:3656-3664

Cattaert, D., El Manira, A. & Clarac, F. (1992) "Presynaptic inhibtion of primary afferents" (in press)

Caudros, M. & Rios, A. (1988) "Spatial and temporal correlation between early nerve fibre growth and neuroepithelial cell death in the chick embryo retina" *Anat. Embryol.* **178**:543-51

Chamak, B. & Prochiantz, A. (1989) "Influence of extracellular matrix proteins on the expression of neuronal polarity" *Development* **106**:483-491

Chang, S., Rathjen, F.G. & Raper, J.A. (1987) "Extension of neurites on axons is impaired by abtibodies against specific neural cell surface glycoproteins" *J.Cell Biol.* **104**:355-362

Chiquet, M. & Acklin, S.E. (1986) "Attachment to Con A or extracellular matrix initiates rapid sprouting by cultured leech neurons" *Proc.Natl.Acad.Sci.* USA **83**:6188-6192

Chiquet, M., Masuda-Nakagawa, L., and Beck, K. (1988) "Attachment to an endogenous laminin like protein initiates sprouting by leech neurons" *J.Cell.Biol* **107**:1189-1198

Chiquet, M. & Nicholl, J.G. (1987) "Neurite ougrowth and synapse formation by identified neurones in culture" *J.Exp.Biol.***132**:191-206

Clark, P.,Connolly, P.,Curtis, A.S.G., Dow, J.A.T. & Wilkinson, C.D.W. (1987) "Topographical control of cell behaviour. I. Simple step cues" *Development* **99**:439-448

Clark, P., Connolly, P., Curtis, A.S.G., Dow, J.A.T. & Wilkinson, C.D.W. (1990) "Topographical control of cell behaviour: II. multiple grooved substrata" *Development* **108**:635-644

Clark, P., Connolly, P., Curtis, A.S.G., Dow, J.A.T. & Wilkinson, C.D.W. (1991) "Cell guidance by ultrafine topography *in vitro*" *J.Cell Sci.* **99**:73-77

Cohen, L.B., Hopp, H.-P., Wu, J.-Y., Xiao, C., London, J. & Zecevic, D. (1989) "Optical measurement of action potential activity in invertabrate ganglia" *Ann.Rev.Physiol.* **51**:527-541

Cohen, L.B., Keynes, R.D., & Hille, B. (1968) "Light scattering and birefringence changes during nerve activity" *Nature* **218**:438-441

Cohen, L.B. & Wu, J.-Y. (1990) "One neurone, many units?" *Nature* **346**:108-109

Colombaioni, L. & Brunelli, M. (1988) "Neurotransmitter-induced modulation of an electrotonic synapse in the CNS of *Hirudo medicinalis*" *Exp. Biol.* **47** pp139-144

Colquhoun, D (1971) *Lectures on Biostatistics: an introduction to statistics with applications in biology and medicine.* Clarendon Press, Oxford.

Condic, M.L. & Bentley, D.(1989) "Pioneer growth cone adhesion in vivo to boundary cells and neurons after enzymatic removal of basal lamina in grasshopper embryos" *J.Neurosci.* **9**:2687-2696

Connolly, P., Clark, P., Curtis, A.S.G., Dow, J.A.T. & Wilkinson, C.D.W. (1990) "An extracellular microelectrode array for monitoring electrogenic cells in culture" Biosensors & Bioelectronics **5**:223-234

Constanti, A. & Galvan, M. (1983) "Fast inward rectifying currents accounts for anomalous rectification in olfactory cortex neurones" *J.Physiol.* **335**:153-178

Craib, W.H. (1927) "A study of the electrical field surrounding active heart muscle" *Heart* **14**:71-109

Craib, W.H. (1928) "A study of the electrical field surrounding skeletal muscle" *J.Physiol.* **66**:49-73

Curtis, A.S.G. (1964) "The mechanism of adhesion of cells to glass. A study by interference reflection microscopy" *J.Cell Biol*. **20**:199-215

Curtis, A.S.G., Forrester, J.V. & Clark, P. (1986) "Substarte hydroxylation and cell adhesion" *J.Cell Sci* **86**:9-24

Curtis, A.S.G., McGrath, M. & Gasmi, L. (1992) "Localised application of anactivating signal to a cell: experimental use of fibronectin boumd t beads and the implications for mechanisms of adhesion" *J. Cell Sci.* **101** (In Press)

Curtis, A.S.G. & Varde, M. (1964) "Control of cell behaviour: topological factors" *J.Natn Cancer.Res.Inst.***33** :15-26

Czéh, G., Kudo, N. & Kuno, M. (1977) "Membrane properties and conduction velocity in sensory neurones following central or peripheral axotomy" *J.Physiol.* **270**:165-180

Das, G.D.,Lammert, G.L. & Allister, J.P. (1974) "Contact guidance and migratory cells in the developing cerebellum" *Brain Res.* **69**:13-29

Davies, J.A.,Cook, G.M.W., Stern, C.D. & Keynes, R.J. (1990) "Isolation from chick somites of a glycoprotien fraction that causes collapse of dorsal root ganglion growth cones" *Neuron* **2**:11-20

Davis, R.L. (1989) "Voltage-dependent properties of electrical synapses formed between identified leech neurones *in vitro*" *J.Physiol.* **417**:25-46

Degeorge, J.J., Slepecky, N., Carbonetto, S. (1985) "Concanavalin A stimulates neuron-substratum adhesion and nerve fiber outgrowth in culture" *Dev. Biol.* **111**:335-351

Dietzel, I.D., Drapeau, P. & Nicholls, J.G. (1986) "Voltage dependence of 5-hydroxytryptamine release at a synapse between identified leech neurones in culture" *J.Physiol.* **372**:191-205

DiFrancesco, D. (1981) "A study of the ionic nature of the pacemaker current in calf Purkinje fibres" *J.Physiol.* **314**:377-393

DiFrancesco, D. & Ojeda, C. (1980) "Properties of the current I_f in the sino-atrial node of the rabbit compared with those of the current I_{k2} in purkinje fibres" *J.Physiol.* **308**:353-367

Dow, J.A.T.,Clark, P.,Connolly, P.,Curtis, A.S.G. & Wilkinson, C.D.W. (1987) "Novel methods for the guidance and monitoring of single cells and simple networks in culture" *J.Cell.Sci. Suppl.* **8**:55-79

Drapeau, P., Melinyshyn, E. & Sanchez-Armass, S. (1989) "Contact-mediated loss of the nonsynaptic response to transmitter during reinnervation of an identified leech neuron in culture" *J.Neurosci.* **9**:2502-2508

Drapeau, P. & Sanchez-Armass, S. (1988) "Selection of postsynaptic serotonin receptors during reinnervation of an identified leech neuron in culture" *J.Neurosci.* **8**:4718-4727

Droge, M.H., Gross, G.W., Hightower, M.H. & Czisny, L.E. (1986) "Multielectrode analysis of coordinated, Multisite, Rhythmic Bursting in cultured CNS Monolayer networks" *J.Neurosci.* **6**:1583-1592

Dunn, G.A. (1982) "Contact guidance of cultured tissue cells:a survey of potentially relevant properties of the substratum" In *Cell Behaviour.* (Ed.Bellairs, R.,Curtis, A.,Dunn, G.) Cambridge University Press. pp247-280

Dunn, G.A. & Brown, A.F. (1986) "Alignment of fibroblasts on grooved surfaces described by a simple geometric transformation" *J.Cell Sci.* **83**:313-340

Dunn, G.A. & Heath, J.P. (1976) "A new hypothesis of contact guidance in tissue cells" *Exp.Cell Res.* **101**:1-14

Ebendal, T. (1976) "The relative role of contact inhibition and contact guidance in orientation of axons extending on aligned collagen fibrills *in vitro*" *Zoon* **2**:99-104

Eckert, R. (1963) "Electrical interaction of paired ganglion cells in the leech" *J.Gen.Physiol.* **46**:573-587

Edell, D.J. (1986) "A peripheral erve information transducer for amputees: Long-term multichanel recordings from rabbit peripheral nerves" *IEEE Trans.Biomed.Eng.* BME **33**:203-214

Edes, R.E. (1892) "On the method of transmission of the impulse in medullated fibres" *J.Physiol.* **13**:428-444

Erickson, H.P. & Bourdon, M.A. (1989) "Tenascin: an extracellular matrix protein prominent in specialised embryonic tissues and tumors" *Ann. Rev. Cell. Biol.* **5** :71-92

Faber, I.C. & Grinvald, A. (1983) "Identification of presynaptic neurones by laser photostimulation" *Science* **222**:1025-1027

Fain, G.L. & Lisman, J.E. (1981) "Membrane conductance of photoreceptors" *Prog.Biophys. & molec.Biol.* **37**:91-147;

Fein, H. (1966) "Passing current through recording glass micropipette electrodes" *IEEE Trans.Biomed.Eng.* **13**:211-212

Fessler, J.H. & Fessler, L.I. (1989) "Drosphila extracellular matrix" *Ann.Rev.Cell.Biol.* **5**:309-39

Fessler, L.I., Campbell, A.G., Duncan, K.G. & Fessler, J.H. (1987) "Drosophilia Laminin: Characterisation and localisation" *J.Cell.Biol.* **105**:2383-2391

Fields, R.D., Neale, E.A. & Nelson, P.G. (1990) "Effects of patterned electrical activity on neurite outgrowth from mouse sensory neurons" *J.Neurosci.* **10**:2950-2964

French, K.A. & Muller, K.J. (1986) "Regeneration of a distinctive set of axosomatic contacts in the leech central nervous sytsem" *J.Neurosci.* **6**:318-324

Fromhertz, P., Offenhausser, A., Vetter, T. & Weis, J. (1991) "A neuron-silicon junction: A Retzius cell of the Leech on an insulated-gate field effect transistor" *Science* **252**:1290-1293

Fromherz, P., Schaden, H., Vetter, T. (1989) "Directed growth of sensory neurons of leech along a photochemical pattern on a laminin-type substrate" *Eur.J.Neurosci.* (Suppl.2) September.

Fuchs, P.A. & Evans, M.G. (1990) "Potassium currents in chick hair cells" *J.Physiol* **429**:529-551

Fuchs, P.A., Henderson, L.P. & Nicholls, J.G. (1982) "Chemical transmission between individual Retzius and sensory neurones of the leech in culture" *J.Physiol.* **323**:195-210

Fuchs, P.A., Nicholls, J.G. and Ready, D.F. (1981) "Membrane properties and selective connexions of identified leech neurones in culture" *J.Physiol.* **316**:203-223

Furshpan, E.J. & Furukawa, T. (1962) "Intracellular and extracellular responses of the several regions of the Mauthner cell of the goldfish" *J.Neurophysiol* **25:**732-771

Garcia, U., Grumbacher-Reinert, S. & Nicholls, J.G. (1989) "Differences in localization of Na^+ and K^+ channels in the soma, axon and growth cones of identified leech neurones in culture" *J.Physiol.* **415**:37P

Gasser, H.S. (1955) "Unmedullated fibres originating in dorsal root ganglia" *J.Gen.Physiol.* **33**:651-690

Gasser, H.S. & Erlanger, J. (1927) "The role played by the sizes of the constituent fibres of a nerve trunk in determining the form of its action potential" *Amer. J.Physiol.*

80:522-547

Geddes, L.A. (1972) *Electrodes and the measurement of bioelectric events.* Wiley-Interscience, London.

Getting, P.A. (1989) "Emerging principles governing the operation of neural networks" *Ann. Rev. Neurosci.* **12**:185-204

Gingell, D. & Todd, I. (1979) "Interference reflection microscopy: a quantitative theory for image interpretation and its application to cell-substratum separation measurement" *Biophys. J.* **26**:507-526

Gise, P.E. & Blanchard, R. (1979) *Semiconductor and integrated circuit fabrication techniques.* Reston Publishing Company, Inc., Virginia.

Glover, J .C. & Mason, A. (1986) "Morphogenesis of an identified leech neurone: segmental specification of axonal outgrowth" *Dev.Biol.* **115**:256-260

Goldman, L. (1961) "The effect of stretch on the conduction velocity of single nerve fibers in *Aplysia*" *J.Cell.Comp.Physiol.***57**:185-191

Gorman, A.L.F. & Mirolli, M. (1972) "The passive electrical properties of the membrane of a molluscan neurone" *J.Physiol.* **227**:35-49

Graham, J. & Gerard, R.W. (1946) "Membrane potentials and excitation of impaled single muscle fibres" *J.Cell. Comp. Physiol.* **28**:99-117

Graubard, K. (1975) "Voltage attenuation within *Aplysia* neurons: the effect of branching pattern" *Brain Res.* **88**:325-332

Grinvald, A. (1985) "Realtime optical mapping of neuronal activity: from single growth cones to the intact mammalian brain" *Ann.Rev.Neurosci.* **8**:263-305

Grinvald, A., Cohen, L.B., Lesher, S. & Boyle, M.B. (1981a) "Simultaneous optical monitoring of activity of many neurons in invertebrate ganglia using a 124-element photodiode array" *J.Neurophysiol.* **45**:829-840

Grinvald, A. & Farber, I.C. (1981) "Optical recording of calcium action potentials from growth cones of cultured neurones with a laser microbeam" *Science* **212**:1164-1167

Grinvald, A., Manker, A., Segal, M. (1982) "Visualization of the spread of electrical activity in rat hippocampal slices by voltage sensitive optical probes" *J.Physiol.* **333**:269-91

Grinvald, A., Ross, W.N. & Farber, I. (1981b) "Simultaneous optical measurements of electrical activity from multiple sites on processes of cultured neurons" *Proc.Natl.Acad.Sci.USA.* **78**:3245-3249

Grinvald, A., Salzberg, B.M., Lev-Ram, V., Hildesheim, R. (1987) "Optical recording of synaptic potentials from processes of single neurones using intracellular potentiometric dyes" *Biophys. J.* **51**:643-651

Gross, G.W. & Hightower, M. (1986) "An approach to the determination of network properties in mammalian neuronal monolayer cultures" *Proc. IEEE conference* on synthetic microstructures in biological research, Virginia. 24-26 March.

Grumbacher-Reinert, S. (1989) "Local influence of substrate molecules in determining

distinctive growth patterns of identified neurons in culture" *Proc.Natl.Acad.Sci.USA* **86**:7270-7274

Grynkiewicz, G., Poenie, M. & Tsien, R.Y. (1985) "A new generation of Ca^{2+} indicators with greatly improved fluorescence properties"*J.Biol.Chem.* **260**:3440-3450

Gunderson, R.W. (1985) "Sensory neurite growth cone guidance by substrate adsorbed nerve growth factor" *J. Neurosci. Res.* **13**:199-212:

Gunderson, R.W. (1987) "Response of sensory neurites and growth cones to patterned substrata of laminin and fibronectin *in vitro" Dev.Biol.* **121**:423-431

Gunderson, R.W. (1988) "Interference reflection microscopic study of dorsal root growth cones on different substrates: Assessment of growth cone-substrate contacts" J.Neurosci. Res. **21**:298-306

Gunderson, R.W & Park, K.H.C. (1984) "The effects of conditioned media on spinal Neurites: Substrate-associated changes in neurite direction and adhesion" *Dev. Biol.* **104**:18-27

Hadley, R.D. & Kater, S.B. (1983) "Competence to form electrical connections is restricted to growing neurites in the snail, *Helisoma*" *J.Neurosci* **3**:924-932

Hagiwara, S., Miyazaki, S., Moody, W. & Patlak, J. (1978) "Blocking effects of barium and hydrogen ions on the potassium current during anomalous rectification in the starfish egg" *J.Physiol.* **279**:167-185

Hagiwara, S. & Morita, H. (1962) "Electrotonic transmission between two nerve cells in leech ganglion" *J. Neurophysiol.* **25**:721-731

Hagiwara, S. & Takahashi, K. (1974) "The anomalous rectification and cation selectivity of the membrane of a starfish egg cell" *J.Membrane Biol.* **18**:61-80

Halfter, W., Reckhaus, W. & Kröger, S. (1987) "Nondirectioned axonal growth on basal lamina from avian embryonic neural retina" *J. Neurosci.* **7**:3712-3722

Halliwell, J.V. & Adams, P.R. (1982) "Voltage-clamp analysis of muscarinic excitation in hippocampal neurons" *Brain Res.* **250**:71-92

Hamill, O.P., Marty, A., Neher, F., Sakmann, B. & Sigworth, F.J. (1981) "Improved patch-clamp techniques for high resolution current recording from cells and cell-free membrane patches" *Pflugers Arch.* **391**:85-100

Hammerback, J.A., Palm, S.L., Furcht, L.T. & Letourneau, P.C. (1985) "Guidance of neurite outgrowth by pathways of substratum-adsorbed laminin" *J.Neurosci. Res.* **13**:213-220

Harrelson, A.L. & Goodman, C.S. (1988) "Growth cone guidance in insects: Fasciclin II is a member of the immunoglobulin superfamily" *Science* **242**:700-708

Harris, A. (1973) "Behaviour of cultured cells on substrata of variable adhesiveness" *Exp. Cell Res.* **77**:285-297

Harris-Warrick, R.M. & Marder, E. (1991) "Modulation of neuronal netwroks for behavior" *Ann. Rev Neurosci.* **14**:39-57

Harrison, R.G. (1911) "On the stereotropism of embryonic cells" *Science* **34**:279-281

Haydon, P.G. (1988) "The formation of chemical synapses betwen cell-cultured neuronal somata" *J.Neurosci.* **8**:1032-1038

Haydon, P.G., Cohan, C.S., McCobb, D.P., Miller, H.R. and Kater, S.B. (1985) "Neuron-specific growth cone properties as seen in identified neurons of Helisoma" *J.Neurosci. Res.* **13**:135-47

Haydon, P.G., McCobb, D.P. & Kater, S.B. (1987) "The regulation of neurite outgrowth, growth cone motility, and electrical synaptogenesis by serotonin" J.Neurobiol. **18**:197-215

Heath, J.P. (1982) "Adhesion to substratum and locomotory behaviour of fibroblastic and epithelial cells in culture" In *Cell Behaviour* (ed. R.Bellairs, A.Curtis & G. Dunn):77-108. Cambridge University Press.

Hedgecock, E.M., Culotti, J.G. & Hall, D.H. (1990) "The *unc-5, unc-6* and *unc-40* genes guide circumferential migrations of pioneer axons and mesodermal cells on the epidermis in *C.elegans*" *Neurone* **2**:61-85

Henderson, L.P. (1983) "The role of 5-hydroxytryptamine as a transmitter between identified leech neurones in culture" *J.Physiol.* **339**:309-324

Henderson, L.P., Kuffler, D.P., Nicholls, J.G. & Zhang, R.-J. (1983) "Structural and functional analysis of synaptic transmission between identified leech neurons in culture" *J.Physiol.* **340**:347-358

Hild, W. & Tasaki, J. (1962) "Morphological & physiological properties of neuron and glia cells in tissue culture" *J.Neurophysiol.* **25**:277-304

Hill, D.K. (1950) "The volume change resulting from stimulation of a giant nerve fibre" *J. Physiol.* **111**:304-327

Hille, B. (1984) *Ionic channels of excitable membranes*. Sinauer Associates Inc., Sunderland, Massachusetts.

Hodes, R. (1953) "Linear relationship between fiber diameter and velocity of conduction in giant axon of squid" *J.Neurophysiol.* **16**:145-154

Hodgkin (1939) "The relation between conduction velocity and the electrical resistance outside a nerve fibre" *J.Physiol.* **94**:560-570

Hodgkin, A.L. & Huxley, A.F. (1945) "Resting and action potentials in single nerve fibres" *J.Physiol. (Lond.)* **104**:176-195

Hodgkin, A.L. & Huxley, A.F. (1952) "A quantitative description of membrane current and it's application to conduction and excitation in nerve" *Ibid.*, **117**:500-544

Hodgkin, A.L. & Katz, B. (1949) "The effect of temperature on the electrical activity of the giant axon of the squid" *J.Physiol.* **109**:240-294

Hodgkin, A.L. & Rushton, W.A. (1946) "Electrical constants and velocity of nerve fibres" *Proc.R.Soc. (Lond.) B* **133**:444-479

Hursh, J.B. (1939) "Conduction velocity and diameter of nerve fibres" *J.Physioi.* **127**:131-139

Hynes, R.O. (1987) "Integrins: A family of cell surface receptors" *Cell* **48**:549-554

Israel, D.A., Barry, W.H., Edell, D.J. & Mark, R.G. (1984) "An array of microelectrodes to stimulate and record from cardiac cells in culture" *Am.J.Physiol.* **247**:H669-H674

Izzard, C.S. & Lochner, L.R. (1976) "Cell-to-substrate contacts in living fibroblasts: an interference reflection study with an evaluation of the technique" *J.Cell Sci.* **21**:129-159

Izzard, C.S. & Lochner, L.R. (1980) "Formation of cell-to-substrate contacts during fibroblast motility: an interference-reflexion study" *J.Cell Sci.* **42**:81-116

Jack, J.J.B., Noble, D. & Tsien, R.W. (1975) *Electric current flow in excitable cells.* Clarendon Press. Oxford.

Jansen, J.K.S., Muller, K.J. & Nicholls, J.G. (1974) "Persistent modification of synaptic interactions between sensory and motor nerve cells following discete lesions in the central nervous system of the leech"*J.Physiol.* **242**:289-305

Jansen, J.K.S. & Nicholls, J.G. (1973) "Conductance changes, an electrogenic pump and the hyperpolarization of leech neurones following impulses" *J.Physiol.* **229**:635-655

Jobling, D.T., Smith, J.G. & Wheal, H.V. (1981) "Active microelectrode array to record from the mammalian central nervous system *in vitro*" *Mol. & Biol. Eng. & Comput.* **19**:553-560

Kassotis, J., Steinberg, S.F., Ross, S., Bilezikian, J.P. & Robinson, R.B. (1987) "An inexpensive dual-excitation apparatus for fluorescence microscopy" *Eur.J.Physiol.* **409**:47-51

Katz, B. "The electrical properties of the muscle fibre membrane" *J.Physiol.* **135**:505-534

Kehoe, J.S. (1978) "Transformation by concanavalin A of the response of molluscan neurones to L-glutamate" *Nature* **274**:866-869

Kerkut, G.A., Sedden, C.B. & Walker, R.J. (1967) "A flourescence microscopic and electrophysiological study of the giant neurones of the ventral nervous cord of Hirudo medicinalis" *J.Physiol* **189**:83-85

Khodorov, B.I. & Timin, E.N. (1975) "Nerve impulse propogation along nonuniform fibres" *Prog. Biophys. Molec. Biol.* **30**:145-184

Klein, M., Shapiro, E. & Kandel, E.R. (1980) "Synaptic plasticity and the modulation of the Ca2+ current" *J.Exp.Biol.* **89**:117-157

Kleinfeld, D., Kahler, K.H. & Hockberger, P.E. (1988) "Controlled outgrowth of dissociated neurons on patterned substrates" *J.Neurosci.* **8**:4098-4120

Kleinfield, D., Raccuia-Behling, F. & Chiel, H.J. (1990) "Circuit constructed from identified *Aplysia* neurons exhibit multiple patterns of persistent activity" *Biophys.J.* **57**:697-715

Kleinhaus, A.L. & Prichard, J.W. (1977) "Close relation between TEA responses and Ca^{2+}-dependent membrane phenomena of four identified leech neurones" *J.Physiol.* **270**:181-194

Kleinman, H.K. & Weeks, B.S. (1989) "Laminin: structure, functions and receptors" *Curr. Opinion in Cell Biol.* **1** :964-967

Konnerth, A., Obaid, A.L., Salzberg, B.M. (1987) "Optical recording of electrical activity from parallel fibres and other cell types in skate cerebellar slices in vitro" *J.Physiol.*. **393**:681-702

Krauthamer, V. & Ross, W.N. (1984) "Regional variations in excitability of barnacle neurons" J.Neurosci. **4**:673-682

Krnjevic, K. & Miledi, R. (1958) "Motor units in the rat diaphragm" *J.Physiol.* **140**:427-439

Kuffler, S.W. & Potter, D.D. (1963) "Glia in the leech central nervous system: physiological properties and neuron-glia relationship"*J. Neurophysiol.* **27**:290-320

Lacey, A.J. (1989) Light microscopy in biology: a practical approach. Practical Approach Series, Oxford University Press.

Lagerspertz, K.Y.H. & Talo, A. (1967) "Temperature acclimation of the functional parameters of the giant nerve fibres in *lumbricus terrestris* L. I. Conduction velocity and the duration of the rising and falling phase of action potentials" *J.Exp.Biol.* **47** :471-480

Larimer, J.L. (1988) "The comand hypothesis: a new view using an old example" *TINS* **11**:506-510

Laurent, G. & Burrows, M.J. (1989) "Intersegmental interneurons control the gain of reflexes in adjacent segments of the locust by their action on non spiking local interneurons"*J.Neurosci* **9**:3030-3039

Lawson, D., Fewtrell, C. & Raff, M. (1978) "Localised mast cell degranulation induced by concanavalin A-sepharose beads. Implication for the Ca^{2+} hypothesis of stimulus secretion coupling" *J.Cell Biol. 79:349-400*

Lent, C.M. (1973) "Retzius cells: Neuroeffectors controlling mucus release by the leech" *Science* **179**:693-696

Lent, C.M. (1981) "Morphology of neurones containing monoamines within leech segmental ganglia" *J.Exp.Zool.* **216**:311-316

Lent, C.M. & Fraser, B.M. (1977) "Connectivity of the monoamine-containing neurones in central nervous system of leech" *Nature* **266**:844-847

Lent , C.M., Ono, J., Keyser, K.T. & Karten, H. (1979) "Identification of serotonin within vital-stained neurones from leech ganglia" *J.Neurochem.* **32**:1559-1563

Letourneau, P.C. (1975) "Possible roles for cell-to-sustratum adhesion in neuronal morphogenesis" *Dev. Biol.* **44**:77-91

Letourneau, P.C. (1979) "Cell substratum adhesion of neurite growth cones, and its role in neurite elongation" *Exp.Cell.Research* **124** :127-138

Lin, S.S. & Levitan I.B. (1987) "Concanavalin A alters synaptic specificity between cultured Aplysia neurons" *Science* **237**:648-650

Lin, S.S. & Levitan, I.B. (1991) "Concanavalin A: a tool to investigate neuronal plasticity" *TINS* **14**:273-277

Lind, R. (1991) *Design and optimisation of extracellular microelectrodes* Ph.d. Thesis

(Glasgow University).

Liu, Y.& Nicholls, J.G.(1989) "Steps in the development of chemical and electrical synapses by pairs of identified leech neurons" Proc.R.Soc.Lond. (Biol) **236**:253-268

Lockery, S.R. & Kristan, W.B.Jr. (1990) "Distributed processing of sensory information in the leech. II. Identification of interneurons contributing to the local bending reflex" *J.Neurosci.* **10**:1816-1829

Loeb, G.E., Marks, W.B. & Beatty, P.G. (1977) "Analysis and microelectronic design of tubular electrode arrays intended for chronic multiple single-unit recording from captured nerve fibres" *Med. Biol.Eng.Comput.* **15**:195-201

Loeb, G.E., Walker, A.E., Uematsu, S. & Koningsmark, B.W. (1977) "HIstological reaction to various conductive and dielectric films chronically implanted in the subdural space" *J.Biomed. Mater. Res.* **11**:195-210

Macagno, E.R. (1980) "Number and distribution of neurones in the leech segmental ganglion" *J.Comp.Neurol.* **190**:283-302

Macagno, E.R., Muller, K.J. & DeRiemer, S.A. (1985) "Regeneration of aons and synaptic connections by touch sensory neurons in the leech central nervous sytstem" J. Neurosci. **5**:2510-2521

Macagno, E.R. Muller, K.J., Kristan, W. DeRiemer, S., Stewart, R. & Granzow, B. (1981) "Mapping of neuronal contacts with intracellular injections of horseradish peroxidase and lucifer yellow in combination" *Brain Res.* **217**:143-149

Macagno, E.R. Muller, K.J. & Pitman, R.M. (1987) "Conduction block silences parts of a chemical synapse in the leech central nervous system" *J.Physiol.* **387**:649-664

Marmor, M.F. (1971) "The effects of temperature and ions on the current-voltage relation and electrical parameters of a molluscan neurone" *J.Physiol.* **218**:573-598

Marsden, C.A. & Kerkut, G.A. (1969) "Flourescent microscopy of the 5-HT containing cells in the central nervous system of the leech *Hirudo medicinalis*" *Comp. Biochem. Physiol.* **31**:851-862

Martin, G.R. & Timpl, R. (1987) "Laminin and other basement membrane components" *Ann. Rev. Cell. Biol.* **3**:57-85

Mason, A. & Leake, L.D. (1978) "Morphology of leech Retzius cells demonstrated by intracellular injection of horseradish peroxidase" *Comp.Biochem.Physiol.* **61A**:213-216

Mason, A., Sunderland, A.J., Leake, L.D. (1979) "Effects of leech Retzius cells on body wall muscles" *Comp.Biochem.Physiol.* **63C**:359-361

Masuda-Nakagawa, L., Beck, K. and Chiquet, M. (1988) "Identification of molecules in leech extracellular marix that promote neurite outgrowth" *Proc.R.Soc.Lond.* **235**:247-257

Mathers, D.A. & Usherwood, P.N.R (1976) "Concanavalin A blocks desentisation of glutamate receptors on insect muscle fibres" *Nature* **259**:409-411

Mayer, M.L. & Westbrook, G.L. (1983) "A voltage-clamp analysis of inward (anomalous) rectification in mouse spinal sensory ganglion neurones" *J.Physiol.* **340**:19-45

Mayer, M.L. & Vyklicky, L. (1989) "Concanavalin A selectively reduces desensitisation of mammalian neuronal quisqualate receptors" *Proc. Natl. Acad. Sci. USA* **86**:1411-1415

McCarthy, R.A., Beck, K. & Burger, M.M. (1987) "Laminin is structurally conserved in the sea urchin basal lamina" *EMBO J.* **6**:1037-43

Mercer, H.D. & White, R.L. (1978) "Photolithographic fabrication and physiological performance of a microelectrode array for neuronal stimulation" *IEEE Trans. Biomed. Eng.* **25**:494-500

Meyrand, P., Simmers, J. & Moulins, M. (1991) "Construction of a pattern generating circuit with neurons of different networks" *Nature* **351**:60-63

Miles, F.A. (1969) *Excitable Cells.* William Heinemann Medical Books Ltd., London.

Miyazaki, S., Takahashi, K., Tsuda, K. & Yoshii, M. (1974) "Analysis of non-linearity observed in the current-voltage relation of the tunicate embryo" *J.Physiol.* **238**:55-77

Muller, K.J. (1981) "Synapses and synaptic transmission" In *Neurobiology of the Leech.* Ed: Muller, K.J., Nicholls, J.G. & Stent, G.S. Cold Spring Harbor Laboratory.

Muller, K.J. & McMahan, U.J. (1976) "The shape of sensory and motor neurones and the distribution of their synapses in ganglia of the leech: a study using intracellular injection of horseradish peroxidase" Proc. R. Soc. lond. B. **194**:481-499

Muller, K.J. & Nicholls, J.G. (1974) "Different properties of synapses between a single sensory neurone and two different motor cells in the leech C.N.S." *J.Physiol.* **238**:357-369

Najafi, K. & Hetke, J.F. (1990) "Strength characterization of silicon microprobes in neurophysiological tissues" *IEEE Trans.Biomed.Eng.* **37**:474-481

Nardi, J.B. (1983) "Neuronal pathfinding in developing wings of the moth *Manduca sexta*" *Dev. Biol.* **95**:163-174

Newgreen, D.F. (1989) "Physical influences on neural crest cell migration in avian embryos: contact guidance and spatial restriction" *Developmental Biol.* **131**:136-148

Nicholls, J.G. & Baylor, D.A. (1968) "Specific modalities and receptive fields of sensory neurons in the CNS of the leech" J.Neurophysiol. 31 :740-756

Nicholls, J.G. & Kuffler, S.W. (1964) "Extracellular space as a pathway for exchange between blood and neurons in the central nervous system of the leech: The ionic composition of glial cells and neurons" *J.Neurophysiol.* **27**:647-671

Nicholls, J.G., Liu, Y. Payton, B.W. & Kuffler, D.P. "The specificity of synapse formation by identified leech neurones in culture" *J.Exp.Biol.* **153**:141-154

Nicholls, J.G. & Purves, D. (1972) "A comparison of chemical and electrical transmission between single sensory cells and a motor nerones in the central nervous system of the leech" *J.Physiol.* **225**:637-656

Novak, J.L. & Wheeler, B.C. (1986) "Recording from the Aplysia abdominal ganglion with a planar microelectrode array" *IEEE Trans. Biomed. Eng. BME* **33**:196-202

Offner, F.F. (1967) *Electronics for Biologists.* McGraw-Hill Book Company, London.

Ohara, P.T. & Buck, R.C. (1979) "Contact guidance *in vitro*" *Exp. Cell Res.* **121**:235-249

Parnas, I., Dudel, J. & Atwood, H.L. (1991) "Synaptic transmission in decentralized axons of Rock Lobster" *J.Neurosci.* **11**:1309-1315

Parsons, T.D., Kleinfeld, D., Raccuia-Behling, F., & Salzberg, B.M. (1989) "Optical recording of the electrical activity of synaptically interacting *Aplysia* neurons in culture using potentiometric probes" *Biophys.J.* **56**:213-221

Pearson, K. G., Stein, R. B. and Malhotra, S.K. (1970) "Properties of action potentials from insect motor nerve fibres" *J.Exp.Biol.* **53**:299-316

Peinado, A., Zipser, B. & Macagno, E.R. (1987) "Regeneration of afferent axons into discrete tracts within peripheral nerves in the leech" *Brain. Res.* **410**:330-334

Pellegrino, M. & Simonneau, M. (1984) "Distribution of receptors for acetylcholine and 5-hydroxtryptamine on identified leech neurones growing in culture" *J.Physiol.* **352**:669-684

Pfenninger, K.H., Maylié-Pfenninger, M.-F., Friedman, L.B. & Simkowitz, P. (1984) "Lectin labeling of sprouting neurons: III. Type specific glycoconjugates on growth cones of different origin" *Dev. Biol.* **106**:97-108

Pickard, R.S. (1979) "Printed circuit microelectrodes" *TINS* **2**:259-261

Pickard, R.S., Collins, A.J., Joseph, P.L. & Hicks, R.C..J. (1979) "Flexible printed circuit probe for electrophysiology" *Med. Biol. Eng. Comput.* **17** :261-267

Pickard, R.S. & Welberry, T.R. (1976) "Printed circuit microelectrodes and their application to honeybee brain" *J.Exp.Biol.* **64**:39-44

Pine, J. (1980) "Recording action potentials from cultured neurons with extracellular microcircuit electrodes" *J.Neurosci.Meth.* **2**:19-31

Prohaska, O.J., Olcaytug, F., Pfundner, P. & Dragaun, H. (1986) "Thin-film multiple electrode probes: possibilities and limitations" *IEEE Trans. Biomed. Eng.* **33**:223-229

Pumphrey, R.J. & Young, J.Z. (1938) "The rates of conduction of nerve fibres of various diameters in cephalopods" *J.Exp.Biol.* **15**:453-466

Rall, W. (1960) "Membrane potential transients and membrane time constant of motorneurons" *Exp.Neur.* **2**:503-532

Rall, W. (1969) "Time constant and electrotonic length of membrane cylinders and neurons" *Biophys.J.* **9** :1483-1168

Rall, W. (1981) "Functional aspects of neuronal geometry. In *Neurones without impulses.* :223-254 Ed: Roberts, A. & Bush, B.M.H. Cambridge University Press.

Ray, C.D. & Walker, A.E. (1965) "Platinized platinum wire brain depth probes: details of construction" *Proc.Staff Meet. Mayo Clin* .**40** :771-804

Rayport, S.G. & Schacher, S. (1986) "Synaptic plasticity *in vitro*: Cell culture of identified *Aplysia* neurons and mediating short-term habituation and sensitization"

J.Neurosci **6**:759-763

Ready, D.F. and Nicholls, J.G. (1979) "Identified neurones isolated from leech CNS make selective connections in culture" *Nature* **281**:67-69

Regehr, W.G. (1988) *Neuron-microdevice connections.* Ph.D.Thesis (Cal.Tec.)

Regehr, W.G., Pine, J. & Rutledge, D.B. (1988) "Long-term in vitro silicon-based microelectrode-neuron connection" IEEE *Trans. Biomed. Eng.* **35**:1023-1032

Regehr, W.G. & Tank, D.W. (1990) "Postsynaptic NMDA receptor-mediated calcium accumulation in hippocampal CA1 pyramidal cell dendrites" *Nature* **345**:807-810

Reichardt, L.F. & Tomaselli (1991) "Extracellular matrix molecules and their receptors:functions in neural development" *Ann. Rev. Neurosci.* **14**:531-70

Retzius, G. (1891) "Zur Kenntniss des centralen Nervensystems der Wurmer" *Biologische Untersuchungen, Neue Folge II* :1-28 Ed. Samson & Wallin, Stockholm. (cited in Muller *et al.* 1981)

Robinson, F.R., & Johnson, M.T. (1961) "Histological studies of tissue reactions to various conductive and bielectric films chronically implanted in cat brains" Wright-Patterson AFB, OH ASD Tech. Rep. pp.61-397 (Quoted in Edell, 1986).

Rosenfalck, P. (1957) "Volume conducted action potentials and their correlation to the intracellular potential" *Acta.Physiol.Scand.* **42** (Suppl. 145):118-119

Rosenthal, F., Woodury, L.W. & Patton, H.D. (1966) "Dipole characteristics of pyramidal cell activity in cat postcruciate cortex" *J.Neurophysiol.* **29**:612-625

Ross, W.N. (1989) "Changes in intracellular calcium during neuron activity" *Ann.Rev.Physiol.* **51**:507-526

Ross, W.N., Arechiga, H. & Nicholls, J.G. (1987) "Optical recording of calcium and voltage transients following impulses in cell bodies and processes of identified leech neurons in culture" *J.Neurosci.* **7**:3877-3887

Ross, W.N., Arechiga, H. & Nicholls, J.G. (1988) "Influence of substrate on the distribution of calcium channels in identified leech neurons in culture" *Proc.Natl.Acad.Sci.USA* **85**:4075-4078

Ross, W.N. & Krauthamer, V. (1984) "Optical measurements of potential changes in axons and processes of neurons of a barnacle ganglion" J.Neurosci. **4**:659-672

Ross, W.N., Lasser-Ross, N. & Werman, R. (1990) "Spatial and temporal analysis of calcium-dependent electrical activity in guinea pig Purkinje cell dendrites" *Proc.R.Soc.* **240**:173-185

Ross, W.N. & Reichardt, L.F. "Species-specific effects on the optical signals of voltage sensitive dyes" *J. Membr.Biol.* **48**:343-356(1979)

Ross, W.N., Salzberg, B.M., Cohen, L.B., Grinvald, A., Davila, H.V., Waggoner, A.S. & Wang, C.H. (1977) "Changes in absorption, flourescence, dichroism and birefringence in stained giant axons:optical measurements of membrane potential" *J.Membrane Biol.* **33**:141-183

Rovensky, Y.A. & Slavnaya, I, L. (1974) "Spreading of fibroblast-like cells on grooved substrates" *Exp.Cell Res.* **84**:199-206

Rutten, W.L.C., van Weir, H.J. & Put, J.H.M. (1991) "Sensitivity and selectivity of intraneural stimulation using a silicon electrode array" *IEEE Trans.Biomed.Eng.* **38**:192-196

Salzberg, B.M. (1989) "Optical recording of voltage changes in nerve terminals and in fine neuronal processes" *Ann.Rev.Physiol.* **51** :507-526

Salzberg, B.M., Obaid, A.L. & Konnerth, A. (1985) "Large and rapid changes in light scattering accompany secretion by nerve terminals in the mammalian neurohypophysis" *J.Gen.Physiol.* **86**:395-411

Sanes, J.R. (1989) "Extracellular matrix molecules that influence neural development" *Ann. Rev. Neurosci.* **14**:491-516

Sargent, P.B. (1977) "Synthesis of acetylcholine by excitatory motorneurones in central nervous system of leech" *J.Neurophysiol.* **40**:453-460

Sargent, P.B., Yau, K.-W., & Nicholls, J.G. (1977) "Extrasynaptic receptors on cell bodies of neurones in the Central Nervous System of the Leech" *J.Neurophysiol.* **40**:453-460

Schain, R.J. (1961) "Effects of 5-hydroxytryptamine on the dorsal muscle of the leech (*Hirudo medicinalis*)" *Br.F.Pharmac. Chemother.* **16**:257-261 (Cited inWalker, 1968)

Silver, J. and Sidman, R.L. (1980) "A mechanism for the guidance and topographic patterning of retinal ganglion cell axons" *J. Comp. Neurol.* **189**:101-111

Singer, M., Norlander, R.H. & Edgar, M. (1979) "Axonal Guidance during during embryogenesis and regeneration in the spinal cord of the newt: The blue print hypothesis of neuronal pathway patterning" *J.Comp.Neurol.* **185**:1-22

Snedecor, G.W. & Cochran, W.G. (1967) *Statistical methods.* Iowa State University Press, USA.

Solomon, F. (1979) "Detailed neurite morphologies of sister neuroblastoma cells are related" *Cell* **16**:165-169

Spitzer, N.C. (1979) "Ion channels in development" *Annu. Rev. Neurosci.* **2**:263-397

Stepnoski, R.A., LaPorta, A. Raccuia-Behling, F., Blonder, G.E., Slusher, R.E. & Kleinfeld, D. (1990) "Noninvasive detection of transmembrane potentials in cultured neurons via light scattering" Preprint AT&T Bell Lab., New Jersey, USA.

Stewart, R.R., Nicholls, J.G. & Adams, W.B. (1989) "Na^+, K^+ and Ca^{2+} currents in identified leech neurones in culture" *J. Exp. Biol.* **141**:1-20

Strong, J.A. & Kaczmarek, L.K. (1986) "Multiple components of delayed potassium current in peptidergic neurons of *Aplysia:* Modulation by an activator of adenylate cyclase" *J.Neurosci.* **6**:814-822

Stryer, L. (1981) *Biochemistry.* W.H.Freeman and Company, New York.

Stuart, A.E., Hudspeth, A.J. & Hall, Z.W. (1974) "Vital staining of specific monoamine-containing cells in the leech central nervous system " *Cell Tissue Res.* **153**:55-61

Syed, N.I., Bulloch, G.M. & Lukowiak, K. (1990) "In Vitro reconstructiomn of the

respiratory central patern generator of the mollusk *Lymnaea*" *Science* **250**:282-285

Tank, D.W., Cohan, C.S. & Kater, S.B. (1986) "Cell body capping of array electrodes improves measurements of extracellular voltages in micro-cultures of invertebrate neurons" IEEE conference on Synthetic Microstructures, Airlie.

Tasaki, I. (1950) "Excitation of single nerve fiber by action currents from another single fibre" *J.Neurophysiol.* **13**:177-183

Thayer, S.A., Sturek, M. & Miller, R.J. "Measurement of neuronal Ca2+ transients using simultaneous microfluorimetry and electrophysiology" *Eur. J.Physiol.* **412**:216-223

Thomas Jr., C.A., Springer, P.A., Loeb, G.E., Berwald-netter, Y. & Okun, L.M. (1972) "A miniture microelectrode array to monitor the bioelectric activity of cultured cells" *Exp. Cell Res.* **74**:61-66

Titmus, M.J. & Faber, D.S. (1986) "Altered excitability of goldfish Mauthner cell following axotomy II. Localisation and ionic basis" *J.Neurophysiol.* **55**:1440-1454

Trisler, D. (1982) "Are molecular markers of cell position involved in the formation of neural circuits" *TINS* **5**:306-310

Tsien, R.Y. (1988) "Flourescence measurement and photochemical manipulation of cytosolic free calcium" *TINS* **11**:419-424

Urban, G.A., Ganglberger, J.A., Olcaytug, F., Kohl, F., Schallauer, R.,Trimmel, M., Schmid, H. & Prohaska, O. (1990) "Development of a multiple thin-film semimicro DC-Prode for Intracerebral Recordings" *IEEE Trans.Biomed.Eng.* BMM **37**:913-917

Verschueren, H. (1985) "Interference reflection microscopy in cell biology: methodology and applications" *J.Cell Sci.* **75** :279-301

Walker, R.J., Woodruff, G.N. & Kerkut, G.A. (1968) "The effect of acetylcholine and 5-hydroxytryptamine on electrophysiological recordings from muscle fibres of the leech, *Hirudo medicinalis*" *Comp. Biochem. Physiol.* **24**:987-990

Wallace, B.G. (1981) "Neurotransmitter Chemistry" In *Neurobiology of the Leech* Ed.: Muller, K.L, Nicholls, J.G. & Stent, G.S. Cold Spring Harbour Laboratory.

Wallace, B.G., Adal, M.N. & Nicholls, J.G. (1977) "Regeneration of synaptic connections by sensory neurons in leech ganglia maintained in culture" *Proc. R. Soc. Lond. B.* **199**:567-585

Weiss, P. (1945) "Experiments on cell and axon orientation *in vitro*: the role of colloidal exudates in tissue organisation" *J.Exp.Zool.* **100**:353-86

Weiss, P. (1958) "Cell contact" *Inter. rev. cytol.* **7**:391-423

Weiss, P. (1959) "Cellular dynamics" *Rev. Modern Physics* **31**:11-20

White, R.L., Roberts, L.A., Cotter, N.E. & Kwon, O.-H. (1983) "Thin-film electrode fabrication techniques" *Ann. N.Y. Acad. Sci.* **405**:183-190

Willard, A.L. (1981) "Effects of serotonin on the generation of the motor program for swimming by the medicinal leech" *J.Neurosci.***1**:936-944

Williams, D.A., Fogarty, K.E., Tsien, R.Y. & Fay, F.S. (1985) "Calcium gradients in single smooth muscle cells revealed by the digital imaging microscope using Fura-2" *Nature* **318**:558-561

Winters, C (1973) "The influence of temperature on membrane processes" In *Effects of temperature on ectothermic organisms: ecological implications and mechanisms of compensation.* Springer, New York. Ed: Wieser, W. pp45-53

Wise, K.D. & Angell, J.B. (1975) "A low capacitance multielectrode probe for use in extracellular neurophysiology" *IEEE Trans. Biomed. Eng.* **22**:212-219

Wise, K.D., Angell, J.B. & Starr, A. (1970) "An intergrated circuit approach to extracellular microelectrodes" *IEEE Trans. Biomed. Eng.* **17**:238-246

Woddington, C.H. (1941) "The genetic control of wing development in *Drosophila*" *J.Genet.* **41**:75-139

Wood, A. (1988) "Contact guidance on microfabricated substrata: the response of teleost fin mesenchyme cells to repeated topographical patterns" J.Cell Sci. **90**:667-681

Wright, S.D., Licht, M.R., Craigmyle, L.S. & Silverstein, S. (1984) "Communication between receptors for different ligands on a single cell: ligation of fibronectin receptors induces a reversible alteration in the function of the complement receptors on cultured human myocytes" *J.Cell. Biol.* **99**:336-339

Yaksta-Sauerland, B.A. and Coggeshall, R.E. (1973) "Neuromuscular junctions in the leech" *J.Comp.Neurol.* **151**:85-99

Zecevic, D., Wu J-Y., Cohen, L.B., London, J.A., Hopp, H-P. & Falk, C.X. (1989) "Hundreds of neurons in *Aplysia* abdominal ganglion are active during the gill-withdrawal reflex" *J.Neurosci.* **9**:3681-3689

Zipser, B. & Cole, R.N. (1992) "A mannose-specific recognition mediates the defasciculation of axons in the leech CNS" *J.Neurosci.* **11**:3471-3480

Zipser, B. & McKay, R. (1981) "Monoclonal antibodies distinguish identifable neurones in the leech" *Nature* **289**:549-554

Zoran, M.J., Doyle, R.T. & Haydon, P.G. (1991) "Target contact regulates the calcium responsiveness of the secretory machinery during synaptogenesis" Neuron 6:145-151

APPENDICES

Appendix 1: Culture medium and physiological salines

Leech Medium

L-15 (without L-glutamine; Sigma) supplemented with:
6mg.ml^{-1} glucose
3 mM glutamate (Sigma, UK),
100 unit.ml^{-1} streptomycin (Flow Labs,UK),
2.5 µg.ml^{-1} amphotericin-B (Gibco,UK).

[For long term cultures >24h, and for removing glial debris when cells were extracted with collagenase/dispase, this medium was supplemented with high quality 2% fetal calf serum; gift from S.Grumbacher-Reinert]

BHK medium *(also known as HECT:Hepes Eagle Calf serum Trypose phosphate; Clark* et al.*,1887)*

Hepes-buffered Glasgow-modified minimum Essential Medium (GMEM; Gibco, UK)

supplemented with:
10% calf serum,
10% trypose phosphate broth (Gibco,UK),
20 mM Hepes (Sigma)
3 mM glutamate (Sigma, UK),
100 unit.ml^{-1} streptomycin (Flow Labs,UK),
2.5 µg.ml^{-1} amphotericin-B (Gibco,UK).

[Modified medium used in bioassay contained only 2% fetal calf serum to avoid saturating the pattern with fibronectin]

Leech Ringer *(Muller* et al., *1981)*

115 mMSodium Chloride (NaCl)
1.8 mM Calcium Chloride ($CaCl_2$)
4 mM Potassium Chloride (KCl)
10 mM Tris Maleate (pH 7.4)

Phosphate Buffered Saline (PBS)

140 mMSodium Chloride (NaCl; 80g)
2.5 mM Potassium Chloride (KCl; 2g)
8 mM Sodium (Na_2HPO_4;11.5g)
1.5 mM Potassium dihydrogen orthophosphate (KH_2PO_4; 2g)

Adjusted to pH 7.4 with HCl
To make 10x stock solution: add amount indicated in brackets to 1 l of double distiled water.

Appendix 2: Estimate of the surface area of isolated neurones.

The morphology of extracted processes was quantified from large images. Each cell was divided up into regions as illustrated below, the dimensions of each region was measured and the surface area calculated (using the equations to the right of the figure). These measurements are likely to underestimate the actual surface area as they do not account for infolding.

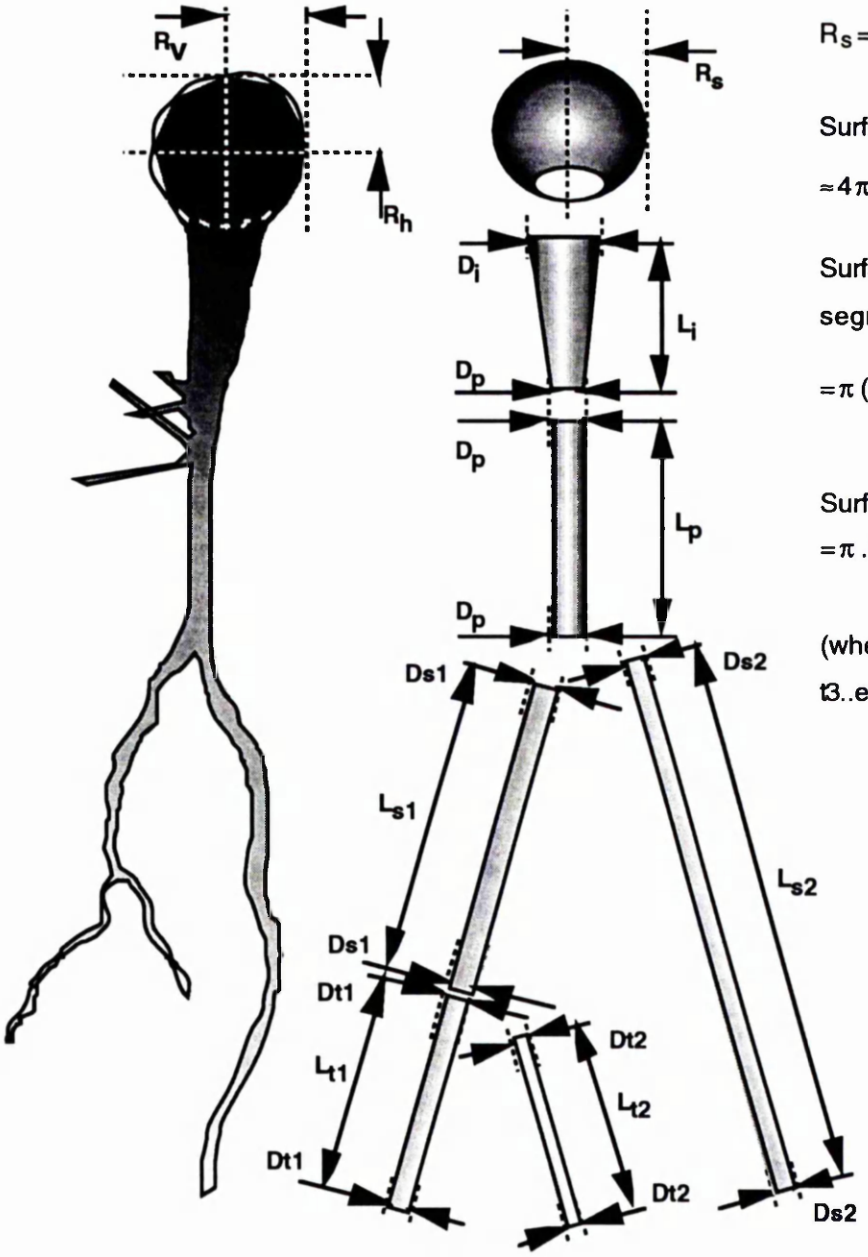

$$R_s = \frac{R_V - R_h}{2}; \quad R_{xn} = \frac{D_{xn}}{2}$$

Surface area of cell body

$$\approx 4\pi R_s^2 - \pi R_i^2$$

Surface area of initial segment

$$= \pi (R_i + R_p)\sqrt{(R_i - R_p)^2 + L_i^2}$$

Surface area of process

$$= \pi . D_{xn} . L_{xn}$$

(where x =p, s1, s2, t1, t2, t3..etc & n=1,2...etc)

KEY:
D:diameter
R:radius
L:length
p:primary process
s1..sn:secondary processes
t1..tn:tertiary processes

Appendix 3: The morphology and passive membrane properties of isolated Retzius neurones

Morphological parameters as defined in appendix 2 and passive membrane properties measured from the cell body of single isolated neurones, after 1 h *in vitro*.

Cell	O	V	Y	R	X	2a	I	p	2e	2i	2j	2l	2h	2b	w	2c
Input Resistance (MΩ)	31.6	37.9	37.1	65.4	18.3	24.1	27.0	23.5	39.7	34.2	26.7	39.5	53.8	22.1	31.1	39.8
Time constant (msec)	82	38	29	88	21	24	88	88	90	254	168	250	93			56
Cell body diameter (µm)	96	91	82	79	86	104	98	80	80.4	72	82.6	80	62.5		98	91
area (µm2)	27339	25515	20770	18930	22963	33665	28207	18849	19712	15611	20340	19490	11807		29733	25484
Initial process length (µm)	74	40.3	38.7	43.5	37.5	40	66	50	70.6	75	62	76	46		45	10.5
width at cell body(µm)	45	24.9	20.9	29	18.3	20	50	40	27.2	29	37	28	24		23.3	26
width at process (µm)	17.7	14.5	12.9	11	10	8.3	11	10	22	19.5	19.5	19.6	22		13.3	26
area (µm2)	7411	2514	2065	2791	1677	1797	6594	4099	5459	5725	5557	5691	3324		2603	857
Primary process length (µm) (to first branch point)	40.3	74.2	96.7	27.4	57	113	75	90				27	0		91	900 µm² †††
width (µm)	11.2	14.5	12.9	11.2	10	8.3	15	8.3				10.8	0		16.6	
area (µm²)	1418	3380	31919	964	1790	295	3534	2347				916	0		4746	1800
Secondary process (1) length (µm) (to end)	274	346	206	72.5	128	28	136	228					28		41	
width (µm)	7.2	8.8	6.45	8.1	8.3	6.6	6.6	6.3					14		5	
area (µm²)	6198	9565	4174	1845	3338	581	2820	4513					1231		644	
(2) length (µm) (to end or second branch point)	100		225	137	78	36.6	118	233	59				22			
width (µm)	7.2		12.9	9.6	8.3	6.6	6.6	6.6	17.4				22			
area (µm²)	2262		9118	4132	2033	729	2447	4831	3225				1520			
Tertiary process (1) length (µm) (to end)	81	80.6†					96††		43							
width (µm)	5.6	4					4		12							
area (µm²)	1425	1013					1206		1621							
(2) length (µm) (to end)	72															
width (µm)	7.2															
area (µm²)	1629															
Total length of processes (µm)	641	541	566	280	300	217	491	601	129	75	62	103	96		177	30
Apparent surface area (µm²)	47682	41987	68046	28662	31801	37067	44808	34621	30017	21336	25897	26097	17882	-	37726	28141

† Branch from 40 µm along the first axon. ††Branch from 50µm along initial process. †††Flat outgrowth at end of stump.